ACCELERATION OF INTENSE HEAVY ION BEAMS IN RIBF CASCADED-CYCLOTRONS

N. Fukunishi#, T. Dantsuka, M. Fujimaki, T. Fujinawa, H. Hasebe, Y. Higurashi, E. Ikezawa, H. Imao, T. Kageyama, O. Kamigaito M. Kase, M. Kidera, M. Kobayashi-Komiyama, K. Kumagai, H. Kuboki, T. Maie, M. Nagase, T. Nakagawa, M. Nakamura, J. Ohnishi, H. Okuno, K. Ozeki, N. Sakamoto, K. Suda, A. Uchiyama, T. Watanabe, Y. Watanabe, K. Yamada, H. Yamasawa,
Nishina Center for Accelerator-Based Science, RIKEN, 2-1 Hirosawa, Wako, Saitama, Japan

Abstract

RIKEN Radioactive Isotope Beam Factory, the world's first next-generation radioactive isotope beam facility, has provided high-intensity light and medium-heavy ion beams since 2006. Our aim is to produce the world's most intense heavy-ion beams, which are essential for exploring nuclei far from the stability line. The new injector RILAC2, which was fully commissioned in 2011, has greatly improved the beam intensity for very heavy ions. As a result, stable operation of highly intense beams such as 415-pnA ^{48}Ca, 38-pnA ^{124}Xe and 15-pnA ^{238}U has been realized.

ACCELERATOR COMPLEX OF THE RIKEN RADIOACTIVE ISOTOPE BEAM FACTORY (RIBF)

The RIBF accelerator complex [1] comprises the RIKEN Ring Cyclotron (RRC) [2], three injectors and three energy-booster cyclotrons (Fig. 1). The injectors are the RIKEN heavy-ion linac complex (RILAC) [3,4], the new injector linac (RILAC2) [5,6] and the K70-MeV azimuthally varying field (AVF) cyclotron [7]. The energy boosters are the fixed-frequency Ring Cyclotron (fRC) [8], the Intermediate-stage Ring Cyclotron (IRC) [9] and the Superconducting Ring Cyclotron (SRC) [10]. The RILAC, the RRC and the AVF cyclotron started operation in 1981, 1986 and 1989, respectively. The three boosters were commissioned in 2006 and the RILAC2 was fully commissioned in 2011.

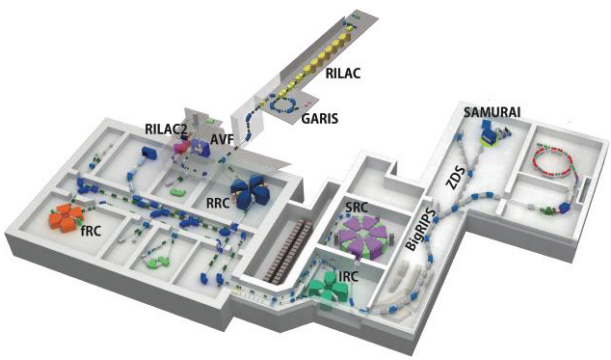

Figure 1: Layout of RIBF.

Acceleration Modes

In addition to standalone applications of the RILAC and the AVF cyclotron for low-energy experiments and direct applications of the beams accelerated by the RRC, the three acceleration modes illustrated in Fig. 2 are available at the RIBF. The variable-energy mode accelerates light and medium-heavy ions such as ^{48}Ca up to 400 MeV/nucleon, where two-step charge-state stripping is usually required. The variable-energy mode cannot accelerate ions heavier than krypton to the same velocity as lighter ions. Hence, very heavy ions, such as uranium, are accelerated further by inserting the fRC between the RRC and the IRC in fixed-energy mode. The RILAC2 replaced the RILAC for this mode in 2011. AVF injection mode is used to accelerate light ions such as oxygen by using three frequency-variable cyclotrons (AVF, RRC and SRC). A polarized ion source (PIS) produces polarized deuteron beams that range in energy from 250 to 440 MeV/nucleon.

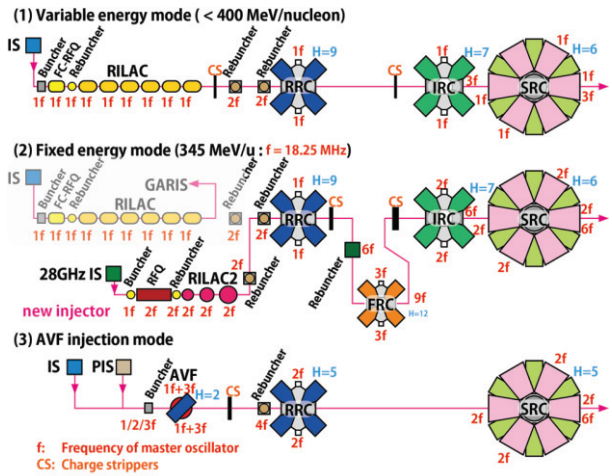

Figure 2: Acceleration modes available at the RIBF.

Ring Cyclotrons Used in the RIBF

Specifications of the four ring cyclotrons are summarized in Table 1. The SRC is the world's first superconducting (SC) ring cyclotron. The others are conventional four-sector cyclotrons. One flat-topping RF resonator is installed in each cyclotron except for the RRC to reduce the energy spread of the beam. The RRC still plays an essential role in the RIBF accelerator complex because of its large velocity gain and the greatly reduced relative energy spread of the beam during acceleration. The fRC was upgraded in 2012; its present K-number is 700 MeV. The isochronous magnetic fields of the SRC are generated by superposition of main and two types of trim coils. The main coil and the four sets of

*fukunisi@ribf.riken.jp

ISBN 978-3-95450-128-1

NEW DEVELOPMENTS AND CAPABILITIES AT THE COUPLED CYCLOTRON FACILITY AT MICHIGAN STATE UNIVERSITY*

A. Stolz#, G. Bollen, A. Lapierre, D. Leitner, D. J. Morrissey, S. Schwarz, C. Sumithrarachchi, and W. Wittmer, NSCL/MSU, East Lansing, MI 48824, USA

Abstract

This brief overview of the Coupled Cyclotron Facility will focus on the newly commissioned gas stopping area and reaccelerated radioactive ion beam capabilities. First commissioning results and operations experience of the combined system of Coupled Cyclotron Facility, A1900 fragment separator, gas stopper, EBIT charge-breeder and ReA linac will be presented.

INTRODUCTION

The Coupled Cyclotron Facility (CCF) at the National Superconducting Cyclotron Laboratory (NSCL) at Michigan State University consists of two coupled cyclotrons, which accelerate stable ion beams to energies of up 170 MeV/u. Rare isotope beams are produced by projectile fragmentation and separated in-flight in the A1900 fragment separator. For experiments with high-quality rare isotope beams at an energy of a few MeV/u, the high-energy rare isotope beams are transported to a He gas cell for thermalization, and then sent to the ReA post-accelerator for reacceleration (Fig. 1). Rare isotope beams in this energy range allow nuclear physics experiments such as low-energy Coulomb excitation and transfer reaction studies as well as for the precise study of astrophysical reactions. In August 2013, the first commissioning experiment using a reaccelerated ^{37}K beam was completed.

COUPLED CYCLOTRON FACILITY

Two coupled superconducting cyclotrons, the K500 and K1200 [1], are used to accelerate stable ion beams produced by ECR ion sources. Two ECR ion sources are available for axial injection into the K500 cyclotron. ARTEMIS is a modified version of the AECR at LBNL operating a frequency of 14.5 GHz. SuSI is a third generation superconducting ECR designed at NSCL, presently operating at 18 GHz [2].

Beams in the range of 8 – 14 MeV/u extracted from the K500 are injected mid-plane into the K1200 through a stripper foil located within one of the dees. Amorphous carbon foils with thicknesses of 300 – 800 μg/cm^2 are used to achieve the required charge ratio of 2.5 between injected and stripped beam. Beams from oxygen to uranium can be accelerated to final energies between 45 – 170 MeV/u. Net beam transmission measured from just before the K500 to extracted beam from the K1200 is often about 30%, resulting in an extracted beam power of about 1 kW for most medium-heavy beams [3].

*Supported by Michigan State University, National Science Foundation and U.S. Department of Energy

#stolz@nscl.msu.edu

Table 1 list a subset of primary beams available from the Coupled Cyclotron facility. Beam intensities in the published beam list are generally not the all-time peak intensities but are the typical intensities that can be used for experiment planning purposes and are considered maintainable for extended time periods.

Table 1: Partial NSCL Primary Beam List (the full list is published on the NSCL website) [4]

Isotope	Energy [MeV/u]	Intensity [pnA]	Isotope	Energy [MeV/u]	Intensity [pnA]
^{16}O	150	175	^{82}Se	140	35
^{18}O	120	150	^{78}Kr	150	25
^{20}Ne	170	80	^{86}Kr	140	25
^{22}Ne	150	100	^{112}Sn	120	4
^{24}Mg	170	60	^{118}Sn	120	1.5
^{36}Ar	150	75	^{124}Sn	120	1.5
^{40}Ar	140	75	^{124}Xe	140	10
^{40}Ca	140	50	^{136}Xe	120	2
^{48}Ca	160	80	^{208}Pb	85	1.5
^{58}Ni	160	20	^{209}Bi	80	1
^{76}Ge	130	25	^{238}U	80	0.2

A1900 FRAGMENT SEPARATOR

The A1900 fragment separator is a high-acceptance magnetic fragment separator consisting of four superconducting iron-dominated dipole magnets and 24 superconducting large-bore quadrupole magnets arranged in triplets [5]. Sixteen of the quadrupoles include a coaxial set of hexapole and octupole coils for aberration correction. Rare isotope beams are produced by projectile fragmentation of the primary beams on a transmission target at the object position of the A1900 fragment separator. Several production targets, usually consisting of beryllium foils with thicknesses between 100 – 2000 mg/cm^2, can be installed on a water-cooled target ladder. The mixture of unreacted primary beam and reaction products is filtered to obtain a single magnetic rigidity in the dispersive first half of the fragment separator. Isotopic selection can be achieved by passing the selected ions through a wedge-shaped energy degrader from which ions with different atomic numbers emerge with different momenta. The second dispersive half of the separator then provides isotopic separation.

ISBN 978-3-95450-128-1

CURRENT STATUS OF THE SUPERCONDUCTING CYCLOTRON PROJECT AT KOLKATA

J. Debnath#, M. K. Dey and A. Chakrabarti *(on behalf of VECC Staff)*
Variable Energy Cyclotron Centre, 1/AF, Bidhan Nagar, Kolkata -700064, India

Abstract

The commissioning of Kolkata superconducting cyclotron with internal ion beam had been reported in the last cyclotron conference [2]. At that time, there was gradual beam loss due to poor vacuum. After installing a higher capacity liquid helium plant the cryo-panels were made functional leading to a substantial increase in the beam intensity. It was hoped that higher beam intensity would help in extraction of a measurable fraction of the beam, but that did not happen. Detailed investigation of beam behavior with the help of three beam probes, installed temporarily at three sectors, revealed that the beam goes highly off-centered while passing through the resonance zone. A plastic scintillator based phase probe was mounted on the radial probe and beam phase was measured accurately [1]. It was quite clear that large amount of field imperfection was prohibiting the beam to be extracted. So magnetic field measurement has been started again and considerable amount of harmonic and average field errors have been found. In this paper we report the important developments since 2010.

INTRODUCTION

A higher capacity Liquid helium plant was installed in 2010. With the help of this plant we could achieve beam chamber vacuum of the order of $3x10^{-8}$ mbar from$7x10^{-7}$ mbar installing 4K-cryo-panels in the valley regions. As a result we got a flat beam profile up to the maximum radius with minimum loss as shown in Fig. 2. The 1st external beam line is ready to take the extracted beam to the experimental hall as shown Fig. 1

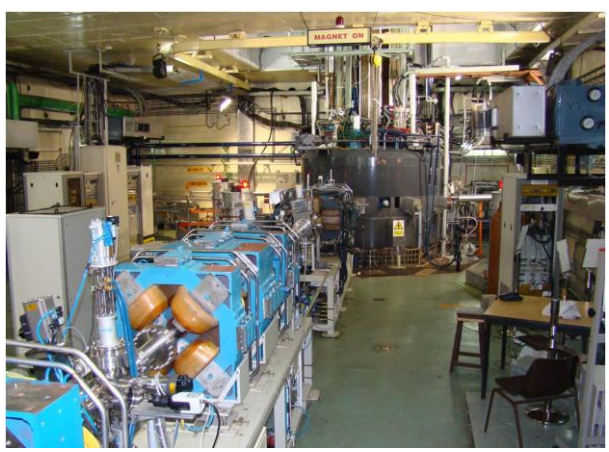

Figure 1: Superconducting cyclotron with beam line.

After getting a good beam profile we carried out the beam extraction trial extensively.

#jdebnath@vecc.gov.in

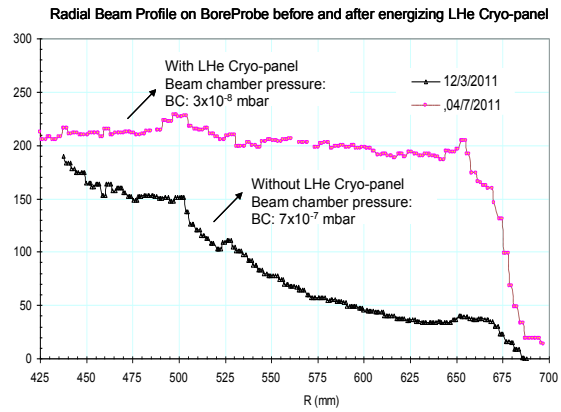

Figure 2: Improvement of beam profile after installing the cryo-panels.

BEAM EXTRACTION TRIAL

In the process of beam extraction trial we have used different diagnostics elements. We have seen the beam profile in the bore-scope monitor at different radii under different settings of magnetic field.

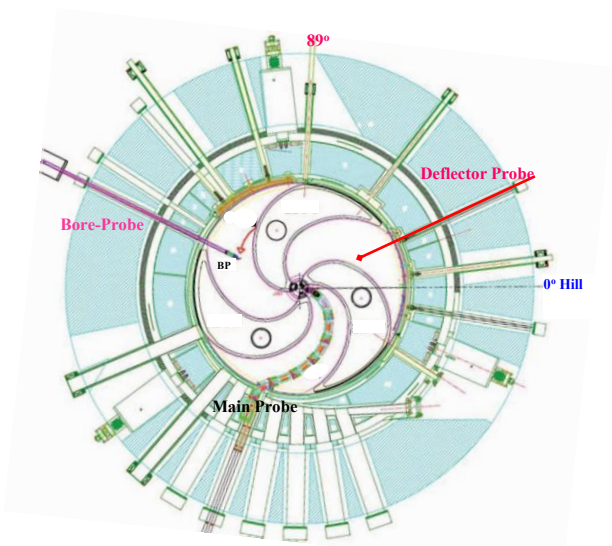

Figure 3: Layout of beam extraction channels and location of the three beam probes.

The schematic of the position of extraction channels and the beam probes are shown in Fig. 3. To get the signature of the extracted beam from the 1st deflector, we put a current reading probe as shown in Fig. 4(b) at the view port at 89°. Then we put an insulated copper plate at the exit of 1st deflector as shown in Fig. 4(c). We could not get any signature of extracted beam from the 1st

ISBN 978-3-95450-128-1

WHAT WE LEARNED FROM EMMA

S. Machida, ASTeC/STFC/RAL, Didcot, United Kingdom
on behalf of the EMMA collaboration

Abstract

After a brief introduction of FFAG accelerators, we discuss the demonstration of serpentine channel acceleration and the fast resonance crossing in non-scaling FFAGs. Then we summarise the findings from the EMMA project so far.

INTRODUCTION

Fixed Field Alternating Gradient (FFAG) accelerators attracted attention in the 1990s as candidates for muon acceleration for a neutrino factory [1-2]. Muons have a very short lifetime (2.2 μs in their rest frame) and the acceleration needs to be very fast to avoid the decay of too many particles in the beam. There is no time to adjust the strength of magnets in the accelerator lattice to match the beam momentum: therefore, synchrotrons are out of question. The only options for fast acceleration are either a linac (including re-circulating versions) or an FFAG [3].

An FFAG accelerator could be classified as one kind of cyclotron. It is especially similar to a synchro-cyclotron in the sense that the magnetic field strength is constant and the rf frequency is swept according to the beam momentum. Nevertheless, a significant difference from a synchro-cyclotron is the strong focusing used in the lattice: alternating field gradients (i.e. focusing and defocusing optics) reduce the beam size and orbit excursion.

Research and development efforts on FFAG accelerators, after a long dormant period following their invention and the construction of a few electron models, aimed for demonstration of proton acceleration with a newly developed rf accelerating cavity using magnetic alloy [4]. Without ramping of magnetic fields, the machine repetition rate could be faster by some orders of magnitude compared with conventional rapid cycling synchrotrons. The goal was set to demonstrate 1 kHz operation; for comparison, the fastest cycling synchrotron (ISIS at Rutherford Appleton Laboratory) achieves 50 Hz.

Regarding the beam optics, proton FFAGs that was developed in Japan at KEK and KURRI [5] followed the conventional "scaling" principle, in which the magnetic field has a profile with strength increasing as r^k, where k is a constant field index and r is the distance from the machine centre. With this scaling law, the tune is constant (independent of beam energy), thus avoiding resonance crossings during acceleration.

In parallel to the development of very rapid cycling proton FFAGs in Japan, design efforts to optimise FFAGs for muon acceleration were carried out in the US and Europe. One outcome from those efforts was the invention of the non-scaling FFAG [6-7]. For muon acceleration, the beam stays in the accelerator for only a short time. Although a non-scaling FFAG is still a circular accelerator, so that the beam goes through the same magnetic channel several times and resonance phenomena emerge, the time scale of resonance blow up can be longer than the whole acceleration cycle. In that case, the beam will not be badly affected by resonances, and constraints on the optics design can be greatly relaxed. Machine parameters can be optimised primarily to squeeze the beam size as well as the orbit excursion.

This novel type of FFAG consists of only dipole and quadrupole magnets, resulting in a large dynamic aperture. Since this design does not follow the conventional scaling law which fixes the transverse tune throughout the acceleration, it is called a non-scaling FFAG, or more specifically a linear non-scaling FFAG.

The advantages of non-scaling FFAGs led to discussions of their application to other areas. For example, the small orbit excursion means that small magnets can be used, which has significant advantages in accelerators for proton therapy.

The biggest question was whether non-scaling FFAGs would work as designed. Although tracking simulations showed promising performance, an experiment had to be carried out to provide a convincing demonstration. The EMMA project (Electron Model for Many Applications) was initiated and construction started at Daresbury Laboratory in the UK [8-10]. Figure 1 shows the layout and Table 1 lists principal parameters.

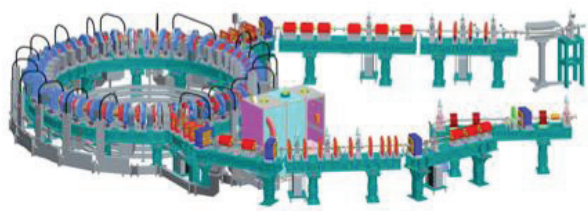

Figure 1: EMMA at Daresbury Laboratory. 10.5 MeV/c electron beams are delivered through beam transport line (bottom right) from ALICE and injected in the EMMA ring (left). The beam is extracted and its properties are measured in the diagnostic line (top right). The lattice does not have dipole magnets. Bending action comes from the shifted quadrupole magnets.

Table 1: Principal Parameters

momentum	10.5 – 20.5 MeV/c
circumference	16.57 m
number of cells	42
focusing	doublet
nominal integrated quad. field	0.402/-0.367 T
rf frequency	1.301 GHz
number of rf cavities	19
tune shift for he momentum range	0.3 to 0.1/cell
acceptance (normalized)	3 π mm rad

ISBN 978-3-95450-128-1

HIGH CURRENT BEAM EXTRACTION FROM THE 88-INCH CYCLOTRON AT LBNL

D.S. Todd, J.Y. Benitez, M. Kireeff Covo, K. Yoshiki Franzen, C.M. Lyneis, L. Phair, P. Pipersky, M.M. Strohmeier, LBNL, Berkeley, CA 94720, U.S.A.

Abstract

The low energy beam transport system and the inflector of the 88-Inch Cyclotron have been improved to provide more intense heavy-ion beams, especially for experiments requiring ^{48}Ca beams. In addition to a new spiral inflector [1] and increased injection voltage, the injection line beam transport and beam orbit dynamics in the cyclotron have been analyzed, new diagnostics have been developed, and extensive measurements have been performed to improve the transmission efficiency. By coupling diagnostics, such as emittance scanners in the injection line and a radially-adjustable beam viewing scintillator within the cyclotron, with computer simulations we have been able to identify loss mechanisms. The diagnostics used and their findings will be presented. We will discuss the solutions we have employed to address losses, such as changing our approach to tuning VENUS and running the cyclotron's central trim coil asymmetrically.

INTRODUCTION

The majority of beams delivered by Lawrence Berkeley National Laboratory's 88-Inch Cyclotron go to users who can be separated into two groups with quite different needs. Users such as those in the National Security Space community perform microchip testing using the cyclotron's ion beams, and they typically require high-charge-state ion beams with relatively low currents. The addition of the fully-superconducting electron cyclotron resonance (ECR) ion source VENUS [2] has increased the variety of beams that can be delivered; for example, Xe^{43+} has recently been added to the 16 MeV/nucleon cocktail. The second group of users are those performing fundamental Nuclear Science research, and these users routinely require high-current, medium-charge-state ion beams. A beam of particular interest for heavy ion physics is ^{48}Ca, where researchers have requested beam currents of nearly 2 pμA. In order to deliver such high currents, a four-year upgrade project was undertaken to identify and correct beam loss mechanisms. Dedicated beam studies showed that there are two primary regions where beam losses occur: along the low energy beam transport (LEBT) system and the center region of the cyclotron.

LOW ENERGY BEAM TRANSPORT

For high current beams, only two of the 88-Inch Cyclotron's three ECR ion sources are typically used: VENUS and the AECR-U [3]. Unlike the fully-superconducting VENUS, the AECR-U is a normal conducting ion source which has been in operation in its upgraded form since 1995. Initial tests of the $^{48}Ca^{11+}$ production capabilities using the AECR-U showed that the cyclotron could only deliver approximately 0.5 pμA, and although the injected current could be increased, no more current could be extracted from the cyclotron [1]. During most of these runs with the AECR-U as the injector, the source extraction voltage was kept at approximately 12.5 kV, but when VENUS, with its higher available extraction voltages, was used as the injector it was found that beam transmission increased. As a result, it was decided to increase source extraction voltage to over 25 kV for both sources (VENUS is already capable of 30 kV) to reduce potential space charge effects along the LEBT and during injection. Additional work was also performed on the AECR-U line to improve the alignment of the transport system, in particular near beam extraction where poor alignment leads to significant beam loss.

The increase in source extraction voltages required upgrades to the cyclotron's axial beam line which is shared by all of the ion sources. In particular, the final solenoid lens that affects the beam trajectory as it nears the cyclotron had to have its maximum current increased. This increase in lens strength required additional water cooling capabilities for that lens. The increase in extraction voltage also led to increases in both the required chopper voltage (upgraded to ±1000 V) and buncher voltage. In order to reduce the necessary buncher voltages, both the fundamental and harmonic bunchers were moved upstream to increase the distance to the cyclotron. The fundamental buncher was moved from 2.54 to 3.1 m away from the cyclotron midplane, while the harmonic buncher was moved from 2.13 m to the former location of the fundamental buncher. These changes result in a nearly 20% reduction of the required bunching voltages for each buncher.

The failure of the VENUS 90° analyzing magnet's power supply during a long, high current run, and the performance of its temporary replacement, illustrated how important the current stability of this supply is. It was found that peak performance required a supply with current stability of at least one part in 10^4.

CENTER REGION

All three of the 88-Inch Cyclotron's ECR ion sources use the same axial line for approaching beams. These sources produce a varied range of beam species (protons to uranium) and beam energies, therefore a gridded mirror inflector is used to bend the approaching beam into the cyclotron's midplane. The mirror inflector is intended to act as a parallel plate capacitor tilted 45.7° above the cyclotron's midplane; the bottom plate may be biased positively while the upper plate is replaced by either grids

ISBN 978-3-95450-128-1

PROGRESS TOWARD THE FACILITY UPGRADE FOR ACCELERATED RADIOACTIVE BEAMS AT TEXAS A&M*

D.P. May, F. P. Abegglen, G. Chubaryan, H. L. Clark, G. J. Kim, B. T. Roeder, G. Tabacaru, R. E. Tribble, Cyclotron Institute, Texas A&M University, College Station, TX 77845, USA
J. Arje, Accelerator Laboratory, University of Jyväskylä, Finland

Abstract

The upgrade project at the Cyclotron Institute of Texas A&M University continues to make substantial progress toward the goal of providing radioactive beams accelerated to intermediate energies by the K500 Cyclotron. The K150, which will function as a driver, is now used extensively to deliver both light and heavy ion beams for experiments. The ion-guide cave for the production and charge-breeding of low-energy radioactive beams has been constructed, and the light-ion guide (LIG) has been commissioned with an internal radioactive source. The charge breeding electron-cyclotron-resonance ion source (CB-ECRIS) has been commissioned with a source of stable 1+ ions, while the injection line leading to the K500 has been commissioned with the injection and acceleration of charge-bred beams. Despite the lack of good field maps, both light and heavy ions beams have been developed for the K150. Progress and plans, including those for the heavy-ion guide (HIG), are presented.

INTRODUCTION

The Texas A&M Cyclotron Institute has been in the process of upgrading the facility since 2005 [1, 2]. The scheme is the following (Fig. 1):

1. The K150 provides either an intense beam of light ions (p, d, α) to a target in the LIG chamber or an intense beam of heavy ions (e. g. argon) to a target in the BIGSOL superconducting-solenoid spectrometer.
2. Products from the target directly enter a helium gas flow in the case of LIG, or in the case of HIG the products are focused through an entry foil in the HIG chamber.
3. Products in either chamber are stopped by the helium and extracted by the helium flow. Since in helium the products remain ionized, after they exit the stopping chamber they are guided by a multipolar rf structure and formed into a beam. The neutral helium is pumped away.
4. This low-charge-state beam of products is focused inside of CB-ECRIS where the products are stopped in the plasma and further ionized by the energetic electrons.
5. Extracted beam from CB-ECRIS is analyzed and a beam of one charge-state is injected into the K500.

Recent progress has focused on: a) improving the intensity and variety of beams from the K150 Cyclotron, which will be used as a driver for the production of short-lived isotopes, b) outfitting the ion-guide cave where these isotopes will be produced and charge-boosted by CB-ECRIS and c) finishing the low-energy injection line connecting CB-ECRIS with the K500 Cyclotron. In conjunction with these tasks a variety of beams have been developed along with a better comprehension of the K150 magnetic fields, charge-breeding has been successfully demonstrated with the CB-ECRIS and the injection-line has been commissioned with beams traveling from source to cyclotron.

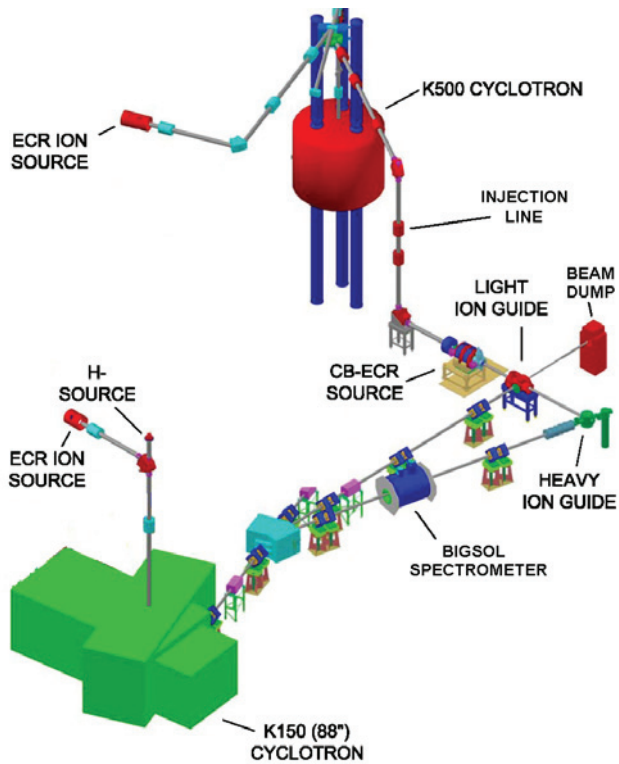

Figure 1: Simplified layout of the Texas A&M Radioactive Beam Facility.

K150 CYCLOTRON

For acceleration by the K150 Cyclotron a multi-cusp ion source produces negative ions of hydrogen and deuterium which are extracted from the cyclotron by stripping to obtain proton and deuteron beams. A two-frequency (14GHz plus 11GHz) ECRIS produces positive-ion beams. The mass and energy range of K150 beams is illustrated by Fig. 2 and includes both first-harmonic and second-harmonic beams (≤ 5 AMeV).

*Work supported by U. S. Dept. of Energy Grant DE-FG02-93ER40773

IMPROVING THE ENERGY EFFICIENCY, RELIABILITY AND PERFORMANCE OF AGOR*

Mariet Anna Hofstee#, Sytze Brandenburg, Jan de Jong, Harm Post, Roel Schellekens,
KVI, University of Groningen, Groningen, The Netherlands

Abstract

Over the past few years the nature of the experiments performed with AGOR has changed from long experiments, to sequences of short experiments, often using different beams. In addition the total demand for beamtime has gone down. This has required a change in operating procedures and scheduling. In view of the changing demands, we are continuing our efforts to improve the energy efficiency and reliability of the cyclotron, while at the same time trying to improve performance. While some of the solutions might be unique to our facility, many will have broader applicability.

HISTORY

- In 1996 a new K600 superconducting cyclotron, AGOR, was installed in Groningen
- In 2003 a new separator was built for the TRIμP program.
- In 2005 a Noctua monitoring system for the electrical power consumption was installed, and expanded in 2007
- Since 2005 the European space agency ESA uses the irradiation facility for radiation hardness testing.
- In 2006 the Irradiation beam line (H-line) was moved from the west to the east side of the building.
- In 2007 a SUPERNANOGAN ECR source was obtained on loan from the Helmholtz Zentrum Berlin (HZB), Germany.
- In the 2007/2008 winter maintenance period a heat recovery system was installed on the big cryo-compressor.
- In 2012 the power distribution system of the building was completely replaced.

BEAMTIME AND USERS

At the time of construction AGOR was intended to provide both polarised light ion beams as well as heavy ion beams. During the initial years several nuclear physics programs were executed with experiments of, usually low intensity, (polarised) light ion beams and typically multi day duration.

In 2003, because of the TRIμP program, requirements changed to high intensity low energy heavy ion beams. Due to the complexity of these experiments the beam development and tuning time required became much longer and experiments eventually took up to two weeks, including the weekends. The TRIμP program will end on 31st of December 2013.

Meanwhile a new category of, partly commercial, users has appeared, using the cyclotron for radiation hardness testing and radiobiology. The available 190 MeV proton beam is well suited for simulating solar flares. The 150 MeV proton and 90 MeV/amu carbon beams are excellent for radiobiology experiments. These experiments are typically short in duration, with a large variety in desired beam intensities and energies. The latter often can be provided from a single high energy primary beam with the use of an automated degrader in the irradiation experimental area.

In 2002 more than 3000 hours of beam were provided to our users for nuclear (astro-)physics experiments with the Big Byte Spectrometer (BBS) and other beamlines, and less than 100 hours for experiments with the multi user facility (2 irradiation experiments). In addition 700 hours of unscheduled maintenance were used, mainly for issues with the cryogenic system [1].

In 2012 a total of nearly 1300 hours of beamtime were provided to our users, distributed over 4 TRIμP experiments (total 490 hours), a long experiment with the BBS (234 hours) and 15 irradiations (326 hours, including one irradiation of 193 hours). In 2012 a little over 200 hours of unscheduled maintenance were needed, mainly due to water leaks in the cyclotron.

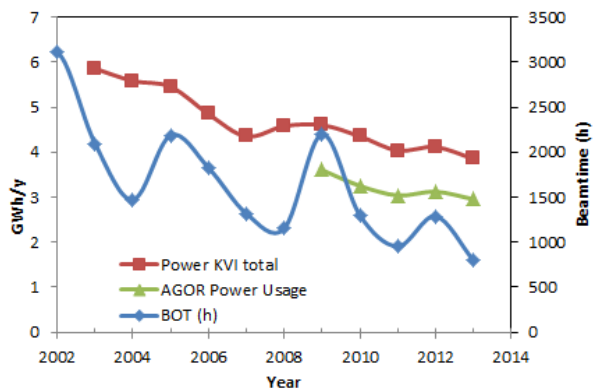

Figure 1: Annual Electrical Energy Usage, AGOR fraction and Total Beam time (hours, right axis). The value for 2013 is a conservative estimate.

SUBSYTEMS

Even though subsystems are discussed separately in the following section, modifications to one subsystem often affect several others.

*Work supported by Stichting FOM, Utrecht, The Netherlands
#m.a.hofstee@rug.nl

ISBN 978-3-95450-128-1

STATUS REPORT OF THE CYCLOTRONS C-30, CS-30 AND RDS-111 AT KFSHRC, SAUDI ARABIA

F. Alrumayan, M. Shawoo and M. Vora
King Faisal Specialist Hospital and Research Centre, Riyadh, Saudi Arabia

Abstract

Experience gained since the commissioning of the IBA C-30 Cyclotron at the King Faisal Specialist Hospital and Research Centre (KFSHRC) in 2010, has shown this facility to be viable entity. In addition to the C-30 Cyclotron, the facility includes two other Cyclotrons, namely: the RDS-111 and the CS-30 Cyclotrons. The latter has dual responsibilities; while it is kept as a backup for the other Cyclotrons for radioisotopes production, it's also used for proton therapy researches and Bragg Peak measurements at that particular energy. Facility operating history, usage and radiopharmaceuticals productions are described.

INTRODUCTION

The production of radioisotopes for use in medical applications such as diagnostic imaging and therapeutic treatment is achieved through nuclear reactions using accelerated charged particles. The latter is accelerated using medical cyclotron which increases its energy to a range of 30 MeV or so. The accelerated charged particles are used to produce radioisotopes that can be used later in nuclear medicine in the form of radiopharmaceuticals. At KFSHRC, there are three medical cyclotrons, the CS-30, the C-30 and the RDS-111. Each of these cyclotrons will be described below.

CYCLOTRONS OPERATIONS

The CS-30 was assembled and tested at TCC in USA before being shipped to Saudi Arabia. Beam tests at the factory started in 1977 and ended in October [1, 2]. The CS-30 can accelerate four different particles with different energy levels [2]. Values are shown in Table 1. Target stations are available on seven beam lines as well as on an internal target. Beam lines #1 and #2 are reserved for FDG production. Beam line #3 terminates in gas target and processing system, which was designed for production of the positron-emitters ^{11}C and ^{15}O. Beam line # 4 consists of two end segments. The 101 degree dipole magnets are used for stack foils experiments. Presently mounted on beam line #5 is production of Krypton-81m generators. Beam line #6 goes to the "isocentric" neutron therapy system. Beam line #7 is used once a week for ^{13}N. A TCC model 4010 internal target system, with isorabbit transfer to the hot cells, is fitted to the cyclotron but has been substantially modified. The cold cathode internal ion source is quite reliable. The life time of tantalum is greater than 100 hours when producing proton [3]. However, this number drops massively when helium beams are accelerated. The C-30 cyclotron, on the other hands, was assembled and tested at IBA in Belgium before being shipped to Saudi Arabia. The Cyclone 30 is 30 MeV, negative ion machine, deep valley magnet and uses cryopumps technology. It has the advantage of simultaneous extraction of two beams rated 350 uA each. The RF system can deliver up to 45 kW of power to accelerate its particles. The C-30 delivers a stable dual beam current up to 750 μA. Maximum efficiency is obtained through the simultaneous bombardment of two different targets for two different isotopes production.

The Cyclone C-30 has three beam lines; beam line #1.1 is connected to five ports through a switching magnet. In each port there is a different target being selected by changing the magnetic field in the switching magnet, they are F-18, N-13, Kr-81m and two as spare for future development. Beam line #2.1 is dedicated for solid target (Thallium, Gallium, etc.) and beam line #2.2 is dedicated for ^{123}I through the well-known nuclear reaction of protons with highly enriched ^{124}Xe.

The RDS-111 cyclotron is a compact machine, installed in 2006. It has the ability to deliver dual beam at 11 MeV with a maximum beam current of 60 μA. It has six ports; three in each line and occupied as follows: two ports are reserved for faraday cup for measuring the beam, two ^{18}F and two ^{13}N targets.

Table 1: Cyclotrons' Characteristics at KFSHRC

Cyclotron Type	Particles	Energy (MeV)	I_{Beam} (μA)
C-30	P	30	750
CS-30	P	26.5	100
RDS-111	P	11	60

Figure 1 shows photos of the three cyclotrons at KFSHRC. Unlike the CS-30 and RDS-111, the C-30 has an advantage of varying its energy smoothly using the radial extraction system. This gives the operator the ability to select between different radioisotopes easily. However, the CS-30 is unique in terms of the number of particles that it can accelerate. Table 1 show the characteristics of these machines.

ISBN 978-3-95450-128-1

STATUS OF THE HZB CYCLOTRON

A. Denker#, J. Bundesmann, T. Damerow, T. Fanselow, W. Hahn, G. Heidenreich, D. Hildebrand, U. Hiller, U. Müller, C. Rethfeldt, J. Röhrich, HZB, Hahn-Meitner-Platz 1, 14109 Berlin, Germany
D. Cordini, J. Heufelder, R. Stark, A. Weber, Charité, Berlin, Germany

Abstract

The therapy of ocular melanomas in Berlin started 1998 as cooperation between the Benjamin-Franklin Klinikum (now Charité) and the Hahn-Meitner-Institut (now Helmholtz-Zentrum Berlin). More than 2222 patients have been treated since. The facility is still the only facility in Germany treating ocular melanomas with protons.

In the beginning, tumour therapy used about 10 % of the overall beam time and its accelerator operation was embedded in the operation for physics experiments. The end of the physics programme in 2006 had severe consequences: Beam time, and consecutively funds and resources, were cut-down remarkably.

The accelerator operation continued mainly for therapy since 2007 with reduced man-power, requiring changes in the set-up and operation regime of the accelerators. Maintaining a high reliability is a key issue. The stability of the proton beam is of utmost importance for the therapy, both on the short-term and the long-term scale.

ACCELERATORS AND OPERATION

The main user of the facility is since 2007 the Charité, using a 68 MeV proton beam for eye tumour therapy. In addition, several small scale experiments, like radiation hardness testing and dosimetry are performed. This changed the operation regime from ~ 4500 hours of beam time to 12 therapy weeks distributed evenly over the year.

Since 2009 our cyclotron is again served by two different injectors. The van-de-Graaff Injector beam line offers the acceleration of a variety of different ion species and a beam bunching for high transmission within the cyclotron. The Radio Frequency Quadrupole, used for heavy ions, has been transferred to iThemba Labs and was replaced by a 2 MV tandetron from High Voltage Engineering Europa B.V. [1]. As standard ion source, the 358 duoplasmatron with direct off axis extraction of negative hydrogen ions was chosen.

Development of the ion source resulted in safe source operation times of more than 600 h and extremely stable beam current [2]. After extensive beam tests, the authorities granted the permit for using the tandetron-cyclotron combination for therapy in 12/2010. The tandetron is in full operation for therapy since 01/2011. It proved to be a reliable machine with extremely high stability, causing no measurable down time.

As shown in Figure 1, operation of the accelerator went very smoothly. Since the successful commissioning of the tandetron the amount of time for beam tests decreased, while more beam time was used by experiments. The downtime of the accelerator over the last five years due to failures was less than 5%. This was achieved by a step by step process addressing all sub-systems of the accelerator complex with:

- Modernisation, e.g. the exchange of the shunt against transducer regulation in the quadrupole power supplies yielding a gain in stability of factor 10 or the replacement of discrete rectifiers by complete 3-phase modules.
- Increased redundancy, e.g. using smaller variety of pumps, vacuum gauges, or power supplies. The operation of the turbo-pumps on 60% of the rotational speed (standby mode) once a good vacuum has been reached increases the service intervals by a factor of five.
- Improved diagnosis, e.g. routinely applied residual gas analysis in the cyclotron for an early determination of a water leak or the logging of the electricity supply.
- Better display of machine parameters like 24 h charts, also available during the periods between the therapy weeks and accessible via world-wide-web interface.

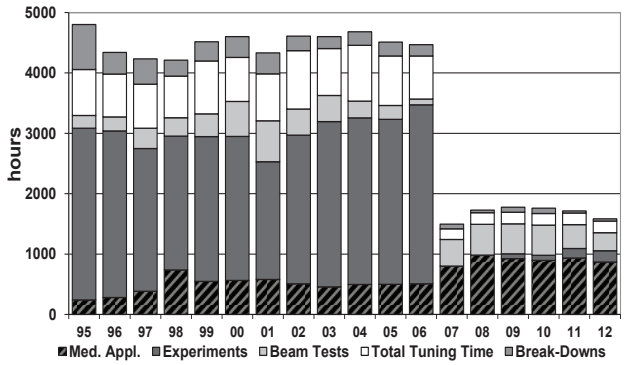

Figure 1: Operation statistics of ISL (1995-2006) and the new operation regime with the main use of the cyclotron for therapy (since 2007).

Between 10 and 30% of the annual downtime is due to failures in the electricity provision by the power supplier. In 2012 alone, six failures of the electricity supply with a duration above 0.1 seconds occurred. However, the peak power consumption of the cyclotron during the ramping procedure of the main magnet would require a large uninterruptible power supply (UPS), which was considered to be too expensive as well as too labour-intense. However, the computers of the control system have been equipped with UPS in order to prevent also data losses.

denker@helmholtz-berlin.de

ISBN 978-3-95450-128-1

20 YEARS OF JULIC OPERATION AS COSY'S INJECTOR CYCLOTRON

R. Gebel, R. Brings, O. Felden, R. Maier, S. Mey, D. Prasuhn,
Forschungszentrum Jülich, IKP-4, Germany

Abstract

The accelerator facility COSY/Jülich is based upon availability and performance of the isochronous Jülich Light Ion Cyclotron (JULIC) as pre-accelerator of the 3.7 GeV/c COoler SYnchrotron (COSY). The cyclotron has passed in total 262500 hours of operation since commissioning in 1968. JULIC provides routinely, for more than 6500 hours/year, polarized or unpolarized negatively charged light ions for COSY experiments in the field of fundamental research in hadron, particle and nuclear physics. The on-going program at the facility foresees increasing usage as a test facility for accelerator research and detector development for realization of the Facility for Antiproton and Ion Research (FAIR), and other novel experiments on the road map of the Helmholtz Association and international collaborations. In addition to the operation for COSY the cyclotron beam is used for irradiation, radiation effect testing and fundamental nuclide production for research purposes.

INTRODUCTION

The Institute for Nuclear Physics (IKP) [1] is focusing on the tasks given by the Helmholtz Association (HGF). This comprises the design and preparations for the High Energy Storage Ring (HESR) of FAIR) [2] with the PANDA experiment. The on-going hadron physics program at the Cooler Synchrotron COSY exploits the internal experimental set-ups ANKE, PAX and WASA as well as TOF with the extracted beam. The new 2 MV electron cooler has arrived from the Budker Institute (Novosibirsk, Russia) at COSY and will be commissioned during the year. IKP is part of the new section “Forces And Matter Experiments” (FAME) of the Jülich-Aachen Research Alliance (JARA). This joins scientists and engineers from RWTH Aachen and Forschungszentrum Jülich for experiments, theory and technical developments for anti-matter (AMS) and electric dipole moment experiments (EDM). The institute is member of the new HGF project Accelerator Research and Development (ARD) and pursues research on various accelerator components. The future project Jülich Electric Dipole Moment Investigation (JEDI) [3] will profit from the availability of polarized beams from the injector cyclotron and the unique capabilities and experiences at the COSY facility.

CYCLOTRON OPERATION

Since 1968 the cyclotron has been operational and provided overall more than 262500 hours availability for experiments and beam development [4-6]. The fraction of the run time since start of commissioning as COSY’s injector in 1992 is shown in Fig. 1. In the first 3 years only H_2^+-beams were used for the stripping injection into the synchrotron ring. For the acceleration of polarized particles beam is provided by a source of the charge exchange type. Two negative ion sources provide beam for routine unpolarized operation [7]. Table 1 reflects the availability of the cyclotron from 2010 to August 2013.

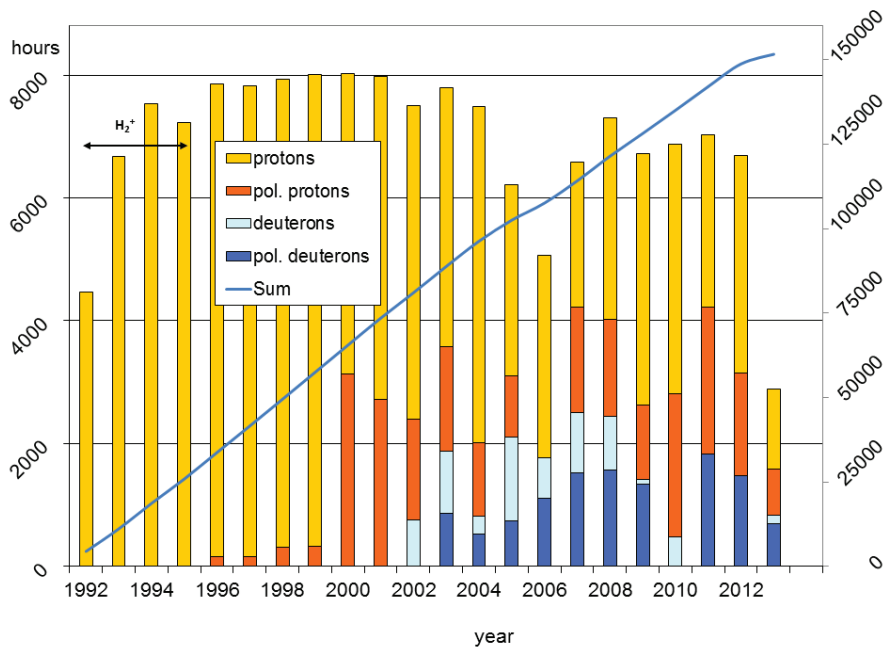

Figure 1: Provided beam hours from the cyclotron since start-up for COSY operation.

ISBN 978-3-95450-128-1

STATUS AND FURTHER DEVELOPMENT OF THE PSI HIGH INTENSITY PROTON FACILITY

J. Grillenberger, M. Humbel, A. Mezger, M. Seidel, W. Tron,
Paul Scherrer Institut, 5232 Villigen PSI, Switzerland

Abstract

The High Intensity Proton Accelerator Facility of the Paul Scherrer Institut is routinely operated at an average beam power of 1.3 MW. Since the last cyclotron conference several highlights have been achieved. The maximum current extracted from the Ring Cyclotron could be increased from 2.2 mA to 2.4 mA during several beam development shifts. Furthermore, the availability of the facility has reached its highest level to date. To even further increase the intensity the beam losses caused by space charge effects have to be reduced to keep the absolute losses at a constant level. This paper gives an overview of the measures taken to increase the beam power while ensuring a high operational reliability. Furthermore, the on-going upgrade program of the RF-system and concepts to compensate for losses caused by space charge effects are presented.

INTRODUCTION

The PSI high intensity proton accelerator facility consists of three accelerators starting with a Cockcroft-Walton type pre-accelerator and a chain of two isochronous sector cyclotrons operated at frequency of 50.6 MHz (Fig. 1). The beam is produced by extracting protons from an Electron Cyclotron Resonance (ECR) source by means of an electrostatic lens system with a voltage of 60 kV. The particles are further accelerated to a kinetic energy of 870 keV by the Cockcroft-Walton pre-accelerator and then vertically injected into the Injector 2 cyclotron. After about 80 turns in Injector 2 the beam is extracted with 72 MeV and then transferred to the Ring cyclotron. The continuous wave beam (CW) is sent to two meson production targets to produce pions and muons used for material research. The targets are realized as rotating carbon wheels of 5 mm (Target-M) and 40 mm (Target-E) thickness respectively [1]. After passing the two targets the beam is collimated and the remaining beam current of 1.55 mA is sent to a spallation target for neutron production. The target installed in the Swiss Spallation Neutron Source (SINQ) consists of a matrix of lead filled Zircaloy tubes. The neutrons produced are moderated in a heavy water tank and are then guided to 13 different user stations. Furthermore, the 590 MeV beam can be kicked towards a pulsed source for the production of ultracold neutrons (UCN) which has successfully been brought into operation in 2010 and is now routinely delivering ultracold neutrons in a pulsed mode mainly for the investigation of the electric dipole moment of the neutron.

OPERATIONAL PERFORMANCE 2012

After almost 40 years of operation, the PSI proton facility has reached its highest availability to date. In 2012 the overall availability of the facility increased from 91.5% in 2011 to 93.5% which corresponds to roughly 30% less outages. Accordingly, the integrated charge delivered to the targets has reached an all-time high (see Table 1). In Fig. 2 the development of the yearly performance of the facility during the past eleven years is shown together with the main reasons causing downtime. Furthermore, in Fig. 3 the outages exceeding 5 minutes of downtime are characterized. It can be noticed that 44% of the downtime in 2012 was caused by failures of the two meson production targets.

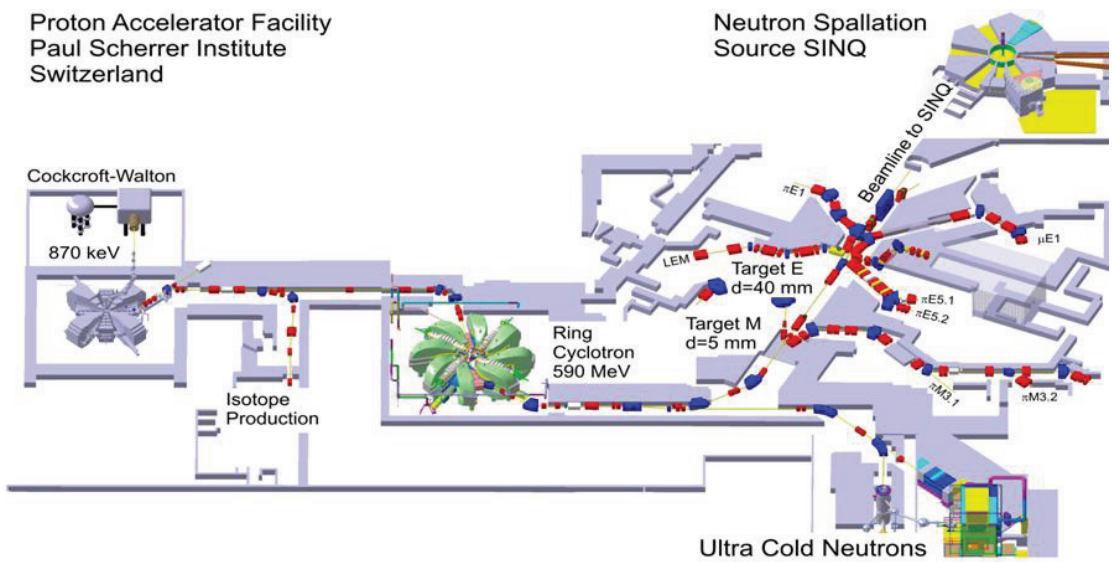

Figure 1: Overview of the PSI high intensity proton accelerator facility confining an area of 120 m × 220 m.

ISBN 978-3-95450-128-1

PRESENT STATUS OF THE RCNP CYCLOTRON FACILITY

Kichiji Hatanaka*, Mitsuhiro Fukuda, Keita Kamakura, Shunpei Morinobu, Takane Saito, Hitoshi Tamura, Hiroshi Ueda, Yuusuke Yasuda, Tetsuhiko Yorita, Research Center for Nuclear Physics, Osaka University, 10-1 Mihogaoka, Ibaraki, Osaka, 567-0047, Japan

Abstract

The Research Center for Nuclear Physics (RCNP) cyclotron cascade system has been operated to provide high quality beams for various experiments in nuclear and fundamental physics and applications. Three ion sources are in operation; atomic beam type polarized ion source, 10 GHz ECR source NEOMAFIOS and 18-GHz Superconducting ECR source. A 2.45 GHz proton source is under development to provide high brightness proton beams. There have been increasing demands for heavy ion beams. A supplementary budget was approved for the restoration of aging facility. Several equipments are under fabrication and the installation will be performed during January and March in 2014.

OPERATION OF THE FACILITY

The RCNP cyclotron facility consists of an accelerator cascade and sophisticated experimental apparatuses. Research programs cover both pure science and applications. Demands for industrial applications have been growing more and more. A schematic layout of the RCNP cyclotron facility is shown in Fig. 1. The accelerator cascade consists of an injector Azimuthally Varying Field (AVF) cyclotron (K=140) and a ring cyclotron (K=400). The maximum energy of protons and heavy ions are 400 and 100 MeV/u, respectively. Figure 2

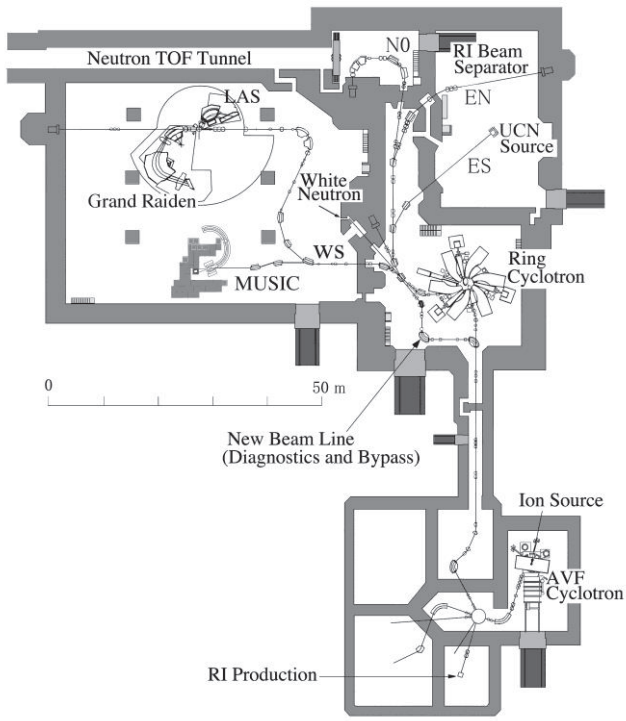

Figure 1: Layout of the RCNP cyclotron facility.

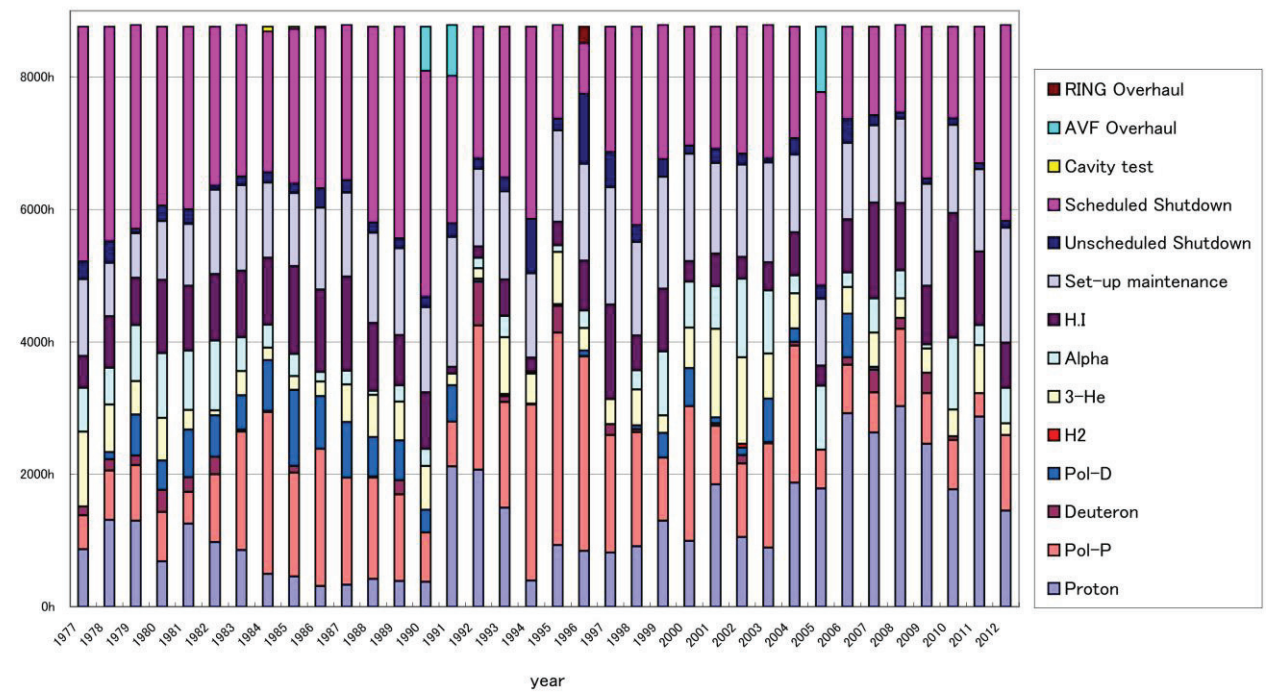

Figure 2: Operating statistics of the RCNP cyclotron facility..

*hatanaka@rcnp.osaka-u.ac.jp

ISBN 978-3-95450-128-1

RECENT PROGRESS AT THE JYVÄSKYLÄ CYCLOTRON LABORATORY

P. Heikkinen, JYFL, Jyväskylä, Finland

Abstract

The Jyväskylä K130 cyclotron has been in use since 1992. It has been used mainly for nuclear physics research but also for applications, such as radioisotope production, space electronics testing and membrane production.

The MCC30/15 cyclotron delivers proton and deuteron beams for nuclear physics research and for isotope production. The experimental set-up has been mainly under construction and so far we have had only a couple of beam tests. Isotope production with the MCC30/15 cyclotron has suffered from severe administrative delays. Finally in December 2012 a preliminary budget study for a GMP laboratory for FDG production (18F) was done. Decisions on the radiopharmaceuticals production at JYFL will be done during 2013. The beam quality dependence on the stripper angle has been studied. The preliminary results will be given.

THE K130 CYCLOTRON

Statistics

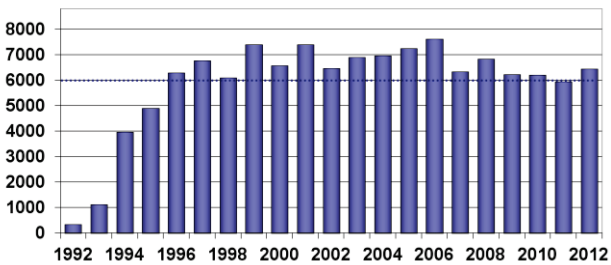

Figure 1: Use of the K130 Cyclotron. The total run time is 124’138 hours at the end of 2012.

The use of the K130 cyclotron during the past few years has been normal. The total use of the cyclotron in 2012 was 6441 hours out of which 4610 hours on target. Three quarters of the beam time was devoted to basic nuclear physics research and one quarter for industrial applications, the main industrial application being space electronics testing. Altogether over 20 different isotopes were accelerated in 2012. Beam cocktails for space electronics testing were the most commonly used beams (26 %). Since the first beam in 1992 the total run time for the K130 cyclotron at the end of 2012 was 124’138 hours, and altogether 32 elements (73 isotopes) from p to Au have been accelerated.

THE MCC30/15 CYCLOTRON

The MCC30/15 Cyclotron, manufactured and installed by the Efremov Institute, St. Petersburg, Russia, was accepted for use in May 2010. However, the re-installation and upgrade of the experimental setup (IGISOL) was still going on, and so far only a few beams have been accelerated by the MCC30/15 cyclotron for experiments and tests.

The emittance of the extracted beam has been measured by a gradient method, i.e. measuring the beam size as a function of quadrupole magnet focusing strengths and finding the emittance and the Twiss parameters by an rms-fit.

The Emittance Measurement Method

The transfer matrix of a beam line gives the position and direction of a particle at the end of the beam line when the initial position and direction is known according to matrix equation

$$\begin{pmatrix} x \\ x' \end{pmatrix}_1 = \begin{pmatrix} C & S \\ C' & S' \end{pmatrix} \begin{pmatrix} x \\ x' \end{pmatrix}_0. \quad (1)$$

The matrix elements above can be used to write a 3x3 transfer matrix for the Twiss parameters as

$$\begin{pmatrix} \beta \\ \alpha \\ \gamma \end{pmatrix}_1 = \begin{pmatrix} C^2 & -2CS & S^2 \\ -CC' & CS' + SC' & -SS' \\ C'^2 & -2C'S' & S'^2 \end{pmatrix} \begin{pmatrix} \beta \\ \alpha \\ \gamma \end{pmatrix}_0, \quad (2)$$

and then the square of the beam half-width at the end of the beam line can be written as

$$\hat{x}^2 = \epsilon\beta_1 = \varepsilon(C^2\beta_0 - 2CS\alpha_0 + S^2\gamma_0), \quad (3)$$

where

$$\gamma = \frac{1+\alpha^2}{\beta}. \quad (4)$$

The transfer matrix elements (C, S, C', S') as functions of the quadrupole magnet strengths (or currents) can be calculated by a linear ion optics program. Measuring the beam sizes (horizontal and vertical) with several different quadrupole settings we get the Twiss parameters and the emittance by an rms-fit.

Measuring Results

The beam transverse emittances were determined in the beam line at the entrance of the first quardrupole magnet. The beam line consists of a quadrupole doublet and a drift. At the end of the beam line the beam size was determined from a scintillation plate with a ccd-camera. First the smallest beam spot was found experimentally and then the quadrupole strengths were varied around these values, and the horizontal and vertical beam diameters were recorded. From the series of quadrupole settings and beam half-widths we get vectors *x(i)*, *C(i)*

ISBN 978-3-95450-128-1

PRESENT STATUS OF CYCLOTRONS (NIRS-930, HM-18) AT NIRS

Satoru Hojo#, Akinori Sugiura, Ken Katagiri, Masao Nakao, Akira Noda, Koji Noda,
NIRS, Chiba, Japan
Yuichi Takahashi, Takanori Okada, Akihito Komiyama, Toshihiro Honma, AEC, Chiba, Japan

Abstract

The cyclotron facility at National Institute of Radiological Science (NIRS) consists of a NIRS-930 cyclotron (Thomson-CSF AVF-930, Kb=110 MeV and Kf=90 MeV) and a small cyclotron HM-18(Sumitomo-Heavy- Industry HM-18, K=20 MeV). The NIRS-930 has been used for production of short-lived radio-pharmaceuticals for Positron Emission Tomography (PET), research of physics, developments of particle detectors in space, and so on. The orbit of a beam in the NIRS-930 cyclotron was simulated with integrated approach for modelling of the cyclotron, including calculation of electromagnetic fields of the structural elements. And some improvements such as installation of extracted beam probe, a beam attenuator and a beam viewer in an injection beam line, were performed in the NIRS-930. The HM-18 has been used for production of short-lived radio-pharmaceuticals for PET. It provides us accelerated H^- and D^- ions at fixed energies of 18 and 9 MeV, respectively. In order to improve the isochronisms, a phase probe has been newly installed in the HM-18. Operational status of the cyclotron facilities and their improvements are to be presented in this report.

INTRODUCTION

There are two cyclotrons, the NIRS-930 and the HM-18, in the cyclotron facility at the NIRS (Figure 1). These two cyclotrons are installed in the same room. The NIRS-930 (Km=110 MeV, Kf=90 MeV) was installed for the main purpose of clinical trial of radio-therapy with fast neutron in 1974. After that, the main purpose of the NIRS-930 changed to proton radiotherapy and has shifted to RI manufacture for molecular imaging. The HM-18(K=20) cyclotron is a negative-ion accelerator that was purchased from Sumitomo Heavy Industry, Ltd. The HM-18 has been operating routinely to produce short-lived radio-pharmaceuticals for PET in conjunction with a heavy ion therapy at HIMAC (Heavy Ion Medical Accelerator in Chiba) since 1994[1].

OPERATION

The NIRS-930 and the HM-18 are operated only during the daytime (9:00-17:00) of weekday, and the NIRS-930 is operated twice per month also on Saturday.

For maintenance, there are three weeks and two weeks shutdowns in summer and spring, respectively. The annual operation time last year of the NIRS-930 is shown in Table.1. The planned operation time was 1648 h, which is multiplication of the days of a scheduled experiment by 8 hours. On the other hand, actual operation time was 1936 h at NIRS-930. The half of the operation time of experiment was used for RI production for radiopharmaceutical products including ^{11}C, ^{18}F, ^{28}Mg, ^{64}Cu, ^{62}Zn, ^{124}I. The other purposes are nuclear and atomic physics experiments, a radiation damage tests with charge beam time fee, studies on radiation damage of material and an electronic device by particle beam or fast neutron, biological experiments, and studies on radiation dosimetries for space radiation. Unscheduled beam stop time by failure was 11 hour; it was 1.8% of total operation time, which was composed of failures in vacuum system, vacuum tube in amplifier of radio frequency system, a current meter for beam monitoring, and human error.

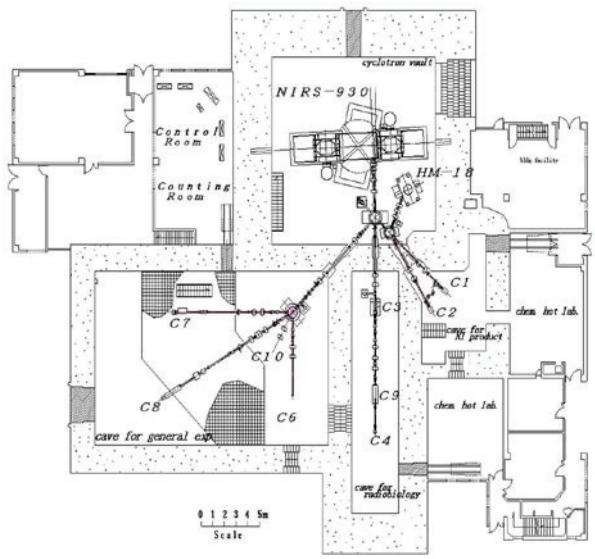

Figure 1: Layout of NIRS cyclotron facility.

Table 1: Annual Operation Time of the NIRS-930 (2012)

Planned time of operation		**1648 h**
Operation time	**Total**	**1936 h**
1. Experiment		1350 h
2. Tuning operation and machine studies		552 h
3. Beam time cancel by operation side *		24 h
4. Unscheduled beam stop by failure		11 h
1 Experiment summary		
RI productions		686 h
Nuclear and atomic physics experiments		304 h
Radiation damage tests (with charge beam time fee)		176 h
Studies on radiation damaged		91 h
Biological experiments		64 h
Studies on radiation dosimeters		29 h

ISBN 978-3-95450-128-1

ON-GOING OPERATIONS WITH THE CYCLOTRON C70 ARRONAX

F. Poirier, S. Girault, Arronax, Saint-Herblain, and IN2P3/SUBATECH, Nantes, France
X.Goiziou, F. Gomez, L.Lamouric, J.Orsonneau, L. Perrigaud, D. Poyac, H.Trichet, Arronax, Saint-Herblain, France
C. Huet, Arronax, Saint-Herblain, and EMN, Nantes, France
E. Mace, Arronax, Saint-Herblain, and INSERM, Nantes, France
N. Varmenot, Arronax, Saint-Herblain, and ICO, Saint-Herblain, France

Abstract

The multi-particle cyclotron C70 Arronax, located at Nantes, France is used to accelerate non- concurrently four types of particles downstream several beamlines. The particle energy and intensity range of the cyclotron has allowed a wide variety of application including radiolysis, neutron and isotope productions, and physics experiments. Also regular operations are performed both with dual beam runs at 2x100 µA for isotope production and at 350 µA for neutron production using 70 MeV proton beams. At low intensity, 70 MeV alpha beam is one distinctive feature of the machine with the possibility to use pulsed beam with variable time between two consecutive bunches. The status of the machine is presented as well as the operational updates on the beamlines, including the alpha particle pulsing system, the newly installed alpha degrader and beam loss monitor being developed for high intensity runs.

INTRODUCTION

The cyclotron Arronax [1] (Accelerator for Research in Radiochemistry and Oncology at Nantes Atlantique), running since 2010, the year of its commissioning, has started in 2011 its hands-on phase. This phase includes, particularly, ramping up the intensity on targets, constitution and optimization of beams for users, as well as issuing the safety of the machine and targets. It is a phase which is being scheduled into regular uses of separated low and high intensity beam periods.

The cyclotron delivers beams separately in six vaults surrounding the main cyclotron vault. In addition to the cyclotron and magnet systems, the main vault houses two particle sources, an injection line, both of which are located on top of the cyclotron, and the secondary water cooling systems used for irradiation stations and faraday cups e.g., distribution manifolds, de-ionisation columns, and pumping. An adjacent room accommodates other technical systems such as vacuum reading devices, source power supplies, and the primary water cooling system. Several upgrades are being studied for Arronax that will use the adjacent room.

C70 ARRONAX

The multiparticle isochronous cyclotron is based on 65 kV RF cavities with a frequency of 30.45 MHz. The maximum radius for the accelerated particles is of the order of 1.2 m with an average hill magnetic field of ~1.6 T. Without beam loading, the RF power is 20 kW. The characteristics of the beam for the four types of particles (proton, alpha, deuterons, HH+) are given in [2].

THE MACHINE OPERATION AND STATUS

The cyclotron has accumulated, over the first 8 months of 2013, 2000 hours RF equivalent time. The high intensity runs in dual-mode have increased to an average intensity on each target of 100 eµA for radioisotope production and several runs have been performed on the neutron activator at 350 eµA for more than 22 hours.

In addition to the existing ones, new beams have been optimized for users which expand the possible use to beamlines and energies, particularly close to the limits of the machine. Great care on the optimization procedure has been applied, relying first on dual-mode optimization when possible (H+ and D+) and second on machine intensity radial scans as discussed later in this paper. Table 1 gives some of the new possibilities.

Table 1: New Optimised Beams at Arronax

Extracted Particles	Energy (MeV)	Beamlines Name
H+	30	Ax1/P1
D+	16	A1/P3/A2/P2
D+	34	Ax
He2+	67.5	Ax5

So far, the best transmission rates measured from the injection down to the end-station are of the order of 30% for protons, 24% for deuterons, and 10% for all other particles. In terms of intensity, the highest losses are at the beginning of the acceleration within the cyclotron (for radius <200 mm) and in some specific locations in the beamlines. The beamline transport strategy described in [2] is focusing on minimizing these later losses.

Arronax has performed regular runs over several days at approximately 2x100 eµA with protons sent simultaneously in two beamlines. A sample of one run is shown in Fig. 1. This sample is 80 hours long and illustrates a very stable run. The mean current on target is $\langle I \rangle$=101.2 eµA with $\sigma_{\langle I \rangle}$=5.3 eµA. Breakdowns are approximately 1.3% of the overall time. For this particular sample the vacuum in the center of the machine is 4×10^{-7} mbar. The neutral current (H^0), mainly due to

ISBN 978-3-95450-128-1

VARIETY OF BEAM PRODUCTION AT THE INFN LNS SUPERCONDUCTING CYCLOTRON

D. Rifuggiato, L. Calabretta, L. Cosentino, G. Cuttone, INFN LNS, Catania, Italy

Abstract

The INFN LNS Superconducting Cyclotron has been operating for almost 20 years. Several beams are currently accelerated and delivered, allowing for a wide variety of experimental activity to be carried out. In addition, clinical activity is regularly accomplished: over 11 years of proton-therapy of the eye pathologies, around 300 patients have been treated. This has stimulated a growing number of interdisciplinary experiments in the field of radiobiology and dosimetry. On the side of nuclear physics, a significant achievement is the production of radioactive beams: several rare isotopes are produced mainly exploiting the in-flight fragmentation method. The development activity carried out on several components of the user oriented facility will be described.

THE SUPERCONDUCTING CYCLOTRON

The LNS Superconducting Cyclotron is a three sectors compact machine [1], see the median plane in Fig. 1.

Figure 1: View of the median plane of the LNS Superconducting Cyclotron.

Beam Production

A considerable amount of beam types have been developed in the 19 years of operation. Almost the whole operating diagram has been covered: for fully stripped light ions (Q/A=0.5) the maximum energy achieved is 80 AMeV, 100 AMeV being the nominal one, concerning the heaviest ions the best performance has been reached with a ^{112}Sn 43.5 AMeV beam and a ^{197}Au 23 AMeV beam.

Reliability has been regarded as one of the most important features of the machine through the whole operation period. Particular attention has been paid to the most critical subsystems, from which most of the failures were originated: radiofrequency, electrostatic deflectors, ion sources and cryogenics. In particular, concerning radiofrequency, aluminum dees were replaced with copper dees and coupler insulators were redesigned; at present, we are considering the problem of obsolescence of the first stage valves in the RF power amplifiers: new tetrodes will replace the present ones, no longer produced, therefore some upgrade of the amplifiers will be necessary. The improvements introduced to the electrostatic deflectors and ion sources are described in the next subsections. Cryogenics are also discussed in a separated subsection.

As a consequence, the annual number of hours of failures, that at the beginning of the Cyclotron operation was a percentage as big as 20% of the hours of delivered beam, was significantly reduced by a factor 10 in the best case, so increasing a lot the accelerator efficiency and allowing for a more dense experimental activity. At present, the maximum annual number of beam hours on target ranges from 3000 to 3500 hours.

The annual number of hours necessary for beam preparation is a quite high fraction of the delivered amount, i.e. from a minimum of 25% to a maximum of 50%, depending upon the number of beam types to be developed: the accelerator operation is not an easy procedure due to the compactness of the machine, which implies a poor diagnostic equipment, and to the accelerator versatility, i.e. its wide operating diagram.

Cyclotron beams are used for research in nuclear physics, mainly multi-fragmentation and nuclear structure, for interdisciplinary experiments, mainly in the field of beam interaction with biological matter and of radiation damage of electronic components, and for proton-therapy of the eye pathologies. A section of this paper is dedicated to proton-therapy. The beam distribution among these three activities is variable from year to year, depending upon the beam requests from users, that are evaluated once per year by a Scientific Committee appointed by the INFN President. In Table 1 the beam time distribution is reported for the years 2009 to 2012. The increasing trend of the applicative research is quite evident.

Table 1: Beam Time Distribution from 2009 to 2012

Year	Nuclear physics	Inter disciplinary	Proton-therapy
2009	63%	23%	14%
2010	44%	33%	23%
2011	32%	48%	20%
2012	34%	39%	27%

ISBN 978-3-95450-128-1

PROGRESS AT VARIAN'S SUPERCONDUCTING CYCLOTRONS: A BASE FOR THE PROBEAM™ PLATFORM

H. Röcken, M. Abdel-Bary, E. Akcöltekin, P. Budz, M. Grewe, F. Klarner, A. Roth, P. vom Stein, T. Stephani, Varian Medical Systems Particle Therapy GmbH, Bergisch Gladbach, Germany

Abstract

During the last 9 years, Varian's superconducting isochronous ProBeam™ medical proton cyclotrons proved their matureness when they accumulated more than 20 operational years at factory testing and patient treatment without any unscheduled down time caused by quenches or failures of the cryogenic supply systems. Their reliable superconductive technology features a fast initial cool-down and low operating costs. Besides the two machines which are in clinical operation in Switzerland and Germany, one more ProBeam™ cyclotron is already fully commissioned and delivering a 250 MeV proton beam at Scripps Proton Therapy Center in San Diego, USA. Several other ProBeam™ cyclotrons are under fabrication or in the phase of factory beam acceptance tests. We report on fast cool-down and time-to-beam-extraction achievements as well as on the latest status and operational experience with Varian's ProBeam™ cyclotrons. Additionally, we give an insight in new developments for further reduction of commissioning time and improvement of reliability.

INTRODUCTION

The driver of Varian's ProBeam™ Proton Therapy Platform is the 250 MeV superconducting (SC) cyclotron, which was already described in previous articles [1]. Since ProBeam™ Cyclotron #3 (delivered to Scripps Proton Treatment Center (SPTC), San Diego) we have the opportunity to pre-commission our cyclotrons with beam in a test cell of our production facility near Cologne (Germany). Up to date, we factory commissioned one more cyclotron (#4, to be shipped to customer site by November, 2013) and the next one (#5) is already moved into the test cell for RF and beam commissioning. Assembly of cyclotron #6 is running and at cyclotron #7 the coil winding is finished and the iron is already in the factory.

The production facility was set up to enable the production of three cyclotrons per year with the possibility of further ramp up.

CYCLOTRON COOL-DOWN

After final assembly and prior to beam commissioning, the cyclotron SC coils are cooled down to liquid helium temperature of 4.2 K on an assembly stand in our productions halls. In order to cool down from room temperature, around 160 MJ heat energy must be carried away from the cryostat. To remove this heat energy by using liquid helium (LHe), around 50.000 liters would be needed. Therefore we apply the reliable and more economical standard solution of cooling down not directly by LHe but via an intermediate step using liquid nitrogen (LN_2), which has a latent heat of evaporation ≈54 times higher than LHe. Cooling down the SC coils from room temperature to LN_2 temperature (77 K) by filling the vessel around the coils takes around 1.400 liters of LN_2. The system is then given some time to thermally settle before the LN_2 is expelled out. A thorough processing has to be followed to avoid any nitrogen freezing when starting the final cooling with LHe. This step then needs only around 1.000 liters of LHe.

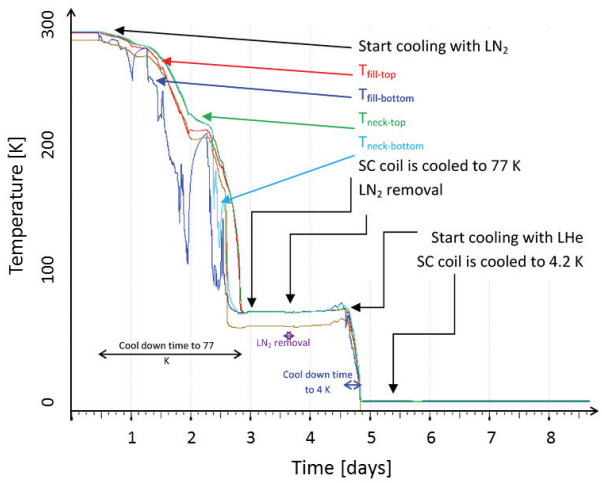

Figure 1: Cool down time of the SC coils from room temperature (300 K) to the LN2 temperature (77 K) and further to LHe temperature (4 K).

In this way the cool down process of the SC coils needs effectively only around 5 days (see Fig. 1), whereas for dry-cooled systems it could easily take several weeks. The time is an important factor because cooling of massive materials cannot be forced. The coils need time to be homogeneously and smoothly cooled to be protected from mechanical stresses due to the different shrinking coefficients at different temperatures all over the coils and LHe vessel. After completing the cyclotron cool-down process, the SC coils can directly be energized to excite the required magnetic field for the mapping and shimming process.

RF COMMISSIONING

After shimming the cyclotron is moved in cold state into the test cell on an air film mover (see Fig. 2). Prior to beam commissioning the RF resonator has to be conditioned. Within approx. 100 h of pulse and cw RF operation, the RF power is stepwise increased to its operational value of nearly 120 kW.

ISBN 978-3-95450-128-1

STATUS REPORT ON THE GUSTAV WERNER CYCLOTRON AT TSL, UPPSALA

D. M. van Rooyen[1], B. Gålnander, M. Lindberg, T. Lofnes, T. Peterson, M. Pettersson
The Svedberg Laboratory, Uppsala University, Box 533, S-75121, Uppsala, Sweden.

Abstract

TSL has a long history of producing beams of accelerated particles. The laboratory was restructured in 2005/2006 with nuclear physics phased out, the CELSIUS ring dismantled and the WASA detector moved to Jülich. The focus of activities became thereby shifted towards, mainly, proton therapy and, in addition, testing of radiation effects using protons and neutrons in a beam sharing mode. The increase in demand on (a) beam time, and (b) consequential faster changes between various set-ups, necessitated some minor upgrades. For the same reason our energy measuring system needed to be streamlined. As a consequence of the restructuring, night shifts were phased out. By switching off certain power supplies overnight a substantial energy saving has been accomplished.

INTRODUCTION

The Gustaf Werner cyclotron, completed in the early 1950s as a fixed-energy 185 MeV proton synchro-cyclotron, was converted to a variable-energy multi-purpose sector-focused cyclotron during the 1980s. Since this upgrade the accelerator is operated both as an isochronous cyclotron and as a synchrocyclotron. Further details can be found in Ref. [1],[2],[3].

Currently the principal users are the proton therapy facility of the Uppsala University Hospital and the irradiation facilities at TSL which provides neutrons and proton beams for science and accelerated electronics testing for industry. [4]. Heavy ions are available from an ECR ion source of an older generation (6.4 GHz) which was upgraded in 2002 in collaboration with JYFL [5].

In this paper we discuss the general status of our facility and describe concluded and ongoing improvements, new developments and conclude with some comments regarding TSL's future.

OPERATIONAL STATISTICS

User and User Statistics

As a result of the restructuring of TSL in 2005/2006 proton therapy has become our primary user with, on average, 36 weeks of patient treatment per year. Our main secondary user is the TSL irradiation facility. As reported earlier [3] the beam is shared between the primary and secondary users. In this beam-sharing mode proton therapy has command over the destination of the beam. Whereas patient treatments are of rather short duration, the beam is mostly available for users at the irradiation facility. Naturally there is then a limitation to the beams available to secondary users, namely being 180 MeV protons. Whereas the latter is the highest proton energy reachable with the Gustav Werner accelerator, this is the beam used for proton therapy treatments.

Although varying from year to year, an approximate number of beam time hours delivered to the Blue Hall irradiation facility is ca 1000 hours per year.

Scheduled Beam Time

Since 2006 beam is scheduled weekdays 06:00 – 18:00 compared to 24-hour shifts, 6 days/week, previously. However, in the recent four years, requested beam time has increased to such an extent that some weeks needed to be scheduled to 22:00 / 24:00 and others having a night shift.

Beams of Interest to our Users in Recent Years

The fact that our primary user (proton therapy) determines our beam and energy as 180 MeV protons – and does so for a large part of a year (Figure 1), unfortunately excludes being more versatile and run other energies and particles. It thus became virtually impossible to use our cyclotron to its full potential.

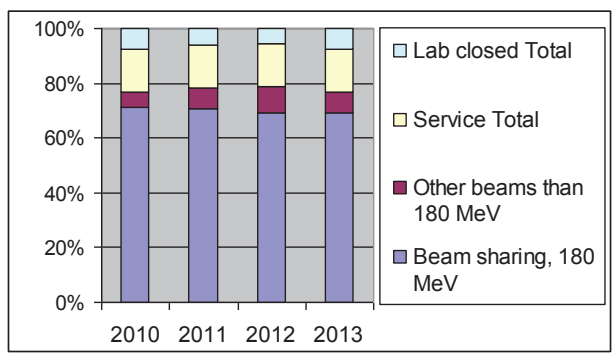

Figure 1: Distribution of total annual hours.

Table 1: Beams of Interest for Current Users other than 180 MeV p

Year	Week number	Mode	Particle	Total energy (MeV)
2010	14	CW	p	25; 50; 100
	19	CW, ECR	Ar9+	400
2011	08	CW	p	25; 50; 80
	15	CW, ECR	C6+; Ar9+	470; 400
	25	CW	p	50; 100
		FM	p	150
	33	CW, ECR	C6+; Ar9+	470; 400

[1] Corresponding author: daniel.vanrooyen@tsl.uu.se

ISBN 978-3-95450-128-1

INSTALLATION AND TEST PROGRESS FOR CYCIAE-100

Tianjue Zhang, Shizhong An, Hui Yi, and Yang Feng, Technology Division of BRIF,
China Institute of Atomic Energy (CIAE), Beijing 102413, P.R. China

Abstract

The 100 MeV high intensity compact cyclotron CYCIAE-100 being built at CIAE adopts an external ion source system, accelerates H- ions up to 100 MeV and provides dual proton beams simultaneously be stripping. The ground breaking ceremony for the building was conducted in April, 2011. Then in September of 2012, the major systems for the machine, including the 435-ton main magnet, two 46.8 kAT exciting main coils, 200-ton hydraulic elevating system with a precision of 0.02 mm, high precision magnetic mapper, the 1.27 m high vacuum chamber with a diameter of 4.08 m, two 100 kW RF amplifiers, magnet power supplies with a stability better than 20 ppm in the power range between 50% and 100%, and water cooling system etc., have been in place for installation.

The paper will demonstrate the results of high precision machining and installation of large scale magnet, magnetic mapping and shimming under the condition with vacuum deformation, study on the multipacting effects under the fields in compact magnet valleys and RF conditioning. The test results for the 18 mA H- ion source and injection line as well as the 2 m long cryopanel and vacuum system will also be presented. The first beam for CYCIAE-100 is scheduled in the latter half of 2013.

INTRODUCTION

The Beijing Radioactive Ion-Beam Facility (BRIF) will be mainly used for productions of intense proton and radioactive ion beam (RIB) in fundamental and applied research, e.g., neutron physics, nuclear structure, material and life sciences and medical isotope production. For this project, a 100 MeV H- cyclotron (CYCIAE-100) with external ion source is selected as the driving accelerator, which will accelerate H- ions and provide dual proton beams of 75 MeV ~ 100 MeV with an intensity of 200 μA ~ 500 μA simultaneously extracted by stripping. In total 7 target stations will be built based on CYCIAE-100 for the fundamental and applied researches. Figure 1 shows the layout of BRIF.

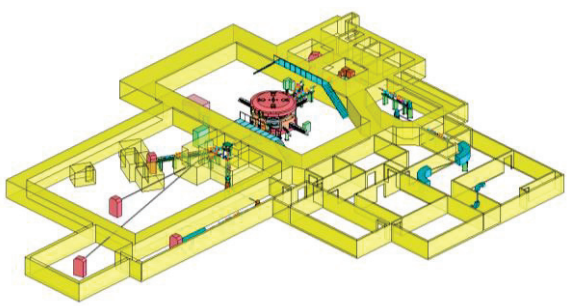

Figure 1: Layout of BRIF.

The status at different stages, including the preliminary design, technical design and construction preparation, as well as progress, has been reported at previous cyclotron conferences [1],[2],[3]. The key parts for CYCIAE-100 have been installed and tested in the main building, such as main magnet, RF cavities, RF amplifiers, main vacuum system, power supplies, etc. The main magnetic mapping and shimming on CYCIAE-100 has been finished. Most of parts testing including RF amplifiers, H- ion source, injection and extraction system, as well as main vacuum system have been finished. The beam commissioning will be started soon and scheduled to get beam in 2013.

MAIN BUILDING OF BRIF

The construction of the main building started on April 28, 2011 and the roof was sealed on January 16, 2012. The on-site installation conditions for the main devices and systems of accelerator have been ready since September 27, 2012. Figure 2 shows the main building.

Figure 2: Main building of BRIF.

MAIN INSTALLATION AND TEST PROGRESS FOR CYCIAE-100

Main Magnet System Installation, Mapping and Shimming

The main magnet of CYCIAE-100 consists of 2 top/bottom yokes, 4 return yokes, 8 poles, 16 shimming bars and 2 central plugs. It is 6160 mm in diameter and 3860 mm in height. The largest single piece weighs 169 tons. The 435-ton main magnet is installed at the cyclotron vault 4 m underground. The installation precision should be better than 0.20 mm in the direction of height and the azimuthal error is required to be no more than 0.50 mm. On the west wall of the building a horizontal hole of 7 m wide and 6 m high is reserved, through which all the parts of the main magnet will be moved into the building. Due to the 4 m height difference between the inside and outside of the building, a steel structure platform is specially made and installed at the inside of the hole with a load bearing of 200 tons. The

ISBN 978-3-95450-128-1

PLAN OF A 70 MEV H- CYCLOTRON SYSTEM FOR THE ISOL DRIVER IN THE RARE ISOTOPE SCIENCE PROJECT

Jongwon Kim#, Yeon-gyeong Choi, Seong-gwang Hong, Jaehong Kim,
Rare Isotope Science Project (RISP), Institute of Basic Science (IBS), Daejeon, Korea

Abstract

A 70 MeV H- cyclotron system has been planned for the rare isotope science project (RISP) in Korea mainly to be used as ISOL driver. The proton beam will be also used for the nuclear and neutron science programs and a maximum beam current requested is 1 mA. A commercial cyclotron with two extraction ports is planned for the facility, and the beam distribution lines have been designed considering some aspects of radiation shielding. The injection beam line has been studied to produce a pulsed beam in the range of 0.01-1 MHz for neutron users to utilize a time of flight technique. A chopper and collimator system is thought as a feasible scheme for beam pulsing. The cyclotron is scheduled to produce a first beam in 2017.

INTRODUCTION

An ISOL facility is planned in the rare isotope science project underway in Korea, in which both ISOL and in-flight fragmentation methods will be utilized [1]. The ISOL driver accelerator is 70-MeV H- cyclotron, whose energy can be varied in the range of 35-70 MeV with a beam current of up to 1 mA. A layout of the ISOL facility is given in Fig. 1, in which two target stations will be installed. A main target material is UC_x to utilize ^{238}U fission reactions. The SPES project of INFN in Italy preciously adopted a similar facility layout including two target stations [2].

An H- cyclotron commercially available will be procured, which is often used to produce radioisotopes for nuclear medicine [3, 4]. Main cyclotron parameters are listed in Table 1. The extracted beam current of 1 mA by electron stripping at 70 MeV has not been tested before. The lifetime of the foil, which is relatively well known in the range of 0.5 mA, cannot be clearly extrapolated to 1 mA. We have studied the dependence of foil lifetime upon its thickness using a high-power electron beam as described in ref. [5]. The electron beam can be used to simulate thermal stress, which is produced by secondary electrons when H- hits a carbon foil. However, it does not simulate radiation effects by proton itself. The current result indicates there is an optimal foil thickness, at which the foil temperature is minimum.

The primary use of the cyclotron will be to provide a cw beam for the ISOL target. The initial target design will be for the beam power of 10 kW and then for 35 kW. A pulsed proton beam has been also considered for the users to apply a technique of time of flight in using mono-energy neutron beams. Beam optics for the injection beam line was studied to produce pulsed beams in the range from 0.01 MHz to 1 MHz with a fast chopper system.

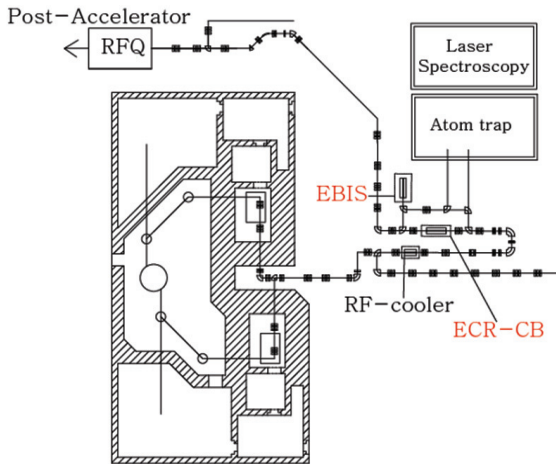

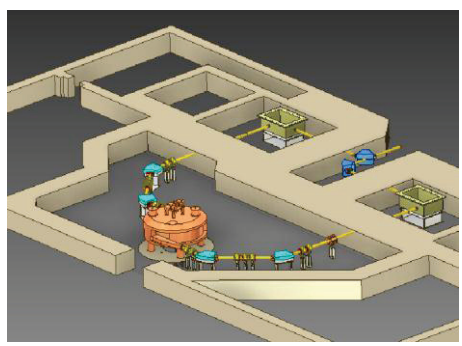

Figure 1: Upper: Layout of the ISOL facility, Lower: view of the cyclotron facility in the RISP.

Table 1: Main Cyclotron Parameters

Item	Value
Beam energy range	35 – 70 MeV
Max. beam current	1 mA
Pulsed beam (option)	0.01 – 1 MHz
Extraction port number	2
Beam size at target	ϕ45 mm
Beam emittance	5 π mm mrad

* Work supported by Rare Isotope Science Program (RISP) through the National Research Foundation of Korea (NRF) funded by Ministry of Science, ICT and Future Planning (MSIP) (2011-0032011).
# jwkim@ibs.re.kr

CONFIGURABLE 1 MeV TEST STAND CYCLOTRON FOR HIGH INTENSITY INJECTION SYSTEM DEVELOPMENT

F. Labrecque, F. Grillet, B.F. Milton, LAC. Piazza, M. Stazyk, S. Tarrant, BCSI, V6P 6T3, Vancouver, Canada
L. Calabretta, INFN-LNS, Catania, Italy
J. R. Alonso, D. Campo, MIT, Cambridge, MA 02139, USA
M. Maggiore, INFN-LNL, Legnaro, Italy

Abstract

In order to study and optimize the ion source and injection system of our multiple cyclotron products, Best® Cyclotron Systems Inc. (BCSI) has assembled in its Vancouver office a 1 MeV cyclotron development platform.

To accommodate different injection line configurations, the main magnet median plane is vertically oriented and rail mounted which also allows easy access to the inner components. In addition, the main magnet central region is equipped with interchangeable magnetic poles, RF elements, and inflector electrodes in order to replicate the features of the simulated cyclotrons.

Multiple diagnostic devices are available to fully characterize the beam along the injection line and inside the cyclotron.

This paper will describe the design of two system configurations: the 60 MeV H_2+ for the DAEδALUS [1,2,3] experiment (MIT, BEST, INFN-LNS) and the BCSI 70 MeV H^- cyclotron.

INTRODUCTION

Over the last decade there has been an important increase in demand for medical radioactive isotopes production. BCSI has a goal to create a line of cyclotrons of differing energies and intensity specific to the isotope production needs of the customer.

Since each system has different cost, efficiency and ease of use requirements for the ion source and injection line, a development platform was assembled in Vancouver to study and optimize beam injection into the appropriate central region. The test stand consists of a fixed high voltage enclosure housing the ion source and a vertically oriented 1 MeV cyclotron mounted on rails to allow various injection line lengths. Other features include interchangeable magnetic poles, RF components, and beam optics, multiple diagnostic devices and a RF system with variable power and frequency.

Construction of the test stand started in November of 2012 and it has been operational since April 2013. The first injection system tested was for a 60 MeV H_2^+ cyclotron for the DAEδALUS experiment in collaboration with MIT and INFN-LNS followed by a 70 MeV H^- cyclotron.

TEST STAND

All elements of the injection system, as well as both halves of the main magnet, are sitting on 6 meter long rails allowing variable injection line configurations. Located at the far right end of the rail (not shown in the figure) is the high voltage enclosure which contains the ion source, its power supplies, and a 25 kW insulation transformer. Located in an insulated rack, the power supplies can be floated up to 40 kV.

An extraction system was not included in the cyclotron design. Instead, the 1 MeV beam is dumped into a copper beam stop bolted onto one of the magnet pole hill.

Main Magnet

Weighing over 7 tons, the four sectors steel structure and both coils of the main magnet are responsible for the creation of the magnetic field. The target field of each platform is achieved through a combination of coil current adjustment and interchangeable elements of the magnetic structure (shims and centre plugs). The different components of the main magnet are shown in Fig. 1.

Having both halves of the cyclotron mounted on a rail facilitates access to its inner components.

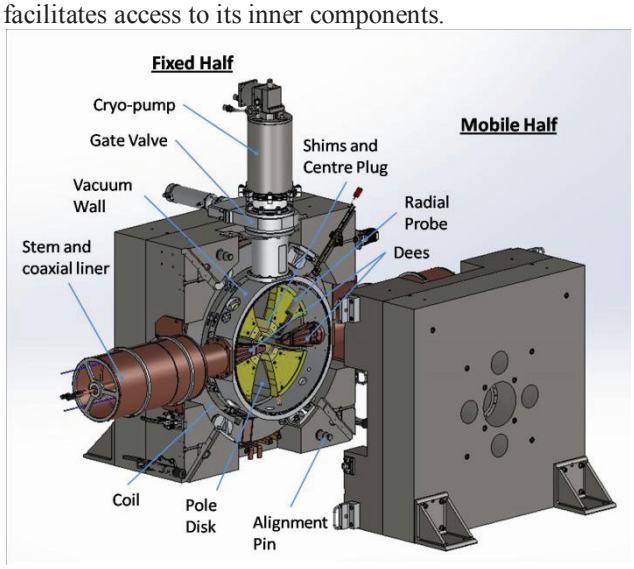

Figure 1: 1 MeV test stand cyclotron and its main components.

Magnetic Field Mapping

To confirm that the target field is reached, a map of the relevant region is made using a temperature compensated hall probe mounted to a dual axis driving system.

Starting with oversized shims and centre plug, the target field is achieved by incremental machining of these elements, followed by field mapping.

ISBN 978-3-95450-128-1

END-TO-END 6-D TRACKING USING EMMA ON-LINE MODEL*

François Méot, BNL C-AD, Upton, New York, USA
David Kelliher, Shinji Machida, Ben Shepherd, STFC/RAL/ASTeC, Chilton, UK

Abstract

Simulation of end-to-end 6-D acceleration over a complete cycle in the prototype linear FFAG EMMA is described. It uses the on-line model code, Zgoubi, and a specific input data file developed in that aim. The optical sequence starts at the entrance of the injection septum, followed by EMMA ring, and ends at the exit of the extraction septum. It includes the injection and extraction kicker pairs and accounts for the time dependence of the septum and kicker fields. This software tool aims at allowing data analysis, following experimental data taking at EMMA.

INTRODUCTION

The Electron Model for Many Applications, EMMA, a 10–20 MeV fixed field alternating gradient ring built at the Daresbury Laboratory, UK, has achieved experimental demonstration of the linear non-scaling FFAG principle and of the serpentine acceleration [1].

EMMA lattice [2] consists of 42 quadrupole-doublet cells. The focusing and defocusing quadrupoles are offset horizontally with respect to the beam axis so to provide a net bending. They are mounted on sliders that allow radial motion, so providing independent setting of time of flight and tunes. The fixed field and absence of nonlinear elements cause the tune to vary from typically 0.3 down to 0.1 per cell, both planes, over the acceleration range.

EMMA FFAG ring parameters are summarized in Table 1, its representation in Zgoubi is displayed in Figure 1. RF cavities are located every two other cell except for two which house injection and extraction equipments. The RF voltage can be varied, to explore acceleration regimes. EMMA is injected at arbitrary momentum, with 40 pC about charge bunches, using DL's ALICE electron recirculator.

The end-to-end simulation tools discussed here use the ray-tracing code Zgoubi [3, 4], the engine for EMMA on-line model [5]. They aim at allowing data analysis, following experimental data taking at EMMA, which included beam position, closed orbit distortion, orbital period as a function of momentum, acceleration.

Table 1: Parameters of EMMA FFAG

circumference	*m*	16.568
Momentum range	*MeV/c*	10.5 - 20.5
Tune shift	/cell	$\sim 0.3 - 0.1$
Lattice		Quad doublet
No of cells		42
Acceptance	mm.mrad	3π
EMMA cell		
cell length	*cm*	39.448
length of F/D quad	*cm*	5.878 / 7.570
Nominal int^d gradient	*T*	0.402 / -0.367
drifts, short/long	*cm*	5 / 21
EMMA RF		
No of RF cavities		19
RF frequency / range	*GHz / MHz*	1.301 / 5.6
RF voltage	*kV/cavity*	20 - 120

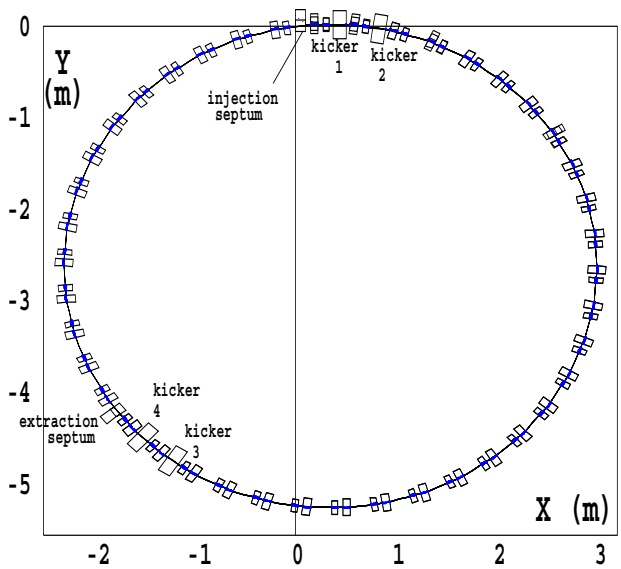

Figure 1: EMMA ring in Zgoubi using the interface software "zpop" [4]. The tracks of $14 - \frac{7}{19}$ accelerated turns are shown (blue), motion is clockwise.

The lattice cell in Zgoubi can be simulated in various different ways, from the most realistic using field maps, to analytical models of the quadrupoles, possibly accounting for overlapping fringe fields. These have been described in detail and compared in earlier works [6, 7]. All necessary mispositioning effects (e.g., to simulate measured horizontal and vertical CODs) and other field defects can be accounted for. These various models of EMMA cell can easily be interchanged. For this reason and for the sake of simplicity, and in addition in order to allow possible direct comparison with matrix methods (using MADX for instance), a simple hard-edge model is used in the present discussion. However, for the analysis of EMMA experimental data, OPERA field maps of the quadrupole doublet will be used instead.

Injection and extraction sections have similar geometry, a series of three successive cells house respectively

* Work supported by Brookhaven Science Associates, LLC under Contract No. DE-AC02-98CH10886 with the U.S. Department of Energy.

A COMPACT, GeV, HIGH-INTENSITY (CW) RACETRACK FFAG*

C. Johnstone#, Fermilab, Batavia, IL 60510, USA
M. Berz and K. Makino, Michigan State University, East Lansing, MI
P. Snopok, Illinois Institute of Technology, Chicago, IL 60616, USA

Abstract

Achieving milliamps of protons at GeV energies in a compact machine format implies both CW operation and high acceleration gradients to control losses. Above a few hundred MeV, beam loss must be well under a per cent to avoid massive shielding and unmanageable activation at high current. As relativistic energies are approached, the orbit separation between consecutive acceleration turns decreases in isochronous or CW accelerators because beam path length must scale proportional to velocity, β. To achieve the orbit separation needed for low-loss extraction, higher acceleration gradients must be deployed in relativistic machines; i.e. RF modules rather than Dee-type cavities. RF module insertion however results in a cyclotron with separated sectors and a greatly increased footprint. In Fixed Field Alternating Gradient Accelerators (FFAGs), the addition of synchrotron-like strong focusing (including reversed gradients to capture both transverse planes) promote inclusion of long, optically stable synchrotron-like straight sections and implementation of high-gradient RF, even SCRF. Further, FFAGs support constant, synchrotron-like machine tunes and tune footprints thus avoiding beam loss from resonances. The next generation of nonscaling FFAG machines not only maintain constant-tune, stable dynamics, these designs have also evolved into compact CW machines up to GeV energies for protons. The most recent innovation is an ultra-compact, 0.2 – 1 GeV FFAG racetrack design with a 3-4m by 5-6m footprint and 2-3m opposing straight sections that achieves both CW operation and low-loss extraction using SCRF. This new FFAG variant is described here. Note that minor lattice revisions would permit a CW ion therapy design capable of 430 MeV/nucleon for ions with charge to mass ratio of ~1/2 and the potential for variable energy extraction.

INTRODUCTION

Historically, cyclotrons are the highest current, most compact accelerator technology, but only at lower energies (hundreds of MeV). Higher energies require separated sectors in the cyclotron - like the 590-MeV PSI [1] or 500-MeV TRIUMF cyclotrons [2] – in order to insert strong accelerating (rf) systems. Stronger acceleration is required to minimize beam losses and radioactivity both during acceleration and during beam extraction (fewer acceleration turns and larger separation between the beams that comprise different acceleration turns facilitate efficient extraction). However, once space is inserted between the magnetic sectors of the cyclotron, the footprint of the cyclotron grows rapidly.

*Work supported by Fermi Research Alliance, LLC under contract DE-AC02-07CH11359 with the U.S. DOE #cjj@fnal.gov

High-intensity applications of relativistic proton accelerators that achieve milliamps of average current require CW operation to mitigate space charge and high acceleration gradients to limit losses to under a per cent to avoid massive shielding and unmanageable component activation. Cyclotron designs utilize Dee-shaped rf components between poles to achieve compactness, however, the accelerating gradient is low. As relativistic energies are approached, the orbit separation on consecutive acceleration turns must decrease to maintain the isochronous condition; i.e. constant revolution frequency for a fixed-frequency acceleration system. To achieve increased orbit separation, especially critical for low-loss extraction, higher acceleration gradients must be deployed; i.e. rf modules must be utilized, forcing separated sectors in a cyclotron, and an unavoidable large increase in footprint. The weak-focusing nature of traditional cyclotron fields does not permit long (several meters) straight sections without a significant scaling up of machine radius and size. However, the addition of strong focusing gradients (and corresponding strong beam envelope control) to conventional cyclotron fields – including reversed gradients to capture both transverse planes – does allow insertion of long synchrotron-like straight sections and thus efficient implementation of high-gradient, multiple-cavity rf modules, even SCRF cryomodules. Further, the nonscaling FFAG designs have evolved into a very compact racetrack shape – essentially a recirculating linear accelerator with FFAG arcs. This new generation of ultra-compact nonscaling FFAGs with constant machine tunes are described in this work, and specifically a 0.2 – 1 GeV proton FFAG with a 3-4 m by 5-6m footprint. With high gradient SCRF structures, described in these conference proceedings [3], the beam undergoes only 40 acceleration turns (1 0MV/m). Complete orbit separation is achieved at extraction for CW operation. The wide horizontal aperture SCRF pillbox design is presented in another submission [3].

DESIGN CONCEPTS

Another key dynamics issue is resonance avoidance, accomplished with stable, constant strong-focusing machine tunes over the entire acceleration energy range. Conventional isochronous cyclotron design cannot maintain both isochronous orbits and stable tunes at relativistic energies. The next generation of nonscaling FFAGs are capable of both, exhibiting strong-focusing machines tunes, tune footprints, and space-charge tune shifts characteristic of synchrotrons. High-intensity operation and tolerance of increased space charge effects has been reported in recent preliminary simulations [4].

ISBN 978-3-95450-128-1

STUDY OF A SUPERCONDUCTING COMPACT CYCLOTRON FOR DELIVERING 20 MeV HIGH CURRENT PROTON BEAM

M. Maggiore, LNL-INFN, Legnaro, Italy
J. V. Minervini, A. Radovinsky, C. Miller, L. Bromberg, MIT-PSFC, Cambridge, MA, USA

Abstract

Compact cyclotrons which accelerate high current of negative hydrogen ions in the energy range 10–30 MeV have been widely used over the last 25 years for medical isotope production and other applications. For a number of applications, low weight, low power consumption, portability, or low radiation background are key design requirements. We have evaluated the feasibility of a compact superconducting cyclotron that would provide proton beams up to 20 MeV by accelerating negative hydrogen ions and extracting them by the stripping process with relatively high beam current of 100 μA. The study demonstrates that the survival of the H- ion under high magnetic field environment could be large enough to guarantee low beam losses as long as the RF voltage is high. The compact cyclotron is energized by a set of superconducting coils providing the needed magnetic field, while the azimuthal varying field is provided by four iron sectors. Additional superconducting coils are added to minimize the stray magnetic field, eliminating the need for a return iron yoke and reducing the total weight of the device. In order to assure adequate vacuum in the accelerating region, an external H- ion source is used.

INTRODUCTION

Cyclotron technology has developed over many decades, and today it is considered a mature technology. The present approach for making cyclotrons includes the use of magnetic iron poles and iron return yokes to decrease the quantity of conductor needed to generate the magnetic field. In addition, magnetic iron sectors are used for shaping the field. The use of superconductivity in cyclotrons opens the potential for compact, high field devices. In this design the use of iron is minimized as both the main field and the return yoke flux are provided by a set of superconducting coils as shown in Fig. 1. The field shaping for the isochronous cyclotron was achieved using a combination of coils and iron pole tips in the bore of the coils, limiting the flexibility of field shaping by coils that are above/below the beam chamber (see Fig. 1). On the other side, the stray field is balanced by the contribute done by a set of superconducting shielding coils placed at outer radii. It results in a very fast decay of the magnetic field with distance away from cyclotron. The choice to operate with high magnetic field allows to maintain extremely compact the size of the machine as the extraction radius is 190 mm. Moreover, the elimination of the iron yoke allows for very large decrease in weight of the cyclotron, resulting in few tons weight machine.

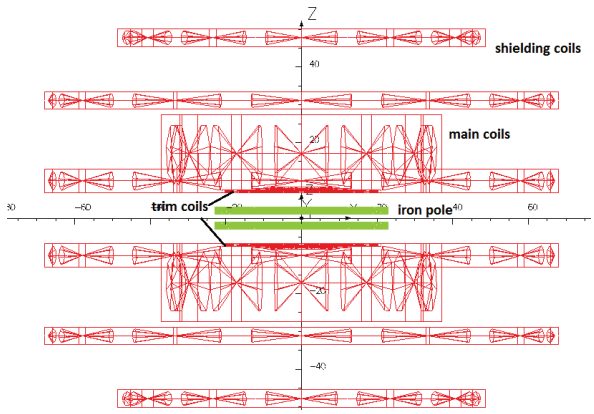

Figure 1: Coils configuration and iron poles location of the cyclotron magnetic system (units are cm).

H-LOSSES AT HIGH FIELD

The beam current loss due to Lorentz stripping of H- is a matter of concern while designing high field cyclotron. Due to the relatively low final energy of 20 MeV, the beam fraction lost during the acceleration can be reduced in two way: by keeping within certain margins the magnetic field values and by decreasing the number of turns necessary to achieve the final energy. Moreover, in order to minimize the residual gas stripping the operational vacuum pressure has to set at 10^{-7} torr.

Beam Losses by Magnetic Lorentz Stripping

When a H- ion is bent in a magnetic field, the electrons and proton are bent in opposite directions. If the magnetic field is strong enough, the slightly bound electron can be stripped.

The beam fraction lost per unit length in the laboratory frame depends on the lifetime τo given by Stinson [1], as

$$\frac{1}{L} = \frac{1}{\beta c \gamma \tau o} \qquad (1)$$

Since the revolution time To of particles travelling into a cyclotron can be assumed constant:

$$To = \frac{2\pi \cdot Eo}{Bo \cdot q \cdot c^2} \qquad (2)$$

with *Eo* rest energy and *Bo* magnetic field at center of the machine, it is possible to estimate the fraction of particle losses during the acceleration from the injection energy (30 keV) to the extraction one (20 MeV), by varying the confining magnetic field at center Bo. The calculations take into account of the magnetic field rise

DESIGN OF NEW SUPERCONDUCTING RING CYCLOTRON FOR THE RIBF

J. Ohnishi, H. Okuno, M. Nakamura, RIKEN Nishina Center, Wako, Saitama, Japan

Abstract

In order to increase the current of uranium beams by more than five times at the RI-Beam Factory (RIBF), we conducted a design study for a new superconducting ring cyclotron (SRC2 in this paper). It is a replacement for the existing fixed-frequency ring cyclotron (fRC) for accelerating U^{64+}, and it will enable us to accelerate U^{35+} extracted from an ion source from a beam energy of 11 MeV/u to 48 MeV/u. The SRC2 consists of four superconducting sector magnets. The maximum magnetic field in the beam orbit area is 3.4 T. This paper discusses electromagnetic forces acting on the coils and their support structure. We also successfully designed the beam injection and extraction system. A superconducting magnetic channel used for the beam injection line has been also designed. We found no significant problems in these fundamental designs.

INTRODUCTION

One of the most important goals for accelerators is to increase the current of primary beams because experiments on nuclear physics using rare RI-beams with a small production cross section are the main types of experiments performed at the RIBF. Because uranium beams are particularly important in the production of these rare RI-beams, increasing the strength of uranium beams is strongly desirable for RIBF experiments. Uranium beams are accelerated by an RFQ, a DTL linac, and four ring cyclotrons (RRC, fRC [1], IRC, and SRC [2]), as shown in Fig. 1. U^{35+} ions extracted from the 28-GHz ECR ion source are converted to U^{64+} at the first charge stripper (CS) after the RRC and to U^{86+} at the second one after the fRC. The converting efficiencies of the two CSs are approximately 18% and 27%, respectively, and the total transmission efficiency from the ion source to the exit of the SRC is approximately 1/200, which is considerably low. Accordingly, we have investigated the design of a second superconducting ring cyclotron (SRC2 in this paper) to replace the fRC, which can accelerate U^{35+} without any need for the first CS. By introducing the SRC2, a more than five-fold increase of the transmission efficiency can be expected by omitting the first CS and a reduction of the beam dispersion caused by the CS. In order to reduce the construction cost, the design policies of the SRC2 are as follows: (1) use of a fixed acceleration frequency, (2) use of four sector magnets, (3) use of cryocoolers, and (4) use of normal-conducting-type trim coils.

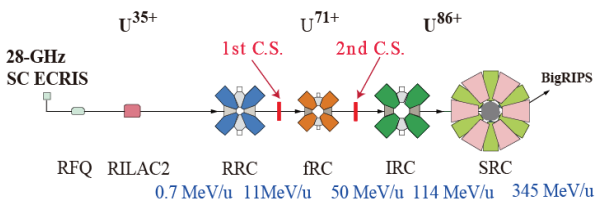

Figure 1: Existing acceleration system for U beam.

NEW SUPERCONDUCTING RING CYCLOTRON

The list of parameters and the plan view of the SRC2 are given in Table 1 and Fig. 2, respectively. The number of sector magnets is four and the K-value is 2200. Two accelerating RF cavities and a flattop cavity are used. The acceleration RF frequency is 36.5 MHz, which is the same as that of RILAC2, and the harmonic number is 9. Although the accelerating RF voltage needs more than 500 kV per cavity, the RF cavities have not yet been designed.

Table 1: SRC2 Parameters

K-value			2220
Energy	injection	MeV/u	10.8
	extraction	MeV/u	48
RF frequency		MHz	36.5
Harmonics			9
Average radii	injection	m	1.775
	extraction	m	3.65
Tune	ν_r		1.09-1.15
	ν_z		0.71-0.76

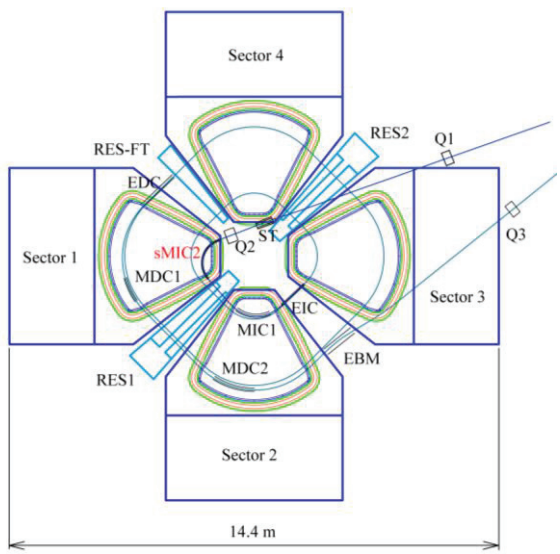

Figure 2: Plan view of new superconducting ring cyclotron.

ISBN 978-3-95450-128-1

RADIAL-SECTOR CYCLOTRONS WITH DIFFERENT HILL AND VALLEY FIELD PROFILES

M.K. Craddock#, University of British Columbia and TRIUMF*, Vancouver, B.C., Canada

Abstract

A new class of isochronous cyclotron is described in which more general radial field profiles *B(r)* are allowed than the simple proportionality to total energy found in conventional radial- and spiral-sector cyclotrons. Isochronism is maintained by using differently shaped field profiles in the hills and valleys. Suitably chosen profiles will produce high flutter factors and significant alternating-gradient focusing, enabling vertical focusing to be maintained up to 1 GeV or more using radial rather than spiral sectors.

INTRODUCTION

In an isochronous cyclotron, the constant orbit frequency, independent of ion energy $\gamma m_0 c^2$ and average radius R (circumference/2π), implies that

$$B = \gamma B_c , \qquad R = \beta R_c , \tag{1}$$

where B denotes the average field around a closed orbit, B_c the "central field" and R_c the "cyclotron radius". Unfortunately the resultant positive field gradient produces a defocusing contribution to the vertical betatron tune ν_z given by $\Delta\nu_z^2 = -\beta^2\gamma^2$. From the beginning, a major problem in cyclotron design has been how to compensate this and ensure vertical focusing. Thomas's [1] suggestion of edge focusing through an azimuthal field variation with N-fold symmetry, and Kerst's [2] of adding alternating focusing by using spiral sectors, have together succeeded in enabling "compact" cyclotrons with spiral sectors to accelerate protons to 230 MeV ($\beta^2\gamma^2 = 0.55$) [3]. *Separate-sector cyclotrons* (SSCs) can achieve higher flutter and so higher energies: the PSI Ring Cyclotron [4] produces 590 MeV protons ($\beta^2\gamma^2$ = 1.65), and designs have been published for energies, up to 15 GeV [5].

Reverse-bend cyclotrons would achieve higher flutter still by making the valley fields negative ($B_v = -B_h$, as in radial-sector FFAGs), rather than zero. Moreover, the alternating-gradient (AG) focusing, minimal in the previous schemes, becomes significant. Thus, if the hills cover a fraction of the orbit h = 0.6, the flutter is expected to maintain vertical focusing only up to 3.75 GeV. But a tracking simulation [6] has shown that positive focusing is in fact preserved up to 7.3 GeV.

HILL AND VALLEY FIELD PROFILES

A common feature of the above schemes is that the hill and valley fields, while of different magnitudes, are assumed to have the same radial profiles, *i. e.*:

$$B_v(r)/B_h(r) = \text{constant}. \tag{2}$$

More elaborate designs have also been proposed to achieve isochronism at high energy without using spiral magnets – basically by introducing more free parameters. Thus Rees [7] has designed a non-scaling muon FFAG that remains isochronous over the range 8-20 GeV (5,900 < $\beta^2\gamma^2$ < 37,000!), relying on AG focusing by "pumplet" cells (OdoFoDoFodO) composed of five straight-sided magnets of three different designs. On a less ambitious scale, Johnstone [8, 9] has designed close-to-isochronous non-scaling proton FFAGs to provide 250-MeV protons and 400-MeV carbon ions for cancer therapy, and 1-GeV protons for ADSR. These all use a 4-cell FDF triplet lattice with straight-sided (though not necessarily radial) edges, and are also remarkable for their low variation in tune, both ν_z and ν_r. In both these authors' studies the *B(r)* profile in each type of magnet is specially determined to produce the desired orbit properties.

Here we propose to explore a simpler possibility for achieving positive vertical focusing at high energy with purely radial sectors – allowing the radial field profiles in hills and valleys to differ. As was found helpful in previous high-energy cyclotron studies [6], we assume hard-edge fields with B_h and B_v each constant along equilibrium orbits. In particular we assume a polynomial variation with energy:

$$B_h(\gamma) = H_0 + H_1\gamma + H_2\gamma^2 + H_3\gamma^3 + ... \tag{3}$$

$$B_v(\gamma) = V_0 + V_1\gamma + V_2\gamma^2 + V_3\gamma^3 + ... \tag{4}$$

As a first step we consider a "compact" design with no drift spaces and negative valley fields. For an orbit of mean radius R crossing a hill-valley edge at radius R_e, we may write $\ell_h = \rho_h\psi_h$ and $\ell_v = \rho_v\psi_v$ for the arc lengths within a half-cell (Fig. 1), where the radii of curvature $\rho_h = B_c R_c \beta\gamma / B_h(\gamma)$, $\rho_v = B_c R_c \beta\gamma / B_v(\gamma)$, and ψ_h and ψ_v are the bending angles.

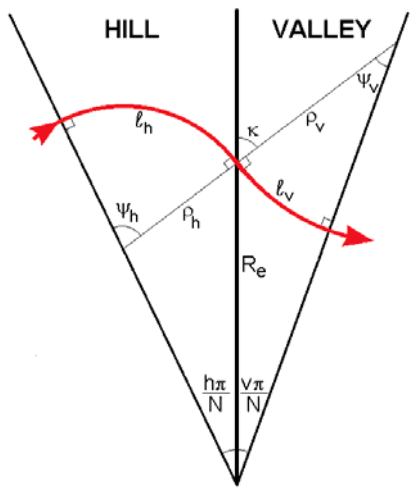

Figure 1: Orbit geometry within a half-cell.

*TRIUMF receives federal funding under a contribution agreement through the National Research Council of Canada.

#craddock@triumf.ca

OPTIMUM SERPENTINE ACCELERATION IN SCALING FFAG

S.R. Koscielniak, TRIUMF, Vancouver, B.C. V6T2A3, Canada

Abstract

Serpentine acceleration is typified by fixed radio frequency, fixed magnetic field and a near (but not) isochronous lattice, radial motion of the orbit, and two or more reversals of the motion in RF phase. This was discovered[1] in 2003 for linear non-scaling FFAGs in the relativistic regime. In 2013, Kyoto University School of Engineering[2] pointed out that serpentine acceleration is possible also in scaling FFAGs and may span the non-relativistic to relativistic regime. As a function of two key parameters, field index and synchronous energy, this paper shows how to optimize the extraction energy and the voltage per turn for the scaling case. Optimization is difficult, and typically leads to poor performance: either extreme voltage or small acceleration range. Nevertheless, designs with credible acceleration parameters can be obtained; and indicative examples are presented herein.

THEORY

Let us contrast the FFAG against the synchrotron. In the latter, the properties of a general particle w.r.t. synchronous are kept (almost) constant by ramping the magnetic field. The "synchronous energy" is a function of time and there is a single orbit. The motion about this is given in power series expansion in small quantities in the longitudinal coordinates momentum P or total energy E. Contrastingly, in a scaling FFAG, any orbit and energy can be used to define the synchronous reference. Due to the remarkable properties of the magnet lattice, the general particle motion can be written in absolute coordinates. In other words, because the momentum compaction is a global property of the lattice, independent of any selected reference energy, we have no need of power series expansions in small deviations.

In the scaling FFAG, the magnet field has the form:

$$B_z(R, z = 0) = (R/R_0)^k \qquad (1)$$

where $k > 0$ is the field index. The general orbit radius is given by $R/R_s = (P/P_s)^\alpha$ where $\alpha = 1/(1+k) < 1$ is solely a property of the lattice. It follows that revolution period T is given by

$$T/T_s = (E/E_s)(P/P_s)^{(-1+\alpha)} = (\beta_s/\beta)[(\beta\gamma)/(\beta_s\gamma_s)]^\alpha \ . \qquad (2)$$

Here γ is the relativistic kinematic factor, $E = E_0\gamma$ and $E_0 = m_0c^2$ is the rest mass energy. We define $T \equiv T(\gamma)$, $T_s \equiv T(\gamma_s)$ and $T_t \equiv T(\gamma_t)$ where $E_s = E_0\gamma_s$ is a synchronous energy and $E_t = E_0\gamma_t$ is the transition energy. One may eliminate $\beta = v/c$ in favour of γ. As the basis for estimations, useful approximations (in the limit $\gamma \gg \gamma_s$ and $\alpha \ll 1$) are $T/T_s \approx \beta_s[\gamma/(\beta_s\gamma_s)]^\alpha$; we set equal T/T_s to unity and solve for $\gamma \approx \gamma_s/\beta_s^k$.

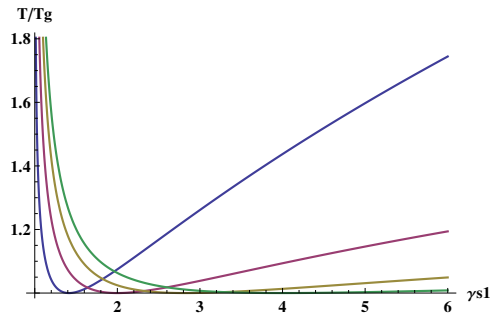

Figure 1: Revolution period versus energy (γ) for α = 1/2 (blue), 1/4 (red), 1/8 (yellow), 1/16 (green).

Figure 1 shows T/T_g curves as a function of γ_s for a variety of α. The curves are "U" or "V"-shaped. $\gamma(T)$ is a double valued function: to each value of T belongs two values of γ. Each curve have a minimum which defines the transition energy. Solving $\partial(T/T_s)/\partial\gamma = 0$, one finds $\gamma_t = 1/\sqrt{\alpha}$. All normalized curves $T/T_g = (T/T_s)/(T_g/T_s)$ for a particular value of α have the identical shape, independent of γ_s.

For energy less than the transition value, the revolution period behaves as if dominated by changing particle speed; and above transition behaves as if dominated by path length. If k is sufficiently large and γ_t sufficiently high, this apparent behaviour persists even in the relativistic regime. The difficulty is of course getting k sufficiently large without compromising the transverse optics. Contrastingly, using moderate values of field index produces a machine which can in principle cover the transition from non-relativistic to relativistic - with constant RF.

For brevity, let $\gamma_{s1} \equiv \gamma_1$ and $\gamma_{s2} \equiv \gamma_2$ be two energies having the same revolution period; there is a continuum of such doublets. We shall adhere to the convention that $\gamma_1 < \gamma_t < \gamma_2$. A certain doublet is chosen to be the synchronous reference when we set the radio frequency (RF) to be co-periodic with the orbit period $T(\gamma_1) = T(\gamma_2)$. Once this is chosen E_1, E_2 become fixed points of the motion. Both values of the synchronous E_s are equally valid! It is a little arbitrary, but we choose to work with the lower E_{s1} because it exists in the narrow range $1 < \gamma_{s1} < \gamma_t$.

The general features of the T/T_g curves in Fig. 1 are a very steep rise as $\gamma \to 1$, and a long slow ramp for $\gamma \gg \gamma_t$. When selecting reference doublets, this has the consequence that as $\gamma_1 \to 1$, so $\gamma_2 \to \infty$. Thus the range of acceleration is unbounded. But this range is illusory, and corresponds to a linac-like regime with prodigious voltage requirement.

ISBN 978-3-95450-128-1

PAST, PRESENT AND FUTURE ACTIVITIES FOR RADIATION EFFECTS TESTING AT JULIC/COSY

S.K. Hoeffgen*, S.Metzger, Fraunhofer INT, Euskirchen, Germany
R. Brings, O. Felden, R. Gebel, R. Maier, D. Prasuhn,
Forschungszentrum Jülich, IKP-4,, Jülich, Germany
M. Brugger, R. Garcia Alia, CERN, Geneva, Switzerland

Abstract

The testing of radiation effects (displacement damage, single event effects) with energetic protons for electronics used in space and accelerators is of growing importance. Setup and past experience of a dedicated test stand used by Fraunhofer INT at the JULIC cyclotron will be presented. During solar proton events, as well as at high energy accelerators (CERN, FAIR), electronics are confronted with protons of much higher energy. Recent scientific studies have shown that for single event upsets as well as destructive failures (e.g, single event latch-ups) a cross section measured at energies in the tens or one/two-hundred MeV range (e.g. PIF@PSI) can significantly underestimate the failure rate. To avoid unnecessary high safety margins there is a growing need for the opportunity to test electronics at several GeV, like the beam provided by the Cooler-Synchrotron COSY in Jülich.

INTRODUCTION

Proton accelerators are a necessary tool for the study of radiation effects in electronics. Protons can produce all kinds of radiation effects, which are generally classified into three categories: effects due to the slow accumulation of ionization (total ionization dose (TID) effects), effects due to transient ionization (single event effects (SEE)), and effects due to the displacement of atoms from their sites in the crystal lattice structure (displacement damage (DD) effects).

While TID effects are usually studied and tested separately with Co-60 gamma sources, proton accelerators are the main tool to study DD effects. The displacement of atoms from their lattice introduces new energy levels in the bandgap of the semiconductor thus affecting its electrical and optical properties [1]. An important quantity for DD effects is the non-ionizing energy loss (NIEL), which for protons increases towards lower energies. For this reason low energy accelerators are very suitable for studying DD effects, provided the beam has enough energy to penetrate the sensitive volume.

Single event effects are noticeable ionization effects produced by a single particle [2]. Protons can produce SEE by two ways. The proton can produce enough charge by direct ionization to trigger an effect e.g. a bitflip (single event upset, SEU) in a memory chip. The equivalent to the NIEL describing ionization effects is the linear energy transfer (LET, in principle the same as the stopping power), which also increases towards lower proton energies. Because protons have much lower LETs as heavier ions, they were until recently not able to produce SEUs by direct ionization. Due to the increasing integration the newest memory technologies have become sensitive to direct ionization by protons [3]. The other way is for the proton to produce recoil atoms or charged fragments by nuclear reactions with the materials in the device. These secondary particles, being heavier ions, have a high enough LET to produce SEE in even quite insensitive devices. While the study of direct ionizing proton SEE calls for a low energy proton accelerator, the study of SEE caused by nuclear reactions needs higher energies.

This paper will look at the experiences and possibilities to study radiation effects at the JULIC/COSY accelerator facility [4] run by the Institute for Nuclear Physics (IKP) at the Jülich Research Centre (FZJ).

TESTING AT JULIC

For the last 15 years Fraunhofer INT has been operating a dedicated radiation effects test facility at an external beam line of the JULIC cyclotron [5], which can be seen in Fig. 1.

Figure 1: Beam line for radiation tests at JULIC.

The energy of the proton beam is fixed to 45 MeV in vacuum. Since the tests are performed in air, the beam has to pass a 2 mm Al foil and about 1.8 m of air, which reduces the energy of the protons to 35 MeV at the surface of the target. The maximum current is 10 µA, but for the typical fluxes needed for testing, the current is about 5 nA to 10 nA. The usable beam diameter at the

*stefan.hoeffgen@int.fraunhofer.de

ISBN 978-3-95450-128-1

SPES PROJECT: A NEUTRON RICH ISOL FACILITY FOR RE-ACCELERATED RIBS

Augusto Lombardi, Alberto Andrighetto, Giovanni Bisoffi, Michele Comunian, Paolo Favaron, Fabiana Gramegna, Mario Maggiore, Leandro AC Piazza, Gianfranco Prete, Demetre Zafiropoulos, INFN/LNL, Legnaro (PD), Italy

Abstract

SPES (Selective Production of Exotic Species) is an INFN project with the aim to develop a Radioactive Ion Beam (RIB) facility as an intermediate step toward EURISOL. The SPES Project is under realization at the INFN Legnaro National Laboratories site. The SPES Project main goal is to provide a production and accelerator system of exotic beams to perform forefront research in nuclear physics by studying nuclei far from stability. The SPES Project is concentrating on the production of neutron-rich radioactive nuclei with mass in the range 80-160. The final energy of the radioactive beams on target will range from few MeV/u up to 11 MeV/u for A=130. The SPES facility acceleration system will be presented.

INTRODUCTION

The aim of the SPES project is to provide relatively high intensity and high-quality beams of neutron-rich nuclei to perform forefront research in nuclear structure, reaction dynamics and interdisciplinary fields like medical, biological and material sciences. SPES [1] is a second generation ISOL radioactive ion beam facility. The SPES project is part of the INFN Road Map for the Nuclear Physics; it involves the Italian national laboratories LNL (Legnaro) and LNS (Catania).

It is based on the ISOL method with an UCx Direct Target able to sustain a power of 10 kW. The primary proton beam is delivered by a cyclotron accelerator with an energy of more than 40 MeV and a beam current of 200 μA. Neutron-rich radioactive ions will be produced by Uranium fission at an expected fission rate in the target of the order of 10^{13} fissions per second with an expected rate on the secondary target of 10^{8} pps.. The exotic isotopes will be re-accelerated by the ALPI superconducting LINAC.

THE SPES PROJECT

General Layout

The SPES project foresees the construction of new facilities on the LNL site as shown in Fig. 1. The SPES building blocks are: a primary proton accelerator; an ISOL source; the beam selection and transport line and the first part of the secondary beam accelerator needed as injector in the existing LNL superconducting accelerator ALPI.

As a primary proton beam accelerator it was decided to acquire a cyclotron from a commercial company in order to focus on the design and the production of the beam transfer and selection line and of the front end accelerator for ALPI.

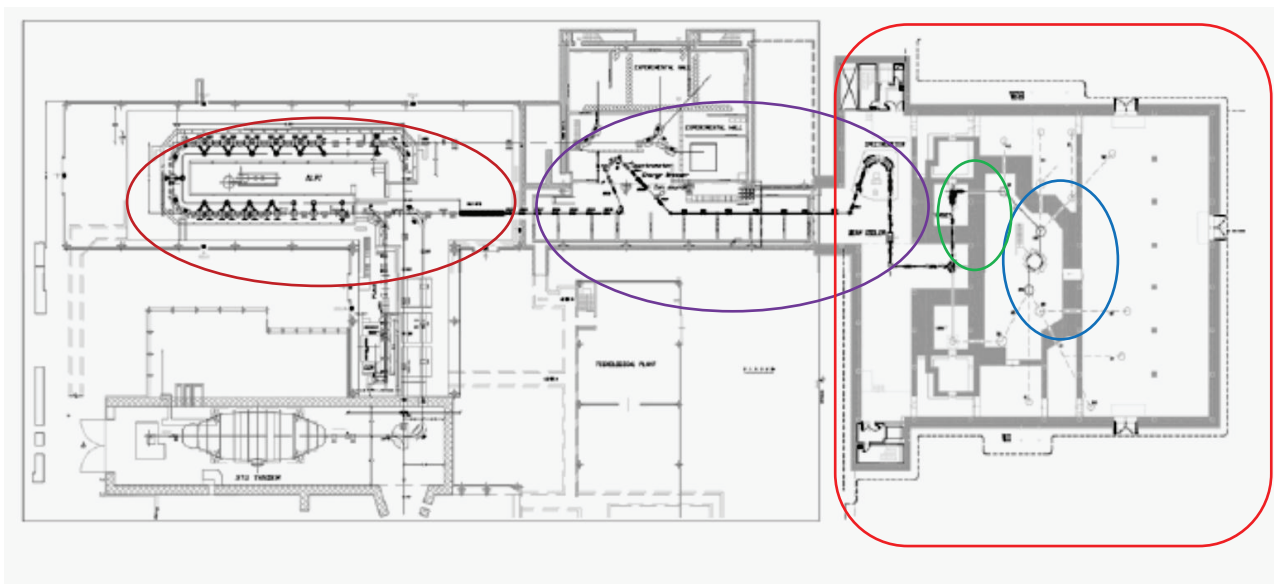

Figure 1: The LNL accelerator complex layout. Starting from the right hand side in the square there is the new building still under construction, inside the ovals in sequence there are from the right hand side: the Cyclotron, the RIB's source, the beam selection and transport line and the re-accelerator which is under construction, namely the RFQ.

ISBN 978-3-95450-128-1

STATUS REPORT AND NEW DEVELOPMENTS AT iThemba LABS

J.L. Conradie, L. Anthony, R. Bark, J.C. Cornell, J.G. de Villiers, H. du Plessis, J.S. du Toit, W. Duckitt, D.T. Fourie, M.E. Hogan, I.H. Kohler, C. Lussi, R. McAlister, H. Mostert, J.V. Pilcher, P.F. Rohwer, M. Sakildien, N. Stodart, R.W. Thomae, M.J. van Niekerk, P.A. van Schalkwyk,
iThemba LABS, P.O. Box 722, Somerset West 7130, South Africa

Abstract

iThemba LABS is a multi-disciplinary research facility in the fields of nuclear physics research, neutron therapy, proton therapy and radionuclide production. Three long-running projects – the construction of a new electron cyclotron resonance ion source, a beam phase measuring system for the separated-sector cyclotron comprising 21 fixed probes and an RF amplitude and phase monitoring system for the 16 RF systems – have been completed. The first results will be reported. The status of the newly developed low-level RF control system will be discussed and an interactive magnetic field calculation method for an injector cyclotron, making use of a database compiled from calculations with the computer program TOSCA, will be presented. Plans to save on the power consumption of the accelerators will be reported on. The beam statistics and the progress with the planning of a radioactive ion beam facility will be discussed.

ELECTRON CYCLOTRON RESONANCE ION SOURCES (ECRIS)

iThemba LABS operates two electron cyclotron resonance ion sources. ECRIS4, which was originally built by GANIL for the Hahn Meitner Institute [1, 2], delivers ion beams from gases and fluids. Since 2011 a second ECRIS, the GTS2, which is based on the design of the Grenoble Test Source [3], has been installed.

In the frame of our collaboration with the ion source group at CERN, experiments for the production of intense argon beams were performed. The source was optimized for the 11+ charge state of argon ions, as it is required for direct injection into the CERN linear accelerator and booster ring. A current of 65 eμA was obtained for the 11+ charge state in CW operation. For injection into the RF linear accelerator at CERN, pulses with a pulse length of 200 μs at a maximum repetition frequency of 5 Hz are required which can be produced from the source in the so-called afterglow regime. In this mode an intensity of 200 eμA with oxygen support gas was achieved. The pulse is stable for more than 500 μs. Additional experiments at iThemba LABS are scheduled to further optimize the beam performance.

RF CONTROL SYSTEM

A modularized version of a digital low-level RF control system has been developed at iThemba LABS. The system is the evolution of the prototype that was reported on previously [4]. The system as illustrated in Fig. 1 utilizes a Xilinx Spartan 6 FPGA that is interfaced with two high-speed 16-bit 500 MHz DACs from Analog Devices to synthesize the RF and local oscillator signals. The RF frequency is programmable in steps of 1 μHz between 5 and 100 MHz and the phase in steps of 0.0001° in the current configuration. High dynamic range of the main RF signal is maintained using a 23-dBm amplifier cascaded with three 32-dB, 0.5-dB digitally programmable step attenuators. The system uses 1 MHz intermediate frequency (IF). The five IF channels are sampled by five 16-bit 10-MHz SAR ADCs from Analog Devices. The dynamic range of each of the IF channels is maintained using 32-dB, 0.5-dB digital step attenuators as well. The amplitude and phase information is extracted from the signals using quadrature demodulation. A closed-loop controller within the FPGA is utilized to keep the phase and amplitude at an operating point and to reject system disturbances. The ARM CPU runs Ubuntu 13.04 and an EPICS IOC. Amplitude and phase information as well as system parameters can be streamed to an EPICS client via Ethernet allowing monitoring and diagnostics of the RF signal to be performed in real time. The system is now in the design verification stage.

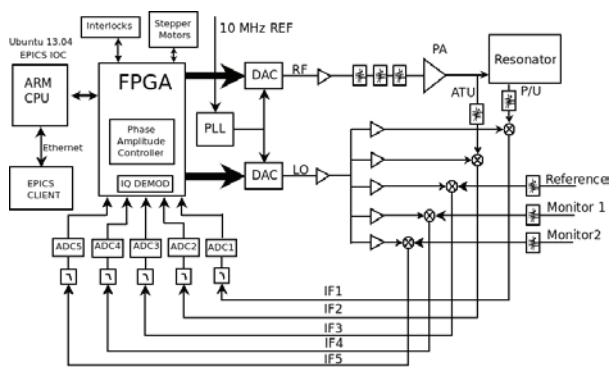

Figure 1: New digital low-level RF control system.

PHASE PROBES FOR THE SEPARATED-SECTOR CYCLOTRON (SSC)

Twenty-one non-destructive fixed phase probes have been installed in the SSC injection valley vacuum chamber. Each probe consists of two double-shielded electrodes symmetrically arranged with respect to the median plane. The upper and lower plates of each probe can be multiplexed to a single output port and are then combined. This reduces the unwanted RF pickup in the system. The second harmonic of the beam bunches is used to extract amplitude and phase information. Selectable 7^{th}-order band-pass filters comprising thirteen 4-MHz band-pass filters, each with a 1-MHz overlap, are used to filter the second harmonic. The filters are designed to reject the fundamental and higher-order harmonics by 60

ISBN 978-3-95450-128-1

AN INVERSE CYCLOTRON FOR MUON COOLING*

T. Hart†, D.J. Summers, University of Mississippi-Oxford, University, MS 38677, USA

Abstract

The production of intense high energy muon beams for the next generation of particle physics experiments is an active area of interest primarily due to the muon's large mass (compared to electrons) and pointlike structure (unlike protons). The muon production and the subsequent preparation into a beam are challenging due the large emittance of the initial muon beam and the short mean muon lifetime. Most muon cooling channels being developed are single-pass structures due to the difficulty of injecting large emittance beams into a circular device. Inverse cyclotrons can potentially solve the injection problem and also reduce the muon beam emittance by a large factor. An end-to-end (injection to extraction) simulation of an inverse cyclotron for muon cooling is presented performed with G4Beamline, a GEANT-based particle tracking simulation program.

INTRODUCTION

Facilities employing intense high energy muon beams, such as neutrino factories [1], muon colliders [2, 3], and neutrinoless muon to electron conversion experiments [4] are current research and development programs for possible next generation particle physics experiments studying neutrinos, the Higgs particle, possible supersymmetric particles, and lepton number violating decays. Muon beams are produced from the decays of pions which, in turn, are produced from collisions of high-energy protons and a high-density target. A tertiary muon beam has a large emittance which must be reduced for a useful beam for experiments. Also, the short lifetime of the muon ($\sim 2.2\ \mu$s) makes the rapid ionization cooling technique necessary as opposed to standard cooling techniques for stable electrons or anti-protons.

Most muon cooling channels are single-pass structures requiring strong radio-frequency gradients and strong transverse focusing to achieve rapid cooling. Multi-pass sychrotron ring-like structures would be much less expensive than linear designs, but injecting large emittance initial muon beams is a limiting difficulty [5]. An inverse cyclotron, a cyclotron in which particles are injected at large radius and lose energy by passing through a moderator material and thus spiral in toward the cyclotron center, is such a multi-pass device with potentially large beam admittance [6].

* Work supported by National Science Foundation Award 757938 and DOE grant DE-FG05-91ER40622

† tlh@fnal.gov

THE INVERSE CYCLOTRON

The inverse cyclotron slows a muon beam to a mean kinetic energy ($K.E.$) and radius of 300 keV and 3300 mm and then to roughly 90 keV and 2200 mm. An inverse cyclotron can accept a large range of initial energies which can be slowed to the common final energy at extraction: higher energy particles will make more turns in the helium moderator and take longer time to spiral in toward the extraction region. While the energy spread of the muons is reduced from injection to extraction, the differing number of turns of muons with different initial energies increases the time spread of the beam. The beam is then extracted and guided out along the positive z direction, slowed by a uniform electric field by about 55 keV and then sent through a section of time-varying electric fields which slow the beam more while increasing the time spread. The final $K.E.$ is about 30 keV which approaches the low energies necessary for frictional cooling for possible further longitudinal phase space reduction. Frictional cooling could reduce the muon beam energy spread down to about 2 keV.

The emphasis for this inverse cyclotron configuration is on manipulation of the final low energy region in a uniform low helium density. Also, the initial beam is not injected in a single turn here, and decay processes are turned off. Some steps for further development are extending the magnetic field outward for larger initial beam energies and varying the moderator density with respect to radius for single-turn injection and more rapid energy loss.

Simulations of this muon inverse cyclotron are done by G4Beamline [7].

The inverse cyclotron consists of three sections:

- A strong focusing cyclotron field containing 0.0001 mg/cm^3 helium which slows down muons injected from outside the cyclotron. The cyclotron field is generated from curved, sectored spirals which provide radial focusing by the increase of $< B_z >$ with radius, and axial focusing through large flutter and coil spiral angle. The muon beam spirals in toward the center of the cyclotron.
- An extraction section which extracts a slowed beam from the inner portion of the cyclotron. Current coils guide the beam out along a path parallel to the z axis.
- A section to manipulate the $(t, K.E.)$ phase space. A short section is an opposing constant electric field to reduce the kinetic energies of each muon. The final section is a series of electric traps which further reduces the kinetic energy of the beam. The section of constant electric field and the series of traps are inside a long solenoid.

ISBN 978-3-95450-128-1

DESIGN STUDY OF A SUPERCONDUCTING AVF CYCLOTRON FOR PROTON THERAPY

H. Tsutsui, A. Hashimoto, Y. Mikami, H. Mitsubori, T. Mitsumoto, Y. Touchi, T. Ueda, K. Uno, K. Watazawa, S. Yajima, J. Yoshida, K. Yumoto, Sumitomo Heavy Industries, Ltd., Tokyo, Japan

Abstract

We have designed a 4 Tesla superconducting AVF cyclotron for proton therapy. Its yoke weight is about 55 tons, which is about one fourth of our normal conducting 230 MeV cyclotron. In order to reduce the size and the weight without deteriorating the beam stability, the hill gap around the outer pole radius should be made small. Calculated extraction efficiency is higher than 60%, by arranging the extraction elements properly. The low temperature superconducting coil using NbTi wire is conduction-cooled by 4K GM cryocooler. Three dimensional electromagnetic finite element codes have been used during all phases of basic design.

INTRODUCTION

Up to now, cyclotrons, synchro-cyclotrons, and synchrotrons have been designed and manufactured as accelerator for proton therapy. Since extracted beam stability by a cyclotron is the best among them, a cyclotron may be the best choice for proton therapy, especially for pencil beam scanning.

Sumitomo Heavy Industries, Ltd. (Sumitomo) started in 1991 with IBA developing a normal conducting azimuthally varying field (AVF) cyclotron named P235, which accelerate proton to 230 MeV, and Sumitomo installed a cyclotron-based proton therapy system at National Cancer Center in Japan in 1998 [1]. This system has two gantries and one fixed port, and its foot print is about 30 m×50 m.

In order to let the system widely accepted by more hospitals, it should be more compact so that it can be easily introduced in a small space. As for the beam delivery system, Sumitomo developed a compact one with a vertical beam transport line and a short-length type gantry, which was installed at Aizawa hospital in Japan in 2013.

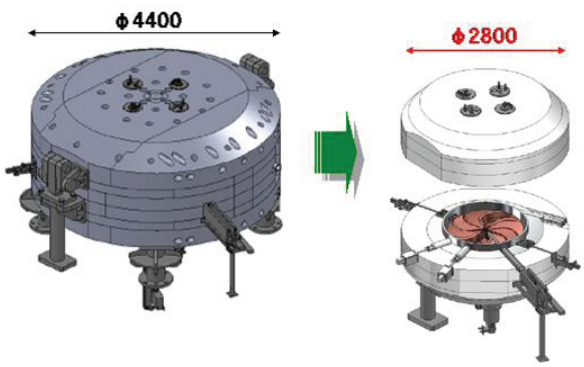

Figure 1: Schematic view of P235 and SC cyclotrons for proton therapy.

In this paper, we present a basic design study of a 4 T superconducting (SC) AVF cyclotron. Comparison between P235 and SC cyclotrons is shown in Fig. 1 and Table 1. It should be noticed that the yoke weight of SC cyclotron is about one fourth of that of P235. This makes the cyclotron transportation from our factory to a hospital, and reinstallation in the hospital much easier.

Table 1: Comparison Between P235 and SC Cyclotrons

	P235	**SC Cyclotron**
Main coil type	Normal	Superconducting
Diameter	4.4 m	2.8 m
Height	2.1 m	1.7 m
Yoke weight	200 t	55 t
Peak power consumption	440 kW	200 kW (RF) + 40 kW (cryocooler)

AVF CYCLOTRON DESIGN

Basic Parameters

Design concept of SC AVF cyclotron is the same as that of the P235, except there is a set of SC main coils in a cryostat. Some basic parameters are shown in Table 2.

Beam extraction radius is set to be 0.6 m, which is the smallest among the AVF cyclotrons for proton therapy. The average magnetic flux density at beam extraction radius calculated is 4 T. According to an approximated formula for the vertical tune,

$$\nu_z^2 \cong 1-\gamma^2+F^2(1+2\tan^2\xi), \qquad (1)$$

where γ, F^2, ξ are the Lorentz factor, flutter, and spiral angle, respectively, the flutter has to be large enough to make the spiral angle reasonably small. Therefore, hill gap is set as small as 12 mm in the outer region.

Magnetic Field

Magnetic field distribution of the magnet is calculated using Opera-3D code [2]. One example of the field calculation is shown in Fig. 2. In the design process, the hill span angle and the spiral angle for each radius are adjusted to get isochronism and vertical beam stability. The magnetic field map obtained has isochronism of 10^{-3} order and is not enough for beam tracking. So, the field map is fine adjusted artificially according to

$$\frac{B_{isochro}(\bar{r},\theta)-B(\bar{r},\theta)}{B(\bar{r},\theta)} \cong \gamma^2(\bar{r})\frac{T(\bar{r})-T_0}{T_0}. \qquad (2)$$

ISBN 978-3-95450-128-1

HIGH GRADIENT SUPERCONDUCTING CAVITY DEVELOPMENT FOR FFAG*

S.V. Kutsaev, Z.A. Conway, P.N. Ostroumov
Argonne National Laboratory, Argonne, IL 60439, USA
C.J. Johnstone, R.D. Ford, Particle Accelerator Corporation, Batavia, IL 60510, USA

Abstract

Like the cyclotron, the Fixed Field Alternating Gradient accelerator (FFAG) is a compact accelerator with a variety of applications in industry and medicine. High intensity, fixed-field compact accelerators require enhanced orbit separation to minimize beam losses especially at extraction. A 900 MeV FFAG, which fits in a 2.4 m x 4.4 m space, requires a total continuous-wave voltage of ~20 MV per turn and the accelerator cavities must fit in two 2 m straight sections. This high voltage can be generated using 4 superconducting (SC) cavities operating at a harmonic of the beam revolution, 150 or 200 MHz in this case. However, as with cyclotrons, the FFAG requires a large horizontal acceptance presenting a challenging problem for SRF cavity design. In this work, we present a SC cavity design with a 50 cm x 1 cm beam aperture, including an electrodynamics optimization, multiphysics analysis and the initial plan for the high-power couplers. Each cavity will be powered by two 100 kW RF couplers to accelerate a 1 mA average beam current

CAVITY TYPE

Several cavity types were considered including a coaxial half-wave resonator (HWR), an H-resonator and a rectangular cavity. Each of these options has advantages and disadvantages. Simulations of the simple non-optimized cavities have been performed to quantify their performance and size. These results are used to determine which option to pursue in more detail for the accelerator design. A peak surface magnetic field of 160 mT was chosen as a design constraint for this analysis because this value is experimentally achievable [1].

The first cavity type considered is a simple HWR model, a section of coaxial line (Fig.1a). As the resonant frequency is determined by the cavity length and the diameter defines optimal beta for acceleration, HWR should be 1 m long and 40 cm in diameter. Table 1 summarizes the main parameters of this cavity. While evaluating the HWR it was noticed that the velocity acceptance of the resonator was not broad enough to provide uniform acceleration over the proton velocity range. This is not possible because the accelerating voltage is a maximum in the center of the cavity and falls off sinusoidally as the protons move to the ends of the HWR; this field non-uniformity gives a varying voltage gain for protons in orbits of varying energies where the voltage gain is low at injection and at extraction. A low voltage gain correlates with a smaller orbit separation and makes injection and extraction difficult. The cavities to be discussed next do not have this issue and therefore the HWR option was dropped.

* This work was supported by the U.S. Department of Energy, Office of Nuclear Physics, under Contract No. DE-AC02-06CH11357 and ANL WFO No. 85F092

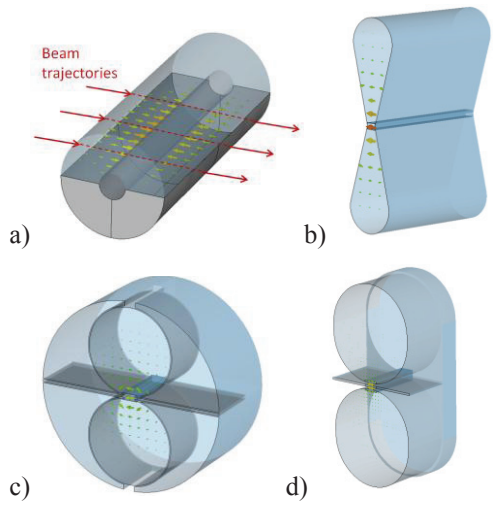

Figure 1: Considered cavity shapes: HWR (a), rectangular (b), H-resonator with (c) and without (d) a tank.

Table 1: RF Parameters of Different Cavity Types (V_{center}/V_{end} – voltage gains of a 200 / 900 MeV proton passing through the center / edge of the gap)

Parameter	HWR	H-resonator	Rectangular
Frequency, MHz		150	
B_{peak}, mT		160	
V_{center}, MV	4.65	2.73	4.11
V_{edge}, MV	1.82	2.51	3.56

To avoid the problem caused by the varying voltage gain in the HWR, it is advantageous to consider a single gap accelerating structure. One option is an H-resonator which performs well at low frequencies and low velocities [2]. Two types of H-cavities were considered: one with (Fig.1c) and one without (Fig.1d) a tank. The cavity with a tank has dimensions of 1m x 1m x 1m and 160 mT peak magnetic fields on the edges limit the voltage gain to a twice less the design value. Removing the tank decreases peak fields and thus increases the maximum achievable voltage. Though peak magnetic field drops under 160 mT, this structure has limits for

ISBN 978-3-95450-128-1

COMPARISON OF SUPERCONDUCTING 230 MeV/u SYNCHRO- AND ISOCHRONOUS CYCLOTRON DESIGNS FOR THERAPY WITH CYCLINACS*

A. Garonna#, CERN, Geneva, Switzerland
A. Laisné, U. Amaldi, TERA Foundation, Novara, Italy
D. Campo, L. Calabretta, INFN-LNS, Catania, Italy

Abstract

This work presents new superconducting compact cyclotron designs for injection in CABOTO, a linac delivering C^{6+}/H_2^+ beams for proton and carbon ion therapy. Two designs are compared in an industrial perspective under the same design constraints and methods: a synchrocyclotron and an isochronous cyclotron, both at the highest possible magnetic field and with an output energy of 230 MeV/u. The SC design features a central magnetic field of 5 T, an axisymmetric pole and a resonant extraction. The IC design features a 3.2 T central magnetic field, four sectors and elliptical pole gaps in the hills and in the valleys.

TERA'S CABOTO LINAC

The cyclinac is a combination of a fast-cycling cyclotron and a high-frequency linac [1]. It presents a unique feature, compared to the cyclotrons and synchrotrons for ion beam therapy. The linac makes it possible to change the beam energy without absorbers and at high repetition rate, paving the way to the treatment of moving tumors. The linac CABOTO accelerates short beam pulses (1.5 µs) of C^{6+}/H_2^+ pulsed at high repetition rate (300 Hz) up to 400 MeV/u [2].

These particular beam characteristics require specialized ion sources of the EBIS type [3-4] and the cyclotron injector should be as green (low consumption) and light (small weight) as possible, as well as reliable and industrially viable. For the determination of the most adapted injector solution, a linac input energy of 230 MeV/u was chosen, as it allows the use of the cyclotron as a stand-alone accelerator for proton therapy. However, existing compact (as opposed to separated-sector) cyclotrons can only reach up to 200 MeV/u (K1200 of Michigan State University) and the 300 MeV/u SCENT [5] and 400 MeV/u C400 [6] designs have not yet been constructed.

Therefore, new superconducting cyclotron designs have been produced: a synchrocyclotron (SC) [7] and an isochronous cyclotron (IC).

FINAL DESIGN PARAMETERS

All the main parameters of the designs are summarized in Table 1.

* Work supported by the TERA Foundation, Novara, Italy
# agaronna@cern.ch

DESIGN METHODS AND CONSTRAINTS

The same constraints were applied to the two cyclotron designs. The underlying philosophy of the designs was to use simplified models, in order to avoid the precise but complex and time-consuming process of three-dimensional modelling. This involved the use of dedicated programs (ALANEW, FIDER, ORBLA, NAJO and CANAL), adapted from previous work [8-9].

Table 1: Comparison of the Two Design Parameters

	IC	SC
q/A	1/2	
Output Energy	230 MeV/u (kinetic)	
Central Field	3.2 T	5.0 T
Pole Type	4 Sectors	Axisymmetric
Pole Radius	1.2 m	1.1 m
Total Current/Coil	1.1 MA.turns	1.9 MA.turns
Ion Sources	At least 2 (external)	
RF cavities	2 (h=4)	1 (h=1)
RF	98 MHz	38-30 MHz
Voltage at Injection	70 kV peak	28 kV peak
Voltage at Ejection	120 kV peak	28 kV peak
RF Power Supply	100 kW	30 kW
Ejection Method	ED	Bump + ED
Yoke Diameter/Height	4.75/2.9 m	4.6/3.3 m
Iron Weight	310 tons	330 tons

First of all, the charge-over-mass ratio (q/A) of the beam was set to 1/2, thus neglecting the 0.8% difference between $^{12}C^{6+}$ and H_2^+.

The cyclotron magnet was modelled using OPERA2D (Vector Fields Ltd). Because of axial symmetry, this approach is exact for the SC. However, for the IC, the azimuthal geometry had to be taken into account by introducing stacking factors. This method can be used to estimate the magnet weight and was found to produce results compatible with existing superconducting cyclotrons and designs by experienced groups [4]. The 3D geometry was approximated using ALANEW and FIDER,

EXPERIMENTAL STUDY TOWARDS HIGH BEAM POWER FFAG *

T. Uesugi,†
Kyoto University Research Reactor Institute, Kyoto, Japan

Abstract

The FFAG complex at KURRI is not only the first proton FFAG accelerator facility for beam users but the one aiming to have high beam power. The talk will present various efforts to increase beam power for the last few years and systematic strategy in near future toward the space charge limit.

FFAGS IN KURRI

Kumatori Accelerator driven Reactor Test (KART) project has been started at Kyoto University Research Reactor Institute (KURRI) since the fiscal year of 2002, aiming to demonstrate the basic feasibility of accelerator driven sub-critical system (ADS) and to develop a 150 MeV proton FFAG accelerator complex as a neutron production driver [1]. The accelerator complex was originally composed of a spiral-sector induction-accelerator, and two radial sector FFAG accelerator [2]. As a first stage, the FFAG accelerator complex has been achieved to output 100 MeV-0.1 nA proton beams at 30 Hz repetition and ADS experiments have been started in March 2009 [3].

In order to raise beam power of the FFAG, the injectors of the FFAG main ring was replaced by an 11 MeV linac with H^- ion source [4] in fiscal year of 2010. With the charge stripping injection of H^- beam, the output beam current of the main ring has reached 1 nA in March 2011 and 10 nA in 2012 with 20 Hz operation. Also acceleration up to 150 MeV has been achieved in 2012. The increased beam intensity attracted beam users in material sciences. Irradiation experiments for material radiation effects are undergoing.

Though the performance of the FFAG is improved every year, it is still far from the limiting current determined by the injector linac. The maximum output of the linac is estimated 3×10^{12} particles per pulse, which corresponds to 10 μA in 20 Hz operation. Main beam loss occurs at beam injection and capture in the main ring. Optimizations of the charge stripping injection and capture efficiency are in progress.

INTENSITY UPGRADE IN KURRI

H^- Injection without Bump System

H^- beams are injected into the FFAG main ring through a charge stripping foil made of carbon. This injection scheme makes it possible to inject a beam at the center of phase space already occupied by a previously injected beam. The circulating beam should escape from the stripping foil as fast as possible, otherwise undesirable effects happen, such as multiple scattering, energy losses and overheating of stripping foil. One method to escape from the stripping foil after injection is to make a bump-orbit. This works very efficiently, but it needs a complicated system. In our facility a fast acceleration is adopted to escape from the stripping foil, using the characteristic feature of FFAG accelerator (Fig. 1). The dispersion is $dR/dE = 2.4$ cm/MeV at the injection energy and rf amplitude is $V = 4$ kV. Therefore, the number of foil-hits for a bunch will be more than 100. This number may be reduced by using offset injection in horizontal space.

Table 1: Machine and Beam Parameters

Parameter	Value
Linac	
Repetition	<200 Hz
Peak current	<5 mA
Pulse length	<100 μs (uniform)
Energy	11 MeV±30 keV (at σ)
Main ring	
Energy	11∼100 or 150 MeV
Field index, k	7.5
Revolution frequency	1557 kHz at injection
Rf voltage	<4 kV

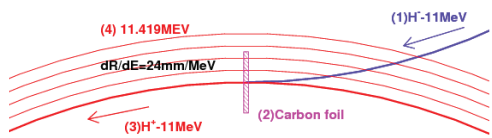

Figure 1: Scheme of charge-strip injection using dispersion.

The stripping foil is installed inside the main magnets and its radial position can be remote controlled. The foil is made of carbon whose dimensions are 25 mm×25mm. The thickness is assumed to be 20 μg/cm^2. Stripping efficiency is higher than 99 %.

Averaged particle energy loss, which is calculated by Bethe's formula, is ΔE_{loss}=760 eV for a 20 μg/cm^2. This energy loss raises the synchronous rf phase as

$$V \sin \phi_s = V \sin \phi_a - \Delta E_{loss} \, ,$$

where ϕ_a is the accelerating phase related to the

* Work supported by Japan Science and Technology Agency
† touesugi@rri.kyoto-u.ac.jp

ISBN 978-3-95450-128-1

THE IBA SUPERCONDUCTING SYNCHROCYCLOTRON PROJECT S2C2

W. Kleeven, M. Abs, E. Forton, S. Henrotin, Y. Jongen, V. Nuttens, Y. Paradis, E. Pearson, S. Quets, J. Van de Walle, P. Verbruggen, S. Zaremba, IBA, Louvain-La-Neuve, Belgium
M. Conjat, J. Mandrillon, P. Mandrillon, AIMA Development, Nice, France

Abstract

In 2009 IBA started developing a compact superconducting synchrocyclotron as part of the small footprint proton therapy system ProteusOne®. The cyclotron has been completely designed and constructed and is currently under commissioning at the IBA factory. Its design and commissioning results are presented.

INTRODUCTION

The ProteusOne® is an innovative single treatment room solution for protontherapy. It consists of the S2C2 superconducting proton cyclotron [1], the new IBA compact gantry [2] and a state-of the-art patient treatment room facility; it is designed for lower cost and compactness to make proton therapy more widely accessible.

In the new gantry, the scanning magnets are placed upstream of the last bending magnet. Figure 1 shows the layout of this new gantry. This configuration offers the combined advantage of compactness and pencil beam scanning with reasonable SAD (source to gantry axis distance). The energy selection system is included in the straight inclined part of the gantry. This also gives a considerable reduction of the facility footprint.

Several presentations on the S2C2 were given at the 2012 European Cyclotron Progress Meeting (ECPM) at PSI [3].

GENERAL CONSIDERATIONS

The average field in an isochronous cyclotron is limited to about 2.5 Tesla. Above this value, the flutter quickly becomes too small to provide sufficient vertical focusing and simultaneously constant orbit frequency. Much higher fields can be used in the superconducting synchrocyclotron where the requirement of isochronism is unnecessary and weak focusing is obtained from the negative gradient of the rotationally symmetric magnetic field. Other important differences exist:

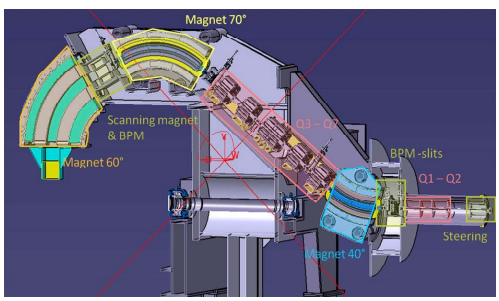

Figure 1: The ProteusOne® compact gantry.

Figure 2: The assembled cyclotron placed in the shielded beam-vault. It can be opened in the median plane as well as at the top of the cryostat. Also visible are the rotco-shield (left), the cryocooler-shield (middle) and the vacuum station (right).

i) the RF frequency is periodically modulated and the beam is pulsed, ii) longitudinal dynamics becomes a major aspect of the beam physics with energy-phase oscillations bound by a separatrix, iii) beam is captured at injection only during a limited time window, iv) regenerative extraction is needed to recover the beam which has a very small turn separation at extraction, v) the extracted beam has a relatively low intensity typically in the order of nAmps (this is perfectly sufficient for proton therapy applications), vi) the central region is strongly reduced in size compared to an equivalent isochronous cyclotron.

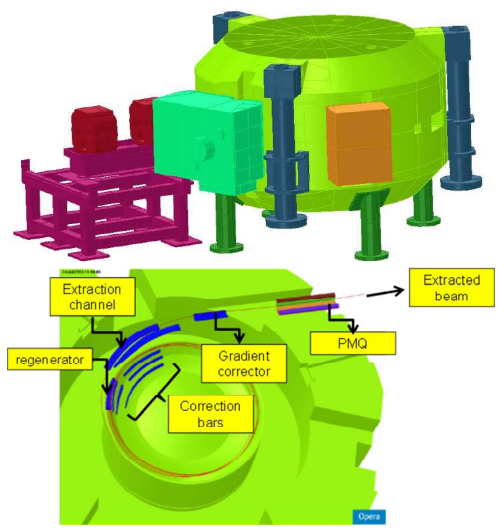

Figure 3: OPERA3D model of the cyclotron.

ISBN 978-3-95450-128-1

ADVANCED FFAG OPTICS, DESIGN AND EXPERIMENT*

J.-B. Lagrange†, Y. Mori,
Kyoto University Research Reactor Institute, Osaka, Japan

Abstract

Much progress has been made in the FFAG design with novel ideas, for example, FFAG straight line, FFAG with race track shape, FFAG with vertical orbit excursion, etc. Some of these were demonstrated experimentally. The talk will review the recent progress around the world.

INTRODUCTION

FFAG accelerators have been designed only in a circular shape, with horizontal excursion until recently, and zero-chromaticity is obtained with the vertical magnetic field B in the mid-plane following the so-called "scaling law" [1]

$$B = B_0 \left(\frac{r}{r_0}\right)^k \cdot \mathcal{F}, \tag{1}$$

with r the radius, r_0 the reference radius, k the constant geometrical field index, $\mathcal{F}$ an arbitrary azimuthal dependent function and $B_0 = B(r_0)$. It constrains the transverse motion, since the machine can only be in a circular shape, and the excursion in the horizontal direction. Recent developments give the possibility to drive particles with no overall bend in FFAGs while keeping zero-chromaticity [2], and vertical excursion FFAGs are investigated these days [3, 4]. Fixed frequency acceleration has also been experimentally demonstrated.

This paper mainly reports on the straight FFAG line, theoretically and experimentally. Other recent developments are then briefly mentioned.

ZERO-CHROMATIC FFAG STRAIGHT LINE

Theory

The motion of a charged particle with a given momentum is described by the following linearized equations for small amplitudes

$$\begin{cases} \frac{d^2x}{ds^2} + \frac{1-n}{\rho^2}x = 0, \\ \frac{d^2z}{ds^2} + \frac{n}{\rho^2}z = 0, \end{cases} \tag{2}$$

in the local curvilinear coordinate system (x, s, z). The field index n is defined as:

$$n = -\frac{\rho}{B}\left(\frac{\partial B}{\partial x}\right)_\perp, \tag{3}$$

with B the vertical component of the magnetic field. The symbol $\perp$ means that the partial derivative is done in the machine mid-plane perpendicularly to the closed orbit, and evaluated at $x = 0$. A necessary and sufficient condition of the invariance of the betatron oscillations along the curves $s = const.$ is

$$\begin{cases} \left(\frac{\partial \rho}{\partial p}\right)_s = 0, \\ \left(\frac{\partial n}{\partial p}\right)_s = 0. \end{cases} \tag{4}$$

From Eq. 4, since the curvature radius ρ does not depend on momentum, the similarity of the reference trajectories is a necessary condition for the invariance of the betatron oscillations. In the cartesian coordinates (X, Y, z), it leads to

$$X_{co}(p, s) = \chi(p) + g(s), \tag{5}$$

where g is independent of momentum and can be seen as the "shape term", common of all the reference trajectories, while χ is the "translation term".

We now focus on the invariance of the field index n with momentum. If we derive in the median plane the equation $p = qB\rho$, for a particle of momentum p and charge q, with respect to x and at $x = 0$, we have:

$$B\left(\frac{\partial \rho}{\partial x}\right)_\perp + \rho\left(\frac{\partial B}{\partial x}\right)_\perp = \frac{1}{q}\left(\frac{\partial p}{\partial x}\right)_\perp. \tag{6}$$

The field index n can thus be rewritten as:

$$n = \left(\frac{\partial \rho}{\partial x}\right)_\perp - \frac{\rho}{p}\left(\frac{\partial p}{\partial x}\right)_\perp. \tag{7}$$

The field index n can then be expressed in the coordinates (χ, s, z):

$$n = \left(\frac{\partial \chi}{\partial x}\right)_\perp \left[\left(\frac{\partial \rho}{\partial \chi}\right)_s - \rho m\right] + \left(\frac{\partial s}{\partial x}\right)_\perp \left(\frac{\partial \rho}{\partial s}\right)_\chi, \tag{8}$$

with m a parameter defined by:

$$m(\chi, s) = \frac{1}{p}\frac{dp}{d\chi}. \tag{9}$$

The parameter m can be rewritten with the magnetic field B as the normalized field gradient

$$m = \frac{1}{B}\frac{dB}{d\chi}. \tag{10}$$

The normalized field gradient m is independent of s, since the momentum is independent of s.

Since ρ does not depend on momentum, it does not depend on χ either:

$$\begin{cases} \left(\frac{\partial \rho}{\partial \chi}\right)_s = 0, \\ \left(\frac{\partial \rho}{\partial s}\right)_\chi = \frac{d\rho}{ds}. \end{cases} \tag{11}$$

* work supported by Japan Science and Technology Agency
† lagrange@rri.kyoto-u.ac.jp

HIGH INTENSITY OPERATION FOR HEAVY ION CYCLOTRON OF HIGHLY CHARGED ECR ION SOURCES*

L. Sun#, Institute of Modern Physics, CAS, 509 Nanchang Rd., Lanzhou 730000, China

Abstract

ECR ion sources have been used as the primary high charge state ion beam injector for cyclotrons for more than 30 years. With the persistent efforts of ECRIS researchers, many high performance ECR ion sources have been built globally, which are capable of producing intense high charge state ion beams. Modern advanced ECR ion source can provide stable and reliable high charge state ion beams for the routine operation of a cyclotron, which has made it irreplaceable, particularly with regard to the performance and efficiency that a cyclotron complex could achieve with the ion source. The 3rd generation ECR ion sources that can produce higher charge state and more intense ion beams have been developed and put into cyclotron operation since early 21st century. They have provided the privilege for the cyclotron performance improvement that has never been met before, especially in term of the delivered beam intensity and energy, which has greatly promoted the experimental research in nuclear physics. This paper will have a brief review about the development of modern high performance high charge state ECR ion sources. Typical advanced high charge state ECR ion sources with fully superconducting magnet, such as SERSE, VENUS, SECRAL, SuSI and RIKEN SC-ECRIS will be presented, and their high intensity operation status for cyclotrons will be introduced as well.

INTRODUCTION

ECRIS (Electron Cyclotron Resonance Ion Source) which is the most efficiency machine to deliver CW or long pulsed highly charged heavy ion beams, has already become an indispensable injector for modern cyclotrons since its first application on the Karlsruhe cyclotron in 1981 [1]. Operation of heavy ion cyclotron needs intense highly charged stable and reliable high quality heavy ion beams, which are typical features that a high performance ECRIS can meet. Nuclear physics research needs high quality, high power, high duty factor ion beams. Cyclotron was a very unique tool for nuclear physics research in last century. The development of cyclotrons has boosted the research activities enormously, and the application of ECRISs with cyclotrons has further promoted the advancement. The main driven force for the development of ECRISs in the 80s and 90s last century was the strong requirements from cyclotron operation for intense high quality highly charged heavy ion beams. After the successful connection of the so-called 1st generation ECRIS PICOHISKA to a cyclotron [1], many innovative techniques have been made by the Grenoble team and other researchers around the world, which made ECRISs more feasible to be employed on cyclotrons. The real breakthrough was the success of Caprice sources in the middle of 1980s [2], which are still widely used on cyclotrons. Caprice source is just the typical example of the 2nd generation ECRISs. In the succeeding 10 years, many prominent sources have been built, such as the ECR4 in GANIL [3], A-ECR in LBNL [4], RIKEN 18 GHz ECRIS [5], and so on. These nice performing machines have helped improve the cyclotrons' performances that have never been met before. Thanks to the great advancement of NbTi superconducting technique, the fabrication of the 3rd generation ECR ion source is possible and cost efficient. SERSE ion source is just a 2.5th generation one with a fully superconducting magnet that enables the source to work at high B mode [6]. Nevertheless, it has provided many technical or theoretical references to later 3rd generation ECRISs such as VENUS in LBNL [7], SECRAL in IMP [8], SuSI in MSU [9], and SCECRIS in RIKEN [10]. Actually, the 5 superconducting ECRISs listed above are all now in routine service as primary heavy ion beam injectors for cyclotrons. These high performance ECRISs can produce very intense heavy ion beams of high charge states that have remarkably pushed the performance of the connected cyclotrons towards the high limit. This paper will give a general presentation on the high intensity operation status of highly charged ECRISs for heavy ion cyclotrons. Although there are so many cyclotrons using high charge state ECRISs as ion beam injectors, as examples, this paper will mainly cover the work in GANIL, INFN-LNS, LBNL, MSU, RIKEN and IMP.

GANIL SOURCES

ECRIS was installed as one of the GANIL injector ion sources in 1985. Several years later, both of the injectors were equipped with room temperature ECRISs working alternatively to produce stable primary ion beams at GANIL. ECR4 and ECR4M are typical 2nd generation ECRISs working at high B mode that enables the high yield of highly charged ion beams. The refined structure ECR4 type ion sources can incorporate external feedings of solid material to the plasma with different techniques, such as inserted rod, resister oven, sputtering sample and MIVOC. The schematic picture of ECR4 ion source is given in Fig. 1. The GANIL injector ion sources can provide highly charged ion beams of all heavy elements from carbon to uranium. Till now, highly charged ion beams from more than 50 isotopes have been delivered. ECR4 is connected to a K25 cyclotron C01 and delivers heavy ion beams with the maximum energy of 100 keV/q by floating the ion source and the beam selection line on a 100 kV high voltage platform. ECR4M is connected to

*Work supported by 100 Talents Program of the CAS, No. Y214160BR0
sunlt@impcas.ac.cn

ISBN 978-3-95450-128-1

ELECTRON CYCLOTRON RESONANCE SOURCE DEVELOPMENT

T.Thuillier*, LPSC, Grenoble Cedex, 38026, France

Abstract

The ECR ion source (ECRIS) is still an active field of research and development, as demonstrated by the numerous contributions to the ECRIS'12 workshop and ICIS'13 conference. It is impossible to present all the interesting ECR development in this paper. Instead, a selection of ECR development for linear accelerator and synchrotrons are presented along with some original recent ECR contributions. A special care is taken to introduce newcomer activity in the ECRIS community.

ECR DEVELOPMENT FOR ACCELERATORS

FRIB Project

The FRIB project relies on the simultaneous acceleration of 220+220 µA of U^{33+}+U^{34+}beams. The VENUS ion source demonstrated the feasibility to produce up to 440+400 µA of U^{33+}+U^{34+}(see Fig. 1).[1] FRIB decided to use the VENUS ECRIS and update slightly its original design. The superconducting coil geometry and magnetic field characteristics of VENUS are kept. The cold mass mechanics, entrusted to LBL superconducting group, will be revised to use the modern key and pad scheme: [2] air inflated bladders are used to deform the coils mechanics and allow the insertion of keys that pre-stress the coils once the bladders are removed. The main advantage of this technique is to allow dismounting a hexapole coil independently from others and modify any coil pre-stress at will, by changing the key dimensions. The cryogenics system is simplified: liquid nitrogen is suppressed and replaced by a set of 2 cryocoolers to cool the 30K shield. The 4.2K cooling power is provided by 2×4.3W GM-JT cryocoolers.

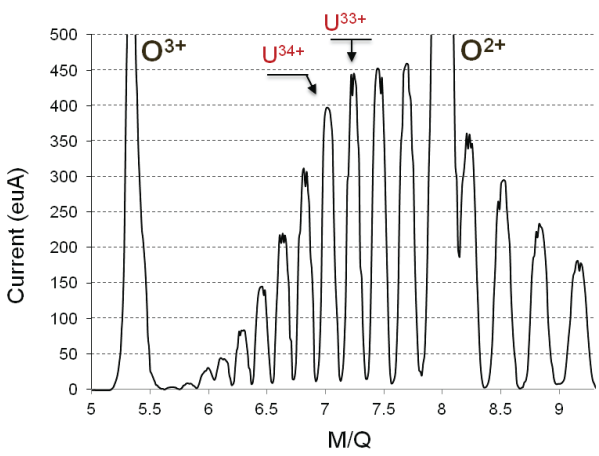

Figure 1: High intensity uranium beam production for U^{33+} and U^{34+} demonstrated by the VENUS source.

SPIRAL2 Project

The new linear accelerator construction is under progress at GANIL. The commissioning source to be used for the A/Q=3 heavy ion accelerator is the 18 GHz room temperature PHOENIX V2. This compact source demonstrated the production of 1.3 mA of O^{6+}, 1 pµA of $^{40}Ca^{16+}$, Ni^{19+}, 7.2 pµA of $^{32}S^{11+}$.[3] these intensities are compatible with the first year beam physics experiments. The higher intensities for heavy mass ions required later (1 mA $^{12}C^{4+}$, 100 µA $^{28}Si^{10+}$, 240 µA $^{32\text{-}36}S^{11\text{-}13+}$, 280-160 µA $^{40\text{-}48}Ca^{14\text{-}16}$ and 60 µA $^{58}Ni^{19+}$) imply the final use a new high performance 28 GHz ECRIS. Funding for such an upgrade is not decided yet. In the meantime, an upgrade of PHOENIX V2, named PHOENIX V3, is under development to increase the plasma chamber volume from 0.7 to 1.4 litre, keeping the overall magnetic confinement unchanged (see Fig. 2).[4] The higher ion confinement time is expected to shift the ion charge state distribution to a higher value, leading to an increase of A/Q=3 ion current. The PHOENIX V3 source is devoted to replace the V2 in 2014/2015 on the LINAC.

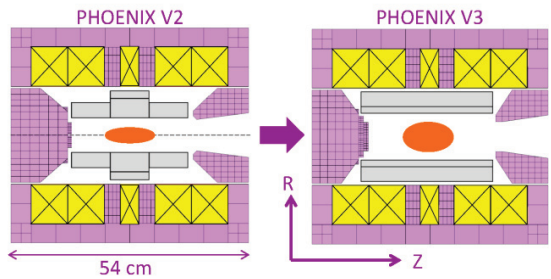

Figure 2: Evolution of the sectional view from PHOENIX V2 to PHOENIX V3.

Korean Projects

The republic of Korea is currently building several facilities involving multi-charged ECR ion sources. First, a new large heavy ion accelerator facility named Rare Isotope Science Project (RISP) is under construction.[5] This facility, based on a superconducting linear accelerator named RAON, will produce various stable and radioactive ion beams. The accelerator specifications are nearby to the FRIB ones. The project needs a high performance ECR ion source to fulfil the beam requirements. The ECRIS superconducting magnet design features 4 axial coils and a classical set of hexapole coils. The team recently built a saddle hexapole coil prototype which reached the target specifications: the other coils are being built now and final assembly will follow shortly. Second, a compact linear accelerator is under construction at the Korea Basic Science Institute in Busan [6]. The goal is to accelerate 1 mA of Li^{3+} beam to 2 Mev/u to produce a fast neutrons flux of 5.3×10^{13}/s applied to radiography. A new 28 GHz SC ECRIS was designed and recently

*thomas.thuillier@lpsc.in2p3.fr

ISBN 978-3-95450-128-1

PIC SIMULATIONS OF ION DYNAMICS IN ECR ION SOURCES

V. Mironov and J. P.M. Beijers,
Kernfysisch Versneller Instituut, University of Groningen, The Netherlands

Abstract

To better understand the physical processes in ECRIS plasmas, we developed a Particle-in-Cell code that follows the ionization and diffusion dynamics of ions. The basic features of the numerical model are given elsewhere [1]. Electron temperature is a free parameter and we found that its value should be about 1 keV to reproduce the experimentally observed performance of our 14 GHz ECR source. We assume that a pre-sheath is located outside the ECR zone, in which ion acceleration toward the walls occurs. Electric fields inside the ECR zone are assumed to be zero. The ion production is modelled assuming ion confinement by a ponderomotive barrier formed at the boundary of the ECR zone. The barrier height is defined by the RF radiation density at the electron resonance layer and is taken as an adjustable parameter. With these assumptions, we are able to reproduce the main features of ECRIS performance, such as saturation and decrease of highest charge state currents with increasing gas pressure, as well as reaction to an increase of injected RF power. Study of the source response to variations of the source parameters is possible.

INTRODUCTION

Electron Cyclotron Resonance Ion Sources are key components of many accelerator complexes, cyclotrons in particular [2]. Often, ECRIS output defines the overall performance of the accelerators, especially for very highly charged ions. Since their invention in the mid-sixties, ECRIS performance has shown a remarkable improvement. This progress is mainly due to increasing the frequency of microwave radiation used for plasma heating, accompanied by an appropriate scaling of the magnetic fields. Semi-empirical scaling laws define the directions for source development [2]. Additional tricks, such as gas-mixing, biased-disk, frequency tuning and others, boost the extracted currents. Each new ECRIS generation brings larger and more expensive sources, particularly since the introduction of fully super-conducting sources, with smaller margins for errors in source design.

Computer simulation of physical processes in ECRIS may pave the way for further improvement of the sources. In order to do so, a computer code should be able to reproduce the main features of ECRIS behaviour. However, this is far from trivial due to difficulties in describing the complex non-linear processes in the source plasma. Calculations are limited by the lack of an adequate understanding of the involved phenomena and by the available computational capabilities. A partial solution could be the use of so-called "toy-models", where some plasma parameters are adjustable or are considered as input, and the relative importance of various effects can be studied.

In this paper we present some new developments of such "toy-model" used in our PIC-MCC code for the simulation of ECRIS behaviour [1]. In the first version of the code, we described the ECRIS performance by assuming that the ECR plasma is free to flow along the magnetic field lines, with no additional mechanisms for plasma confinement. The experimentally observed charge-state-distributions of the extracted ion currents could be reproduced, as well as the spatial distributions of the extracted ion beams. The ion density gradients play a crucial role, being defined in the calculations by the length of the plasma. Despite the success in modelling, at least one important feature of ECRIS operation was missed – saturation and decrease in the currents of the highest charge states with increasing gas flow into the source chamber. Reaction of the extracted currents to changes in injected RF power was also not correctly described by the model.

As a next step in the development, we suppose that the ECRIS plasma is mainly localized inside ECR zone and that the ions are transported toward the source wall beyond this zone by a (pre)sheath electric field. However, an additional confining mechanism is now needed to reproduce the experimental CSD of the ion currents, and we assume that it is due to a ponderomotive barrier close to the ECR boundary [3]. Indeed, there is experimental evidence of a modification of the plasma profile caused by intense microwave radiation. A ponderomotive force pushes electrons from regions where the radiation power density is highest, and the emerging potential barrier confines ions. Such regions occur for example when the plasma density is close to the critical or quarter-of-critical value [4], or the magnetic field is close to the ECR condition.

There are models [5] that describe absorption of the microwave radiation at the ECR surface and electron heating in terms of non-linear decay of microwaves into electrostatic electron waves that propagate along the magnetic field lines toward the upper-hybrid-resonance (UHR) layer, where they are absorbed. We remind that the UHR layer is situated where $\omega^2_{RF}=\omega^2_p+\omega^2_c$, with ω_{RF} the microwave frequency, ω_c the cyclotron frequency, and ω_p the plasma frequency. In this approach, the highest gradients of the wave electric field are at the UHR layer.

We present the results of calculations based on the assumption that the ECRIS plasma is located mainly inside the UHR layer and is confined by a potential barrier. Despite the unavoidable simplifications and assumptions, we are able to reproduce the charge-state

ISBN 978-3-95450-128-1

STATUS OF THE RIKEN 28-GHZ SC-ECRIS

Y. Higurashi#, J. Ohnishi, K. Ozeki, M. Kidera, T. Nakagawa,
RIKEN, 2-1 hirosawa Wako Saitama, Japan

Abstract

Ever since we obtained the first beam from RIKEN 28-GHz SC-ECRIS in 2009, we have been trying to increase the beam intensity using various methods. Recently, we observed that the use of Al chamber strongly enhances the beam intensity of a highly charged U ion beam. Using this method, we obtained ~180 eμA of U^{35+} and ~230 eμA of U^{33+} at an injected RF power of ~4 kW by the sputtering method. The advantage of this method is that a large amount of the material can be introduced into the plasma chamber; therefore, long-term beam production without a break is possible. In fact, we already produced intense U beams in the RI Beam Factory (RIBF) experiments for over a month without a break. For the long-term operation, we observed that the consumption rate of the U metal is ~5 mg/h. In this spring, we also produced a U beam using a high-temperature oven through two-frequency injection. In these test experiments, we observed that the beam intensity of the highly charged U ions is strongly enhanced. In this contribution, we report the results of the various test experiments on the production of highly charged U ion beams. We also report the analysis of the long-term production of U ion beams in RIKEN RIBF experiments.

INTRODUCTION

Ever since we obtained the first beam in a RIKEN RIBF project, we have been trying to increase the beam intensity of the heavy ions to achieve our final objective of 1 pμA for all target heavy ion beams [1]. Intense uranium (U) ion beam is a strong tool to produce radio isotope beams through in-flight fission reaction. For this reason, we constructed and developed a new superconducting ECR ion source at an operational frequency of 28 GHz for the production of heavy ion beams including U ions [2]. In 2011, we successfully injected 28-GHz microwaves into the ion source and produced highly charged Xe ion beams [3]. Simultaneously, we tried to produce highly charged U ion beams by the sputtering method. In 2012, we replaced the stainless steel chamber (SS chamber) with an aluminum chamber (Al chamber)). Using the Al chamber, we observed the strong enhancement of the U ion beam intensity in comparison to that using the SS chamber.

In this paper, we present the recent results of the production of highly charged U ions and analysis of the long-term operation in the RIKEN RIBF experiment.

#higurasi@riken.jp

DESIGN OF THE ION SOURCE

The detailed structure and first experimental results using 28-GHz microwaves are described in [2, 3]. The main feature of the ion source is that it consists of six solenoid coils to produce a mirror magnetic field, which produces flexible magnetic field distribution from classical B_{min} to "flat B_{min}" [4]. Using this configuration, we can independently change the magnetic field gradient and surface size of the ECR zone. Recently, we installed an additional GM-JT refrigerator, which has a cooling power of 4.2 W at 4.2 K, in order to increase the cooling power. At present, there are two GM-JT refrigerators available to cool the cryostat. Figure 1 shows the cooling power of the two refrigerators vs. aperture size of the JT valve. The cooling power is strongly dependent on the aperture size, which was optimized to maximize the

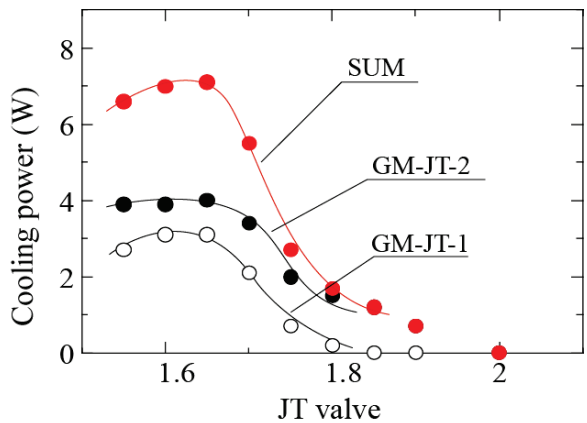

Figure 1: Cooling power of the GM-JT refrigerators vs. aperture of the JT valve.

cooling power. A maximum cooling power of ~7.4 W was obtained using a tow GM-JT refrigerator. Under this condition, the cooling power is ~8 W against the X-ray heat load in the cryostat.

With regard to the external ion source of the heavy ion accelerator, the production of stable beams is a critical issue, particularly for the RIKEN RIBF project. In 2011, we modified the power supply of the gyrotron to stabilize the beam intensity [5]. We observed large power ripples in the output microwaves, which render some difficulties in the operation of the ion source at an RF power lower than 1 kW. These ripples can be reduced by increasing the electric capacitance in the rectified circuit of the cathode power supply. We also observed long-wave irregularity of the beam intensity, which is correlated with the RF power. This is mainly because of the irregularity in the temperature in the room where the power supply to the

ISBN 978-3-95450-128-1

A STUDY OF MULTIPACTING EFFECTS IN LARGE CYCLOTRON CAVITIES BY MEANS OF FULLY 3-DIMENSIONAL SIMULATIONS*

Chuan Wang#, Bin Ji, Pengzhan Li, Zhiguo Yin, Yu Lei, Jiansheng Xing, Tianjue Zhang,
CIAE, Beijing, China
Andreas Adelmann, Achim Gsell, Mike Seidel, PSI, Villigen PSI, Switzerland

Abstract

Field emission model and secondary emission models, as well as 3D boundary geometry handling capabilities, are needed to efficiently and precisely simulate multipacting phenomena. These models have been implemented in OPAL, a parallel framework for charged particle optics in accelerator structures and beam lines. The models and their implementation are carefully benchmarked against a non-stationary multipacting theory. A dedicated multipacting experiment with nanosecond time resolution for the classic parallel plate geometry has also shown the validity of the OPAL model.

Multipacting phenomena, in the CYCIAE-100 cyclotron, under construction at the China Institute of Atomic Energy, are expected to be more severe during the RF conditioning process than in separate-sector cyclotrons. This is because the magnetic stray fields in the valley are stronger, which may make the impact electrons easier to reach energies that lead to larger multipacting probabilities. We report on simulation results for CYCIAE-100, which gives us an insight view of the multipacting process and help to develop cures to suppress these phenomena.

INTRODUCTION

Multipacting phenomena have been observed in various RF structures of accelerators. Multipacting is appearing in high-Q RF cavities of cyclotrons [1, 2]. The primary or seed electrons will impact the cavity surface, and produce an avalanche of secondary electrons. Under certain conditions (material and geometry of the RF structure, frequency etc.), the electron secondary emission yield (SEY) coefficient will be larger than one and lead to exponential multiplication of electrons. This kind of discharge will limit the power level until the surfaces will be cleaned through a very time-consuming conditioning process [1, 2]. The appearance of magnetic field in cyclotrons will make the impact electrons easier to reach energies that lead to larger secondary emission yields and make the prediction of electron trajectories in cyclotron cavities more difficult. Large scale multipacting simulations based on reliable data of surface material, full size geometry of RF structures and parallel computing allow more thorough analysis and a deeper understanding of these phenomena even in early design stage of RF structures. To make OPAL [3] a feasible tool to perform these large scale multipacting simulations, first we implement a 3D particle-boundary collision test model into OPAL. We have implemented surface physics models including two secondary emission models, developed by Furman-Pivi and Vaughan respectively. The above mentioned models and their implementation in OPAL have been benchmarked against both a non-stationary theory [4] and a nanosecond time resolved multipacting experiment with a parallel plate geometry. The time evolution of the particle density among simulation, theory and experiment agrees very well.

*Work partially supported by The Beijing Radioactive Ion-Beam Facility upgrading project.
#cwang@ciae.ac.cn

MODEL IMPLEMENTATIONS IN OPAL

Geometry Handling

The particle-boundary collisions test is crucial to multipacting simulations. Since complex 3D geometries are hard to be accurately parameterized by simple functions, we use oriented triangulated surfaces, which are extracted from volume mesh generated by GMSH [5], to represent the complex geometry of real RF structures. Subsequently we can make use of efficient 3D line segment-triangle intersection (LSTI) tests [6] to find exact locations of particle-boundary collisions. Even though the implemented LSTI algorithm use pre-computed oriented triangles, early rejection strategy is necessary to bring the computational time down to an acceptable level. By using an early rejection strategy (see Fig. 1), the number of LSTI tests in each time step has been greatly reduced. In that example, only the red particles will be tested in each time step. If we have M triangles and N particles in the simulation, both in the magnitude of tens of thousands to millions, the number of LSTI tests in single time step without the described early rejection technique would be prohibitive. The details of this early rejection strategy have been documented in our previous reports [7].

Surface Physics Models

Electron field emission is a major source of primary particles in the secondary emission process. The Fowler-Nordheim (F-N) model has been used to model these seed electrons in OPAL [7].

We have implemented two secondary emission models. The first one is a phenomenological model developed by M.A. Furman and M. Pivi [8]. The Furman and Pivi's secondary emission model calculates the number of secondary electrons that results from an incident electron of a given energy on a material at a given angle. For each of the generated secondary electrons the associated process: true secondary, re-diffused or backscattered is recorded, as is sketched in Fig. 2

THE NEW AXIAL BUNCHER AT INFN-LNS

A. Caruso, G. Gallo, A. Longhitano INFN-LNS, Catania, Italy
J. Sura, Warsaw University, Warsaw, Poland
F. Consoli, Associazione Euratom-ENEA sulla Fusione, Frascati, Italy
Li Pengzhan, China Institute of Atomic Energy, Beijing, China

Abstract

A new axial buncher for the K-800 superconducting cyclotron is under construction at LNS [1]. This new device will replace the present buncher [2] installed along the vertical beam line, inside the yoke of the cyclotron at about half a meter from the medium plane. Maintenance and technical inspection are very difficult to carry out in this situation. The new buncher will still be placed along the axial beam line, just before the bottom side of the cyclotron yoke. It consists of a drift tube driven by a sinusoidal RF signal in the range of 15-50 MHz, a matching box, an amplifier, and an electronic control system. A more accurate mechanical design of the beam line portion will allow for the direct electric connection of the matching box to the ceramic feed-through and drift tube. This particular design will minimize, or totally avoid, any connection through coaxial transmission line. It will reduce the entire geometry, the total RF power and the maintenance. In brief, the new axial buncher will be a compact system including beam line portion, drift tube, ceramic feed-through, matching box, amplifier and control system interface in a single structure.

BUNCHER STUDY

This new device will be driven by a simple sinusoidal voltage, as the rough approximation of the ideal saw-tooth signal [3]. The sine wave choice will reduce the total efficiency and performance of the system, but the generation of a high frequency saw-tooth in the range 15-50 MHz remains difficult still today. The basic two-gap buncher structure [4] is shown in Fig.1, between the SERSE ion source [5] and the K-800 superconducting cyclotron.

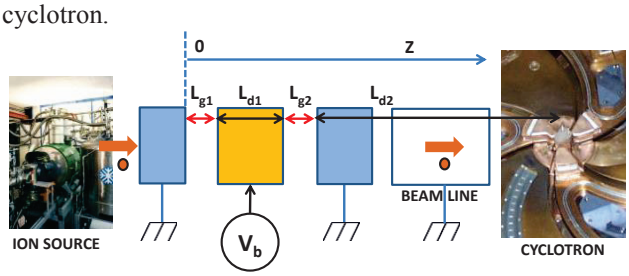

Figure 1: Basic structure of the axial buncher.

It is a drift tube, fed by the sinusoidal voltage $V_B = V_{MB}\sin(\omega t + \varphi_0)$, and placed between two grounded tube electrodes. L_{g1} and L_{g2} are the two gaps of 5 mm length. The distance between the Buncher and the inflector at the cyclotron central region is 3011 mm, and it is imposed by mechanical constraints. Particles generated by the ion source have $v_{z0} = \sqrt{2q_iV_s/m_i}$ velocity, being q_i and m_i their charge and mass, and V_s the voltage of the source output electrode. The drift tube length L_{d1} is 83.5 mm. This length is chosen so that L_{d1}+L_{g1} is an odd integer multiple of the $\beta\lambda/2$ quantity. In particular, $\beta\lambda = v_{z0}/f$ (with f cyclotron frequency) is the path of the particles in one period and, because of the fixed geometry of the cyclotron central region, has to be constant.

The basic theoretical study of the bunching effect in the present structure [4] has been analytically performed here by considering a time-varying and spatially uniform electric field within the two L_{g1} and L_{g2} gaps. Here particles undergo a time varying acceleration, whereas they will move in uniform linear motion within the following drift tubes. We now illustrate the typical case for α particles. It gives: $V_{MB} = 73.8078$ V, $V_S = 24.72$ kV, $f = 43.617$ MHz, and then $\beta\lambda = 35.28$ mm. The cyclotron acceptance interval phase is 35°. Each particle of the continuous flow coming from the ion source arrives at the position z = 0 at the t_0 time instant (Fig. 1). The calculated particle trajectories are shown in Fig. 2a-2b in the Applegate diagrams, referred to one period. The trajectories grouping is apparent. The time instants when they reach the cyclotron inflector is t_{d2}. In Fig. 2c-2d the plot of t_{d2} versus t_0/T is shown. The V_{MB} voltage has been tailored to optimize the particle transmission within the cyclotron acceptance time, referred to the 35° phase. This is clearly shown in Fig. 2c-2d, where the curve is tangent to the dotted boundaries.

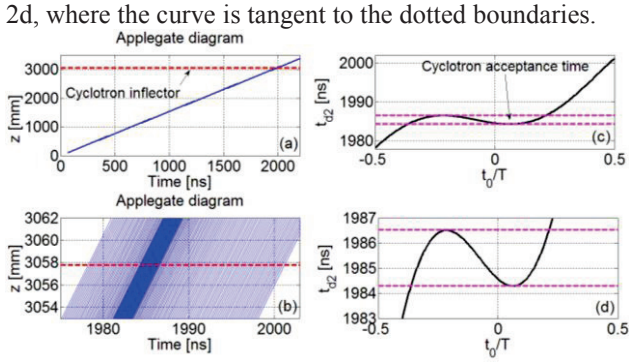

Figure 2: (a) and (b) Applegate diagrams with different scales; (c) and (d) t_{d2} versus t_0/T.

Under these conditions the particle transmission to the cyclotron is TR = 57.6%, and the energy spread is $\Delta E/E$ = 1.15%.

ISBN 978-3-95450-128-1

HEAT TRANSFER STUDY AND COOLING OF 10 MeV CYCLOTRON CAVITY

S. Saboonchi, H. Afarideh*, Department of Energy Engineering & Physics, Amirkabir University of Technology, Tehran, 15875-4413, Iran
M. R. Asadi, Islamic Azad University (PPRC) Science and Research Branch of Tehran, Tehran, 147789-3855, Iran
M. Ghergherehchi, J. S. Chai, Department of Energy Science/School of Information & Communication Engineering, Sungkyunkwan University, Suwon 440-746, Korea

Abstract

The most important problem in mechanical design of RF cavity of cyclotron is generated heat by RF power loss. An optimized cooling system for cavity is necessary to prevent Dee damaging and minimizing error function of cyclotron created by displacements. Also optimization of water circuit and water flow is essential because it affects unwanted vibrations and manufacturing. In this paper an attempt has been done to design an optimized cooling system for the cavity of a 10MeV cyclotron using ANSYS CFX and CST MICROWAVE STUDIO software.

INTRODUCTION

This paper describes the simulation and design methodology of cooling line for a single-stem, room temperature, copper resonator operating on the fourth harmonic. The RF system is designed to accelerate H− ions to 10MeV with the relevant performance requirements outlined in Table 1.

Table 1: Relevant Design Parameters

Parameter	Value
Resonant Frequency	69 MHz
Dee Tip Voltage	50 kV
Water flow at inlet	0.180 kgr / sec
Diameter of cooling line pipe	7 mm

Using the 3D CAD program Solid Works. Model of the resonator was created. This model (Figure 1, 2) consists of the copper resonant structure; all copper is oxygen-free high conductivity (OFHC).

For this study, mechanical interfaces between components are considered perfectly connected, both thermally and mechanically .stability of temperature is essential during the operation of cyclotron .cooling lines in Dee and stem considered perfectly connected it means there is a single cooling line used per quarter of RF cavity. Cooling line inters form stems and at the first it is crossed stem in spiral shape because the hottest part of RF cavity are stems after stem passed from middle of Dee near the boundary and surface then water exits form the centre of stem this is general shape of cooling line in RF cavity . We analysis too geometry of cooling line and compare them. In designing we considered two important problems first the cooling line can decrease temperature in acceptable range to avoid displacement without generating considerable Vibration and it can be fabricated easily. Vibration occurs because of flow of water in cooling line special in spiral part of it in stems. Generally in experimental velocity of water in this type of pipe has to be under 10 m/s but this is only the limitation of velocity in pipe, for decrease the vibration this value must be more less than 10 m/s , by trying and error in cooling line geometry we tried to archive optimized design in cooling system. These two designs of geometry of cooling line in Dee and stem are shown in Figure 1 and Figure 2. In Figure 1 step of spiral cooling line in stem is changed along the stem but in Figure 2 cooling line has a same step along the stem. First design is harder to fabricate but has less unwanted vibrations and second design is easier to fabricate and has more efficiency in heat transfer but it has more vibration than first one.

Figure 1: Geometry of cooling line first design.

*corresponding author: hafarideh@aut.ac.ir

ISBN 978-3-95450-128-1

RESONATOR SYSTEM FOR THE BEST 70 MeV CYCLOTRON

V. Sabaiduc, G. Gold, B. Versteeg, BCSI, Vancouver, BC, V6P 6T3, Canada
J. Panama, Best Theratronics Ltd., Ottawa, ON, K2K 0E4, Canada

Abstract

Best Cyclotron Systems Inc. (BCSI) is presently developing a 70MeV cyclotron for radioisotope production and research purpose. The RF system comprises two separated resonators driven by independent amplifiers to allow for the phase and amplitude modulation technique to be applied for beam intensity modulation. The resonators are presently in the commissioning phase consisting of cold test measurements to be later followed by high power commissioning in the cyclotron. The electromagnetic modeling has been done with CST Microwave Studio. All simulation results showed a very conservative design with typical parameters for the energy and size of the resonators.

INTRODUCTION

General Description

The RF System is composed from two independent resonators insulated at the center region, amplifiers and LLRF control systems interconnected through local oscillator synchronisation, clock signals and master/slave operation mode as shown in Fig. 1. The high level operation is implemented at the level of the cyclotron PLC control and graphic interface. All RF operational procedures are implemented at the level of the LLRF control digital processing module with FPGA and micro-controller technology.

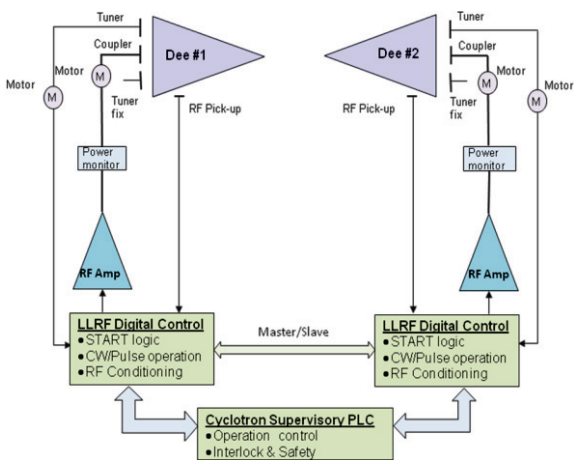

Figure 1: RF System diagram.

The RF system has to operate within specific stability requirements regarding the dee voltage amplitude and phase: dee voltage stability < 5 x 10^{-4} and phase stability <±0.1 degrees. The initial beam intensity is designed for 700μA of negative hydrogen ions to be accelerated to 70MeV.

There are a few advantages in designing separate resonators for high energy cyclotrons that have been considered:

- Symmetric dee voltage distribution
- Reduced coupling power per cavity making the coupler design less critical
- Minimizes cavity mismatch with beam loading, lower VSWR
- Allow for beam intensity control through phase modulation of the accelerating electric field.

RESONATORS

Electromagnetic Model Simulations

Preliminary electromagnetic modeling has been done with CST Microwave Studio and simulation results have been reported [1] and presently updated as the detail design was completed.

The resonators are operating on 4th harmonic and are λ/2 resonant cavities with single stem design. Each resonator cavity is equipped with capacitive coupling and tuning mechanism. An additional fix tuner has been added per cavity to compensate for the slightly difference in frequency due to the dee tip configurations while keeping the same stem length.

Final simulation results are listed in Table 1.

Table 1: Resonator Simulation Results

Parameter	Value
Frequency (4th harmonic)	56.2MHz
Quality factor Q	6800
Power loss per resonator	17.3kW
Shunt impedance	103kΩ
Dee tip/outer voltage	60 to 70.4kV
Maximum current density	5200A/m

Dee voltage distribution is shown in Fig. 2.

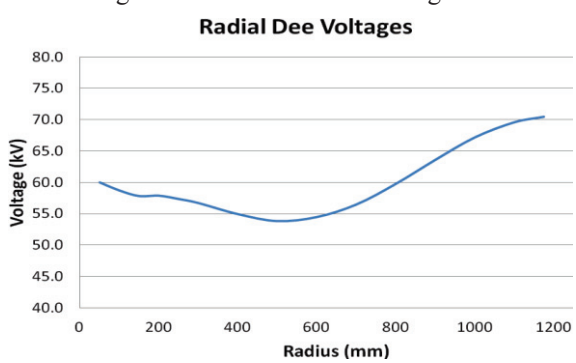

Figure 2: Radial dee voltage distribution.

ISBN 978-3-95450-128-1

CONTROL SYSTEM OF 10-MEV BABY CYCLOTRON

A. Abdorrahman, S. Malakzade, H. Afarideh*, G. R. Aslani, Department of Energy Engineering & Physics, Amirkabir University of Technology, Tehran, 15875-4413, Iran
A. Afshar, Department of Electrical Engineering, Amirkabir University of Technology, Tehran, 15875-4413, Iran
M. Ghergherehchi, J. S. Chai, Department of Energy Science/School of Information & Communication Engineering, Sungkyunkwan University, Suwon 440-746, Korea

Abstract

For controlling all the equipment and services required for operating the 10 MeV baby cyclotron and optimizing various parameters, an extensive control system is used. Most of the control systems are located in the control room which is situated outside the biological shield. The control console in the control room has switches for all the power supplies like main magnet, radio frequency system, vacuum system, ion-source, deflector, etc. Several Programmable Logic Controllers (PLC's) which are located near the equipment control the whole system. A technique of Supervisory Control and Data Acquisition (SCADA) is presented to monitor, control, and log actions of the PLC's on a PC through use of I/O communication interface coupled with an Open Process Control/Object Linking and Embedding [OLE] for Process Control (OPC) Server/Client architecture. In order to monitor and control different part of system, OPC data is then linked to a National Instruments (NI) LabVIEW. In this paper, details of the architecture and insight into applicability to other systems are presented.

INTRODUCTION

As you are designing the cyclotron control system, some requirement must be considered:

• Control subsystems should be integrated into the control system easily.

• The programming system for application programs should be programmer-friendly.

• Incremental amendment and extension should be possible.

• To minimize man-power and efforts, the international collaboration or commercially available products should be applied.

- Easy data access and analysis
- Remote control/diagnostics based on Network
- High level security
- Well defined auto/manual control mode
- Practicable to local control in emergency
- Stable beam current
- Control various devices in real time
- Convenient operation
- Easy maintenance

*corresponding author: hafarideh@aut.ac.ir

The control of Cyclotron is a typical complex real-time system. Generally, it is a hybrid system including both continuous control and dynamic discrete events. But for time response requirements, closed-loop controls are implemented by hardware such as PLC in most cases of cyclotron.

Supervisory control and data acquisition is the basic requirements for distributed control system of industrial process and large-scale equipment like cyclotron, which has high channel counts that demands for keeping track of a large number of data points. Normally, SCADA provides effective approaches to system's high-level monitor and control by combining real-time/historical data collection, logging and trending with friendly dynamic graphic indicators

Control architecture of system control is a three layer architecture comprising of device layer, server layer and user Interface layer. The device layer consists of PLCs which controls the automatic process sequence operations. The PLCs and the process components are configured to satisfy fail-safe operation [1].

The user interface layer consists of the control computers where the operators issue, the set points and the mode of operation commands. The alarm and historical archive are also running in this layer.

PLC OVERVIEW

Programmable Logic Controllers (PLCs) [2] are diskless compact computers including all the necessary software and hardware interfaces to the process. They are generally used for automation control application either standalone or connected to distributed inputs/outputs, to other PLCs and/or to supervision PCs. The connections are established by means of field buses such as PROFIBUS or Ethernet. An example of this connection is shown in Fig. 1.

ISBN 978-3-95450-128-1

THE DEVELOPMENT OF CONTROL SYSTEM FOR 9 MeV CYCLOTRON*

Y.S. Lee, J.K. Park, Y.H. Yeon, S.H. Lee, S.H. Song, H.S. Kim, S.H. Kim, S.Y. Jung, S.W. Shin, J.C. Lee, H.W. Kim, J.S. Chai,#
College of Information & Communuication Engineering / WCU Department of Energy Science
Sungkyunkwan University,Korea
K. H. Park, PAL, POSTECH, Pohang, Korea

Abstract

The Sungkyunkwan University has developed the 9 MeV cyclotron for producing radio isotopes. In order to operate the cyclotron stably, all sub-systems in the cyclotron are controlled and monitored consistently. Each sub-system includes its own control devices, which are developed based on PLC or DSP chip and the sub control modules interface with main control system in real time. For the main control system, we choose the Compact-RIO platform from NI (National Instrument) to take into account for a fast latency and a robust control. The main control system has high-performance processor running hard real-time OS so that the system can control the cyclotron in a fast and an exact manner. In addition, the system can be remotely accessed over the network to monitor the status of cyclotron easily. The configuration of the control system for 9 MeV cyclotron and performance test result will be presented in this paper.

OVERVIEW OF THE 9 MeV CYCLOTRON

The cyclotron accelerates the negative hydrogen particle to produce radioisotopes, and a couple of sub-systems make the particle acceleration possible. The cyclotron consists of magnet system, RF system, ion source system, vacuum system, and cooling system. The detail configuration of cyclotron is demonstrated in Fig. 1.

In order to accelerate the particle stably, it is necessary for the environment to maintain the constant temperature and humidity, fundamentally. In addition, the degree of vacuum inside cyclotron should be under 1 x 10^{-6} mbar. A double-stage high-vacuum system has been installed to improve the vacuum state as the time to reach the vacuum level. The cyclotron includes a panning ion gauge (PIG) type ion source for generating negative hydrogen from plasma by the use of arc power supply outside of cyclotron. The electromagnet field made by both RF system and magnet system accelerates the negative hydrogen for the desired energy level. The RF system is composed of two parts which are RF resonator and RF amplifier. The RF amplifier provides the high power RF signals to RF cavity to increase the dee voltage up to 40kV for electric field inside the cyclotron. The electric field is regulated by RF tuner. The average magnetic field is 1.36T generated by about 138A coil current from magnet power supply (MPS) [1].

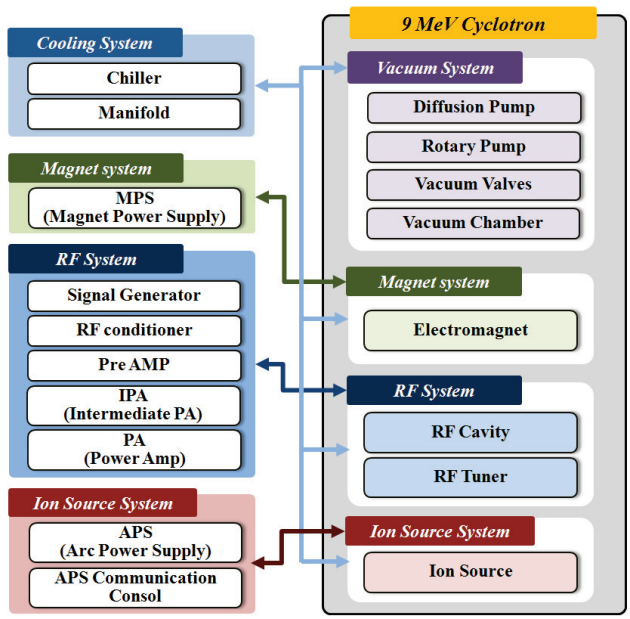

Figure 1: Configuration of 9 MeV cyclotron.

Table 1: Specification of Primary Control Parameters

System	Parameter	Specification
Magnet	Coil current	138A (±10ppm)
RF	Frequency	83.2 MHz
	RF mode	CW / Pulse
Ion source	H_2 gas flow rate	0 ~ 10 SCCM
	Arc current	0 ~ 2 A
	Arc voltage	0 ~ 2 kV
Vacuum	Degree of vacuum	1 x 10^{-6} mbar
Cooling	Water Temp.	< 20 ℃
	Water Resistivity	> 10 MΩ

*Work supported by Nuclear R&D program through the National Research Foundation of Korea funded by the Ministry of Education, Science and Technology (2012-0925001)
#jschai@skku.edu

ISBN 978-3-95450-128-1

TEMPERATURE STABILITY OF THE TRIUMF CYCLOTRON RF CONTROLS

M. Laverty, K. Fong, Q. Zheng, TRIUMF, Vancouver, Canada

Abstract

Factors which contribute to ambient temperature sensitivity in the TRIUMF cyclotron RF control system are examined and characterized. Seasonal temperature variations together with air conditioning system limitations can give rise to unwanted temperature variations in the rack space housing the control system. If these are large enough, they can cause excursions in the cyclotron accelerating voltage. The critical components responsible are characterized and some possible remedies outlined.

INTRODUCTION

The current cyclotron control system has been in operation for a number of years [1]. The megawatt or so of power circulating in the resonators is controlled using a feedback signal from two centrally located voltage probes. A network of monitoring probes is used to fine tune individual resonators, and can also be summed and averaged to give a dee voltage reference reading that is independent of the control system. Recently, some discrepancies have been noted between the voltage reported by the control system and that given by these voltage probes.

In an attempt to shed some light on the causes of these discrepancies, both the rf control system and the voltage probe monitoring system were investigated in some detail. The results of those investigations form the subject of this paper.

CYCLOTRON VOLTAGE PROBES

Since these probes were being used as a reference, and no performance data on them was available, a closer examination was undertaken. There are 60 of these probes distributed across all four quadrants of the cyclotron. These lead to the bank of detectors shown in Fig. 1. Approximately 2-3 watts of power is drawn from each probe, which must be dissipated by the detector electronics. Finned aluminium extrusions are used. It may be noted that these are located horizontally, and spaced quite close together, which somewhat reduces their efficiency.

To get a picture of the temperature gradients experienced at the detectors, measurements were taken at each end of the heatsink serving a bank of eight detectors. These measurements, which were taken at an ambient temperature of 22.7 degrees, are summarized in Table 1. A range of temperatures spanning 7.5 degrees can be observed, with the coolest temperatures at the detectors located at the bottom of the array, and the warmest in the upper central region.

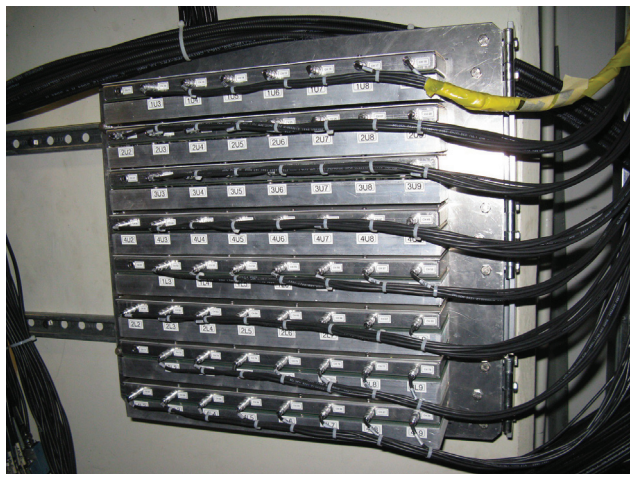

Figure 1: Cyclotron voltage probe detectors.

Table 1: Detector Temperatures (degrees C)

Detector	Left	Right
Upper Q1	44.4	44.5
Upper Q2	47.9	47.1
Upper Q3	49	47.7
Upper Q4	47.1	47.1
Lower Q1	47.1	46.5
Lower Q2	46.5	43.6
Lower Q3	45.9	43.9
Lower Q4	43.5	41.5

To determine if these temperature variations as well as potential ambient temperature variations were significant, information on the temperature sensitivity of the detector circuit was required. Since this was not available, the detector circuit was examined in more detail. A photo of the detector circuit is shown in Fig. 2. The circuit used is a conventional half wave diode detector. The heat sink mounted 50 ohm terminating resistor is visible, as is the detector diode, low pass filter, and an output clamp diode.

To determine the temperature sensitivity without a proper environmental chamber, the heatsink was insulated, and self heating used to gradually raise the temperature of the detector. This limited the temperature range to 10-15 degrees C or so, but this covers the observed operating range of the detector array, and also leaves room for some ambient temperature variation.

ISBN 978-3-95450-128-1

THE DEVELOPMENT OF RADIAL PROBE FOR CYCIAE-100

FengPing Guan, HuaiDong Xie, LiPeng Wen, TianJue Zhang, ZhenGuo Li, ZhiGuo Yin, Chuan Wang, CIAE, Beijing, China

Abstract

In the design of CYCIAE-100 beam diagnostics system, three radial probe targets distribute on three directions above magnetic pole and in the valley on the median plane of cyclotron. These radial probe targets can be used for beam center measurement. By blocking beam on five fingers and one stopping block, the radial probe target can measure the radial and axial distribution of H^- beam at the same time. During beam commissioning, the radial probe targets can also be used for beam intensity measurement. The changeable target tip design makes it possible to replace the damaged part and optimization of the structure. The mechanical and control part of radial probe target system is finished, assembly and prime test of the whole system will be carried out in September.

DESIGN OF RADIAL PPROBE

The project of Beijing Radioactivity Ion-beam Facility (BRIF) is being constructed at China Institute of Atomic Energy (CIAE). As a major part of the BRIF project, a 100MeV compact cyclotron (CYCIAE-100) will provide proton beam with an intensity of 200μA～500μA [1].

CYCIAE-100 is a compact isochronous cyclotron. The radius of magnetic pole is 2000 mm, yoke is 3080 mm, air gap between 46-60 mm. Large radius with small axial space plus high requirement of isochronous magnetic field, all these factors lead to the following design of radial probe target: 4580 mm long, placed on the median plane of CYCIAE-100 cyclotron, above the surface of magnetic pole, bellows with compression ratio as high as 0.234 is chosen for vacuum seal. The moving range of radial probe target is 2020 mm to assure the radial probe measurement range near the centre of CYCIAE-100 [2]. When not measuring, radial probe target is blocked off from main vacuum chamber by a gate valve. The position of three radial probe targets on CYCIAE-100 is shown in Fig. 1.

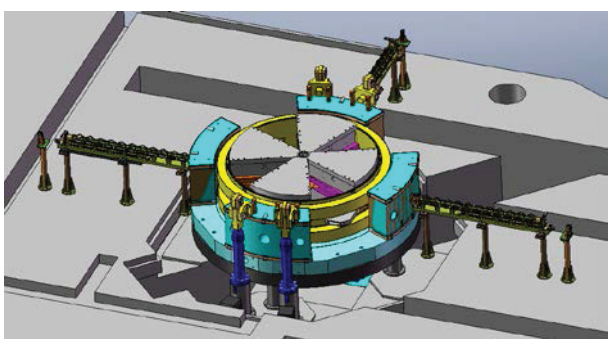

Figure 1: Radial probe targets on CYCIAE-100.

For the purpose of beam center measurement, three radial probe targets will be installed on three directions above magnetic pole and in the valley on the median plane of CYCIAE-100 cyclotron. Meanwhile, at low energy, radial probe target with water cooling can get real time beam intensity which is important parameter for prime beam commissioning. The main functions of radial probe target are as follows:

Get Beam Distribution on Axial and Radial Directions at the Same Time

The radial probe target tip, making up by five fingers and one stopping block in front, get the beam distribution on axial and radial directions by blocking the beam. Radial probe target tip is made by copper. The five fingers' positions are decided according to the calculated axial beam distribution. The five cuboid fingers with 0.5mm cuneate tip outside the stopping block can satisfy the radial resolution requirement. The five fingers are symmetrical to the median plane of CYCIAE-100, as shown in Table 1.

Table 1: The Size of Five Fingers

Finger No.	Position	Size
1	Top	9mm
2	Upper	6mm
3	Middle	4mm
4	Lower	6mm
5	Bottom	9mm

Between the five fingers and the stopping block is a layer of heat conducting ceramic, this can enhance the effect of water cooling. The structure of radial probe target tip 1 are shown in Fig. 2.

Figure 2: Structure of radial probe target tip 1.

ISBN 978-3-95450-128-1

A PROFILE ANALYSIS METHOD FOR HIGH-INTENSITY DC BEAMS USING A THERMOGRAPHIC CAMERA

Ken Katagiri*, Satoru Hojo, Akira Noda, Koji Noda, NIRS, Chiba, Japan
Toshihiro Honma, Accelerator Engineering Corp., Chiba, Japan

Abstract

A new analysis method for the digital-image processing apparatus has been developed to evaluate profiles of high-intensity DC beams from temperature images of irradiated-thin foils. Numerical calculations were performed to examine the reliability and the performance of the profile analysis method. To simulate the temperature images acquired by a thermographic camera, temperature distributions were numerically calculated for various beam parameters. The noises in the temperature images, which are added by the camera sensor, were also simulated to be taken its effect into account. By using the profile analysis method, the beam profiles were evaluated from the simulated-temperature images, and they were compared with the exact solution of the beam profiles. We found that the profile analysis method is adaptable over a wide beam current range of $\sim$0.1$-$20 μA, even if a general-purpose thermographic camera with rather high noise ($\Delta T_{\mathrm{NETD}} \simeq$ 0.3 K; NETD: Noise Equivalent Temperature Difference) is employed.

INTRODUCTION

Beam profile measurement in a beam transport line is important for providing high-quality beams at accelerator facilities. To measure the beam profile, one can employ several types of beam monitors, such as wire monitors and scintillation screens [1]. Wire monitors such as wire scanners and profile grids have a high tolerance for high-current beams, and are thus widely used, especially in high-intensity accelerator facilities. However, when measuring beam profiles including hollow structures, the wire monitors fail to give the correct profile, because information from wire monitors is a one-dimensional projection of the beam profile along the x- or y-axes [1]. Scintillation screens are also employed to measure the profiles of high-intensity beams, but are not suited to measure high duty factor DC beams because the CCD camera pixels usually used in scintillation screen systems are easily damaged by secondary neutrons. A new improved monitor is required for the stable measurements of the beam profile in high-intensity accelerator facilities.

Under those background, we proposed a simple diagnostic system including a thermographic camera and a thin foil, in which the heat source distribution caused by beam irradiation and heat conduction can be treated as two-dimensional. The microbolometer used in the thermographic camera is tolerant of neutron radiation in the accelerator facilities that provide high-intensity DC beams[2]. Also, the diagnostic system can be quasi-nondestructive if the target plate can be thin for the incident beams. For those reasons, the simple diagnostic system can be expected to be used in high-intensity accelerator facilities. To evaluate an accurate beam profile from the temperature distribution obtained by the thermographic camera, we developed a new algorithm for a digital image processing apparatuses. The algorithm accurately converts a temperature profile to a beam profile using a discretized Poisson equation with averaging and filtering procedures.

Temperature images acquired by a thermographic camera contain noise from the camera sensors. To investigate degradation of the converted beam profile due to noise and evaluate reliability of the algorithm, we performed numerical analyses using simulated temperature images. To simulate temperature images acquired by a thermographic camera, temperature distributions were numerically calculated for various beam parameters. Camera noise was also simulated to consider its effect. We then converted the simulated temperature images into beam profiles using the algorithm. The converted beam profiles were compared with exact solutions of the beam profiles. We present the results of the comparison between the converted beam profiles and the exact solutions. From these results, we discuss how noise in the temperature images affects the accuracy of converted beam profiles. We then examine the effect of averaging and filtering procedures to obtain more accurate beam profiles.

CONVERSION ALGORITHM

The simple diagnostic system including a thermographic camera and thin foil is shown in Fig. 1. Beams incident on the thin foil pass through it. The beams then irradiate the main target, which is installed downstream for the primary purpose, such as radioisotope or neutron beam production. A thermographic camera installed at an angle diagonal to the beam axis measures the temperature distribution in the thin foil.

The conversion method requires simplification to minimize its calculation cost for use in digital image processing apparatuses. The conversion method is therefore represented by a two-dimensional rather than three-dimensional model. If the beam intensity is constant, and the foil is thin enough to consider energy deposition of the incident beams as uniform along the z-axis, then the relation between the temperature distribution $T(x, y)$ and the heat-source distribution caused by the incident beams $S(x, y)$ is expressed by a two-dimensional steady-state heat conduction equation,

$$\frac{\partial^2 T(x,y)}{\partial x^2} + \frac{\partial^2 T(x,y)}{\partial y^2} = -S(x,y)/\lambda(T). \qquad (1)$$

* tag410@nirs.go.jp

ISBN 978-3-95450-128-1

DEVELOPMENT OF RAPID EMITTANCE MEASUREMENT SYSTEM

Keita Kamakura*, Kichiji Hatanaka, Mitsuhiro Fukuda, Tetsuhiko Yorita, Hiroshi Ueda, Takane Saito, Shunpei Morinobu, Keiichi Nagayama, Hitoshi Tamura, Yuusuke Yasuda, Mitsuru Kibayashi, Hirofumi Yamamoto, Noriaki Hamatani, RCNP, Osaka, Japan

Abstract

We have developed a new system to measure the beam emittance [1]. With our conventional emittance measurement system, it takes about 30 minutes to get emittances in both the horizontal and vertical plane. For quick measurements, we have developed a new system consisting of a continuously driven slit with a fixed width and a BPM83 (rotating wire beam profile monitor). BPM83 uses a rotating helical wire made of tungsten, the speed is 18 rps. Continuously driven slit consists of a shielding plate with two slits, and is inserted into the beam path at an angle of 45 degrees.

The slit is driven by PLC controlled stepping motor, and it takes 70 seconds to move the full stroke of 290 mm. While moving the slit, the output from BPM83 and the voltage of potentiometer that corresponds to the slit position are recorded simultaneously. We are using CAMAC for data acquisition. Trigger signals are generated by BPM83 and NIM modules. Data analysis takes about 1 second. With this system we can get the horizontal and vertical emittance plots within 75 seconds. This system will definitely make it easier to optimize parameters of ion sources and the beam transport system.

INTRODUCTION

At RCNP, various ion beams are generated in three ECR ion sources and accelerated with AVF Cyclotron (K = 140 MeV) and Ring Cyclotron (K = 400 MeV). The schematic diagram of RCNP cyclotron facility is shown in Fig. 1. Beams are used widely for fundamental and applied physics experiments e.g. precise nuclear physics

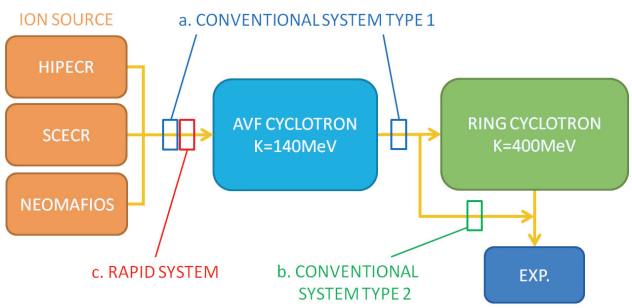

Figure 1: Schematic diagram of RCNP cyclotron facility. One type of conventional emittance measurement systems and the rapid emittance measurement system that will be discussed in this paper are installed in the downstream of three ECR ion sources [2].

* keita@rcnp.osaka-u.ac.jp

experiments that combines light ion beam with high energy precision ($\Delta E \sim 0.01\%$) and ultra-high resolution spectrometer Grand-RAIDEN, furthermore experiments using secondary particles (UCN, muon, etc.) by high energy proton beam. At present, the current of 400 MeV proton beam is confined to about 1μA after Ring Cyclotron. However an improvement for beam current intensity and quality is planned for experimental demands e.g. increasing of statistics for precise nuclear physics experiments using high quality beam, supplying halo-free beam for 0° experiments, UCN and muon experiments. For that purpose, an improvement of transport efficiency, furthermore speeding up of beam diagnosis and control are getting to be essential.

One of the causes to lower the beam transport efficiency is the problem that the beam extracted from ion source is not injected to AVF Cyclotron effectively. To solve the problem, it is important to match the injection beam emittance with the acceptance of AVF Cyclotron. In order to attain that, we have to minimize the ion-source beam emittance and maximize its intensity, namely, to increase brightness. Besides, parameters of ion source and beam transport system should be modulated to match phase space distribution of injection beam with the phase space area of AVF-Cyclotron's acceptance.

To bring up the brightness of the beam extracted from ion source, we need to measure emittance repeatedly, and optimize the parameter for ion source. Though, conventional emittance monitor with beam slits and three-wire profile monitor takes about 20∼30 minutes to acquire data for emittances in both the horizontal and vertical plane, furthermore, we needed to calculate manually for getting emittances and phase space distributions. Therefore it is difficult to measure repeatedly to optimize operation parameter. For this purpose, reduction of data acquisition time and analysis time in emittance measurement is getting to be a crucial issue.

RAPID EMITTANCE MEASUREMENT

There are two types of conventional emittance measurement systems in our facility. Both systems use three-wire profile monitor (TPM), and it takes about 1 minute to acquire a beam profile with TPM. Although it depends on the position resolution we set, the whole data acquisition takes about 20∼30 minutes for that reason. In conventional systems the profile measurement is a rate-limiting step. If the interval of profile measurement is short enough compared to the slit movement, we can reduce measuring time drastically by measuring profiles and moving the slit simultaneously (Fig. 2).

ISBN 978-3-95450-128-1

VARIANTS OF GROUNDING AND SHIELDING IN A BEAM DIAGNOSTICS MEASUREMENT OF LOW SIGNAL CURRENTS

R. Dölling, Paul Scherrer Institut, CH-5232 Villigen PSI, Switzerland

Abstract

The performance of several variants of grounding and shielding of long measurement cables for small currents against ground potential differences has been estimated analytically.

INTRODUCTION

In the large part, the beam diagnostics at the PSI cyclotrons and beam lines utilize low signal currents of low frequencies generated by the beam. This includes collimators, segmented aperture foils, wire scanners, harps, and ionization chamber based loss, current and profile monitors. The current measurement electronics, in most cases logarithmic amplifiers, are located outside the vault in order to prevent radiation damage and to allow for permanent service access. Hence, signal cables of 30 to 150 m length are needed. In order to preserve the signal quality, the prevention of ground loops is the most important factor. An appropriate grounding scheme, using "floating" amplifiers, has been applied at PSI by L. Rezzonico and U. Frei since 1989 [1]. Nevertheless, in some instances, with the presence of strong noise sources, this comes to its limits. This can be e.g. motors driven by switching power supplies over long cables, having insufficient EMI measures.

There are many possible variants for grounding and connecting the individual cable shields. Figure 1 depicts several variants which have been examined analytically and are discussed in the following. Variant b1) is used at the present diagnostics of the HIPA facility [2], variant c) at the Proscan beam line diagnostics [3]. Variants d1), d2) are under consideration for the diagnostics in the beam lines to the new Gantry 3 at Proscan. Although we restrict ourselves here to a single cable length (50 m) and the parameters of our "LogIV" logarithmic amplifiers [1], quite general conclusions can still be drawn. This is helpful for assessing quantitatively the determining factors and guiding the way to improvements.

MODEL AND DERIVATION

The model for the variants d) and e) (two shields), taking into account or not the "bridge elements" introduced by the DC-DC converters and differential amplifiers isolating a group of four logarithmic amplifiers from "rack ground", is depicted in Fig. 2. For variants b) (only one shield) and a) (only a "shield", which is part of a ground loop) this model is stripped down accordingly.

Based on Maxwell Equations, the definition of conductivity and the utilization of symmetries, the theory of shielded cables was developed in the 1930s. A systematic description is given in the book of Kaden [4], including coaxial cables, skin effect, conductive and magnetic shields and the coupling of a perturbing signal from outside to inside. We adopt this formalism with the additional boundary condition that the shields #1 and #2 are connected galvanically only at one end (and not at both ends or many locations in between as assumed in [4]). Furthermore the capacitive and inductive coupling through the small holes in the braided shield is added in the way given by Vance [5, 6]. Hereby the variants have been described approximatively by analytical equations which have been evaluated numerically [7]. In the following, this procedure can only be adumbrated.

References to equation numbers from [4] are given in curly brackets. We adopt the notation of [4], borrowing in some instances from [6]. Apostrophes are added to indicate the normalization to unit cable length. Tildes are added to indicate time-varying parameters. The subscript notation is adapted to indicate the involved shield numbers according to Fig. 2. The purely ohmic resistance is indicated by the subscript "ohm" (instead of "0" which is used here for the center conductor).

The assumed source of disturbance is the periodic potential difference $\tilde{U}_\mathrm{g} = \hat{U}_\mathrm{g} \sin \omega t$ between "detector ground" ($\equiv 0$ V) and "rack ground" which establishes linearly over the inner surface of "shield" #3 (which substitutes the cable tray). The local current difference $\tilde{I}'_2(s) \approx C'_{23}\, \boldsymbol{\alpha}_{23}\, \dot{\tilde{U}}_{3\mathrm{i}}(s)$ at shield #2 is generated (and mainly determined) by capacitive coupling. (For frequencies below 100 kHz it is $\boldsymbol{\alpha}_{23} \approx 1$.) The integral local current is then $\tilde{I}_2(s) \approx \int_s^{s_\mathrm{max}} \tilde{I}'_2(s)\, \mathrm{d}s$, which causes a local voltage drop and hence a potential at the outside of shield #2 of $\tilde{U}_{2\mathrm{e}}(s) = \int_0^s \tilde{U}'_{2\mathrm{e}}(s)\, \mathrm{d}s = \boldsymbol{R}'_2 \int_0^s \tilde{I}_2(s)\, \mathrm{d}s$ with $\boldsymbol{R}'_2 = R'_2 + \mathrm{i}\omega L'_2 = R'_{2\mathrm{ohm}}\, k_\mathrm{Cu} d_2^* \coth(k_\mathrm{Cu} d_2^*)$ {L23, E23} the inner impedance. The local voltage drop at the inside of shield #2 is then $\tilde{U}'_{2\mathrm{i}}(s) = \boldsymbol{Z}'_2\, \tilde{I}_2(s)$ with the transfer impedance $\boldsymbol{Z}'_2 = \boldsymbol{R}'_{\mathrm{K2diff,1layer}} + \mathrm{i}\omega M'_2$ of shield #2 including the coupling resistance (named also diffusion part) $\boldsymbol{R}'_{\mathrm{K2diff,1layer}} = R'_{2\mathrm{ohm}}\, k_\mathrm{Cu} d_2^* / \sinh(k_\mathrm{Cu} d_2^*)$ {L25} and already a term for coupling inductively through the braid. If the 1-layer shield is replaced by a compact 3-layer shield with central magnetic layer, the corresponding term is $\boldsymbol{R}'_{\mathrm{K1diff,3layer}} = \frac{\boldsymbol{R}'_{\mathrm{K1Cu}}\, \boldsymbol{R}'_{\mathrm{K1Cu}}}{\boldsymbol{R}'_{\mathrm{1Cu}} + \boldsymbol{R}'_{\mathrm{1Cu}} + \mathrm{i}\omega L'_{\mathrm{1Mu}}}$ with coupling resistance $\boldsymbol{R}'_{\mathrm{K1Cu}}$, inner impedance $\boldsymbol{R}'_{\mathrm{1Cu}}$ {E23} and interspace inductance L'_{1Mu} {L27}. Integration gives the local potential $\tilde{U}_{2\mathrm{i}}(s) = \int_0^s \tilde{U}'_{2\mathrm{i}}(s)$ along the inside of shield #2.

The same procedure is performed for shield #1 including terms for the bridge elements and capacitive coupling through the braid of shield #2.

Coupling to the inner measurement loop is derived using Fig. 2B with the assumption that C_det, C_inj are relatively small.

ISBN 978-3-95450-128-1

MEASUREMENT OF TURN STRUCTURE IN THE CENTRAL REGION OF TRIUMF CYCLOTRON*

T. Planche, Y.-N. Rao, R. Baartman, TRIUMF, Vancouver, BC, Canada

Abstract

To get the most out of the existing beam diagnostics in the TRIUMF cyclotron, we started in 2011 to develop new data processing and visualization tools. The main advantage of these Matlab©-based tools, compared with old VMS-based tools, is that they can benefit from a much larger library of modern data processing and visualization algorithms. This effort has already shown itself very useful to highlight essential features of the beam dynamics which remained unnoticed before. In this paper we present measurement results displaying beam dynamics processes taking place in the central region of the TRIUMF 500 MeV cyclotron.

INTRODUCTION

The TRIUMF 500 MeV cyclotron is equipped with five radially moving probes primarily dedicated to beam diagnosis. Among these five probes, two are low energy (LE) probes, covering the region between $R = 13.89$ and 161.5 inch (corresponding to $\sim$ 0.5 − 85 MeV). These two probes move along identical rails placed 180° apart (see Fig. 1). The two LE probes have identical heads. They consist of five horizontal fingers, plus a large plate, which shields them from the beam except for the leading 0.075 inch (see Fig 2). The probe heads can take no more than about 0.5 μA, which requires that measurements are taken at very low duty cycle. Details concerning the design of the head can be found in this reference [1].

Measurement results presented in this paper have been chosen to highlight key features of the beam dynamics in the central region of the TRIUMF cyclotron.

PHASE-DEPENDENT DYNAMICS

The TRIUMF 500 MeV cyclotron accelerates H^- ions, and uses charge exchange extraction. No turn separation is required for extraction, which allows a very large phase acceptance (up to 60° [2]). The ion source produces a cw beam, which can be bunched by means of two rf cavities in the injection line. The first bunching cavity works at the same frequency that the cyclotron (first harmonic), which is the fifth harmonic of the revolution frequency; the second one works at twice this frequency to partially compensate the non-linearity of the first harmonic sine wave.

The azimuthal field variation is practically negligible in the central region, due to the fact that the injection radius ($\sim$ 11 inch) is smaller than the magnetic gap height (18 inch). Without azimuthal field variation, the sole source of vertical focusing is the rf gaps. This makes vertical focusing in the central region of TRIUMF cyclotron phase dependent.

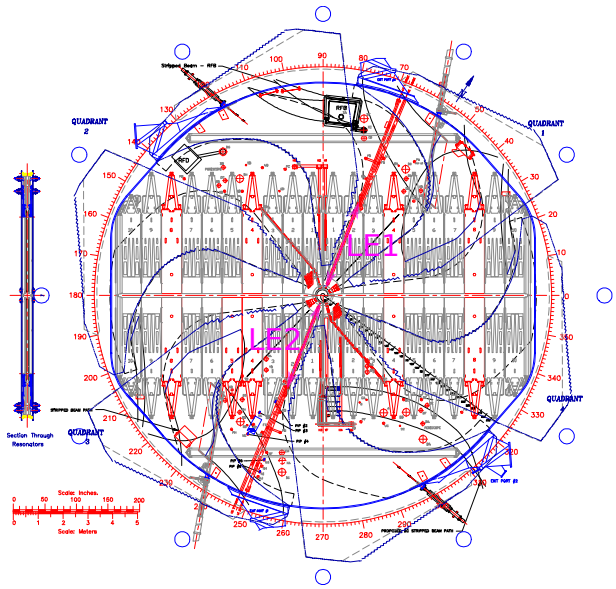

Figure 1: Schematic view of the TRIUMF cyclotron. The two low energy probes are indicated in magenta.

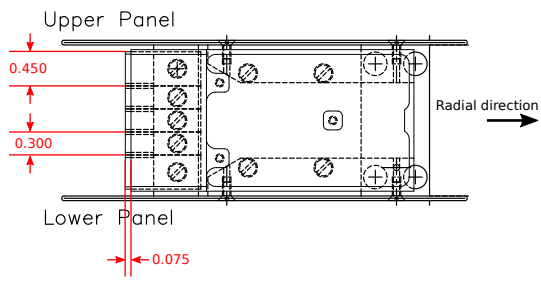

Figure 2: Schematic drawing of the low energy probe head. Dimensions are given in inch.

To study the behavior of each individual phase we inject very short bunches, and follow their evolution with the LE probes. To achieve very short bunches, space charge is greatly reduced by inserting in the injection line, upstream of the bunchers, a pepper pot. This device reduces the charge by a factor $\sim$ 50 without affecting the beam emittance. We set the amplitude of the first harmonic buncher to arrive at the injection gap with most of the particles gathered within a narrow phase window, as illustrated in Fig. 3 (a) and (b). After injection into the cyclotron and acceleration though the Dee gaps, the particle distribution as seen by the LE probes generally presents two peaks (see

*TRIUMF receives federal funding via a contribution agreement through the National Research Council of Canada.

ISBN 978-3-95450-128-1

SIMULATION OF SUFFICIENT SPINDLE CUSP MAGNETIC FIELD FOR 28 GHz ECRIS

M. H. Rashid# and A. Chakrabarti, VECC, 1/AF- Bidhannagar (Salt Lake), Kolkata 700064, India

Abstract

A cusp magnetic field (CMF) configuration is proposed for achieving more plasma confinement. It is an improved version of CMF compared to the classical one used earlier to design arbitrarily ECR ion source (ECRIS) of low frequency. The CMF has been reconfigured here adopting a simple, novel and cost-effective technique to shrink the loss area and to achieve denser plasma than in traditional ECRIS. It consists of a mid-iron disk, two end-plugs and a pair of superconducting magnet coils cooled by cryo-coolers. It is designed for high-B mode operation of the cusp ECRIS of as high as 28 GHz RF frequency for producing an intense beam of highly charged heavy ions. The electric current in the coil at the extraction end can be manipulated to optimize the operation to achieve high extracted beam current of highly charged ions.

INTRODUCTION

Significant developments took place in fabrication of ECRIS after its invention in Grenoble, France by the ion source group led by Geller in 1970's. They built early ECRIS'es, MAFIOS and its variant [1, 2] and show their superb feature in terms of charge state of ions achievable and ion beams extractable. The salient features of the ECR plasma including its production and confinement in minimum-B field and techniques to improve further the workings of an ECRIS have been described in detail [3]. With special design of superconducting magnets for as high frequency as 28 GHz of powerful microwave, Gammino et al [4] explored the possibility of constructing third generation ECR ion source called GyroSERSE, which opened the way to a new operational domain having the highest plasma densities, ~10^{13} cm^{-3}.

The electrons crossing the iso-Gauss surface, B_{ECR}, gain energy due to transfer of energy from the EM wave to electrons through ECR process when electron gyration is in resonance with RF ($f_G = f_{RF}$). A magnet system for a conventional source using higher microwave frequency is complex, consume more electric power and more complicated forces act on the coils and coil bands. Thus, the magnet system becomes complex. The scaling laws for ECR ion source design are well known [3].

The motivating factors of the present study are i) constructing a simple and compact but superb ECRIS of higher RF frequency, ii) producing dense large volume of plasma consisting of high charge state ions (HCI's), iii) more confinement of electrons for heating the electrons electromagnetically through ECR process, iv) sufficient confinement of ions for further step-wise stripping and v) shorter magnetic cusp line of plasma loss region. Some earlier attempts were taken to understand theoretically the plasma confining feature of the simulated sufficient spindle CMF for lower frequencies [5]. After we are satisfied for higher and higher frequencies in generation and confinement of high density plasma theoretically, we should go for experimental test of the superior CMF principle and proposed design. There is an on-going effort by the LPSC-IN2P3 group at Grenoble for development of a 60 GHz ECRIS based on shouldered CMF configuration. They produced the required magnetic field [6] related to the frequency using helix-coils in agreement with the scaling laws. Here we are proposing field design for 28 GHz RF frequency in a larger chamber volume immersed in the CMF.

#E-mail: haroon@vecc.gov.in

SUPERIOR SPINDLE CMF

We assume that axial length and diameter of the chamber are 2L. The radial ($B_r(r,z)$) and axial ($B_z(r,z)$) field components on the point cusp (PC) and ring cusp (RC) are of magnitude B_0; they are given by Eqs. 1 and 2 respectively derived from A_θ in Eq. 3 to maintain field symmetry and effective mirror action.

$$B_r(r,z) = -Gr - 3\,\mathrm{Pr}\,z^2 - Qr^3 \quad (1)$$

$$B_z(r,z) = 2Gz + 2Pz^3 + 4Qr^2 z \quad (2)$$

$$A_\theta(r,z) = -Grz + Pz^3 r + Qr^3 z + C \quad (3)$$

Where *G, P, Q* and *C* (say 0) are constants. The magnetic field is taken to be that of vacuum and the plasma current effect is neglected. The constants G, P and Q are evaluated adopting three constraints. The first constraint, must be satisfied as there is no electric current inside the chamber, which sets the constant Q = - (3/4)P. Another two boundary constraints $B_r(L,0) = -B_0$ and $B_z(0,L) = B_0$ set the constants $G = (11B_0)/(14L)$ and $P = (-2B_0)/(7L^3)$. Thus, A_θ and desired field components are defined, in general, to generate symmetric and spindle CMF. The theoretically obtained field for L=16 cm and B_0=40 kG can be numerically reproduced in reality as under.

PROPOSED CMF ECRIS DESIGN

Earlier, application of old CMF of low and asymmetric magnetic field to confine plasma was limited because of huge plasma loss mainly at the RC position. Some crucial attempts to understand the features and associated problems of the old CMF have been reported recently. The papers [5] deal with the technique to get an improved configuration of CMF for microwave frequency 14.4 and 18.0 GHz. Superconducting coils can be used to achieve it corresponding to higher microwave frequencies. Here a design is described for f_{RF} =28 GHz and B_{ECR} =10 kG with improved field mainly at the RC, which at least is

ISBN 978-3-95450-128-1

CHARACTERIZATION OF THE VERSATILE ION SOURCE (VIS) FOR THE PRODUCTION OF MONOCHARGED LIGHT ION BEAMS

L. Celona#, S. Gammino, L. Calabretta, G. Castro, D. Mascali, L. Neri, G. Torrisi and G. Ciavola, INFN- LNS, via S.Sofia 62, 95123 ,Catania, Italy
F. Di Bartolo, Università degli Studi di Messina, Dipartimento di Fisica e Astronomia, Ctr. Papardo Sperone, Messina, Italy

Abstract

The Versatile Ion Source (VIS) is an off-resonance Microwave Discharge Ion Source (MDIS) which produces a slightly overdense plasma at 2.45 GHz of pumping frequency. In the measurements carried out at INFN-LNS in the last two years, VIS was able to produce more than 50 mA of proton beams and He^+ beams at 65 kV, while for H_2^+ a current of 15 mA was obtained. The know-how obtained with the VIS source has been useful for the design of the proton source of the European Spallation Source, to be built in Lund, Sweden, and it will be useful also for other facilities. In particular, the paper deals about the design modifications of VIS, in order to use it as injector of H_2^+ of the ISODAR facility, will be also presented.

INTRODUCTION

The VIS source [1] is a MDIS installed at INFN-LNS as test-bench for the production of high intensity, low emittance proton and light ion beams and for studies of plasma physics [2]. In VIS a slightly overdense plasma is generated by means of a 2.45 GHz off-resonance discharge in the 0.1 T magnetic field produced by a movable permanent magnets system. A four electrodes extraction system allows extracting the ion content and injecting it in the LEBT. The entire source has been designed in order to present many advantages in terms of compactness, high reliability, capability to operate in cw mode or in pulsed mode, reproducibility, and low maintenance.

VIS is able to produce up to 50 mA of low emittance (< 0.2 π.mm.mrad) proton beams, but opportune modifications in the experimental set-up are needed depending on the ion to be optimized. In particular, in the following paper we focus our attention to the production of H_2^+. The use of this molecule instead of H^+ may represent a solution of the space charge effects affecting the acceleration of high intensity proton beams. H_2^+, indeed, allows the decrease of the generalized perveance, the parameter which measures the space charge effect, because of the larger m/q ratio with respect to protons. Generation of a high intensity (25-50 mA) H_2^+ beam is key point of the IsoDAR [3] and DAEδALUS [4] experiments. Both these experiments will make use of a MDIS as injector of a new high power cyclotron. Since the intensity of H_2^+ beams generated by VIS is not enough to satisfy the IsoDAR requirements, a series of studies and design modifications on the VIS source to increase H_2^+ intensity has been carried out.

#celona@lns.infn.it

He^+ AND H_2^+ PRODUCTION WITH VIS

The production efficiency of different ions is strictly related to the characteristics of the plasma which generate them. Modification of the VIS experimental set-up can affect directly the plasma parameters; it has been shown that the shift of the permanent magnets affects the plasma electron temperature [5], while the insertion of insulators, like BN at the endplates of the source, or an alumina tube embedded along the walls of the plasma chamber, can affect the ion lifetime and density [6,7]. He^+ ions are generated by means of ionization of the neutral helium due to electron impact. The cross section of the ionization reaction gets the maximum above 100 eV electron temperature, a value much larger than the usual electron temperature in MDIS (20-25 eV). The plasma temperature has been modified by shifting the permanent magnets with respect to the plasma chamber. The magnets system has been moved with steps of 2 mm from the home position towards the microwave line, over a maximum shift of 6 mm. The best results have been obtained when magnets were placed at the reference position (Z=0) and with a $6 \cdot 10^{-5}$ mbar pressure [8]. Furthermore both the BN disks and the alumina tube were inserted in the source to increase the electron density and the extracted current ($I_{extr.} \propto n_e$). The comparison of He^+ obtained at different values of the permanent magnets positions are shown in Fig. 1.

In a hydrogen plasma, four reactions have the largest possibility to occur:

$$H_2 + e^- \rightarrow H+H + e^- \quad (1)$$

$$H_2 + e^- \rightarrow H_2^+ + 2e^- \quad (2)$$

$$H_2^+ + e^- \rightarrow H^+ + H + e^- \quad (3)$$

$$H + e^- \rightarrow H^+ + 2e^- \quad (4)$$

The plasma parameter which mainly affects the H_2^+ production is the ion lifetime. H_2^+ molecules, indeed, are metastable in a plasma because the possible collisions with electrons (reaction n.3) can lead to the molecule break-up. Ion lifetime can be decreased in a MDIS by removing the alumina tube and the BN in the extraction region. Such a modification of the experimental set-up allows an improvement of the H_2^+ fraction from 5-10% up to 50%. Unfortunately, the increase of the H_2^+ fraction is

ISBN 978-3-95450-128-1

A CENTER REGION UPGRADE OF THE LBNL 88-INCH CYCLOTRON

K. Yoshiki Franzen*, J. Benitez, A. Hodgkinson, M. Kireeff Covo, C. Lyneis, B. Ninemire, L. Phair, P. Pipersky, M. Strohmeier, and D.S. Todd,
Lawrence Berkeley National Laboratory, 1 Cyclotron Road, Berkeley, CA 94720, USA
D. Leitner, Michigan State University, East Lansing, MI 48824, USA

Abstract

The design and results of an upgraded cyclotron center region in which a mirror field type inflector was replaced by a spiral inflector is described. The main goals of the design were to facilitate injection at higher energies in order to improve transmission efficiency and to reduce down-time due to the need of replacing mirror inflector wires which rapidly break when exposed to high beam currents. The design was based on a detailed model of the spiral inflector and matching center region electrodes using AMaze, a 3D finite element suite of codes. The spiral inflector was used to extract a 2.0 pμA 250 MeV ^{48}Ca beam from the cyclotron thus meeting design goals. Furthermore, the inflector was utilized during an eight week experiment without any issues delivering around 1 pμA ^{48}Ca as requested by the users.

INTRODUCTION

The Lawrence Berkeley National Laboratory 88-Inch Cyclotron has a more than 50 years track record of producing beams to support the nuclear science community. The present mission of the cyclotron is two-fold: 1) to serve the National Space Security community and other users with beams for radiation tests of microcircuits, and 2) to serve the local nuclear science community with a focus on super-heavy element research. For the first of these users groups the beam intensity levels produced by the cyclotron is usually adequate. Instead it is the ability to produce ion species at higher charge states that is of main interest. On the other hand, for the second user group the beam intensity plays an important role. Especially of interest for the Berkeley Gas Separator (BGS) group is the availability of a high current ^{48}Ca ion beam in the ~250 MeV energy region [1,2]. Previous measurements have routinely utilized such a beam of currents up to 0.6 pμA with the ions produced by the Advanced Electron Cyclotron Resonance (AECR) ion source. However, as shown in Fig. 1 it was not possible to increase this maximum cyclotron output current above this value due to space charge effect causing beam losses along the beam lines and the cyclotron center region. Another limitation was that the maximum output current of $^{48}Ca^{10+}$ and $^{48}Ca^{11+}$ from the ion source was limited to around 50 μA. It was therefore decided to use the more powerful VENUS ECR ion source to obtain a higher current level and to improve the transport efficiency by increasing the extraction voltage from 14 kV to 25 kV or higher. Preparing VENUS required the development of a new low-temperature oven and has been reported elsewhere [3]. Increasing the source extraction voltage required an increase in maximum current of the final focusing element of the injection beam line, and a redesign of the cyclotron center region geometry in order to handle the increases in injected beam currents and energies. The goal was also to improve the transmission of the center region which is where the majority of losses occur between the source and the cyclotron extraction.

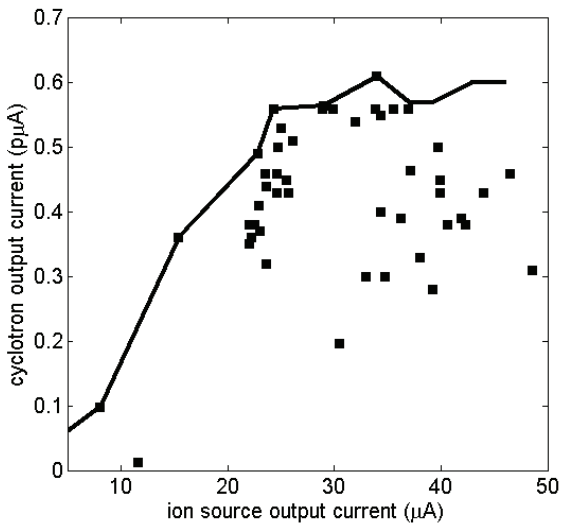

Figure 1: Each data point indicates an optimized tune of $^{48}Ca^{10+}$ or $^{48}Ca^{11+}$ in the 250-270 MeV region prior to the intensity upgrade (February 2011 and earlier).

INJECTION LINE UPGRADE

Using a set of Allison scanners [4] positioned after VENUS' analyzing magnet, emittance data and Twiss parameters were obtained for a 25 kV $^{40}Ar^{9+}$ ion beam extracted at different currents. This particular beam was chosen since its mass-to-charge ratio is similar to that of $^{48}Ca^{11+}$. Using TRACE 3-D [5] the phase-space ellipses were propagated through the system to a plane 1600 mm above the cyclotron mid-plane. All optical elements were tuned in the calculation such that the beam envelopes were well within each beam line aperture along the way. Starting from 1600 mm above the cyclotron mid-plane and onward the beam was represented by an ensemble of particles with Gaussian phase-space distributions of each transversal axis as $\psi(x,x') = \frac{1}{2\pi\varepsilon} e^{-\frac{\left(x^2+(\alpha x+\beta x')\right)^2}{2\beta\varepsilon}}$ in

*Correspondence address: Mevion medical systems, 300 Foster St., Littleton, MA 01460, USA

ISBN 978-3-95450-128-1

DEVELOPMENTS OF ION SOURCE COMPLEX FOR HIGHLY INTENSE BEAM AT RCNP

T. Yorita , K. Hatanaka, M. Fukuda, H. Ueda, Y. Yasuda, S. Morinobu, A. Tamii, K. Kamakura,
Research Center for Nuclear Physics (RCNP), Osaka University, Osaka, Japan

Abstract

Several developments of Ion Source Complex at RCNP have been carried for the purpose of beam quality improvement. For 18 GHz superconducting (SC)-ECR which produces highly charged heavy ions, the new extraction system to increase the beam current has been developed and the heavy ion current has been improved. Studied for relation between this extraction and beam emittance and transmission also has been done, and it is found that there are some aperture limitations and the beam transport line should be modified to obtain more ions. Highly intense proton (HIP)-ECR the 2.45GHz permanent magnet ECR which provides highly intense proton beam has also been developed for further beam brightness improvement. Some modifications have been done and the proton beam quality also has been improved.

INTRODUCTION

Ion source complex at RCNP consists with four ion sources as shown in Figure 1. The 18 GHz SC-ECR is installed in order to increase beam currents and to extend the variety of ions, especially for highly charged heavy ions which can be accelerated by cyclotrons at RCNP. The mirror magnetic field is produced with four liquid-helium-free superconducting coils and the permanent magnet hexapole is of Halbach type with 24 pieces of NEOMAX-44H material. The production development of several ion like B, C, O, N, Ne, Ar, Ni, Kr and Xe has been performed and these beams are already provided to experimental users[1,2,3]. For further improvement of beam quality and intensity, it is needed more improvement not only for the SC-ECR itself like extraction system but also for the beam transport line. For that purpose, the extraction electrode has been modified to increase extracted beam from plasma chamber of SC-ECR. The detail studies for transmission and emittance also have been carried. Another ion source, 2.45 GHz HIP-ECR is installed to extend the proton beam power[4]. Intense 400 MeV proton beam accelerated by Ring Cyclotron at RCNP is required for ultra cold neutron experiment, neutron irradiation test of semiconductors, muon source, RI production for medical application, and so on. The beam current requirement is over 10 uA although the maximum present current is about 1.1 uA. So the high brightness proton ion source with low emittance and high current of over 1 mA is needed. This 2.45 GHz ECR using a set of ring-shaped permanent magnets was originally developed at CEA-Saclay to produce a 100 keV CW proton beam with the intensity more than 100 mA [5]. The design of our HIP-ECR is similar to this CEA-Saclay source, but the extraction system was optimized for 15 keV protons to match with the injection system of the RCNP AVF cyclotron which is the injector of Ring cyclotron. The development of proton beam production with this source has been carried successfully[4]. For further improvement of beam quality, some modification has been done.

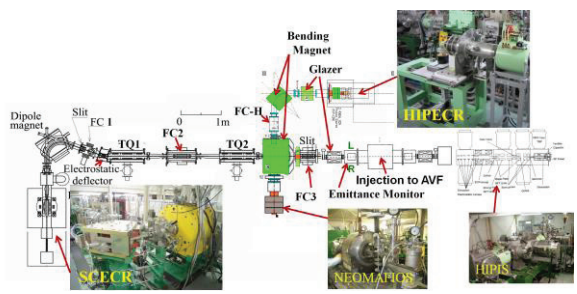

Figure 1: Ion Source Complex at RCNP: The room for ion sources is upstairs of AVF cyclotron; the transport line is 5980mm behind of median plane of cyclotron. There are 4 ion sources; HIPIS for polarized p, d, 2.45 GHz HIP-ECR for intense p, 10 GHZ NEOMAFIOS for p~Mg and 18GHz SC-ECR for highly charged heavy ions.

#yorita@rcnp.osaka-u.ac.jp

EXTRACTION ELECTRODE MODIFICATION FOR 18GHZ SC-ECR

Plasma electrode, extraction electrode and einzel lens are modified in order to increase the ion beam current. Figure 1a) shows the original electrodes and 1b) shows the electrodes after modification. The new extraction electrode can be applied to -20 kV against the plasma electrode which applied to +15kV. The baffle slit downstream of einzel lens is ground level. The position of

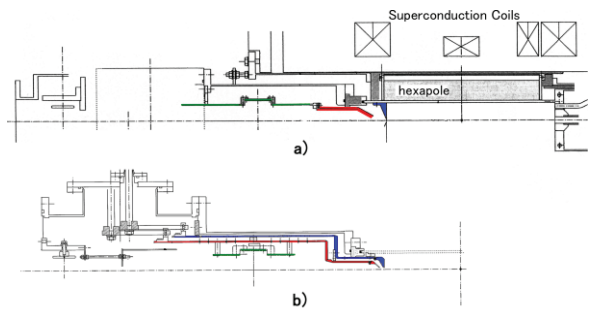

Figure 2: The schematic views of extraction system before modified in a) and after in b).In case of b) both positions of plasma and extraction electrode can be controlled from outside of vacuum chamber. New extraction electrode also can be applied to -20 kV. The baffle slit downstream of einzel lens is ground level.

ISBN 978-3-95450-128-1

CRITICAL ANALYSIS OF NEGATIVE HYDROGEN ION SOURCES FOR CYCLOTRONS

Sergey Korenev, SIEMENS Medical Solutions, Knoxville, TN 37932, USA

Abstract

The negative hydrogen ion sources found applications as injectors for cyclotrons. The efficiency for internal and external ion sources is one important question for industrial cyclotrons, which are used for production of medical isotopes. The short critical analysis of PIG and MULTICUSP ions sources for production of negative hydrogen ions is given in this paper.

INTRODUCTION

The industrial cyclotrons for production of medical isotopes found large number of applications [1]. The Positron Emission Tomography requires radioactive markers, which are produced using irradiation of target by proton beam from cyclotron [2]. The industrial cyclotrons use negative hydrogen ions with following converting to protons before input of beam to target [3]. The ion source is important device of cyclotrons, which determines physical parameters of beam for injection to accelerating and magnetic fields.

The history of R&D for ion sources is long. The ion source consists from plasma emitter with required ions and extraction electrode system. The general structure of negative hydrogen ions source is given on Fig. 1. The more detail structure of negative hydrogen ion source is presented on the Fig. 2. The generation of hydrogen negative ions in plasma emitter is complex task. The selection of type of electrical discharge determines by applications of ion source. The focus of this paper is negative hydrogen ion source for industrial cyclotrons.

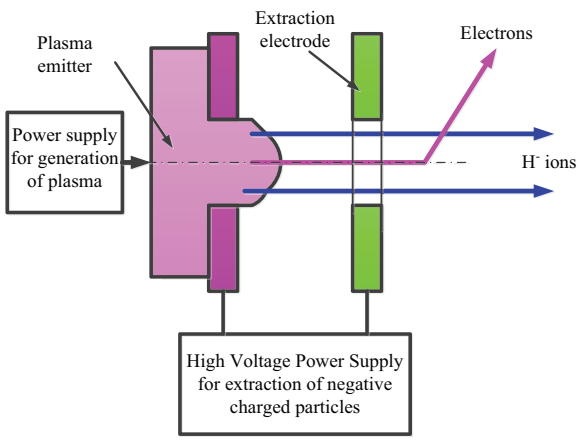

Figure 1: The general structure of H^- ion source.

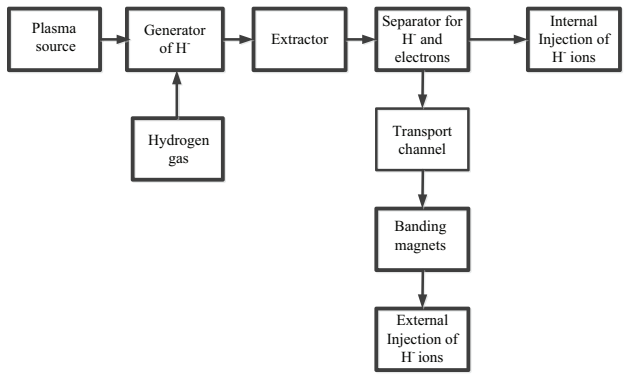

Figure 2: The structure of H- ion source.

PHYSICAL MECHANISMS FOR GENERATION OF H^- IONS

The main question for negative hydrogen ion source is acceptable and effective method for production of these ions. The adding of second electron on the orbit of hydrogen atoms leads to forming negative hydrogen ions. The logical solution for production of hydrogen negative ions is plasma chemical reactions in plasma with hydrogen gas [4]. The methods for forming of gaseous plasma with negative ions are very broadly and known [5]. The plasma chemistry for generation of hydrogen negative ions is complicated [6]. The physical processes in plasma emitter of ion source are following: i) the forming of gaseous plasma and ii) the generation of negative hydrogen ions using plasma chemical reactions. The forming of gaseous plasma is simple task and presents the standard solution based on glow electrical discharge. The second task is complex and has different solutions, based on the plasma chemical reactions for production of negative hydrogen ions. The basic principle of production negative hydrogen ions is combination of ionization and dissociation processes.

The common basic mechanism for production of negative hydrogen ions is following:

1. The forming of excited positive charged hydrogen molecule by electron impact:

$$H_2 + e^- = {}^*H_2 + 2e^-. \quad (1)$$

2. The capture of low energy electron by

$${}^*H_2 + e^- = {}^*H_2^-. \quad (2)$$

3. The dissociation of these excited hydrogen molecules on the negative hydrogen ions:

$${}^*H_2^- = H^- + {}^*H. \quad (3)$$

ISBN 978-3-95450-128-1

DEVELOPMENT STUDY OF PENNING ION SOURCE FOR COMPACT 9 MeV CYCLOTRON*

Y.H. Yeon, M. Ghergherehchi, K.M Gad, X.J. Mu, S.Y. Oh, Y.S Lee, H.W. Kim, S.W. Shin, S.Y. Jung, S.H. Lee, H.S. Kim, S.H. Kim, T.V. Cong, J.S. Chai,#
School of Information & Communication Engineering/ WCU Department of Energy Science
Sungkyunkwan University, Korea

Abstract

Penning Ion Gauge (PIG) source has been used in internal source for cyclotron. The PIG source produces H^- ions. This source consists of cold cathode which discharges electrons for producing H^- ions and anode for making plasma wall. Tantalum which is cold cathode was used for emitting electrons and tungsten copper alloy was used for anode. Optimization of cathode and anode location and sizing were needed for simplifying this source for reducing the size of compact cyclotron. Transportation of electrons and number of secondary electrons has been calculated by CST particle studio. Calculation of PIG source in 9 MeV cyclotron has been performed by using various anodes with different size of expansion gap between the plasma boundary and the anode wall. In this paper design process and experiment result is reported.

INTRODUCTION

The compact 9 MeV cyclotron which is constructed in Sungkyunkwan University accelerates the H^- ions in order to extract proton beams. The negative ions are stripped by carbon stripper. The internal PIG source is widely used for producing and accelerating H^- ions. The cold cathode type PIG source consists of a hollow anode cylinder with two cathodes on each end. Electrons emitted from two cathodes collide with H_2 gas for making plasma.

The electron collision processes such as dissociative electron attachment and polar dissociation with neutral molecules are the responsible of production of H^- ions in the low density plasma [1, 2] . The size of PIG source is related with transition region of this low density plasma.

In the compact 9 MeV cyclotron, the magnetic field of the cyclotron center is 1.366 T and the pole gap of magnet is 60 mm. The hollow anode cylinder's length and the position of cold cathodes should be in this space. The calculations of the length of transition region, transportation of electrons and number of secondary electrons are done by CST Particle Studio [3] for concluding the length of PIG source. The magnetic field of permanent magnet is calculated by TOSCA [4].

DESIGN STUDY OF PENNING SOURCE

The Penning ion source (Fig. 1.) consists of a hollow anode cylinder with a cathode on each end. Electrons emitted from cathode move towards to the anode under electric field, while a homogeneous parallel magnetic field distributed between the two cathode electrodes confines the electrons inside the anode. This magnetic field also keeps the electrons oscillating between two cathodes to produce greater ionization efficiency.

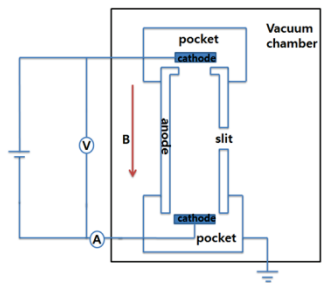

Figure 1: Schematic of the PIG ion source.

In the PIG ion source, the hydrogen plasma is weakly ionized. The length of transition region is related to the length of cathode to anode. In the transition region, electrons are collisional equilibrium and the charge neutrality is not preserved. The strong electric field from cathode penetrates in this region. We assume this situation in CST particle studio and simulate the trajectory of electrons and electric field.

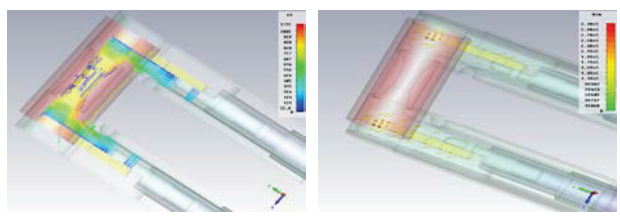

Figure 2: The electron trajectory and electric field of ion source.

For the weakly ionized plasma, we assume the fluid equation for calculating the length of transition region (see Eq. 2).

$$n_e = n_0 \exp(-\frac{eE}{T_e} x) \quad (1)$$

From the results of Chen's experiment [5], the ratio of the electron density n_e and the charge density at the plasma edge n_0 (where x=the length of transition region) is 0.2. As the result of Eq. 1, we can get the electric field

* This work was supported by Nuclear R&D program through the National Research Foundation of Korea funded by the Ministry of Education, Science and Technology (2012-0925001).
#jschai@skku.edu

ISBN 978-3-95450-128-1

A 20 mA H⁻ ION SOURCE WITH ACCEL-ACCEL-DECEL EXTRACTION SYSTEM AT TRIUMF

K. Jayamanna, I. Aguilar, I. Bylinskii, G. Cojocaru, R.L. Dube, R. Laplante, D. Louie, M. Lovera, B. Minato, M. Mouat, S. Saminathan, T. Tateyama, E. Tikhomolov
TRIUMF Canada's National Laboratory for Particle and Nuclear Physics,
4004 Wesbrook Mall, Vancouver BC, Canada V6T 2A3

Abstract

During the last three decades, TRIUMF has developed H⁻ cusp ion sources for the 500 MeV, TR30, TR13 cyclotrons, as well as many other machines. These ion sources can be categorized as high current versions, producing up to 20 mA of DC H⁻ beam within a normalized emittance (4RMS) of 0.6 π-mm-mrad and low current versions, producing up to 1 mA of CW current within a normalized emittance (4RMS) of 0.16 π-mm-mrad. A new state-of-the-art test stand is being built to further enhance H⁻ knowledge while improving the brightness and filament life. The preliminary results of the test stand performances, as well as relevant emittance measurements, are discussed.

INTRODUCTION

TRIUMF's 500 MeV cyclotron has been fed by an arc discharge H⁻ ion source developed in-house 20 years ago. Since then, new additions to TRIUMF like ISAC have required more and more beam current from the cyclotron. To satisfy the growing intensity of experiment demands, the source beam current and brightness needed to be improved. Due to historical reasons, the initial beam energy has been limited to 12 kV and the power to the source filament limited to 2.5 kW. Finding reasonable time slots for beam development has also been difficult due to heavy usage of the ion source. Filament life has been an additional concern as every three weeks there was a loss of two to three shifts due to interruptions for filament changes and re-tuning. Consequently, the need for a state-of-the-art test stand became an increasingly prominent concern. This new test stand was designed to develop a high brightness ion source with a long filament life. One of the unused on-line terminals was chosen to build said test stand so it would be available for use as a hot spare if required.

EXPERIMENTAL SETUP

The test stand was built in a terminal; a metal enclosure of 6 m by 5 m by 3 m (see Fig. 1) built on 300 kV high voltage insulators and additionally powered by a 100 kVA isolation transformer. The test stand was built on rails for easy access to any element in the system. The source is located in a second high voltage enclosure capable of up to 75 kV and powered by a 45 kVA isolation transformer. This secondary high voltage rack consists of several power supplies: a 10 V * 1000 A filament one, a 200 V * 50 A arc one, a 10 kV * 400 mA lens one, and a few other small power supplies, including virtual coil ones. Another 100 kV x 2 kVA transformer is utilized to supply uninterrupted power to the controls and the safety devices at the secondary stage so that the sparking and the vigorous testing will not affect them.

The vacuum system employs four turbo pumps, a root blower and a scroll pump and is capable of reaching 2e-9-Torr in the source side without gas loading.

The beam line (see Fig. 2) is equipped with a cusp source, a 4-electrode extraction system, a focusing solenoid and diagnostic components such as emittance scanners, and a graduated Faraday cup. All the focusing and steering elements are magnetic and no electrostatic elements were used other than in the extraction system.

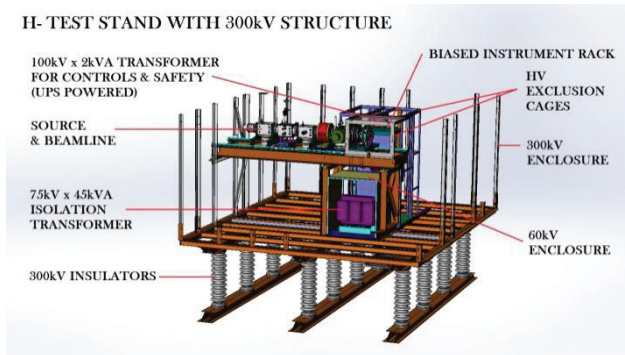

Figure 1: H⁻ test stand with the 300 kV platform.

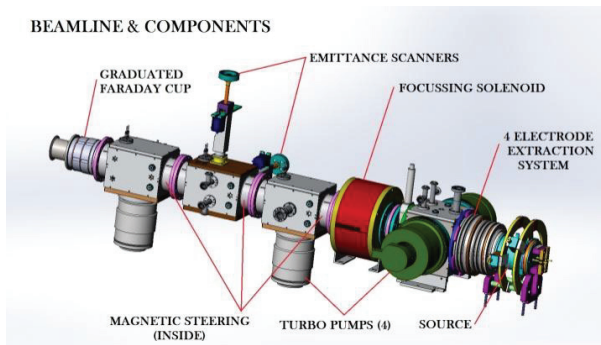

Figure 2: The beam line with the source, extraction system, diagnostics elements and the vacuum components.

The Ion Source (see Fig. 3) employs a 20 row Halbach array type magnetic configuration. Four electro magnets have been built to provide virtual filter magnetic fields so that they can be optimized to various arc voltages and different plasma conditions.

A new accel-accel-decel extraction system is being developed in order to run the source at optimum source

ISBN 978-3-95450-128-1

DESIGN AND SIMULATION OF CAVITY FOR 10 MeV COMPACT CYCLOTRON

V. Afzalan, H. Afarideh*, R. Azizi, Department of Energy Engineering & Physics, Amirkabir University of Technology, Tehran, 15875-4413, Iran
M. Ghergherehchi, J. S. Chai, Department of Energy Science/School of Information & Communication Engineering, Sungkyunkwan University, Suwon 440-746, Korea

Abstract

RF system is known as one of the most vital parts to produce the efficient accelerator system [1]. In this paper, the RF system and cavity of 10 MeV AVF (Azimuthally Varying Field) Cyclotron for radioisotope production are designed. The Cyclotron works on 4th harmonic with Dee's voltage of 50 KV. In order to supply the expected accelerating voltages RF power coupling and RF tuner has been considered. The RF system is simulated using commercially available simulator, CST Microwave Studio code. In contrast the geometry of cavity is optimized to achieve suitable Q value in desired frequency. Since the factors are non-ideal during the fabrication process, the actual Q value of cavities is estimated.

INTRODUCTION

This paper mainly describes a development study of cavity for 10 MeV AVF cyclotron. The cyclotron is being designed for producing short-life isotope, such as F-18 for Positron Emission Tomography (PET). The AVF cyclotron will be injected by penning ion source (PIG) for getting F-18. Because of the limitation caused by magnet, we satisfied the condition of λ/2 by adjusting stem, liner, the gap of Dee, etc. Cavity is designed to have a few thousands of Q value with resonance frequency of 69MHz, which is based on the magnet design. In addition, in order to obtain a good Q value in desired frequency, geometry of cavity is optimized.

CST studio suite offers a lot of options for parametric design. This structure has defined when some objects which relatives to each other change simultaneously. The model of the cavity is designed by this code has many parameters like Dee's angel, valley gap, stem dimension, etc. Parametric geometry of structure can change easily in order to determine the optimum geometry of cavity [2]. 3D modeling was investigated by using Solid Works program to study the non-ideal factor during the fabrication process [3].

RF CAVITY DESIGN

General Concept

The geometric model of the double gap delta cavity housed inside the valley of the magnetic system of cyclotron; so the structure of the RF system is double gap λ/2 coaxial type resonator. This structure is useful for compact cyclotron because they are suitable for applications where a special radial voltage profile (along the acceleration gaps) is desired [4].

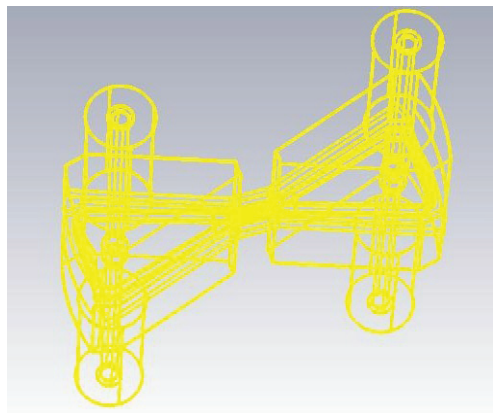

Figure 1: Wire frame of cavity.

The RF system specifications of 10 MeV RF cavity are shown on table 1. Material of RF Cavity is OFHC copper to get better electric conductivity. In addition, this material does not affect magnetic-field intensity. Using the CST Microwave Studio, a parametric model of the resonator was created (Figure 1). Dee's angle is 35°, which are located in both of valleys. Total length of each Dee is about 42cm. Total lengths of Dees, hill gap (3cm), and stem reaches λ/2 in rough design and Dee's radius is 35cm. 4th harmonic mode has been adopted, and length of Dee's gap corresponds to the hill gap.

Table 1: 10 MeV Cyclotron RF System Specifications

Parameters	Values
Energy	10 MeV
Pole radius	0.45m
Extraction radius	0.40m
Hill / Valley gap	0.03 / 0.48m
Number of cavities	2
Cavity angle	40 degrees
Dee angle	35 degrees
Dee voltage	50 kV
Harmonic mode	4
Resonant frequency	69 MHz

*corresponding author: hafarideh@aut.ac.ir

DESIGN OF A DIGITAL LOW-LEVEL RF SYSTEM FOR BEST MEDICAL CYCLOTRONS

G. Gold, V. Sabaiduc, Best Cyclotron Systems Inc., Vancouver V6P 6T3, Canada

Abstract

A versatile digital Low-Level Radio Frequency (LLRF) system has been designed for the various energy cyclotrons being developed by Best Cyclotron Systems Inc. (BCSI). Primary design considerations are given to robustness, low cost and the flexibility to be used on all BCSI resonator designs. As such, the system allows for operating frequency selection from 49 to 80 MHz and is compatible with single or double resonator configurations through the use of local oscillator synchronization and high-speed command exchange. An I/Q demodulation/modulation scheme is employed allowing for frequency and amplitude control. High-speed phase control of separated resonators allows for beam intensity modulation techniques to be applied. This paper discusses the overall system design as well as integration results for a single resonator cyclotron.

INTRODUCTION

To accommodate with the variety of BCSI cyclotrons being established, a frequency selectable digital LLRF controller was designed [1] [2]. The controller fits into a standard 19 inch rack-mounted module and contains all of the necessary electronics, inputs, outputs and power supplies to be a fully self-contained unit.

Figure 1: The front panel of the LLRF module showing status lights, local control potentiometers and RF I/O.

A discussion of the internal components will follow, along with a description of the control procedures and their testing.

ARCHITECTURE

Hardware

The major hardware subsystems of the LLRF are the analog RF front- and back-end, Digital Control Card (DCC), motor drivers and power supplies. Each of these components were designed to be modular and easily replaceable. A block diagram of the subsystems and their interconnections is seen in Fig. 2.

Incoming RF signals are routed through filtering, mixed to an intermediate frequency and I/Q modulated before being converted to digital signals. Similarly, outgoing RF signals are converted to analog, filtered, I/Q demodulated and frequency mixed up to the cyclotron frequency.

Digital signals are routed directly between the analog board and the Altera Cyclone III FPGA on the DCC via two 80 pin connectors. This allows for fast signal processing to occur with minimal latency. The Analog Devices Blackfin microcontroller handles the higher level interface with the motor drivers and Host PC. The motor driver boards are based off the MicroSystems A4988 chip and are socket mounted for quick replacement.

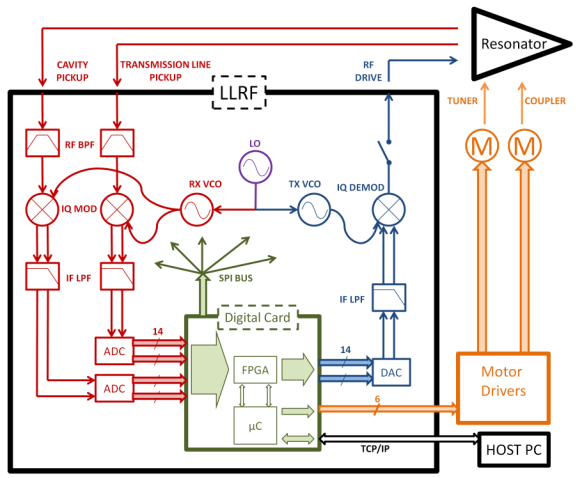

Figure 2: Hardware architecture of the LLRF board showing the major logical sections.

Software

The FPGA and microcontroller are tightly bound in function by using Direct Memory Access over Serial Peripheral Interface (SPI) and Parallel Peripheral Interface (PPI). They share a bank of 60 read-only and 60 read-write registers to communicate. This same set of registers, albeit with different read-write privileges, is shared between the microcontroller and the host PC over TCP/IP.

The FPGA is responsible for the high-speed signal processing such as the amplitude control loop, spark recovery, interlocks and safety. Additionally, all of the IC programming is handled at this level including the data converters and operating frequency selection using a dedicated SPI bus.

Higher level procedures are contained within the microcontroller. These include the RF drive state machine, motor control, host PC communication and automated frequency control loop.

ISBN 978-3-95450-128-1

RESONATOR SYSTEM FOR THE BCSI TEST STAND CYCLOTRON

G. Gold, LAC Piazza, V. Sabaiduc, J. Zhu, BCSI, Vancouver, V6P 6T3, Canada
J. Panama, Best Theratronics Ltd., Ottawa, ON, K2K 0E4, Canada

Abstract

Best Cyclotron Systems Inc. (BCSI) is presently developing a test facility for beam injection into a center region cyclotron operating at maximum 1MeV [1]. The test stand cyclotron will operate at various fixed frequencies that will cover the entire range from 49MHz to 80MHz as estimated for the current cyclotron models under development at BCSI. The resonator was designed with a variable coaxial section allowing for the frequency to be continuously adjusted as required for the particular model in study. Having interchangeable dee tip geometries presented various thermal management challenges which have been addressed. Three operational frequencies, 49MHz, 56MHz and 73MHz have been simulated with CST Microwave Studio. The paper is reporting the theoretical parameters of the cavity, resonator mechanical design considerations and radiofrequency system integration with the amplifier and LLRF control.

INTRODUCTION

The resonator system has been designed and optimised driven by the following requirements:

- Simplicity and modularity of the system (mechanically simple to easily switch between the three operational frequencies).
- Lower power dissipation (to reduce costs of amplifiers).
- Optimization of the quality factor of the cavity.

The entire resonator structure is operational for all frequencies with the exception of the dee tips and center region that are replaced for each particular case. The resonator structure operates on the 4th harmonic and half-wave design for all frequencies. A general view of the resonator system is represented in Fig. 1.

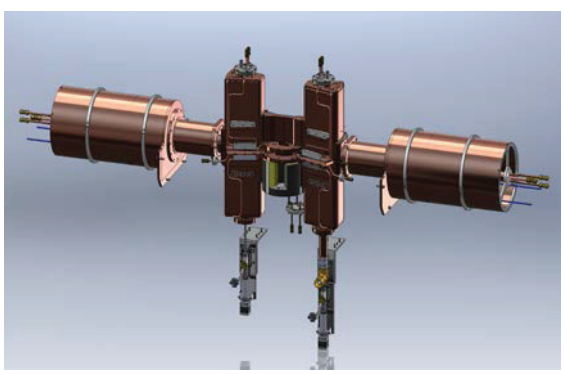

Figure 1: Test stand resonator system

The resonators are connected together at the dee tip and driven by a single amplifier. The accelerating field amplitude and phase stability is controlled by the standard LLRF control circuit designed for BEST cyclotrons [2].

MULTI-FREQUENCY SIMULATIONS

The simulations were performed in CST Microwave Studio environment using the Eigenmode solver. No symmetry planes were used. To speed up and simplify the simulations, just one cavity was simulated per case.

All solid materials were treated as Perfect Electromagnetic Conductor (PEC) via the electric boundaries condition to find the resonant frequency, EM fields and radial voltage distributions of the simulated structures.

Power dissipation, quality factor and numerical evaluation of the EM fields were estimated considering the structure made of copper. The copper surface conductivity value was reduced to $5.0 \cdot 10^7$ S/m to include the roughness imperfection of the copper surface.

The simulated output results were normalized to the voltage distribution values as per the input requirements listed in Table 1. The radial voltage distribution was evaluated increasing the radius with a step of 30mm and the R(1MeV) indicates the radius at which the beam reaches an energy slightly below 1MeV.

Table 1: Input Requirements

	14MeV	**70MeV**	**60MeV**
Frequency	72.8MHz	56.2MHz	49.2MHz
Dee voltage	40kV	60kV	70kV
Dee angle	32 deg	30 deg	28 deg
R(1MeV)	11.9 cm	15.6 cm	26.8 cm

Design Parameters

The complete set of design parameters for the variable frequency resonator has been compiled with the particular design characteristics of each of the three frequency resonators resulting in a coherent unique design with very similar quality factors that are listed in Table 2.

Table 2: RF Cavity Simulated Performance

	14MeV	**70MeV**	**60MeV**
Frequency	72.6MHz	55.9MHz	48.8MHz
Quality factor	6225	6156	6131
Power/cavity	1.67kW	3.76kW	4.97kW
Max Surface currents	44 A/cm	66 A/cm	75 A/cm
Max Electric field	3.3MV/m	12.3MV/m	8.3MV/m
Cavity length	810mm	950mm	1050mm

ISBN 978-3-95450-128-1

THE DESIGN AND TESTING OF AN AUTOMATIC RF CONDITIONING SYSTEM FOR THE COMPACT MEDICAL CYCLOTRON

Lei Yu, Yin Zhiguo, Li Pengzhan, Ji Bin, Zhang Tianjue, Wang Chuan, Wei Junyi,
China Institute of Atomic Energy, P.O.Box 275(3), Beijing 102413, China

Abstract

The multipacting phenomenon for the compact medical cyclotrons is special, due to the present of the fringing magnet filed inside the accelerating structure. And it will become more interesting, when the vacuum system is equipped with diffusion pump. A method used for CYCIAE-14 cyclotron cavity conditioning was reported in this paper, together with the testing results of an automatic conditioning circuits designed on such basis. Apart from traditional Low Level RF control, in which close-loop regulation is played as an important role, the automatic conditioning system emphasis on the cavity startup process. It takes advantage of the modern digital signal processing technique, combined with the direct digital synthesizer to accurately limit the reflection, will condition the cavity by means of the sweeping frequency, using the low RF driven power, in continuous wave mode. After successful establishment of the accelerating voltage, the system would maintain turning of the resonator and would decrease driven power once in a while, until the driven power is below a preset limit or the Dee voltage collapse again. In the latter case, the system will repeat the whole process until reaches the first one or interrupt by the operator. The electronics are designed and tested first; it will be used later in the commissioning of the RF system of other compact medical cyclotrons built by BRIF division of CIAE.

INTRODUCTION

The RF system is an important part of CYCIAE.-14 cyclotron [1]. It is very important to condition the RF cavities effectively. Since it determined that whether the cyclotrons can turn into the normal operational stage as quickly as possible.

When the cyclotrons are in operation, usually, the periodical servicing and maintenances will break the vacuum. To achieve the required resonator voltage as soon as possible, we should condition the RF cavities again after regaining the vacuum degree .

At present, a lot of kind of accelerator which including the linear accelerators, the energy storage rings and the synchrocyclotrons were all faced with the problem that the RF cavities need to be effectively conditioned to restrain the multipactor in them. The science researchers of them had made a lot of study on it. They had attempted to use various conditioning methods and make them automation [2] [3] [4]. Thus it can be seen that it is significant to study and implement a safe and efficient automatic conditioning system for the operation of the RF system of the cyclotrons.

THE METHODS OF THE AUTOMATIC CONDITIONING SYSTEM

The multipactor were discovered by Gutons in 1924 [5] [6] [7], and in 1934 Philo T.Farnsworth presented the multipactor and confirmed it with experiments. At present, the multipactor in the valley magnetic field of the cyclotron can be simulated through the large-scale programs which is the parallel numerical calculation. Through observing and studying, we find that the multipactor of the CYCIAE-14 usually appears at the power from 1 kilowatt to 1.5 kilowatt.

Therefore, we have presented a new method of the RF cavities conditioning, it concluded four steps as follows: a). At first, the system use the low duty ratio pulse wave as the input signal. When the multipactor appears, demarcating the driven power and the voltage of the cavities, as the Fig.1. b). Secondly, without the magnetic field, the input signal changes to the CW power.The CW power sweeps the RF cavities frequency and condition the cavities, in order to bake the surface of the cavities for gassing. c).Thirdly, with the magnet field, using the CW power sweeps the resonance frequency point of RF cavities. After the power going through all regions of the multipactor, add the amplitude modulation. The amplitude of CW decreased with the time, to condition the cavities. d). Finally, with the magnet field, we use new method to keep the tuning frequency. To ensure that the high power and low duty ratio wave condition the cavities is achieved.

The conditioning method above is summarised from the conditioning process of the CYCIAE-10, the CYCIAE-14 and the metallic experimental cavities of the CYCIAE100. The automatic conditioning system of this article would achieve the step b), step c) and step d) to avoid the complexity of the aritificial operation.

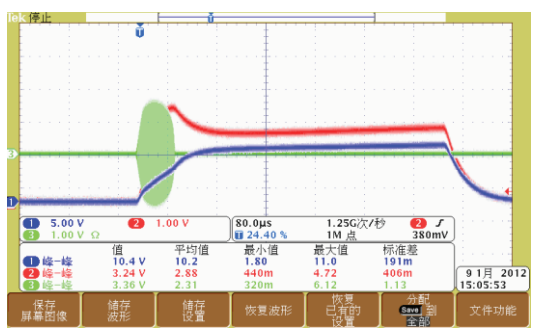

Figure 1: Demarcating the multipacting power.

ISBN 978-3-95450-128-1

DEVELOPMENT OF 20 kW RF AMPLIFIER FOR COMPACT CYCLOTRON*

Seung Hyun Lee, H.S. Song, J.H. Kim, T.V. Cong, H.S. Kim,
Lee Y. S., Y. H. Yeon, Jong Seo Chai,#
WCU Department of Energy Science / School of Information & Communication Engineering,
Sungkyunkwan University, Suwon 440-746, Korea

Abstract

Compact cyclotron for PET RI production accelerates H- ions using electric field. For accelerating ions in cyclotron, RF amplifier is developed to transmit RF power to RF resonating cavity.

RF amplifier generates high-power RF signal up to 20 kW with narrow band frequency. The amplifier device was used of triode vacuum tube operated in cathode-driven. Impedance matching systems were composed of bridge-network system. Components of impedance matching system had rigid structure to endure high-power RF signal. Variable inductors of matching components have been used of short-bar movement system for changing reactance of characteristic impedance. The experiment results were measured by VSWR meter and network analyzer.

INTRODUCTION

Compact cyclotron for PET RI production has a role to accelerate H- ions to 9 MeV energy level. For accelerating ions from PIG ion-source, electric field (E-field) is needed up to 40 kV in this cyclotron. In RF cavity, acceleration gap is about 3 mm and loaded Q-factor is about 1500. It means that RF amplifier would transmit 8 kW RF signal [1]. Also RF amplifier could satisfy stability in operation, because cyclotron emits continuous beam in continuous wave (CW) RF operation mode [2].

This paper describes the development of power amplifier stage of RF amplifier from design to manufacture. The operation is accomplished in CW mode for cyclotron operation and pulse wave modulation (PWM) for RF cavity conditioning. The result of experiments to transmit RF signal has been measured by VSWR meter. And network analyzer is confirmed frequency response.

AMPLIFIER REVIEW

Figure 1 shows the scheme of RF amplifier system. It consists of power supply stage and RF amplification stage. Operation sequence was controlled by PLC unit. Filament source is consisted of AVR transformer.

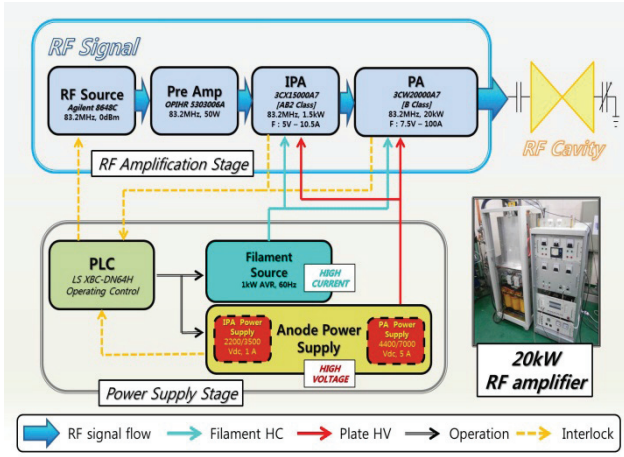

Figure 1: Scheme of RF amplifier system.

Anode Power Supply (APS) in power supply stage could generate DC voltage with two values. It makes the difference gain of amplification. Power amplifier (PA) stage is a main stage for 20 kW RF amplification. It consists impedance matching circuits to match the characteristic impedance as 50 Ω, and filter circuits to block RF leakage signal for filament and plate stage. Table 1 is summarised of RF amplifier operating parameters.

Table 1: Operating Parameters

Parameter	Value
Resonating frequency	83.2 MHz
Maximum Driving RF Power	1.5 kW
Maximum Output RF Power	10/20 kW
Maximum DC anode voltage	4000/7000 V
Maximum DC anode current	5 A
Idling DC anode current	180 mA
Characteristic Impedance	50 Ω
Main Power source	380 V / 92 A - 3rd Phase
Maximum Gain of amplifier	15 dB
Operating Efficiency	65 %

* This work was supported by Nuclear R&D program through the National Research Foundation of Korea funded by the Ministry of Education, Science and Technology. (2012-0925001)
# jschai@skku.edu

DESIGN STUDY OF A 83.2 MHZ RF CAVITY FOR THE 9 MEV COMPACT CYCLOTRON*

SeungWook Shin, Jong Chul Lee, Jong-Seo Chai#,
Sungkyunkwan University (SKKU) Department of Energy Science, Suwon, Korea
Byung-No Lee, Korea Atomic Energy Research Institute (KAERI), Daejeon, Korea

Abstract

A compact cyclotron accelerating H^- ion for producing a radioactive isotope FDG (FluoroDeoxyGlucose) for PET (Positron Emission Tomography) has been designed at Sungkyunkwan University. The H^- ion which generated from the PIG (Panning Ion Gauge) ion source will be accelerated at the normal conducting RF cavity which uses 83.2 MHz of resonance frequency and extracted at the carbon foil striper at the energy of 9 MeV. This cyclotron has to be small to install local hospital while FDG production needs more than 9 MeV of proton beam energy. Chasing two hare at once, deep valley type of magnet has been selected for high energy and compact cyclotron. Due to the small size of valley space where RF cavities will be installed, lots of difficulties have been introduced. Despite of those difficulties at the designing process, we could achieve resonance frequency of 83.2 MHz and Q-factor of 4500 with very compact size of RF cavity.

INTRODUCTION

Application of cyclotron has been expanded significantly for a past few decades at various field since it was invented by Ernest O. Lawrence in 1932. One of the major application of the cyclotron to the public is to produce radiopharmaceuticals especially FDG for a PET machine [1].

A compact 9 MeV cyclotron has been developed for the FDG production at Sungkyunkwan University [2]. A proton beam is used for the FDG production and this proton beam is extracted by stripping H^- beam which is produced from PIG ion source located at the centre of the cyclotron. The created H^- beam is accelerated at the RF cavity which provides electric field activating at the frequency of 83.2 MHz. A main specification of 9 MeV cyclotron is shown at Table 1 while Fig. 1 and Fig. 2 show layout and cross-section view of whole system

THE RF SYSTEM

To accelerate charged particles, one needs to introduce electric field at the pass of beam path by RF cavity. RF cavity mainly consists of DEE, liner for a RF ground, stem, RF power coupler for feeding high RF power and fine tuner for a fine frequency tuning. RF cavity of cyclotron can be expressed by R-L-C equivalent circuit and those specific values determines RF cavity's characteristics such as resonance frequency, Q-factor, shunt impedance etc.

Table 1 : 9 MeV Cyclotron Main Parameters

Parameters	Values
Beam Energy	9 MeV
Accelerated Ion	H^-
Type of Ion source	PIG
Diameter	1.25 meter
Maximum magnetic field	1.9 T
Harmonics	4^{th}
RF Frequency	83.2 MHz, Normal conducting
Accelerating voltage	40 kV
Q-factor	4500

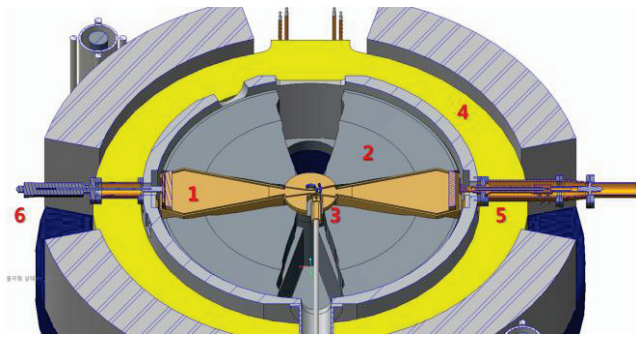

Figure 1: Layout of 9 MeV cyclotron: 1. RF cavity, 2. Magnet, 3. PIG ion source, 4. Magnet coil, 5. RF coupler, 6. fine tuner.

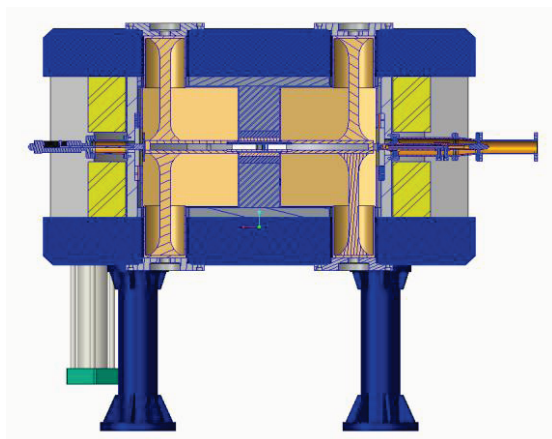

Figure 2: Cross-section view of 9 MeV cyclotron.

*Work supported by National Research Foundation of Korea funded by the Ministry of Science, ICT and Future Planning (NRF-2010-0025952)
#jschai@skku.edu

ISBN 978-3-95450-128-1

DEVELOPMENT OF 1.5 kW RF DRIVER FOR COMPACT CYCLOTRON*

H.S. Song, S.H. Lee, J.H. Kim, T.V. Cong, H.S. Kim, Y.S. Lee, Y.H. Yeon, S.Y. Jung, S.W. Shin, J.S Chai#
WCU Department of Energy Science / College of Information & Communication Engineering, Sungkyunkwan University, Suwon 440-746, Korea.

Abstract

The 1.5 kW RF driver was designed and manufactured with the resonance of frequency of 83.2 MHz. 3CX1500A7 / 8877 triode vacuum tube was used for RF power amplification, and grounded-grid amplifier (G.G. Amp.) type was adopted for this RF driver since the circuit design and manufacturing process is simple [1]. Anode, and cathode voltage of RF driver is approximately 3500 V, and 5 V respectively. In this paper, impedance matching process of RF driver is described. Variable capacitor and variable inductor is utilized to implement the impedance matching for cathode and anode. In addition, RF power output characteristics compare with RF input is shown.

INTRODUCTION

The 9 MeV compact cyclotron was designed and manufactured for getting F-18 at medium-small PET facilities. 1.5 kW, 83.2 MHz RF driver plays a role for providing RF power to RF cavity through 20 kW RF amplifier. RF driver employs 3CX1500A7 / 8877 triode, which has a high amplification factor of 200. This triode is grounded–grid, and cathode-driven amplifier. This amplifier has several advantages; first, this amplifier is a zero bias. Second, grid is grounded, so circuit configuration is simple compared with tetrode, and pentode. Third, this type of amplifier prevents from positive feedback. It can be operated in high frequency. Last, drive output is obtained by drive input plus output power. Figure 1 shows signal flow diagram of 1.5 kW RF driver. This RF amplifier can produce power of 1.5 kW at the maximum, however, since maximum power of final RF amplifier which transmits power to RF cavity was designed for 10 kW, RF driver provides about 1 kW. RF power is cathode-driven by 50 W pre-amplifier. It is a solid-state broadband amplifier, and operating frequency is from 20–500 MHz [2]. Anode voltage of this RF driver is provided by full-wave bridge regulator circuit. The circuit includes high voltage transformer, and capacitor. Transformer boosts voltage from 3-phase 380 V to 3500 V, and then capacitor regulates to DC. Automatic variable regulator is used to provide constant cathode voltage of 5 V even if there is a small signal fluctuation. Table 1 demonstrates main specification of RF driver for 9 MeV compact cyclotron.

* This work was supported by National Research Foundation of Korea funded by the Ministry of Science, ICT and Future Planning. (NRF-2010-0025952)
# jschai@skku.edu

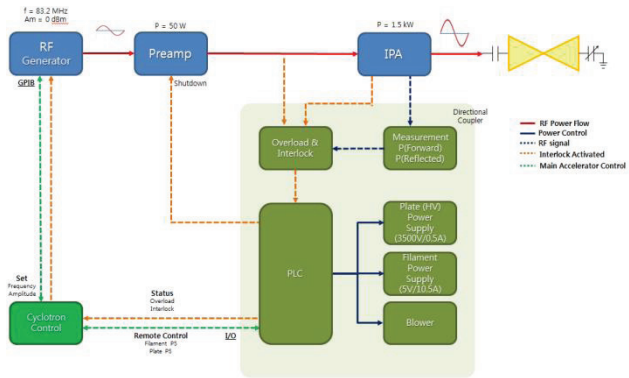

Figure 1: Signal flow diagram of 1.5 kW RF driver.

RF DRIVER DESIGN

For RF driver circuit design, we have composed pi matching network for both cathode and anode. Pi network is normally used when matching between high impedance source and 50 ohm load [3]. For fine tuning, two variable capacitors were used for RF matching in cathode, and two variable inductors were utilized in anode. Q value of RF driver affects circulating current, and bandwidth. In our case, we designed Q value below 5 in order to prevent from damage of RF component especially in anode with high circulation current.

Table 1: Main Specification of RF Driver for 9 MeV Compact Cyclotron

Parameters	Values
RF driver vacuum tube	3CX1500A7
Resonant frequency	83.2 MHz
Anode voltage / current	3500 V / 0.5 A
Cathode voltage / current	5 V / 10.5 A
Rated maximum power	1 kW / 1.5 kW
Characteristic impedance	50 Ω
Main Power source	380 V / 92 A - 3rd Phase

DESIGN AND CONSTRUCTION OF COMBINATION MAGNET FOR CYCIAE-100

S. Wei, S. An, M. Li, C. Wang, M. Yin, T. Zhang, X. Zheng, CIAE, China

Abstract

The high intensity compact cyclotron CYCIAE-100 being constructed at China Institute of Atomic Energy (CIAE) is designed to extract proton beam from 75MeV to 100MeV in two opposite directions by stripping foil. Two combination magnets have been designed to bend the proton beams with different energies into one common beam line. The combination magnets have been designed into the return yoke of the main magnet of CYCIAE-100 for the dynamic reason. 2 D and 3D simulation of these combination magnets have been finished, the machining of them have also been finished. The magnetic field of the combination magnets have been measured and the results shows that the measurements are very closed to the calculation, indicating these two magnets can be used in the BRIF project.

INTRODUCTION

CYCIAE-100, the high intensity compact cyclotron is being installed at CIAE [1,2]. The proton beams are extracted in two opposite directions with different energies. Two combination magnets are designed to bend beam with different energies into one common beam line, as shown in Fig. 1 [3].

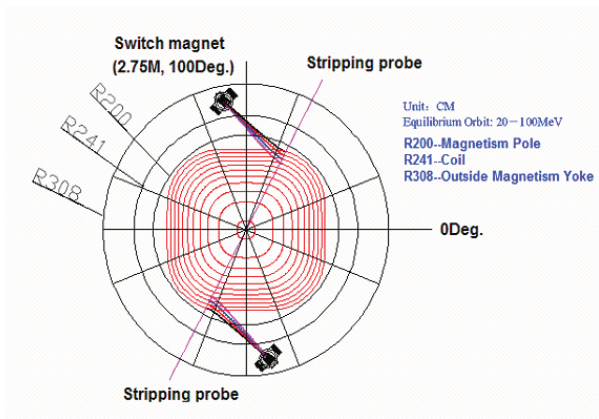

Figure 1: Layout of CYCIAE-100 and the combination magnet.

Simulation results show that the beam envelop is smaller when the combination magnet put into the return yoke of the main magnet than that put outside the return yoke, that is the reason to install the combination magnet into return yoke.

Beam from 75 MeV to 100 MeV are bending to common line through combination magnet, the maximum bending angle is 5°,detailed design will presented.

DESIGN OF THE MAGNET

Maximum bending angle of beam with energy 75 MeV to 100 MeV is 5°, the magnetic rigidity of proton beam with given energy is certainly, then we can take a balance of the magnetic field and the magnet size, the main parameters are shown in Table 1.

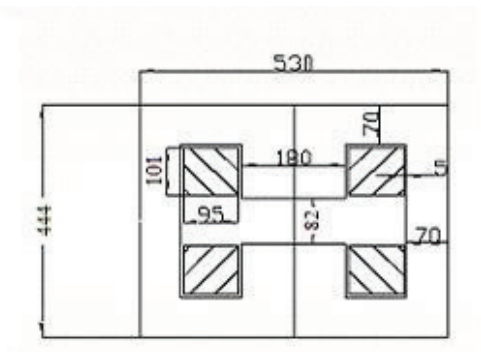

Figure 2: Layout of the magnet.

Table 1: Main Parameters

Parameter	Value
Bmax	0.53 T
Bending radius	2968 mm
Gap	82 mm
Effective length	322 mm
Ampere-turn	17500 AT
Conductor	5 mm×5 mm−Φ3 mm

Figure 2 shows the intersecting surface of the magnet, the main dimensions are also shown in this figure. Simulations based on this model have been done and shown below.

2D Field Distribution

2D simulation has been taken to ensure the main parameters of the magnet as well as to decide the size of the shimming bar that at the edge of the pole face.

POSSION [4] code is used to give the field distribution, shimming bars with height 1mm on the edge of the pole are used to increase the uniformity of the field. Different shapes of shimming bars were simulated and field uniformity were compared to get a better one.

ISBN 978-3-95450-128-1

CONCEPTUAL DESIGN OF A 100 MeV INJECTOR CYCLOTRON

M. Li, J.J. Yang, T.J. Zhang, J.Q. Zhong, CIAE, Beijing, China

Abstract

This paper outlines the conceptual design work of a 100 MeV injector cyclotron for the 800 MeV ring cyclotron, which was proposed by the China Institute of Atomic Energy (CIAE) as a high power proton source of diverse application purpose. For high intensity operation, a straight-sector magnet structure and low magnetic field are preferable. This cyclotron is very similar to PSI Injector II cyclotron, but with higher extraction energy.

INTRODUCTION

In the BRIF-III proposal, an 800 MeV high power proton cyclotron complex was proposed to provide high power proton beam for ADS, neutron science, proton radiography, radioactive ion production and other applications [1], [2]. In this solution, the ECR source will provide a 40~50 mA quasistatic proton beam for a Cockcroft-Walton high voltage generator or a RFQ, which can accelerate the proton to around 1 MeV. Then a low-energy beam line will transport and inject the beam into the injector cyclotron, in which the beam is accelerated to 100 MeV by two double-gap RF cavities and will extracted by electrostatic deflector at its final turn. A medium-energy beam line delivers the beam to the 800 MeV ring cyclotron. The block diagram of the facility is shown in Figure 1.

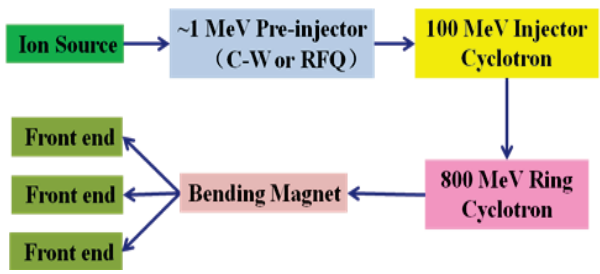

Figure 1: The block diagram of the BRIF-III proposal.

The choice of the energy relies on the feasibility within the BRIF project. This BRIF-III project is divided into two phases. For the first phase, it is proposed to construct the 800 MeV ring cyclotron and to utilize the 100 MeV, 200 μA compact H- cyclotron CYCIAE-100 of the BRIF-II project as its injector. The CYCIAE-100 is under construction at CIAE and is scheduled to start commissioning in 2014. Then in the second phase, in order to achieve a high beam current, the CYCIAE-100 will be superseded by a dedicated separated-sector injector cyclotron, which is described in this paper. The layout of the BRIF facility is shown in Figure 2.

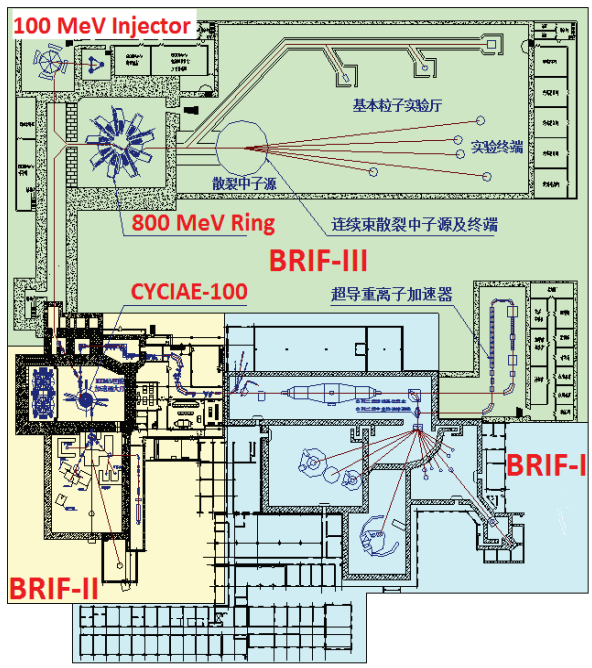

Figure 2: The layout of the BRIF facility.

OVERALL DESIGN

For high beam intensity operation, one must take beam loss control into account at the very beginning of the design. A large pole diameter is preferable for achieving low beam loss. There are two reasons. Firstly, in cyclotrons which accelerate bare proton particle, a large inter-turn separation for the last two turns is required to insert the septum of electrostatic deflector in between. The inter-turn separation is proportional to the orbit radius. Along with the increase of the beam current, the beam's radial size will be enlarged because of the large emittance of injected beam and space charge effects during accelerating. Secondly, we have more space in the valley to insert the auxiliary elements to do fine adjustment for the beam, such as collimators, dipole and quadruple magnets. In the preliminary design, the key parameters are given out for the dedicated injector cyclotron, which is listed in Table 1 and the layout is sketched in Figure 3. Two 3rd harmonic cavities are kept in the baseline design. But according to PSI Injector II experience, most probably they are not required for high current operation because a compact stationary beam will develop during the accelerating because of the strong vortex motion in the horizontal-longitudinal plane, which is introduced by the strong space charge force and the intrinsic coupling between the horizontal and longitudinal directions. In that case, all the four valleys can be used to install the accelerating cavities to enlarge energy gain per turn. Accordingly the total turn number can be reduced by half

ISBN 978-3-95450-128-1

INVESTIGATION OF CYCLOTRON CARBON FOIL LIFETIME IN RELATION TO ITS THICKNESS*

J.H. Kim#, S.G. Hong, J.W. Kim,
Rare Isotope Science Project (RISP), Institute for Basic Science (IBS), Daejeon, Korea
Y.G. Choi and Y.S. Kim,
Nuclear & Energy Engineering Department, Dongguk University, Gyeongju, Korea

Abstract

Thin carbon foils are used as positive-ion extractors in negative-ion accelerators by stripping two electrons. Power deposited in foils via stripping H^- ions and accompanying two electrons generates heat. The energy loss of protons and electrons in carbon foil can be estimated by the multiplication of stopping power (dE/dz) and its thickness. The stopping powers are estimated as the values of 8.51 and 7.25 MeV/(g/cm^2) for the proton and electron, respectively. In cyclotron the stripper is located in a strong magnetic field of ~1.7 Tesla, which makes electrons circular motion around the foil and eventually stops by it. In this study, three carbon foils (200, 400, and 800 μg/cm^2) are tested to investigate the correlation of foil temperature and its lifetime at 1-mA proton extraction. Lifetimes of stripping foils are needed to be as long as possible before replacement of broken foils. Effective lifetimes of carbon foils are investigated as a function of a foil peak temperature, using 38-keV DC electron beam with 2~3 mm diameter.

INTRODUCTION

In negative-ion accelerating cyclotrons a thin carbon foil is usually used to stripe two electrons from the negative ions shown in Fig. 1. Each negative hydrogen (H^-) ion consists of one proton and two electrons, which travel together during accelerating up to 70 MeV in cyclotron. Therefore the kinetic energy of electron is 38.13 keV at the moment of stripping. Power deposited in foils via stripping H^- ions includes energy losses by the proton and also by accompanying electrons. These energy losses of protons and electrons have been calculated by using PSTAR [1] and ESTAR [2] programs. When ions (protons and electrons) pass through a carbon foil, heat is generated mainly through the ionization loss and transferred by the radiation emission. After a time the foil is at thermal equilibrium, heat is emitted by thermal radiation, which is dominant because typical carbon foils have a relatively large ratio of area to volume. It is desirable to have foils running as long as possible before replacement, in order to minimize cyclotron downtime. However, an ion-induced damage, removal of atoms from the foil via elastic and inelastic collision is not considered. In this study, three carbon foils with different thicknesses (100, 200, 400, and 800 μg/cm^2) are investigated in order to find long-lived stripper foils for proton at the extracted energy of 70 MeV. The lifetime of the foil is defined as when the downstream beam is reduced by 10% of its initial value as shown in Fig. 1 (right side). Stripper foils have tested in order to estimate their lifetimes with energetic electron beams corresponding to the practical operating condition.

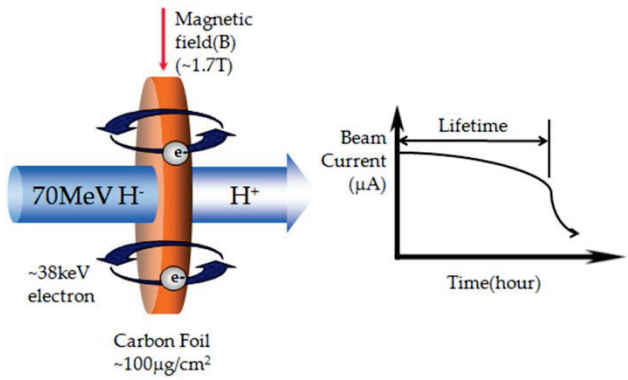

Figure 1: Schematic diagram of stripping two electrons from a negative ion by a carbon foil. As the foil is rupturing, the extracted beam current is decreasing. Since the electrons are travelling with 70-MeV protons together the kinetic energy of electron is 38.13 keV at the moment of stripping.

THEORY

A simplified adiabatic model could be used for an estimation of thermal distribution on the foil. Deposited power densities through the carbon foil by 70-MeV negative hydrogen ions with 1-mA current and by accompanying electrons are estimated by using PSTAR and ESTAR programs, respectively. The density of carbon foil is used as a value of 2.0 g/cm^3 [3].

Stopping Power for Protons

The energy loss of accelerated protons in matter is primarily due to ionization and atomic excitation as shown in Fig. 2. An electronic stopping power, average rate of energy loss per unit path length due to Coulomb collision is the main contribution for generating heat in matter. A nuclear stopping, energy loss per unit length due to the transfer of energy to recoiling is less effective when the ion's energy becomes high.

ISBN 978-3-95450-128-1

DEVELOPMENT OF A NEW ACTIVE-TYPE GRADIENT CORRECTOR FOR AN AVF CYCLOTRON

M. Fukuda#, N. Hamatani, H. Ueda, K. Hatanaka, T. Yorita, S. Morinobu, K. Nagayama, K. Kamakura, T. Saito, Y. Yasuda and H. Tamura, RCNP, Osaka University, Ibaraki, Japan

Abstract

A new type of a gradient corrector with active coils has been developed for beam focusing and bending in the extraction region of the RCNP AVF cyclotron. The gradient corrector is of quadrupole type consisting of a pair of a C-type iron yoke separated each other. A sixteen-turn hollow conductor was coiled around each side yoke, and the two iron dipoles generate a linear field gradient independently. A field gradient up to 9 T/m are available under excitation of a cyclotron main coil for focusing a heavy ion beam with magnetic rigidity up to 1.6 T-m. The position of the gradient corrector is variable within +/-20 mm from a beam extraction axis. Production of the designed field gradient was verified by a field measurement using a Hall-element under excitation of the main coil. We have succeeded in focusing an extracted beam at an object point of the MEBT optics by a combination of the gradient corrector and a quadrupole triplet. Correction of an extracted beam orbit was also demonstrated by optimizing the coil current and position of the gradient corrector.

INTRODUCTION

At the RCNP cyclotron facility the project for improving proton beam intensity and quality is in progress [1]. The cyclotrons will be upgraded to give intense proton beam more than 10 μA with little beam loss on the way from the AVF cyclotron to a target. In the extraction region of the AVF cyclotron, mismatching of the extracted beam trajectories to the MEBT system and insufficient beam focusing in the extraction region caused beam loss and activation of the extraction components.

A horizontal beam spread in the extraction region, caused by a steep fall of a main coil field is compensated by a field gradient corrector placed on the way to a medium energy beam transport (MEBT) system before extraction. A field gradient more than a few T/m is needed to focus the extracted beam, and the required gradient value depends on the magnetic rigidity Bρ of the beam. In a conventional AVF cyclotron, a typical field gradient corrector was of passive type, which has dipole iron pieces whose pole shape was optimised to form a linear field gradient for generating horizontal focusing force using the fringing magnetic field of a main magnet in the extraction region. If the position of the gradient corrector was fixed, the field gradient was uniquely determined by the excitation level of the main magnet. The focal distance of the gradient corrector was not always optimum for each Bρ of particles. The field gradient was tuneable in the limited conditions that the position of the pole tips is changeable.

Gradient correctors of active type were developed by IBA for a small self-extracting 14 MeV H^+ cyclotron using a permanent magnet [2] and by JAEA for the JAEA K110 AVF cyclotron using active coils [3]. The gradient correctors were quite useful for beam focussing and well-matching between the cyclotron extraction axis and the MEBT line. However, fine tuning of the field gradient including non-linear components was difficult.

A new type of a field gradient corrector was developed for the RCNP AVF cyclotron. It consists of a set of quadrupole with active coils and generates a tuneable independent field gradient on both sides of the poles. This paper describes the design and performance of the new gradient corrector of active type.

BEAM OPTICS FOR MATCHING THE EXTRACTED BEAM WITH MEBT

The extraction system of the RCNP AVF cyclotron consists of an electrostatic deflector with a span angle of 120 degrees, a magnetic channel with coils above and below the iron channel to compensate the first harmonic components in the acceleration region, a magnetic shielding iron channel for generating zero-field just before extraction of the cyclotron. The layout of the extraction system is shown in Fig. 1. The magnetic shielding channel was followed by a deflection magnet and a quadrupole triplet lens for adjusting the extracted particle trajectories to the MEBT line and forming a doubly-focussed object for MEBT optics. Beam loss occurred downstream of the magnetic shielding channel because of non-existence of horizontal focussing elements. Thus we decided that the magnetic shielding channel was

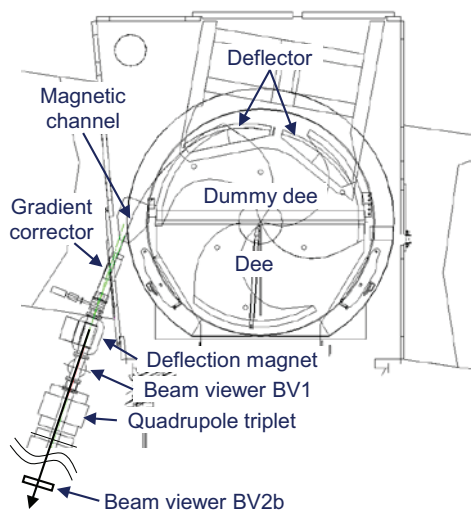

Figure 1: Layout of the RCNP AVF cyclotron.

#mhfukuda@rcnp.osaka-u.ac.jp

IMPROVEMENT IN DESIGN OF 10 MeV AVF CYCLOTRON MAGNET

R. SolhjouMasouleh, H. Afarideh*, B. Mahdian, Department of Energy Engineering & Physics, Amirkabir University of Technology, Tehran, 15875-4413, Iran
M. Ghergherehchi, J. S. Chai, Department of Energy Science/School of Information & Communication Engineering, Sungkyunkwan University, Suwon 440-746, Korea

Abstract

Design study of a 10MeV baby cyclotron which accelerates H− ions is started in March, 2012 at Amirkabir University of Technology (AUT). Up to this point, conceptual design of the cyclotron magnet is finished. This process has been done in two steps: initial design and then optimization.

After finishing the initial design of the magnet by the CST software [1] and adopting hard-edge approximation for finding the pole tip [2], an optimization process has been followed to smooth the pole edge in order to decrease the tension in sharp edges of the pole. In this paper, we are going to explain about the optimization process in details. Actually, we tried to fit the best curve at the pole edges of the magnet with goal of having minimum magnetic field error. Also a short report of results which was obtained before optimization is provided here. Precision of this design is ensured by checking the magnetic field and beam dynamic parameters during the optimization.

INTRODUCTION

The 10 MeV cyclotron magnet is designed to be made of steel-1008 with 4 sectors. Conceptual design of the magnet using the CST software is finished so far and its latest result has been presented previously. Figure 1 provides a short report of magnet design before applying the optimization method:

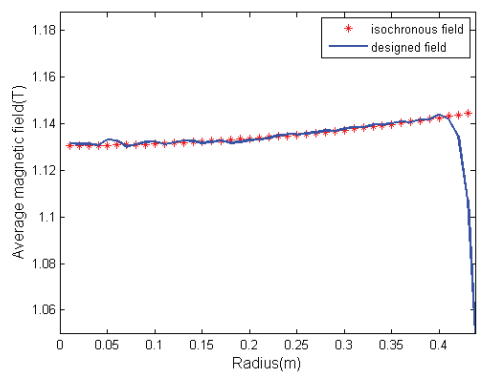

Figure 1: Average magnetic field before applying the optimization method.

Also betatron oscillation frequencies have been calculated considering the formulas [3] (Fig. 2).

*corresponding author: hafarideh@aut.ac.ir

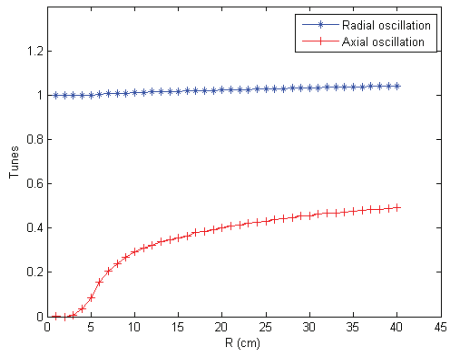

Figure 2: Betatron oscillation before applying the optimization method.

Dividing conceptual design of the magnet into two steps, the first one includes finalizing the magnet model by matching the average magnetic field to the isochronous field. And the second step consists of an optimization process that has been done subsequently. One of the activities which had been applied in order to optimize the model is explained in this paper.

METHOD EXPLANATION

A certain design might seem to be finalized but when you start the engineering design you may face some other aspects of modelling. One of the problems that may occur after manufacturing of the magnet is to have tension in the edges of the magnet. Usually this problem becomes more evident at the pole edge. As it is shown in Fig. 3, this area is not uniform; however the intensity of magnetic field is very sensitive here. So in order to solve this problem we tried to remove the uneven edges.

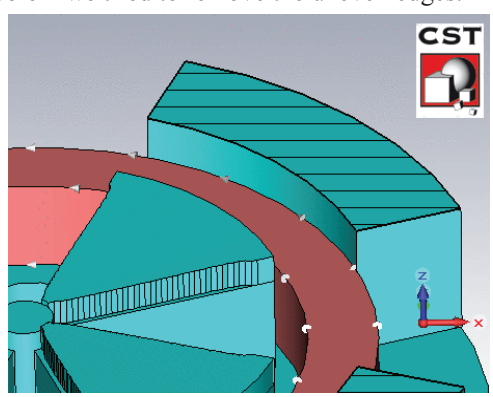

Figure 3: Pole edge before applying the optimization method.

ISBN 978-3-95450-128-1

CONCEPTUAL DESIGN OF 100 MeV SEPARATED SECTOR CYCLOTRON

B. Mahdian, H. Afarideh*, R. SolhjouMasouleh, Department of Energy Engineering & Physics, Amirkabir University of Technology, Tehran, 15875-4413, Iran
M. Ghergherehchi, J. S. Chai, WCU Department of Energy Science/School of Information & Communication Engineering, Sungkyunkwan University, Suwon 440-746, Korea

Abstract

The 100 MeV separated sector cyclotron, aimed for various applications including radioactive ion-beam (RIB) production and proton therapy, was designed at Amirkabir University of Technology (AUT). It has four separated sector magnets. The cyclotron magnet design was based on an iterative process starting from a simple model requiring the vision of the complete cyclotron and the possibility of integration of all subsystems. By computer simulation with the 3D (CST) and 2D (POSSION) codes, principle parameters of the cyclotron magnet system were estimated (pole radius 180 cm, outer diameter 640 cm, height 300 cm). The results showed that the isochronous deviations between simulated values and the calculation one are smaller than 5 Gauss at most radii; therefore, it fulfilled the requirements. This work has been done with high accuracy, proved by particle trajectories and considered mesh range. It has been concluded that it can be possible to design and develop this high energy cyclotron by introducing simple model without using trim and harmonic coils.

INTRODUCTION

Due to the increasing need for accelerators in various research fields such as nuclear physics, atomic physics, material science, biology, and medical science, Amirkabir University of Technology (AUT) has aimed to design isochronous cyclotrons. One of the applications of cyclotrons these research fields are interested in is producing radioactive ion-beam (RIB), can be obtained by a 100 MeV separated sector cyclotron. Magnet, designed based on an iterative process, is considered as one of the most important parts of cyclotron. Two main goals were satisfied in this paper; first, obtaining an average field, rising appropriately with radius, and then, maintaining orbit stability. The main parameters of the magnet will be presented in Table 1. The whole structure of the designed magnet is shown in Fig. 1.

BASIC CONSIDERATIONS

Because of the fact that small gap between poles reduces the number of ampere-turns, necessary to produce the required magnetic field [1], 3 cm pole gap was selected. Four-fold configuration was adopted not only to avoid the effects of the resonances like and [2] but also to increase the acceptable maximum energy [3].

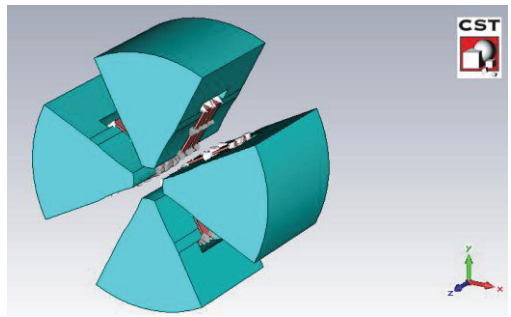

Figure 1: Whole structure of the magnet.

Table 1: Main Magnet Parameters

Parameters	Values
Pole radius	180 cm
Height	300 cm
Sector angle	46-54 degree
Sector Gap	3 cm
Number of sectors	4

MAGNET MODEL CORRECTION

The hard-edge magnet model was used to give an approximate solution to convert magnetic field error to corresponding sector angle error, as shown in Eq. (1),

$$\Delta\eta(r) = \Delta B(r).\frac{2\pi/N}{B_{hill}(r) - B_{valley}(r)} \quad (1)$$

Usually, $\Delta\eta(r)$ used for model correction needs to be multiplied with a scaling factor σ with the value between 0.5 ~ 0.9 to avoid oscillation of field error during iteration [4]. Shimming process was followed as an iterative process until the magnetic field error along radius become minimum value. All the diagrams and error calculations were obtained using MATLAB program.

HAND CALCULATIONS

Prior to 3D simulation with CST code [5], basic dimensions of the magnet had been calculated. Under consideration of magnetic rigidity, calculated according to the following equation, extraction radius and maximum magnetic field on the hill regions were figured out respectively 148.7 cm and 1.7 Tesla. Based on the ampere law, the number of ampere-turns was estimated to be 26.4 kA*turns.

*corresponding author: hafarideh@aut.ac.ir

MAGNETIC FIELD MAPPING OF THE BEST 70 MeV CYCLOTRON

F.S. Grillet, B.F. Milton, Best Cyclotron Systems, Vancouver, Canada
D.T. Montgomery, Cedarflat Precision, Burnaby, Canada

Abstract

As is well known, the mapping of a cyclotron magnet presents several key challenges including requirements for a high degree of accuracy and difficult space constraints in the region to be measured. Several novel solutions were used to create the mapper for the Best 70 MeV cyclotron, which is based on an earlier version used to map the Best 14 MeV cyclotron. Based on a temperature compensated 3-Axis hall probe that is continuously sampled while the probe travels along a radial arm a high degree of positional accuracy is achieved by simultaneously sampling optical encoders located with the probe. A novel implementation using air bearings and air jets provides axial rotation of the arm with almost no metal parts. The mapper has achieved a full 360 degree map in 1 degree theta steps, and 2.5mm radial steps in 2 hours and 40 minutes, with a relative radial accuracy of ±0.02 mm and angular accuracy of ±0.003 degrees. These tolerances are required due to the steep gradients in field, in the centre region the field varies radially by approximately 150 Gauss/mm. This translated to a 3 Gauss variation per 0.02 mm step, while the measurement accuracy target was ±1 Gauss. This paper will describe how the simultaneous challenges of designing with no metal parts while achieving a high degree of rigidity and precision have been addressed.

INTRODUCTION

Mechanical Requirements

The key challenges of mapping cyclotron magnets comes from the tight space constraints together with the requirement for high accuracy. The area to be measured had a diameter of 2.8 m; the vertical gap in which the mapper sat was 55 mm at the centre and 45 mm at the outer radius. The mapper had to rotate a full 360 degrees (in 1 degree theta steps) and map from the edge of the hill to 150 mm past the centre. Since measurements were taken 'on the fly' there had to be no metal parts moving while measurements were being taken and no magnetic parts whatsoever. The maximum allowable deviation from the median plane was 0.25 mm, absolute radial position accuracy of ±0.5 mm and relative angular accuracy of ±0.003 degrees. The hall probe had to be aligned to the magnetic field to better than 1 degree and the maximum rotation of the probe during a map was 0.25 degrees. As can be seen these are not easily attainable targets, especially when little or no metal parts could be used. As well as meeting the accuracy requirements, the mapper had to be transportable. This resulted in manufacturing the beam in three 1m sections, which also resulted in parts which were more easily manufactured.

Overview of Design

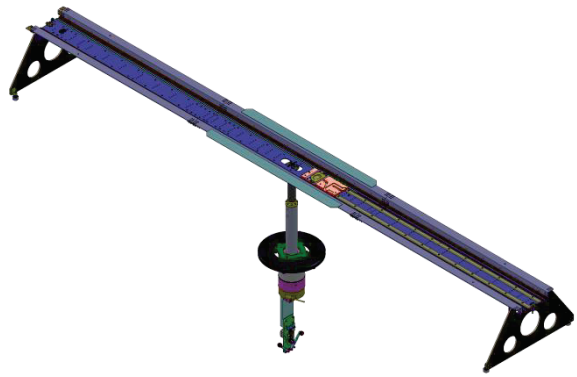

Figure 1: Solid model of the mapper assembly.

The design is based on a rotating shaft to which a carbon fibre beam is connected at its centre, as shown in Fig. 1. At each end of the beam are air bearings which are activated when the mapper rotates, these are mounted on balsa filled carbon fibre legs. Radial motion of the hall probe is achieved by being mounted to a carriage which is driven along the length of the beam by a string and pulley assembly using a stepper motor as drive. A 3-axis probe was used since the 2 "secondary" axes can be used to level the probe in the median plane and verify median plane symmetry.

SYSTEM DESIGN

Carriage Design

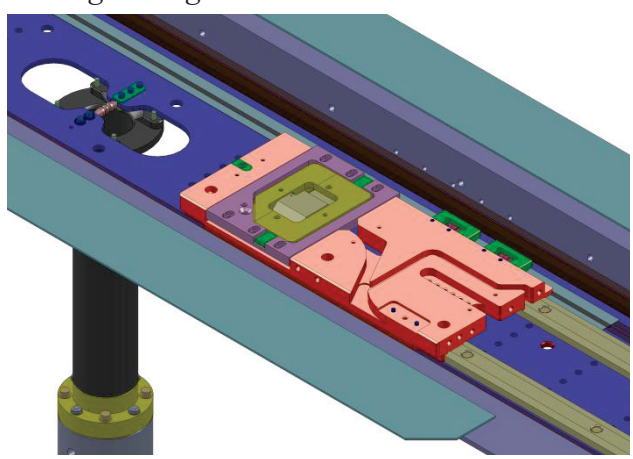

Figure 2: Complex machining is required for carriage and its components.

Since field measurement was to be done while the carriage was moving through the field there had to be no metallic parts due to the formation of eddy currents. The

ISBN 978-3-95450-128-1

DEVELOPMENTS OF HTS MAGNETS AT RCNP

Kichiji Hatanaka*, Mitsuhiro Fukuda, Keita Kamakura, Shinya Takemura, Hiroshi Ueda, Yuusuke Yasuda, Kumiko Yokoyama, Tetsuhiko Yorita, Research Center for Nuclear Physics, Osaka University, 10-1 Mihogaoka, Ibaraki, Osaka, 567-0047, Japan
Takeo Kawaguchi, KT-Science, 1470-1-803, Fujie, Akashi, Hyogo, 673-0044, Japan

Abstract

At RCNP, we have been developing magnets utilizing high-temperature superconducting (HTS) wires for this decade. We built three model magnets, a mirror coil for an ECR ion source, a set of coils for a scanning magnet and a super-ferric dipole magnet to generate magnetic field of 3 T. They were excited with AC/pulse currents as well as DC currents. Recently we fabricated a cylindrical magnet for a practical use which polarizes ultracold neutrons. It consists of 10 double pancakes and the field strength at the center is larger than 3.5 T which is required to fully polarize 210 neV neutrons. It was successfully cooled and excited. One dipole magnet is under fabrication which is used as a switching magnet after the ring cyclotron and is excited by pulse currents. It becomes possible to deliver beams to two experimental halls by time sharing.

INTRODUCTION

High-temperature superconductor (HTS) materials were discovered in 1986 [1]. Significant efforts went into the development of new and improved conductor materials [2] and it became possible to manufacture relatively long HTS wires of the first generation [3]. Although many prototype devices using HTS wires have been developed, so far these applications have been rather limited in accelerators and beam line facilities [4].

At the Research Center for Nuclear Physics (RCNP) of Osaka University, we started to investigate the performance of HTS wires applied for magnets excited by alternating (AC) and pulsed currents as well as direct current (DC) more than ten years ago. We have fabricated three types of prototype magnets. They are a cylindrical magnet [5], a scanning magnet with race-track shape coils [6] and a super-ferric dipole magnet [7]. The coil of the dipole magnet has a negative curvature and the magnet successfully generated the field higher than 3 T at operating temperature of 20 K. Recently, we fabricated a cylindrical magnet for a practical use which polarizes ultracold neutrons. At RCNP, we have been developing a superthermal ultracold neutron (UCN) source to search for the neutron electric dipole moment (nEDM) [8,9]. The critical energy of UCN from the RCNP source is 210 neV which is determined by the Fermi potential of the He-II bottle. The neutron magnetic potential is 60 neV/T. Then the magnetic field is required to be larger than 3.5 T in order to fully polarize UCNs from the source. We decided to apply HTS wires for a practical use after our developments on HTS magnets. One dipole magnet is under fabrication now. The magnet is used as a switching magnet after the ring cyclotron and is excited by pulse currents. It becomes possible to deliver beams to two experimental halls by time sharing.

*hatanaka@rcnp.osaka-u.ac.jp

3 T DIPOLE MAGNET

In order to investigate feasibilities of synchrotron magnets using HTS wire, we have built a super-ferric dipole magnet to be operated by lumping currents. The specification of the magnet is summarized in Table 1.

Table 1: Design Parameters of the HTS Dipole Magnet

Magnet	Bending radius	400 mm
	Bending angle	60 deg.
	Pole gap	30 mm
	Number of turns	600 x 2
Coils	Winding	3 Double pancakes/coil
	Temperature	20 K
	Rated current	300 A

The HTS wire consists of a flexible composite of Bi-2223 filaments in a silver alloy matrix with a thin stainless steel lamination that provides mechanical stability and transient thermal conductivity. The wire, DI-BSCCO Type HT-SS, was supplied by Sumitomo Electric Industries, Ltd. [10]. The wire is 4.5 mm wide and 0.3 mm high in average. Upper and lower coils consist of 3 double pancakes of 200 turns. Critical current Ic of wire measured at 77 K and self-field was higher than 160 A. Ic values of double pancakes were 60-70 A at 77 K. After stacking, they were 47 A and 51 A for the upper and lower coil, respectively. There were no damages in wire during winding process. Stacked pancakes are sandwiched by ion plates to reduce magnetic fields on the wire surface, since the Ic is lowered by fields on surface. Figure 1 shows the lower coil which has a negative curvature inside.

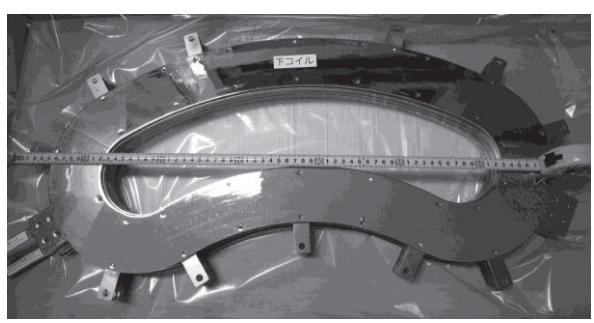

Figure1: Lower coil of the dipole magnet.

ISBN 978-3-95450-128-1

THE DEVELOPMENT OF HIGH STABILITY MAGENT POWER SUPPLY*

K. H. Park# , Y. G. Jung, D. E. Kim, H. S. Suh, H. G. Lee, H.S. Han and S. C. Kim,
PAL, POSTECH, Pohang, Korea
Y. S. Lee and J. S. Chai,
Schoolof Information & Communuication Engineering Sungkyunkwan University,Korea

Abstract

This paper presents the magnet power supply (MPS) for the beam correction magnet. The required current to the magnet was ±20 A. The MPS has been implemented using the digital signal processing technology using the DSP, FPGA, ADCs and analogue and digital circuits. An embedded module was adapted for the Ethernet connection. The output current stability of the MPS showed about 10 ppm peak-to-peak in short term experiment. The long term stability was also ~10 ppm for eight hours. The other experimental results such as line regulation, and bandwidth were given in this paper.

INTRODUCTION

The Pohang Light Source(PAL) has been constructing the PAL-XFEL accelerator that needs many kinds of magnet power supply (MPS). The MPSs are nowadays developed by the digital technologies using digital signal processor (DSP), FPGA, ADC and so on. The DSP was primarily optimised for the various digital signal processing with the fast calculation time such as feedback control, digital filters, stand alone controller etc. And it includes many hardware functions to make it easy to interface the peripheral devices through the SPI, CAN, RS232C, I2C, ADCs etc. Thus the application areas of the DSP increased sharply in the various applications, especially in power conversion systems – high quality power supply, UPS, inverter, etc. [1].

The other trend in circuits design for the electronic system is that the FPGA gets popularity in the wide application area because it gives flexibility in circuits design to the designer. It can be made the complicated random logic simple. The FPGA makers also provide various useful IPs thus circuits design is very easy, furthermore it gives very high performance and density [2]. The high stable MPS circuits generally combined a DSP with FPGAs to get the fast calculation time. The digitally controlled MPS was at the many accelerator laboratories. The performance of MPS improved better but its size smaller by every year. The MPS was also required the embedded Ethernet connection for EPICS which was the general control architecture in accelerator machine [3].

In this paper, we present the various design schemes and experimental results of the high stabile MPS for corrector magnet of the PAL-XFEL.

* Work supported by Ministry of Science, ICT & Future Planning
# pkh@postech.ac.kr

SYSTEM CONFIGURATION

The system configuration of the designed MPS is shown in the Fig. 1. The input stage is rectifier circuits with a damped low pass filter to get stable output stability. The bandwidth of the input filter should be less than 30 Hz with a small under damp. The out stage is H-bridge topology using the four FETs with cascaded low pass filters to make the output current smooth and remove the switching noise. The output stage was isolated to the control circuits in order to minimize the switching noise influence.

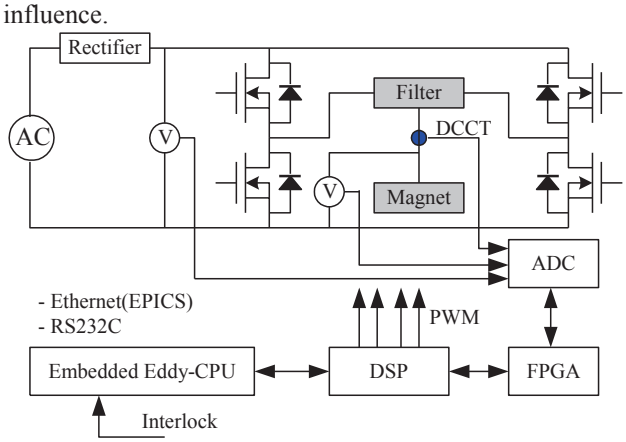

Figure 1: Block diagram of the magnet power supply.

The DSP TMS320F28335 from TI Co was adapted to control the overall power supply system. It has six high resolution PWM outputs with 150ps micro edge position which is the absolutely required function to archive the ~10 ppm output stability [4].

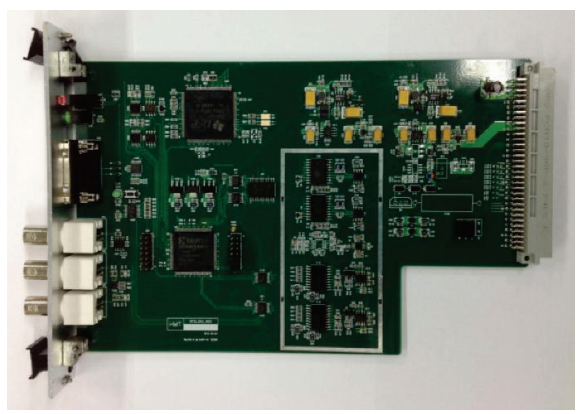

Figure 2: DSP Board that includes DSP, FPGA, ADCs and the other logics.

ISBN 978-3-95450-128-1

DESIGN STUDY OF 10 MeV H- CYCLOTRON MAGNET

H. S. Kim[1], M. Ghergherehchi[1], H.W. Kim[2], S.H. Lee[1], S.H. Kim[1], J.S Chai[#1,2]
[1]WCU Department of Energy Science / [2]College of Information & Communication Engineering
Sungkyunkwan University, Suwon, 440-746, Korea

Abstract

For the past decades, PET (positron emission tomography) has been remarkable growth in market. PET using ^{18}F is widely provided for cancer screening and expected to be installed at small and medium hospital for convenience of patients. At Sungkyunkwan University, 10 MeV H^- cyclotron, which produces ^{18}F is being developed. In this paper, we demonstrated main magnet design and whole design procedure was explained. The result of design is verified by orbit analysis and single particle tracking. The description of the obtained result is presented in this paper.

INTRODUCTION

9 MeV H^- cyclotron for production of ^{18}F has been designed and manufactured and successfully operated at Sungkyunkwan University. In this research, 10MeV energy cyclotron is selected in order to yield more ^{18}F [1]. Design procedure is described from initial calculation to verification of the result. Modelling and optimization method with the assistance of three dimensional magnetic field calculation are simulated by OPERA-3D [2]. The magnetic field analysis is performed by beam code CYCLONE [3]. It consists of 3 part. Part 1 and 2 is used at centre of the cyclotron and at first 5 turns. Part 3 is suitable for turn 5 to extraction. Based on CYCLONE Part 3, we could manufacture magnet in accordance with our designed magnetic field which satisfies focusing and isochronous condition. In addition, magnet shimming was carried out by analysis of obtained results by simulation codes. Design requirements were satisfied by iteration process.

MAGNET DESIGN

Magnet design started from determining RF frequency, harmonic number and magnetic rigidity.

$$B \bullet \rho = \frac{1}{300\ Z}[T^2 + 2\ T\ E_0]^{1/2}. \qquad (1)$$

From equation (1), size of magnet pole can be approximately determined. Cross-section view is shown as Fig. 1. Radius of magnet and pole is 830 mm and 460 mm. The gap ratio of valley/hill is 15 and hill sector angle is 47°. Differences between hill and valley magnetic field could increase vertical tune by 0.6. However, the above geometry need more ampere turn. To reduce it, radio frequency was set at 67.23 MHZ. Main parameters of magnet are shown in Table 1.

Magnetic field calculation was done by OPERA 3D. Material adapted in this magnet is a low carbon steel AISI 1008 that contains maximum 0.1% of carbon and used to enhance magnetic properties. Figure 2 shows the B-H curve of magnet material. Local mesh method with 8732146 elements and 1/8 boundary condition was used for fast and accurate calculation. Calculated vertical magnetic field component data in midplane is used as an input of beam code. In CYCLONE code, it is extended to field out midplane. Figure 3 shows field distribution in magnet pole.

Table 1: Main Parameters of 10 MeV Cyclotron Magnet

Parameters	Values
Maximum Energy	10 MeV
Accelerated particle	Negative hydrogen
Radio frequency	67.23 MHZ
Harmonic number	4
Pole radius	0.46 mm
Hill / Valley gap ratio	15 (360 mm/24 mm)
Sector angle	47°
B-field (min., max.)	0.26, 1.96 T
Dimension (Diameter, Height)	1660 mm×860 mm

EQUILIBRIUM ORBIT ANALYSIS

In order to get a stable isochronous field, tunes and phase error should be considered. Equilibrium orbit information was calculated by CYCLONE code. Energy gain per Dee is 0.0398 MeV. Equilibrium orbit is spaced from 0.0150 MeV to 10.6364 MeV. Energy gain per Dee is used for spacing among adjacent orbits. Figure 4 shows that energy of orbit at average radius.

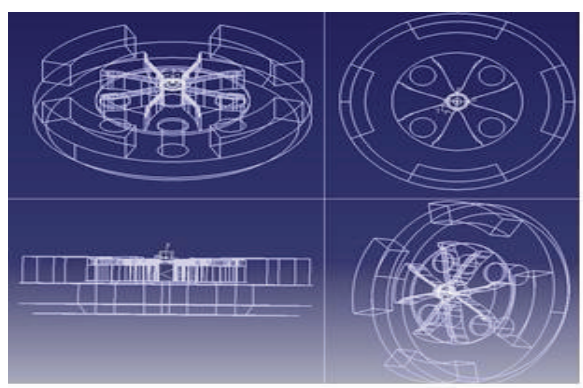

Figure 1: Cross section view of magnet.

ISBN 978-3-95450-128-1

AN INTEGRATED SELF-SUPPORTING MINI-BEAMLINE FOR PET CYCLOTRONS

Morgan Patrick Dehnel, David Edward Potkins, Thomas Maxwell Stewart
D-Pace, Inc., PO Box 201, Nelson, BC, V1L 5P9, Canada

Abstract

A commercial Fluorine-18 water-target can now handle 150 micro-amperes of 10-19 MeV proton current [1-5]. The days of a few tens of micro-amperes bombarding a PET target with low residual activity on a self-shielded cyclotron are over. Now an integrated self-supporting mini-beamline is essential for safe, optimized and reliable operation of PET cyclotrons especially with high power liquid or solid targets. The high levels of prompt/residual radiation are moved (~1 m) away from the cyclotron so local-shielding can be placed around the target/selector assembly, which minimizes cyclotron component damage due to prompt neutrons/gammas, and ensures the high residual target radiation is attenuated, so maintenance personnel can work on the cyclotron in a "cool" environment. Beam diagnostic readbacks from baffles/collimators provide steering and focusing control of the beam. This "plug-n-play" beamline is an integrated self-supporting unit cantilevered from the cyclotron. The single aluminum sub-structure acts as mounting flange, support structure, beampipe, and magnet registration device. A cross-shaped vacuum envelope through the compound quadrupole/steering magnets result in maximum beam throughput and optimization.

MINI-BEAMLINE DESCRIPTION

The mini-Beamline is an evolution of the D-Pace Compact Beamline for PET [6-8], which was short yet used large elements (radially), and was more expensive. The mini-Beamline is a light-weight integrated unit with options. It is intended for any cyclotron used for Positron Emission Tomography (PET) radioisotope production. IBA has facilitated a first installation opportunity and this paper shall illustrate the system's performance and set-up for the case of a Cyclone® 18.

Ion-Optics

IBA provided the Twiss parameters (α,β,γ) describing the 18 MeV proton beam at each of the four extraction ports with unnormalized emittance 15 π·mm·mrad (90% of the beam intensity) in both phase planes. A conservative momentum dispersion of 0.35% was utilized. Ion-optics were undertaken with Beamline Simulator [9] to confirm high transmission from each of the main tank ports to a target (ϕ = 10 mm) at ~1.4 m from the main tank (~ 1 m from cyclotron yoke). Table 1 gives the mini-Beamline element parameters, Figure 1 shows a cross-section of the largest beam envelope which is in the X plane at the centre of the horizontally focusing quadrupole magnet. Note the unique shape of the extruded aluminum vacuum tube. It increases the beamline acceptance and is a stronger mechanical section as compared to a round pipe. Figure 2 gives the X & Y beam profiles for extracted beams from each of the four ports to target. This establishes the mini-Beamline's efficacy on any port.

Table 1: Mini-Beamline Ion-Optical Parameters

Parameter	Value	Unit
Drift 1	489	mm
VQ: L, ϕ_{bore}, B_{max}	150, 33, 0.3	mm, mm, T
Drift 2	50	mm
HQ: L, ϕ_{bore}, B_{max}	150, 33, 0.3	mm, mm, T
Drift 3	600	mm

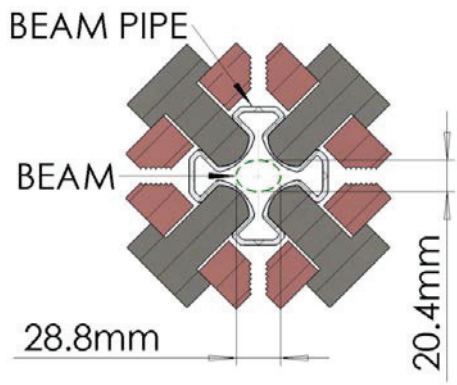

Figure 1: Cross-section at widest beam envelope.

Features

Figure 3 shows the 3D layout of the mini-Beamline. The light-weight integrated aluminum sub-structure provides several functions. It is a low residual activity vacuum vessel with specialized interior shape for high transmission, and large-section exterior for strength. It self-supports the entire beamline and is cantilevered from the magnet yoke by way of an adjustable foot. It has precision machined features for tightly toleranced magnet registration. The upstream flange mates to the cyclotron main tank, and houses an aluminum entrance collimator electrically isolated with VESPEL™ stand-offs and has beam current readback to the control system (bnc).

The unique quadrupole doublet is divided into ambient air-cooled quadrants with the yokes primarily in the longitudinal direction. For asymmetric focusing and XY Steering a circumferential yoke is used for differential flux. The X & Y compound magnets utilize one small power supply per thermally-interlocked coil (Total = 8).

ISBN 978-3-95450-128-1

TRIM COIL UNBALANCE OF THE 88-INCH CYCLOTRON*

M. Kireeff Covo#, M. Strohmeier, A. Ratti, B. Bingham, B. Ninemire, C. Lyneis, D. Todd, L. Phair, and P. Pipersky, LBNL, California, USA
K. Y. Franzen, Mevion Medical Systems, Massachusetts, USA

Abstract

The 88-inch cyclotron Dee probe shows large losses inside the radius of 20 cm and suggests problems in the ion beam injection. The current of the top and bottom innermost trim coil 1 is unbalanced to study effects of the axial injection displacement. A new beam profile monitor images the ion beam bunches, turn by turn, and the beam center of mass position is measured. The technique allows increasing the beam transmission through the cyclotron.

INTRODUCTION

The ions produced by the electron cyclotron resonance ion sources are injected inside the 88-inch cyclotron by a mirror inflector. The inflector assembly is a grounded grid mounted with standoffs on a biased plate that is tilted 45^0 above the cyclotron horizontal midplane. The ions entering the grid inflector experience an electrostatic force that directs them to the cyclotron middle plane.

After the ions enter the cyclotron, they are accelerated by a radiofrequency (RF) electric field and held to a spiral trajectory by a static magnetic field. The RF fields cause the ions to bunch up into packets.

The cyclotron has a set of 17 adjustable concentric trim coils [1] located on the pole pieces inside the magnet gap. They are used to modify the distribution of vertical magnetic fields and compensate for the relativistic mass increase to keep an isochronous motion as the ions gain velocity and the orbit increases with radius. The ions that are not synchronized with the RF are lost.

The Dee probe [2,3] is mounted at the end of a shaft that moves radially inward. The probe is unsuppressed, but it is partially magnetically shielded by the main magnet field. The probe measures the beam current hitting a water cooled copper block. The measured signal corresponds to the internal beam intensity inside the cyclotron and exhibits the radial beam losses.

Low cross section experiments that produce super-heavy elements have increased the demand for high intensity heavy ion beams at energies of about 5 MeV/nucleon [4]; nevertheless initial measurements with the Dee probe show large losses inside the cyclotron radius of 20 cm. The poor transmission suggests problems in the ion beam injection may be caused by off-centered initial orbits with bunches partially hitting the lips of the Dee inserts.

The next sections show the unbalance of innermost trim coil 1 and measurements of the beam center of mass position to correct the initial off-center orbits and improve the transmission through the cyclotron. This work is in continuation of the High-Voltage Upgrade Project [5] and aims to increase the intensity of the ion beam.

INNERMOST TRIM COIL 1 UNBALANCE

Figure 1 shows in black the 750 A power supply connected to trim coil 1 using a reversing switch. The switch can invert the electrical current orientation of the coils and consequently the orientation of the magnetic field. The coils are arranged in series, so all the current of the top coil goes to the bottom coil.

Initially, two CM600HA-5F IGBT transistors displayed in red were connected in parallel to the coils in order to shunt the current around the top and bottom coils, i.e., from the busbar between the top and bottom coils to the power supply positive and negative outputs.

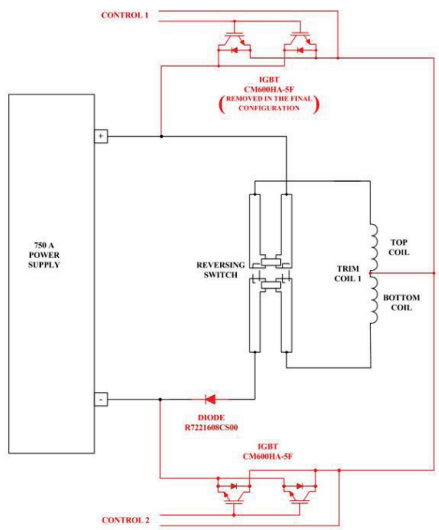

Figure 1: Trim coil unbalance circuitry. The original trim coil system is displayed in black and the modifications are in red. Two parallel IGBT transistors are connected across each coil. The top IGBT transistors connected to the positive output are removed in the final configuration. A power diode is also added in the final configuration between the power supply negative output and the reversing switch, allowing to shunt half of the trim coil current.

This configuration has the advantage of weakening the top or bottom vertical magnetic fields with the same control signal, independently of the position of the reversing switch. For instance, if the magnetic field produced by trim coil 1 has the same direction of the

*Work supported by by the Director, Office of Energy Research, Office of High Energy and Nuclear Physics, Nuclear Physics Division of the U.S. Department of Energy under Contract DE-AC02-05CH11231.
#mkireeffcovo@lbl.gov

BUNCH-SHAPE MEASUREMENTS AT PSI'S HIGH-POWER CYCLOTRONS AND PROTON BEAM LINES

R. Dölling, Paul Scherrer Institut, CH-5232 Villigen-PSI, Switzerland

Abstract

Longitudinal-transversal 2D-density distributions of the bunched 2.2 mA CW proton beam can now be measured at the 13 last turns of the Injector 2 cyclotron, at several locations in the connecting beam line to the Ring cyclotron, at the first two turns of the Ring cyclotron (all at energies around 72 MeV), as well as behind the Ring cyclotron (at 590 MeV). In the large part, distributions can be taken from several angles of view, separated each by 45°.

The measurement systems at our facility have evolved with time; this paper gives the present status, performance, limits and typical results. Due to the limited space, we refer in the large part to our previous publications [1, 2, 3] and concentrate on recent findings and measurements and ideas for next steps.

INTRODUCTION

In contrary to its predecessor in 1992 [4], the "old" detector setup (Fig. 1a) operating in 2000 [1] already had a time resolution allowing to resolve the bunch time structure at the last two turns of Injector 2. Since 2004 it is (with a single detector) also used in the Ring cyclotron [5]. The "new" detector setup from 2010 [2, 3] provides a larger count rate and thereby much shorter measurement durations. Here it was intended to again allow the determination of time resolution, but by a simpler design [2]. This failed as is discussed later.

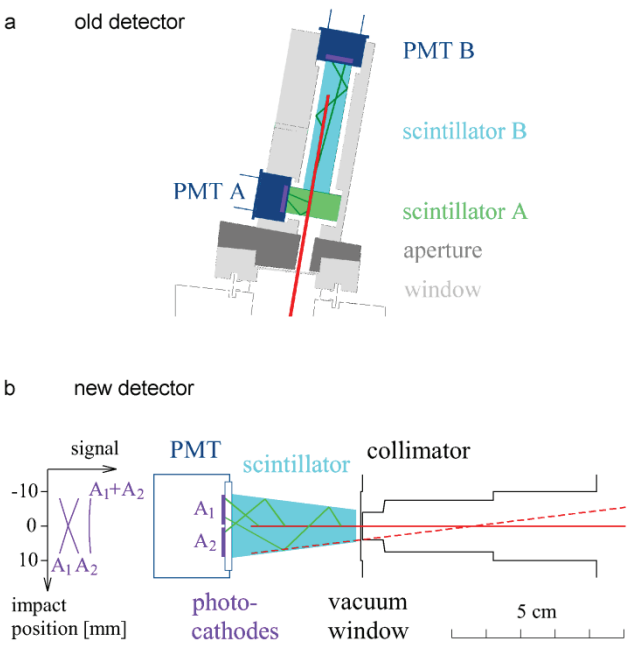

Figure 1: a) Old detector setup (at RIZ1). b) New setup.

The evaluation procedure with several corrections is described in [3] and the background correction needed for the measurement in the Ring cyclotron in [2]. Bunch shapes measured at full beam current at all locations are presented in [3]. (Here we have to note, that at the location MXZ1 shortly after the Injector 2, the wire 0 is not melted by a too dense beam as assumed in [3]. Unchanged, this measurement is now operational. The reason for the repeated wire failure is not clear.)

PULSE HEIGHT SELECTION

Protons are scattered elastically at the wire or inelastically, loosing discrete energies, or other particles are created with an energy spectrum. The time-of-flight from wire to detector is different for these species, as well as the photo-multiplier tube (PMT) output pulse heights generated. Pulse-height selection allows to derive the timing information from only a single species. At present, pulse height selection and timing both use leading-edge discriminators (LED) [2], accepting pulses above a certain height. Both discriminator levels are set fixed. The pulse height is adjusted by varying the PMT gain via the PMT voltage while observing the bunch time structure with the wire placed at a fixed position in the beam.

Significant differences in discrimination characteristics are visible for different detectors, locations and beam energies. At ~72 MeV (Fig. 2a-c), the signal is a folding of the bunch shape with the (much sharper) peak structure resulting from the different delays of elastically (left peak) and inelastically (following peaks) scattered protons. The diagonal slope results from discriminator walk at the changing pulse height. To the right, the increase of accepted counts with the PMT voltage is depicted. The steps due to the species with different energy loss are visible. The blue line marks the level, where all elastically scattered protons are accepted. To the far right, the 1σ-length of the distribution is displayed. The red line indicates the voltage level, which gives a good resolution and, if possible, allows the use of all elastically scattered protons. The protons are stopped in the scintillator, a sharp step in the count rate of the elastically scattered protons (ESP), which give the highest pulses, is expected, when a certain voltage is surpassed. This is the case at Fig. 2a,c and with all ESP utilized, the displayed bunch length is still minimal. In contrary, at Fig. 2b there is a gradual increase, the pulse heights seem to be "smeared out". Here not more than ~40% of the ESP can be used without increasing the measured bunch length. The reason for this is not clear. Possibly, the stronger coupling of RF noise to the PMT base-line signal observed in this case plays a role. The old detector (Fig. 2a) exhibits a linear walk while the new detector

ISBN 978-3-95450-128-1

DEVELOPMENT OF A SCINTILLATOR PROBE BASED ON FIBER OPTICS FOR RADIAL BEAM DIAGNOSTICS OF THE ION BEAM OF THE 88-INCH CYCLOTRON *

M. Strohmeier†, P. Pipersky, K. Yoshiki Franzen, M. Kireeff-Covo, C. Lyneis, J. Benitez, B. Ninemire, L. Phair, D. Todd, LBNL, Berkeley, CA 94720, USA

Abstract

The complex 3-D magnetic field structure of the 88-Inch Cyclotron combined with the large number of tuning parameters such as trim coils, valley coils, the main field itself and the injection/extraction components makes it challenging to tune the Cyclotron. Furthermore, beam diagnostic devices to help tuning were limited to a stationary Faraday cup at the exit of the machine and a so-called Dee-probe which allowed for beam current measurements as a function of the turn radius. Motivated to improve the transmission of the Cyclotron due to misalignment of the ion beam in the center region and insufficient beam diagnostics, we have developed an optical beam viewer which we can move radially in and out of the machine. It allows us to image the beam cross section and its axial position with high spatial resolution as a function of radius. In this paper, we describe the mechanical development of the device which consists of a KBr scintillator disc, a fiber bundle and a digital camera and we present data from its initial commissioning.

INTRODUCTION

The 88-Inch Cyclotron at Lawrence Berkeley National Lab has been operating for more than 50 years, supplying numerous nuclear science programs with ion beams. More recently, two distinct user groups with very different beam needs have developed. The first group is composed of members of the National Space Security community who performs chip testing and requires low intensity beams of highly charged ions such as Xe^{43+}. The second is the Nuclear Science Community which requires medium charge states at relatively high intensities. For example, the heavy element research group has recently requested a $^{48}Ca^{11+}$ beam of 2 pµA. In order to meet these high current needs, a 4-year project was launched where the low energy injection beam lines and the Cyclotron center region were evaluated and upgraded. It became clear that in order to identify losses and increase the transmission of the Cyclotron, more detailed diagnostics were needed. Historically, a beam current readout of the inflector, a radial Dee-probe (a water cooled copper plate with a current readout) and a 3-finger probe were the only available diagnostic tools inside the Cyclotron. The 3-finger probe is composed of 3 segmented electrodes with individual current measurements that give a rough indicator of the axial beam position. However, there was no information about the beam shape and whether or not it was being clipped at some point along its trajectory. This led to the development of a radial scintillator probe to replace the 3-finger probe, which would give much more detailed information about the beam properties. The new probe utilizes most of the motion and vacuum components of the 3-finger probe which kept the amount of modifications at a minimum. The design and its implementation will be described in this paper.

HARDWARE OF THE PROBE

The radial scintillator consists of three main components: The Scanner Head, a Fiber Bundle and the CCD camera which are all described below. A schematic view of the device is shown in Figure 1 and its technical details are summarized in Table 1.

Table 1: Specifications of the Essential Viewer Components

Camera:	Allied Vision Tech - GigE Manta
	1392 (H) x 1040 (V) pixels
	4.6 µm x 4.6 µm per pixel
	1/2” chip size, C-mount connectors
Fibers:	SCHOTT North America, Inc.
	10 µm mono-fiber size
	≈ 100 µm spatial resolution
Scintillator:	KBr from Alfa Aesar, 4mm thick

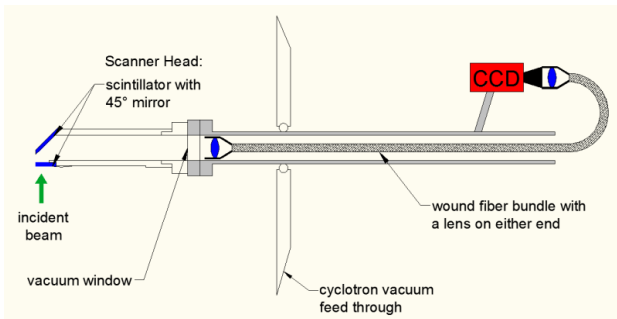

Figure 1: Schematic view of the radial scintillator probe commissioned at the 88-Inch Cyclotron at LBL.

* This work was supported by the U.S. Department of Energy under Contract No. DE-AC02-05CH11231.

† MMStrohmeier@lbl.gov

ISBN 978-3-95450-128-1

R&D OF HELIUM GAS STRIPPER FOR INTENSE URANIUM BEAMS

H. Imao*, H. Okuno, H. Kuboki, O. Kamigaito, H. Hasebe, N. Fukunishi, Y. Watanabe, M. Fujimaki, T. Maie, T. Dantsuka, K. Kumagai, K. Yamada, T. Watanabe, M. Kase, Y. Yano
RIKEN Nishina Center for Accelerator-Based Science, Saitama, Japan

Abstract

Intensity upgrade of uranium beams is one of the main concerns at the RIKEN Radioactive Isotope Beam Factory (RIBF). The lifetime problem of carbon-foil strippers due to the high energy loss of uranium beams around 10 MeV/u was a principal bottleneck for the intensity upgrade in the acceleration scheme at the RIBF. We have developed a recirculating He-gas stripper as an alternative to carbon foils for the acceleration of high-power uranium beams. The new stripping system was actually operated in user runs with U^{35+} beams of more than 1 puA. Electron-stripped U^{64+} beams were stably delivered to subsequent accelerators without serious deterioration of the system for six weeks. The new He-gas stripper, which removed the primary bottleneck in the high-power uranium acceleration, greatly contributed to the tenfold increase of the average output intensity of the uranium beams in 2012 from the previous year.

INTRODUCTION

Intensity upgrade of uranium beams up to our ultimate goal intensity of 1 puA is one of the main concerns at the RIKEN Radioactive Isotope Beam Factory (RIBF) [1]. A new injector, RILAC2 [2, 3], which includes a 28-GHz superconducting electron cyclotron resonance ion source (ECRIS) [4], has been successfully developed and became fully operational in fiscal 2011. To further accelerate the uranium beams generated by this powerful injector, one of the highest priorities is to explore a new charge stripper for the high-power uranium beams. The possible output intensity of uranium beams at the RIBF was mainly limited by the lifetime problem of the carbon foil strippers.

Figure 1 shows the acceleration scheme for ^{238}U and ^{48}Ca ions before 2011 at the RIBF, where the charge state of ions are converted twice with thin carbon foil strippers [5]. In the acceleration of for ^{238}U, highly charged uranium ions, $^{238}U^{35+}$, generated by 28-GHz ECRIS [4] are accelerated with RILAC2 up to the energy of 0.67 MeV/u. They are further accelerated to 11 MeV/u in the RIKEN Ring Cyclotron (RRC) and then converted to $^{238}U^{71+}$ beams using a thin carbon foil with a thickness of approximately 0.3 mg/cm^2. After the beams are further accelerated to 50 MeV/u by the fixed frequency cyclotron (fRC), the charge state is converted to 86+ with a relatively thick carbon foil stripper (approximately 17 mg/cm^2). $^{238}U^{86+}$ beams are accelerated to the final energy of 345 MeV/u by the intermediate-stage cyclotron (IRC) and the superconducting ring cyclotron (SRC), and then sent to the RI production target with the RI beam separator BigRIPS.

* imao@riken.jp

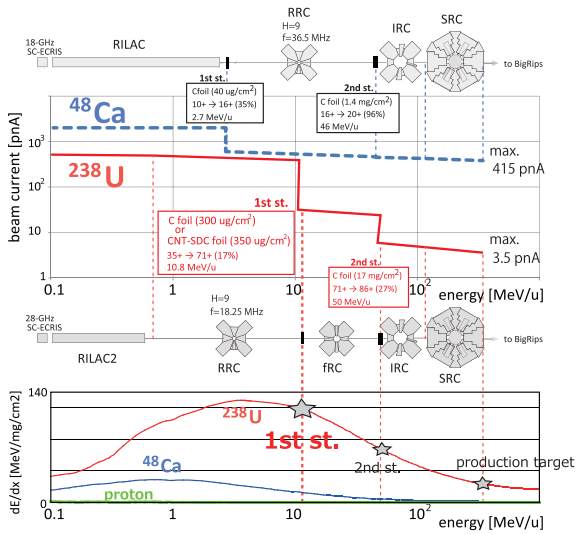

Figure 1: The acceleration scheme of uranium and calcium ions before 2011 at the RIBF. Calculated energy dependences of dE/dx for ^{238}U, ^{48}Ca and proton are also shown at the bottom of the figure.

There are some intrinsic difficulties in the electron stripping of uranium ions compared with that of calcium ions. For very heavy ions such as uranium ions, the binding energies of the inner shell electrons are very large. One requires sufficient injection energy to increase the charge–mass ratio q/m of uranium ions by stripping strongly bound electrons. As shown in Fig. 1, the injection energies for the first stripper at the RIBF are 2.7 MeV/u for ^{48}Ca and 10.8 MeV/u for ^{238}U. The stripper thickness correspondingly increases at the higher injection energy. Increased stripper thickness causes emittance growth, which reduces the beam transmission efficiency in the subsequent cyclotrons.

The most serious problem for the acceleration of the high-intensity uranium beams is the damage caused to the strippers by high energy loss of uranium ions as shown at the bottom of Fig. 1. The energy loss ($\propto \sim Z_p^2 Z_t/A$) of uranium ions is thousands times higher than that of protons and near maximum at the injection energy of 11 MeV/u at the first stripper.

The foil thickness required at the energy of the first carbon foil stripper is very thin less than 1 μm. The problems of using such thin foil stripper for high-power uranium beams include the fragility, thickness non-uniformity, and poor thermal conductivity. The previously measured lifetime of the fixed carbon foil stripper is as short as 15 h when it is irradiated by uranium beams with intensities of up to 20 pnA [6]. The use of rotating foil strippers of

ISBN 978-3-95450-128-1

TRIUMF EXTRACTION FOIL DEVELOPMENTS AND CONTAMINATION REDUCTION*

Y.-N. Rao, R. Baartman, I. Bylinskii, V. Verzilov, TRIUMF, Vancouver, Canada
J.M. Schippers, Paul Scherrer Institut, Villigen, Switzerland

Abstract

Progress has been made in understanding of failure modes and activation issues surrounding the extraction probes and stripping foils of the TRIUMF 500 MeV cyclotron. The radioisotope ^{7}Be has in the past decade been observed near the main extraction stripper, and relatedly, stripping foils warped or even broke during use. This is now understood to be due to over-heating in the foil and the frame, caused by the stripped 270 keV electrons migrating up the foil before dissipating their energy in the foil frame. As well, it is desirable to reduce beam spill along the high intensity primary beam lines. The spills are primarily caused by the large angle scattering from the stripping foil. It was thus suggested that thinner foils be used to minimize the scattering. In view of these 2 issues, improvements were made such that (1) highly-orientated pyrolytic graphite foils, of thickness around 2 mg/cm^2, are now used; (2) Tantalum frame is now used in place of the previous stainless steel. These changes, plus additional heat relief features introduced, have resulted in 4 times longer lifetime with the foil, and 5 to 10 times reduction to the tank contamination level around the extraction probe. Also, these improvements have led to significantly reduced amount of beam spill monitor trips.

INTRODUCTION

The 500 MeV H$^-$ cyclotron has been using stripping foils to extract multiple proton beams simultaneously. It has extracted increasingly intense proton beams during the past 40 years. Over the last 10 years, routine operation delivered peak currents up to 320 μA in total to the three primary beamlines, where the two high energy beams for the beamlines (1A and 2A) are extracted with the stripping foils operated in a radial shadow mode to obtain the desired beam split ratio. In such a shadow case, the beam density on the foils is 40% higher than in the single extraction case.

In the 2004 year-end shutdown it was observed that the ^{7}Be contamination near the 1A stripper was higher than in previous years by at least one order of magnitude. The activity was almost completely from ^{7}Be. It was speculated to be due to the dense beam spots on the 1A and 2A foils as a result of the shadowing technique used. A possible scenario was that the higher density spot produced a higher density electrons which spiraled around the magnetic field and passed though the foil repeatedly, ending up in the foil or the metallic holder and causing an overheat to the foil, thereby driving off ^{7}Be that had been produced there by nuclear reactions.

*TRIUMF receives funding via a contribution agreement through the National Research Council of Canada.

The foil frame did show evidence of excessive heating, as shown in Fig. 1 as an example. During those years, after an accumulation of ~60 mA-hrs, which could take three to five weeks, the foil began to warp and even crack, producing beams with poorer quality and requiring frequent retuning and increasing spills along the beam line.

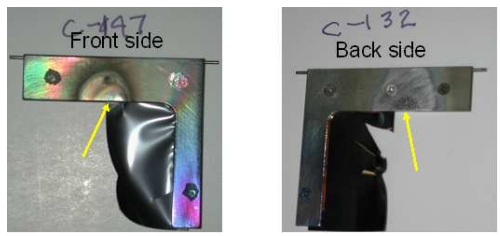

Figure 1: Used foils showing the signs of overheated frame and cracked and warped foil.

These foils were standard pyrolytic graphite, of thickness [1] 4.5±1 mg/cm^2, unchanged over decades because it was thought that thicker foils are stronger and therefore more durable. For a 5 mg/cm^2 carbon foil, Monte Carlo simulation result [2] shows that $> 6 \times 10^{-5}$ of particles are scattered beyond 3.3 mrad. These particles already run outside the 4″ beam pipe as the beam line transfer matrix element R_{34} or R_{12} reach 1.5 cm/mrad at maximum. This means that at 100 μA, there is >6 nA lost along the beamline. These losses are localized in a couple of spots and trigger beam trips by safety system, as only beam loss of <1 nA/m can be tolerated in order to retain access to the beamlines for service. Thus, it was suggested to use 2.5 to 5 times thinner foils to minimize the scattering.

ELECTRON HEATING SIMULATIONS

Simulations [2, 3] were performed to calculate the distribution of energy deposited by the electrons that are stripped from the H$^-$ ions of 500 MeV. Simulations began with the geometry and size of the original standard foil assembly (1st generation), which consisted of two plates (stainless steel, of thickness 0.031 inches) screwed together with a foil (pyrolytic graphite) and a pivoting pin clamped between them. A representative beam spot of H$^-$ used in the simulation was 2 mm wide and 8 mm tall, with a linear distribution in x (maximum at the edge) and a quartic distribution in y. The whole area was divided into grids of uniform size 0.1 mm in both directions.

When H$^-$ enters the foil, the electrons are stripped. The stripped electrons pass through the foil, and then spiral around the magnetic field and cross the foil multiple times. At every crossing, the electrons lose energy longitudinally

ISBN 978-3-95450-128-1

MAPPING OF THE NEW IBA SUPERCONDUCTING SYNCHROCYCLOTRON (S2C2) FOR PROTON THERAPY

J. Van de Walle#, W. Kleeven, C. L'Abbate,V. Nuttens, Y. Paradis,
IBA, Louvain-la-Neuve, Belgium
M. Conjat, J. Mandrillon, P. Mandrillon, AIMA, Nice, France

Abstract

The magnetic field in the Superconducting Synchrocyclotron (S2C2) has been measured with a newly developed mapping system during the commissioning of the machine at IBA. The major difference with other mapping systems at IBA is the usage of a search coil, which provides high linearity over a large magnetic field range and the possibility to measure in a more time efficient way. The first mapping results of the S2C2 were compared with OPERA3D calculations. The average field, the tune functions and the first harmonic were the main quantities which were compared with calculations. The horizontal position of the main coil was found to be a crucial parameter to get a good agreement between calculation and measurement. The vertical position of the main coil was optimized based on measured vertical forces on the main coil.

INTRODUCTION

The newly developed superconducting synchro-cyclotron (S2C2) is the first non-isochronous and superconducting cyclotron build at IBA. It's compact size (2.5 m diameter) is crucial to reduce the footprint and overall cost of existing proton therapy solutions. The compact single room proton therapy system called ProteusONE® aims at making proton therapy available to more people at a reduced cost and with less impact on building and infrastructure.

THE MAPPING SYSTEM

The mapping system is shown in Figure 1 and consists of a search coil (MagnetPhysik, FS 2800 W), a Hall probe (Arepoc s.r.o., LHP-NP) and a NMR probe (Metrolab) which are all mounted on a wheel which covers 360 degrees azimuthally and has a radial range of about 50 cm. The NMR probe can be positioned in the centre of the S2C2, where the field homogeneity is good enough to measure the 5.72 Tesla field with high precision. This NMR measurement is the starting value for the relative measurement with the search coil, which moves from the centre to a maximum radius with a speed of 6 cm/s. The voltage induced in the search coil is integrated with a Metrolab PDI5025. The integration intervals are defined by an optical ruler along the track of the search coil which has a radial pitch of 50 μm. The radial resolution chosen for the mapping of the S2C2 is 1 mm. The magnetic field at radius r is given by :

$$B(r) = B_0 + \int_{t_1}^{t_2} \frac{V(t) - V_{offset}}{A_{eff}} dt$$

where B_0 is the field measured in the centre with the NMR probe, t_1 and t_2 are the trigger interval time limits defined by the optical ruler, V_{offset} is the measured voltage offset on the integrator input and A_{eff} is the effective surface of the search coil. The latter was calibrated separately in a calibration magnet [1]. The Hall probe present on the mapping wheel was used to compare the field profiles measured with Hall probe and search coil at different main coil currents. In this way, the effective surface calibration of the search coil was checked. The dimensions of the search coil were chosen carefully in order to minimize the influence from the finite size of the search coil [2]. Prior to each radial track with the search coil, the voltage offset on the integrator input is measured. It was found that this offset varies about 25 μV over the full mapping time (maximum 24 hours). With a total measurement time of about 10 seconds for each radial track, an offset of 25 μV would contribute about 8 Gauss of "artificial" field at the end of the track. Figure 2 shows the measured field map at nominal current (652 A) in color scale. The regions indicated in Figure 2 are (1) the regenerator region, (2) the region between azimuth 180° and 270° where the radial range of the search coil is limited due to the presence of the septum in the median plane, (3) the region where the beam enters the extraction channel.

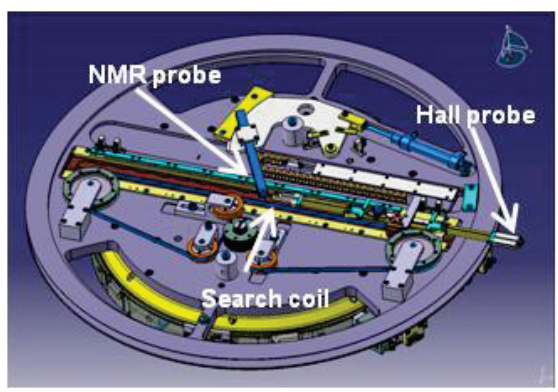

Figure 1: Layout of the mapping wheel.

e-mail : jarno.vandewalle@iba-group.com

STRUCTURAL AND MAGNETIC PROPERTIES OF CAST IRON FOR CYCLOTRONS

S. Zaremba, E. Forton, IBA, Louvain-la-Neuve, Belgium
E. Ferrara, F. Fiorillo, L. Martino, E. Olivetti, L. Rocchino, Istituto Nazionale di Ricerca, Metrologica (INRIM), Torino, Italy

Abstract

At IBA, the steels used to build the magnets of the Cyclone230® cyclotron are cast on demand, using very strict criteria, casting procedure, requirements and quality control. Among the various steps performed at the foundry, a thermal annealing is made. In this work, we assess the usefulness of such thermal treatment.

Samples of pure iron casts have been magnetically and structurally characterized. Progressive magnetic softening was observed upon successive annealing steps. These changes of the magnetic properties were attributed to the relief of internal stresses.

Results, obtained by X-ray diffraction, electron microscope and precise determination of magnetization curve and hysteresis loop, will be presented and commented.

INTRODUCTION

The fabrication of a Cyclone230® cyclotron [1] magnet requires operations like casting, cooling, annealing, machining among others. A very good understanding of each production step and an impact of each operation on the cyclotron quality are mandatory. In addition the suppression of one operation may generate significant cost reduction leading towards more affordable system. In this case, it could make protontherapy a bit less expensive. In this context, we were encouraged to perform an extensive study of the iron casting procedure.

IBA started to collaborate with the INRIM to deploy a program of structural and magnetic studies of iron.

IRON SAMPLES

Figure 1: The selection of tested iron samples.

Tested iron samples, provided by the iron supplier, created a large variety taking into account: shape (disks, toroids and rods), thermal treatment (unannealed, annealed at 820 C), location in the original iron casts (4 positions in the cast) and numerous samples from nearly the same position (see Fig. 1).

During analysis, some samples:

- have been ground, polished, cleaned and/or etched using a nitric acid in ethanol solution (Nital)
- have been additionally annealed in different temperatures during cycles controlled in time

MICROSTRUCTURAL INVESTIGATIONS

Grain Size

An optical microscope and a Scanning Electron Microscope (SEM) have been used to count the number of grains intercepted by arbitrary chosen sufficiently long straight lines. The number of intercepts is related to the grain size. Acquired statistics permitted to calculate the average intercept length $\bar{x}$ and the standard deviation σ. The condition: $\sigma \geq \bar{x}$ implies large variation in observed grain size. For different samples, measurements gave values: 0.77 mm $< \bar{x} <$ 1.52 mm, $x_{max} = 8$ mm and 0.84 mm $< \sigma <$ 1.64 mm.

It should be noted that irregularly shaped large grains and inclusions of impurities produce multiple intersections with arbitrarily selected test lines. In this way the average intercept length and consequently the grain size are underestimated.

Some samples have been photographed in large magnification (150x) before and after thermal treatment to verify the effect of annealing on grain boundaries and to detect recrystallization or the occurrence of grain growth. From the comparisons, no changes in grain shape or grain size have been observed between unannealed state and fully annealed state of samples. The thermal treatment does not produce any recrystallization or grain growth.

Chemical Composition Of Impurities

Information on the chemical composition of the cast iron is a standard request of IBA. An example is shown in Fig. 2. The impurities content has been once again determined using a Scanning Electron Microscope (SEM) and an Energy Dispersive Spectroscopy X-ray Diffraction (EDS XRD) detector.

A high magnification (4000x) of the SEM was needed to detect different shapes and sizes of inclusions.

Unetched iron samples presented different types of inclusions like: sharp edge shapes, bar shapes, cross-shaped crystals and tree-like shapes of monocrystals or multicompound agglomerates.

ISBN 978-3-95450-128-1

DESIGN OF A MgB_2 BEAM TRANSPORT CHANNEL FOR A STRONG-FOCUSING CYCLOTRON*

K. Melconian, C. Collins, K. Damborsky, J. Kellams, P. McIntyre, N. Pogue, A. Sattarov
Accelerator Research Laboratory, Department of Physics and Astronomy, Texas A&M University, TX 77843, USA

Abstract

A superconducting strong focusing cyclotron is being developed for high current applications. Alternating-gradient focusing is provided by ~6 T/m superconducting beam transport channels which lie in the sectors along the arced beam trajectory of each orbit of the cyclotron. The ~1 T sector dipoles, corrector dipoles, and Panofsky type quadrupoles utilize MgB_2 superconductor operating around 15-20 K. The operating temperature provides a valuable margin for a cost-effective cryogenic design, and large thermal stability in the event of occasional heat loads from intercepted beam or other sources. The main dipole windings are designed with sufficiently large curvature so that they can be fabricated using react-and-wind procedure; the quadrupole windings require small-radius end bends and so must be fabricated using wind-and-react procedure. Initial magnetic modelling on the end field region is presented. This paper is a duplicate of work previously presented [1].

INTRODUCTION

High-current proton accelerators are being developed for use as neutron and muon sources, accelerator driven systems (ADS) for nuclear transmutation, high energy physics and nuclear physics research experiments, cancer therapy, and isotope production. The Accelerator Research Lab at Texas A&M University (TAMU) is developing an accelerator-driven subcritical molten salt system to destroy the transuranics in spent nuclear fuel. Details of the ADS can be found in references [2] and [3]. The proton driver for the system is a flux-coupled stack of 10 mA 800 MeV CW strong-focusing cyclotrons (SFC) which incorporate several novel techniques to provide low-loss acceleration of such high-current beams.

There are a number of challenges in accelerating high current beams in a cyclotron: including crossing betatron tune resonances, space charge effects, and sufficient turn separation at high energies. These challenges are addressed in the SFC through several innovations: novel superconducting RF cavities [4] combined with a low dipole field make it possible to fully separate the orbits; multiple cyclotrons can be stacked in a flux-coupled arrangement to provide reliability by redundancy; and strong-focusing is accomplished using alternating-gradient beam transport channels (BTC) located in the aperture of the sector dipoles.

*Work supported by Texas ASE Fund and by the Mitchell Family Foundation.
KarieMelconian@tamu.edu

SECTOR DIPOLE

The SFC accelerator system, shown in Fig. 1, consists of an injector cyclotron (TAMU100) and a main cyclotron (TAMU800). Each cyclotron is an isochronous continuous-wave (CW) sector cyclotron containing wedge-shaped sector dipoles and superconducting RF cavities. The flux-coupled stacked configuration of the cyclotrons was chosen to minimize the overall footprint, provide the required current for our accelerator-driven molten salt system, and provide reliability by redundancy.

The sector dipole is designed using the levitated-pole strategy first developed for the RIKEN ring cyclotron [5]. The main dipole field is provided by MgB_2 superconducting windings around a pair of cold-iron flux plates. Each assembly of two flux plates is suspended symmetrically in the vacuum gap of the overall warm-iron flux return. The back-side gaps between each flux plate and its warm-iron flux return segment is designed so that net vertical forces on each cold-iron flux plate cancels. This means the thermally insulating supports for each flux plate need only support the gravitational force plus modest de-centering forces. The fields along the design orbits required for isochronicity are obtained by shaping the beam side of the cold pole pieces. A list of some of key parameters of the TAMU 100 and TAMU 800 are given in Table 1.

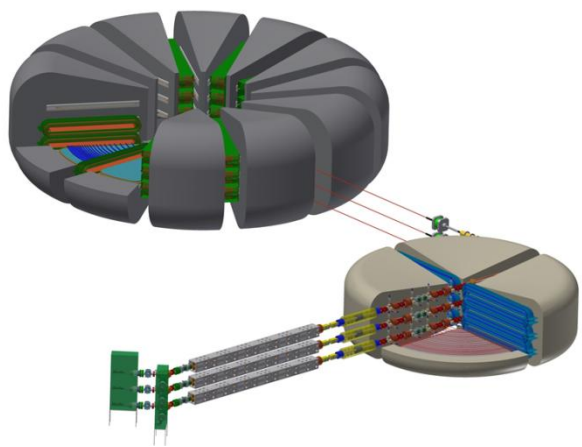

Figure 1: Sequence of strong-focusing cyclotrons consisting of two stacked cyclotron systems. The TAMU 100 accelerates protons from the RFQ to 100 MeV and feeds into the TAMU 800 which accelerates the protons to a final energy of 800 MeV.

ISBN 978-3-95450-128-1

METHODS OF INCREASING ACCURACY IN PRECISION MAGNETIC FIELD MEASUREMENTS OF CYCLOTRON MAGNETS

N. Avreline, W. Gyles, R. Watt, ACSI, Richmond, BC, V6X 1X5, Canada

Abstract

A new magnetic field mapper was designed and built to provide increased accuracy of cyclotron magnetic field measurements. This mapper was designed for mapping the magnetic fields of TR-19, TR-24, and TR-30 cyclotron magnets manufactured by Advanced Cyclotron Systems Inc. A Group3 MPT-141 Hall Probe (HP) with measurement range from 2 G to 21 kG was used in the mapper's design. The analogue monitor output was used to allow fast reading of the Hall voltage. Use of a fast ADC NI9239 module and error reduction algorithms, based on a polynomial regression method, allowed the reduction of noise to 0.2 G. The HP arm was made as a carbon fibre foam sandwich. This rigid structure kept the HP arm in a flat plane within 0.1 mm. In order to measure the high gradient field, the design of this mapper provided high resolution of HP arm angle within 0.0005° and of radial position within 25 µm. A set of National Instrument interfaces connected through a network to a desktop computer were used as a base of control and data acquisition systems. The mapper was successfully used to map TR-19 and TR-24 cyclotron magnets.

MAPPING SYSTEM OVERVIEW

The mapping system consists of a mechanical motion device (MMD), acquisition and control electronics and software for operation and data processing.

Mechanical and Measurement Specifications

- Magnetic field accuracy: $5*10^{-5}$ T (in hills)
- Azimuthal, radial resolutions: 0.0005°, 25 µm
- Magnetic field range: 0.4 – 2.2 T
- Scanning speed: 75 – 500 mm/s
- Duration of 360° measurement: 70 min (at 150mm/s)
- Number of samples per scan: 52000

Mechanical Motion Device (MMD)

MMD moves the Hall Probe (HP) to any point in the mid-plane of the cyclotron's magnet through radial and azimuthal components of motion. Those components of motion are achieved by stepper motors mounted onto two shafts inserted through the center of a cyclotron's magnet.

The HP is located on the HP cart that slides along the rails of the HP arm (see Figure 1) which in turn is attached to the main (larger) shaft. This shaft allows azimuthal rotation of the HP arm through a Harmonic Drive (HD), which is a stepper motor that is operating in servo mode. According to the specifications of this motor, the accuracy of positioning is 30arc-s (2.8×10^{-4} degrees) [1]. An Inductosyn encoder [2] with resolution of 0.0001° is used for reading the angle of HP arm's position. Each angle position is read by an Inductosyn before and after scanning to guarantee the HP arm did not move. Compressed air brakes are applied to hold the angle. If the difference between readings is more than 0.0005°, the HP arm is reset and the process is repeated. Rigid bellows are used to join the HD to the main shaft without applying extra force to the HD bearings. Furthermore, the shaft is supported by two spherical bearings that allow for alignment adjustment.

Figure 1: The magnetic field mapper.

A second (smaller) shaft is located inside the main shaft and its stepper motor rotates a timing pulley. The timing pulley pulls a timing belt that is attached to the HP cart. This produces radial motion. The suspension system for the HP cart is made from sliders moving along the rails. For vibration reduction an adjustable mechanical system with shock absorbers is used.

A linear optical encoder with 2 mm period stripes is used for reading radial coordinates. The signal obtained by the HP arm's optical sensor (collected at 5 kHz for 150 mm/s) from this encoder is presented in Figure 2.

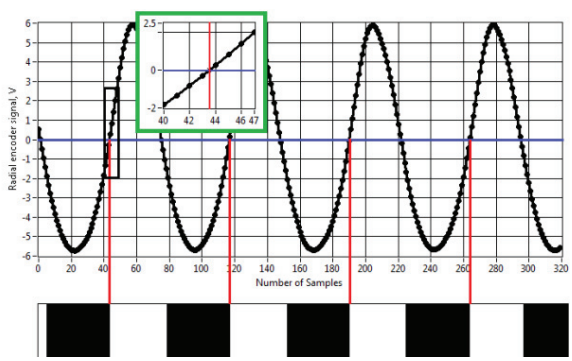

Figure 2: Determination of radial position.

The precise strip edge positions are defined where the optical sensor signal crosses zero voltage (i.e. where

ISBN 978-3-95450-128-1

THE HOUGHTON COLLEGE CYCLOTRON: A TOOL FOR EDUCATING UNDERGRADUATES

M. Yuly, Houghton College, Houghton, NY 14744, USA

Abstract

The cyclotron is an ideal undergraduate research project because its operation and use involve so many of the principles covered in the undergraduate physics curriculum -- from resonant circuits to nuclear reactions. The physics program at Houghton College, as part of an emphasis on active learning, requires all majors to complete a multiyear research project culminating in an undergraduate thesis. Over the past ten years, seven students have constructed a working 1.2 T tabletop cyclotron theoretically capable of producing approximately 400 keV protons. The construction and performance of the cyclotron will be discussed, as well as its use as an educational tool.

THE SCIENCE CURRICULUM AT HOUGHTON COLLEGE

Houghton College is committed to providing a rigorous and practical curriculum to undergraduates majoring in science. In additional to the wide range of traditional coursework offered in the division, there is a strong emphasis on hands-on experiences that will develop the problem solving and applied skills needed by scientists in the real world. Traditional coursework usually focusses on the content of the discipline, but not on developing the traits needed to be a successful scientist. Today's science students need to become practical problem solvers able to apply their content knowledge to difficult problems, with the laboratory skills and character qualities needed to be successful. They need undergraduate experiences in analyzing real problems that do not have nice "textbook" solutions. Furthermore, these problems should develop more than intellectual problem solving skills, but also practical laboratory skills, as well as character qualities including patience, confidence and perseverance.

This applied emphasis led Houghton College to introduce the Summer Research Institute (SRI) [1] in 2007 and the Science Honors Program [2] in 2009. In the physics department, the emphasis is seen in the requirement that all physics majors complete an individualized research project that starts during their sophomore year and culminates in their senior year in a thesis and a presentation at a scientific meeting. Students receive course credit for working one-on-one with faculty members on their research projects, and the faculty receives teaching load credit. The long three-year project timeframe allows the students to make significant progress toward solving a difficult problem.

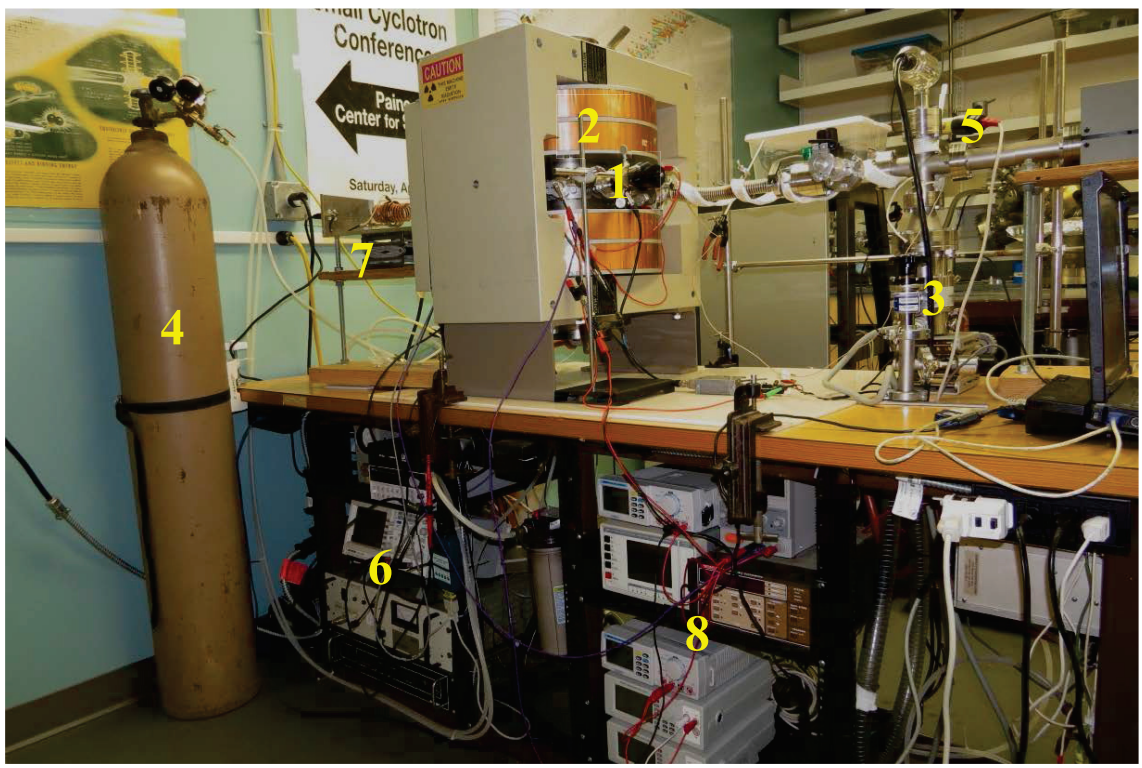

Figure 1: A photograph of the Houghton College Cyclotron, showing the (1) vacuum chamber and target linear motion feedthrough, (2) electromagnet, (3) turbopump, (4) hydrogen cylinder, (5) vacuum gauges and residual gas analyser, (6) RF system, (7) tuning coil, and (8) filament controls and beam current electrometer.

ISBN 978-3-95450-128-1

THE RUTGERS CYCLOTRON: PLACING STUDENT'S CAREERS ON TARGET*

K. Ruisard#, G. Hine, T. Koeth, University of Maryland College Park, MD, U.S.A.
A. Rosenberg, Stanford University, CA, U.S.A

Abstract

The Rutgers 12" Cyclotron is an educational tool used to introduce students to the multifaceted field of accelerator physics. Since its inception, the cyclotron has been under continuous development and is currently incorporated into the modern physics lab course at Rutgers University, as a semester-long mentored project. Students who participate in the cyclotron project receive an introduction to topics such as beam physics, high voltage power, RF systems, vacuum systems and magnet operation. Student projects have led to three different focusing pole geometries, including, most recently, a spiral edged azimuthally varying field (AVF) configuration. The Rutgers Cyclotron is often a student's first encounter with an accelerator, and has inspired careers in accelerator physics.

INTRODUCTION

The Rutgers 12" Cyclotron (Fig. 1) is a 1.2 MeV particle accelerator dedicated to student education and exploration. Originally built as an extracurricular project by two Rutgers undergraduates, the majority of cyclotron development has been accomplished by current and former students.

Rutgers University, like many schools, does not offer any courses specific to accelerator physics. Even the number of graduate degree programs with accelerator research programs is limited. The Rutgers Cyclotron provides a unique opportunity for students to learn accelerator physics at the undergraduate level, and can serve as a model for other schools looking to develop an accelerator education program.

The cyclotron currently resides in a laboratory classroom at Rutgers University. Because of its low energy, the machine does not activate during operation and can safely be approached and incorporated into lab work. The 12-inch diameter H-frame iron core magnet provides a nominally 1 Tesla vertical field in the 2-inch magnetic gap. Interchangeable iron pole tips allow for application of various focusing schemes. The vacuum chamber, which operates at 10E-5 Torr, holds a 5-inch radius DEE and dummy DEE with a peak applied RF voltage of 10 kV and tunable frequency 2 - 30 MHz. Protons and $_2H^+$ are generated by an internal cold-cathode Penning Ion Gauge (PIG) source. Chamber diagnostics are a radial probe and a deflector, each equipped with a phosphor screen/current collector.[1]

In the first section, we will review the structure of student cyclotron projects and summarize the history of the cyclotron's development in a student-project timeline. Next we will motivate a specific project to implement edge focusing in the cyclotron. The third section will expand on the procedure of this project, while the fourth reviews results and conclusions. Finally, we comment on the Rutgers Cyclotron's contributions to the accelerator community.

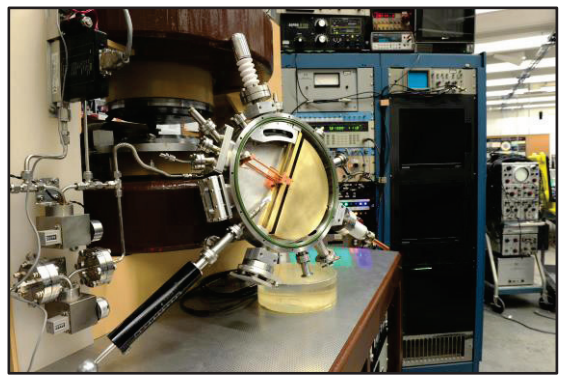

Figure 1: The Rutgers Cyclotron.

CYCLOTRON HISTORY

The cyclotron was originally conceived in 1995 by Rutgers undergraduates Timothy Koeth and Stuart Hanebuth. Koeth continues to play an important role as steward of the cyclotron system and mentor for student projects. Since 2001, cyclotron R&D has been driven and executed by undergraduate students, with significant contributions from both independent study students and participants in the Rutgers University Modern Physics Laboratory course.

Students enrolled in the Modern Physics course have the option of engaging in a semester-long cyclotron project as an alternative to the standard syllabus. In a typical cyclotron project, a small group of 1-3 students work closely with a mentor (typically a cyclotron staff member) in an independent study format, with well-defined goals that can reasonably be met within a semester.

Student Involvement

The following is a brief summary of student contributions to the cyclotron. In 2002, Chun and MacLynne designed a pair of weak focusing pole tips to replace the original perfectly parallel poles. The weak focusing tips were later installed and shown to dramatically increase deliverable beam current.[2] The weak focusing tips are pictured in Fig. 2a. The following year, Friedman and McClain measured the

*Work privately supported by the Rutgers Cyclotroneers and a Rutgers Physics Department donor-funded Instructional Equipment Fund.
#kruisard@umd.edu

ISBN 978-3-95450-128-1

COLUMBUS - A SMALL CYCLOTRON FOR SCHOOL AND TEACHING PURPOSES

Ch. Wolf, M. Frank, E. Held Gymnasium Ernestinum, Coburg, Germany

Abstract

A small cyclotron has been constructed for school- and teaching purposes. The cyclotron uses a water-cooled magnet with adjustable pole-pieces. The magnet provides a field up to 0.7 T.

The vacuum chamber is positioned between the two poles. The vacuum chamber provides ports for different subsystems, measuring tools and some viewports.

A turbo molecular pump backed up by a dry compressor vacuum pump is used to evacuate the chamber to a pressure of 10^{-5} mbar.

The ions are accelerated between two brass RF electrodes, called dee and dummy-dee.

In the center of the chamber there is a thermionic ion source. A mass flow controller fills it with hydrogen gas ionized by electrons from a cathode.

The required 5.63 MHz RF power is supplied by a RF transceiver. A matching box adjusts the output impedance of the transceiver to the input impedance of the cyclotron.

The expected final energies of the protons are 24 - 48 keV after 6 - 8 revolutions. These energies don't produce any radiation outside the chamber.

The purpose of this project is to realize a low-cost cyclotron using standard devices as far as possible.

INTRODUCTION

In principle a cyclotron is an easily understandable accelerator. It is found in every textbook descriptions and tasks on the cyclotron, but in contrast a real cyclotron is a very complex device so that most of the students have never seen a working cyclotron in reality.

The project COLUMBUS intends to change this situation by providing a minicyclotron for school and teaching purposes.

TECHNICAL DATA

In order to build such a small cyclotron one has to meet two conditions:

- Vacuum, magnetic field, frequency etc. must be so low that one can use standard components as far as possible, otherwise the costs will go to infinity
- The final energy of the cyclotron must be small enough so that no harmful radiation can arise, so that the students can do experiments with the cyclotron.

Table 1 shows the technical data of COLUMBUS. One can easily recognize that COLUMBUS meets all the conditions mentioned above.

In addition no beam will be extracted to make sure that no harmful radiation can escape during the experiments.

Table 1: Technical Data

Diameter of the Dees	140 mm (5.5 in)
Flux-density of the magnetic field	0.38 T
Vacuum in the chamber	10^{-5} mbar
dto with H_2	10^{-4} mbar
Cyclotron frequency	5.63 MHz
Number of revolutions	6 - 8
Voltage between the dees	2.0 -3.0 kV
Final energy	24 - 48 keV

MAGNET AND VACUUM-CHAMBER

At the very beginning there were two big problems:

- How to get a magnet for the homogenous field and
- How to get a suitable vacuum-chamber.

The first problem was solved by the Research Institute of Jülich. Prof. Dr. Maier and his team donated a Bruker BE-15. This is a laboratory magnet with two water-cooled coils. The pole-diameter is 150 mm (~ 6 in). The pole pitch is adjustable from 50 - 120 mm (~ 2 - 5 in). The flux-density is up to 2 Tesla depending on the spacing of the poles. At a distance of 100 mm the flux-density is up to 0.7 Tesla.

The second problem was solved by VACOM, a company specialized in vacuum-components. VACOM built the vacuum-chamber, i.e. Fig. 1, for us free of charge.

It has got ten ports, as shown in Fig. 2, the pumping-port, a port for instruments, another one for the RF, some view-ports, two ports for the filament-heating. Between these ports there is the gas-inlet for the ion source.

Figure 1: The vacuum chamber.

ISBN 978-3-95450-128-1

A NOVEL OPTICAL METHOD FOR MEASURING BEAM PHASE AND WIDTH IN THE RUTGERS 12-INCH CYCLOTRON

J. Gonski, S. Burcher, S. Lazarov, J. Krutzler, Rutgers University, New Brunswick, NJ 08901, USA
T. Koeth, B. Beaudoin, University of Maryland, College Park, MD 20740, USA

Abstract

We present an optical based measurement of beam bunch length and time of arrival (phase wandering) for protons accelerated in the Rutgers 12-inch Cyclotron. This technique is necessary to test the isochronicity of various magnetic field configurations, including radial and spiral azimuthal varying fields [1]. We discuss our inaugural measurements in a constant gradient weak focusing field and compare with simulation. Preliminary success with this method justifies continued exploration and refinement of this technique. By necessity, this method is insensitive to the DEE gap voltage and enables all cyclotron facilities to perform longitudinal measurements within their central region.

INTRODUCTION

The Rutgers 12-Inch Cyclotron is an educational accelerator dedicated to student training by experimental exploration of beam phenomena. Over a decade of experimentation has been focused on transverse beam measurements without any knowledge of the longitudinal behavior. This is because the large residual electric field of the radio frequency (RF) accelerating potential makes standard electronic beam phase and bunch length measurements impossible. RF filtering permits average beam current measurements, but removes any time structure within an RF cycle. We have developed an optical based measurement that is insensitive to DEE voltage using a fast (3 ns) phosphor screen viewed by a gated camera to create "time sliced" images which longitudinally profile the beam. The phosphor plate is located on the end of a radial positioner that can sweep the entire chamber radius and hence any ion revolution. Because a number of technical obstacles had to be mastered, we performed our first experiments in a weak focusing field, which is our simplest magnetic field configuration.

We recall that in a weak focusing field, the axial magnetic field decreseases with increasing radius so as to form axial-restoring radial field components above and below the median plane. As a consequence, the cyclotron condition can only be met at one point in the ion's flight from source to target; at all other locations, there is a mismatch between the cyclotron frequency and the RF accelerating frequency. When the two are not perfectly matched, each ion revolution acquires a phase error [2]. This error is acceptable, as long as the overall integrated phase slippage is less than 90°. The accelerating DEE voltage can be increased to reduce the number of turns and keep the phase slippage blow 90°. Alternatively, if one starts the ions in a magnetic field that is too high, they can acrue a phase slippage in one direction that permits the cyclotron condition to be met midway. At this point, a reversal of the phase slippage leads to a net zero phase error, illustrating phase stability as displayed in Fig. 1. In contrast, in an isochronous field, ions return to the same azimuthal location every RF cycle. In this paper, we measure the bunch length and phase slippage under differing magnetic field strengths in the definitively non-isochronous weak focusing field.

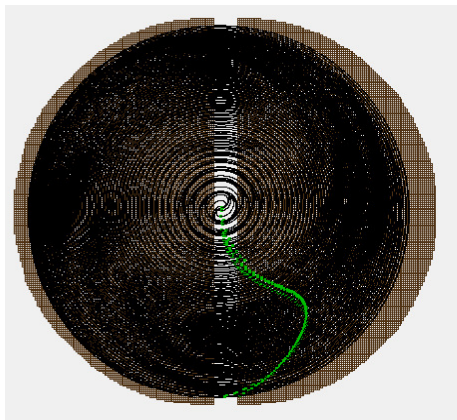

Figure 1: Simion demostration of phase slippage of proton in weak focusing field; green markers indicating ion location once per Radio Frequency Accelerating Voltage cycle.

SIMULATIONS

In order to anticipate the measurement's signature, the experiment was modelled in SIMION. A model of the weak focusing field generated by Poisson Superfish (PSF) was imported into SIMION. Flight time and ion paths were simulated in SIMION by tracking groups of ions through the cyclotron's 3D magnetic and RF electric fields [3]. Data such as ion position, time of flight (TOF), and energy were recorded for post processing. The fast phosphor target was modelled as a terminating plate with the same dimensions, and located at the corresponding experimental azimuth and radii position. The relative phase shift as a function of magnetic field was determined by the ion TOF, where flight termination occurred upon collision with the plate.

For each magnetic field value used in data acquisition, a separate PSF field was created and used in SIMION to generate ion flight simulations under experimental operating conditions. Comparison to measurements revealed a proportionality of relative phase shift between simulation and data. Precise definition of this relationship can be found in later sections. We expect a linear relationship between relative phase shift and magnetic

ISBN 978-3-95450-128-1

THE CYCLOTRON KIDS' 2 MeV PROTON CYCLOTRON

H. Baumgartner, MIT, Cambridge MA, USA

Abstract

Over several summers, two high school students constructed a self-designed at Jefferson Lab. This paper describes the design of their 2 MeV proton cyclotron. The machine is now at Old Dominion University, where it will be used as an educational tool in the accelerator physics program.

INTRODUCTION

There has never been a better time for amateurs interested in science or engineering to find information online and to get in touch with others who share their interests. When Heidi Baumgartner and Peter Heuer (the "Cyclotron Kids"), met at an astronomy summer camp in their freshman year of high school, they decided that they wanted to take on the ambitious project of designing their own small cyclotron. Inspired by previous successful independently built cyclotron projects, they based their designs on information about other amateur particle accelerators that they found on the Internet.

There have been approximately a dozen previous amateur particle accelerator projects, including Fred Neill's 1999 winning submission to the Intel International Science and Engineering fair, in which he built a 4-inch diameter cyclotron at home. Dr. Timothy Koeth, then an undergraduate student at Rutgers University in 1995, built another cyclotron, which he continued to improve over the past decade, and has used to mentor many other Rutgers undergraduates. There are others, including the machine built at Knox College by Jeff Smith and by Mark Yuly at Houghton College.

The Cyclotron Kids drew basic designs for their machine inspired by those of other amateurs that had completed such an ambitious project, and then looked for a company to sponsor them to build their machine and enter it into a science fair. The donation of a diffusion pump from Capitol Vacuum Parts, a company in Chantilly, VA, further encouraged them. One of their funding request emails was forwarded to Andrew Hutton, the associate director of Jefferson Lab in Newport News, VA, at the time. Against their expectations, Dr. Hutton invited them to construct their cyclotron at the national lab, under the guidance of scientists and engineers there.

OVERVIEW OF CYCLOTRON DESIGN

Target Energy

When the project moved to Jefferson Lab, the project scaled up from what the Cyclotron Kids had planned on building in a basement. The target energy became 2MeV, with the goal of being able to produce electron-positron pairs from collisions of the protons with a stationary target [1].

Electromagnet

One of the most expensive parts of a cyclotron project is attaining a homogeneous magnetic field over a large cross-section. Jefferson Lab provided left over 1060 steel scrap, from which the 1.6 Tesla H-shaped electromagnet was designed. The Jefferson Lab machine shop then machined the pieces of the magnet and wound the coils of the magnet

The magnet (Fig. 1). has two excitation coils, each 360 turns of copper wire of 1/4 inch square cross-section, with an internal water cooling channel. Because of the difficulty of handling and winding such stiff wire, it was found easiest to assemble the magnet out of ten "double-pancakes," or coils of 18 turns of wire two layers thick, individually wrapped in insulating cloth and potted in epoxy. The ten double-pancakes were then all together cast in epoxy.

The magnetic field strength in the gap of the H-magnet is given by the following equation:

$$\mathrm{B} = \frac{\mu_0 NI}{g} \quad (1)$$

The magnetic field is inversely proportional to the gap in the middle of the magnet, so it is advantageous to keep the gap between the magnet poles small. This tight spacing made the design of the vacuum chamber more difficult, but it was essential for achieving the target magnetic field strength of 1.6 Tesla.

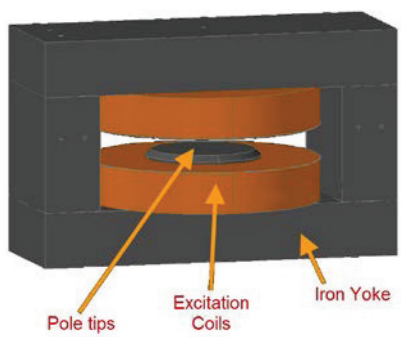

Figure 1: Overview of the electromagnet.

The design of the pole tips is also very important for particle beam focusing effects. A slight decreasing gradient along the radius of the magnet is necessary because the outward curving magnetic field lines provide a restoring force of the particle beam back to the midplane if it has some axial velocity. This gradient is achieved by a linear 0.02 inch taper from the center of the pole face outwards. POISSON Superfish, a magnetostatic modeling program from Los Alamos, was used to verify the design of the electromagnet, the portions of the

ISBN 978-3-95450-128-1

SPACE CHARGE LIMIT IN SEPARATED TURN CYCLOTRONS*

R. Baartman, TRIUMF, 4004 Wesbrook Mall, Vancouver, BC, V6T 2A3, Canada

Abstract

From both simulations and measurements, it is known that at sufficiently high charge per bunch, the bunches in an isochronous cyclotron undergo a vortex effect whose ultimate result is that the bunches reshape into circularly-symmetric distributions in the radial-longitudinal plane. This state cannot exist for arbitrarily high charge since at some point the space charge force will overwhelm the cyclotron's radial magnetic focusing. We apply envelope equation (or "second moment") formalism to determine (a) the particle motion frequencies (b) the self-consistent size, or turn width, and (c) the upper limit for the bunch charge for a given size of the bunch. This work is partly a review of work by Sacherer, Kleeven, and Bertrand-Ricaud, and partly a synthesis of those works. Some comparisons are made to published data for the PSI high intensity cyclotrons and new data from the TRIUMF cyclotron.

VORTEX EFFECT, QUALITATIVELY

The basic physics of the "vortex" effect is that leading particles are "pushed" by space charge, but cannot advance because of isochronism and instead gain energy and so go sideways to higher radius. Trailing particles do the reverse. Particles at the outside move back and those at the inside move forward. Mort Gordon [1] made the perceptive connection to Coriolis force in rotating frames. He made the following points in regards to space charge forces in cyclotrons. Referenced to the rotating frame in which the bunch is stationary, the motion of the particles due to space charge is a *steady-state velocity ... directed along the equipotential curves associated with F [the electric field due to space charge]*. Gordon realized that this motion applies locally to individual turns, but then since he had dealt only with cyclotrons with little or no turn separation, stated: *Since the length $R\Delta\theta$ of the turn is generally much greater than the radius gain per turn, the local vortices are so small and feeble that their presence can be neglected entirely*. But in high intensity machines, turn separation is required all the way out to extraction, so Gordon's case does not apply and contrarily, the local vortices dominate. Moreover, Gordon probably did not realize that the local vortex effect can impede the usual bunch stretching where R increases and $\Delta\theta$ remains constant: above a threshold amount of bunch charge, $\Delta\theta$ will decrease rather than remain constant, in order to maintain the circular stationary state.

A crucial ingredient in the physics of the evolution of the vortex effect is that the equipotentials of space charge are different than the distribution density contours. Specifically, for $a,\ b$ as semi-axes, the form of the equipotentials is

$$\text{constant} = \frac{x^2}{a(a+b)} + \frac{y^2}{b(a+b)}, \tag{1}$$

when the distribution has the form

$$\text{constant} = \frac{x^2}{a^2} + \frac{y^2}{b^2}. \tag{2}$$

And in fact the two only agree when the distribution is circular.

In 1981, Werner Joho [2] presented a model that used Gordon's mixed turns with constant $R\Delta\theta$. This results in a distribution of charge that looks like a pie sector, and was therefore called the "sector model". From this, he derived a limit beyond which the additional energy spread due to space charge would cause turns to no longer be sufficiently separated for clean extraction. The result was a current limit proportional to the cube of the energy gain per turn. The (local) vortex effect was subsequently discovered at PSI and although it invalidates the sector model, the limit nevertheless still is proportional to the cube of the energy gain per turn. We shall see why.

SIMPLIFIED MODEL

Bertrand and Ricaud [3] have presented an elegant simplified model, from which they derive the relation between bunch charge and size. Since it is known that the bunches tend to circular, for the case where the vertical size is equal to the horizontal (often a fairly good approximation), the bunches are spheres. Spheres with constant inside density of charge have a very simple form for the electric field:

$$\vec{E} = \frac{1}{4\pi\epsilon_0}\frac{Q}{r^3}\,\vec{r} \equiv k\,\vec{r} \tag{3}$$

Further, we assume a flat magnetic field B. Then the magnetic and electric forces on a particle of charge q, mass m give, in the lab frame:

$$\begin{aligned} m\ddot{x} &= +qB\dot{y} + qk(x - x_0) \\ m\ddot{y} &= -qB\dot{x} + qk(y - y_0) \end{aligned}$$

where $(x_0, y_0) = R(\cos\omega t, \sin\omega t)$ is the equilibrium orbit and $\omega = qB/m$.

Solve using complex $z = x + iy$, let $z = R\exp(i\omega t) + C\exp(pt)$, find

$$p^2 - i\omega p - \frac{qk}{m} = 0 \rightarrow p = \frac{i\omega}{2} \pm \sqrt{-\frac{\omega^2}{4} + \frac{qk}{m}} \tag{4}$$

Divide p by $i\omega$ to get the tunes of the modes:

$$\nu_{r\pm} = \frac{1}{2}\left(1 \pm \sqrt{1 - \frac{Q}{Q_{\max}}}\right) \tag{5}$$

*TRIUMF receives federal funding via a contribution agreement through the National Research Council of Canada.

ISBN 978-3-95450-128-1

VLASOV EQUATION APPROACH TO SPACE CHARGE EFFECTS IN ISOCHRONOUS MACHINES

A.J. Cerfon*, O. Bühler, J. Guadagni, NYU CIMS, New York, NY 10012, USA
F.I Parra, J.P. Freidberg, MIT PSFC, Cambridge, MA 02139, USA

Abstract

Starting from the collisionless Vlasov equation, we derive two simple coupled two-dimensional partial differential equations describing the radial-longitudinal beam vortex motion associated with space charge effects in isochronous cyclotrons. These equations show that the vortex motion can be intuitively understood as the nonlinear advection of the beam by the $\mathbf{E} \times \mathbf{B}$ velocity field, where $\mathbf{E}$ is the electric field due to the space charge and $\mathbf{B}$ is the applied magnetic field. The partial differential equations are also formally identical to the two-dimensional Euler equations for a fluid of uniform density. From this analogy, we explain why elongated beams develop spiral halos and a stable round core while round beams are always stable. Solving the coupled equations numerically, we find good agreement between our model and Particle-In-Cell simulations.

INTRODUCTION

Modern applications of cyclotrons in fields such as materials science, nuclear medicine and national security require high quality beams at high intensities. In order to design cyclotrons that are capable of producing such beams reliably, one needs to be able to understand and predict the effects of space charge forces on beam evolution. Because of the complexity of beam dynamics and of the magnetic field geometry in modern machines, the theoretical work is now largely numerical.

Recently, very sophisticated numerical tools based on the Particle-In-Cell (PIC) method have been developed to design modern cyclotrons and analyze experiments [1, 2, 3]. Codes based on the PIC approach are very intuitive and can be conveniently parallelized for large-scale computations. These are critical points given the complexity of the problem at hand. The evolution of charged particle beams in high intensity cyclotrons is indeed described by the seven-dimensional Vlasov-Poisson system in complicated geometries [1]. However, there are also drawbacks with direct PIC simulations of the exact Vlasov-Poisson system. First, precisely because of the conceptual simplicity of the PIC formulation, it often does not provide insights on the basic phenomena involved in the dynamics until one runs the simulations and extracts information from the numerical results. More importantly, the conventional PIC method is subject to difficulties associated with statistical noise, which require the simulation of a very large number of particles to bring the statistical uncertainty to an appropriately low level. Accurate fully self-consistent PIC simulations of beam dynamics in modern cyclotrons are thus very computationally intensive [1]. While these high performance numerical tools are very valuable for in-depth calculations, the computational times – measured in hours – are impractical for fast scoping studies of novel designs and for the fast interpretation of results during experimental runs.

In a wide class of cyclotrons, space charge forces are important because of their cumulative effect after many turns, but they only slightly disturb the single-particle dynamics on a given revolution. For these machines, the quasi-periodicity of the single-particle motion can form the basis for an averaging procedure that reduces time resolution requirements and the dimensionality of the Vlasov-Poisson problem. Adam relied on this fact to develop the successful two-dimensional PIC code PICS based on the "Sphere Model" [4]. A very similar averaging procedure known under the name gyrokinetics (e.g. [5]) is also succesfully used in plasma physics for accurate and tractable simulations of fusion and astrophysical plasmas [6, 7, 8, 9].

This paper belongs to the early stage of an ongoing project to derive averaged equations for the Vlasov-Poisson system in modern cyclotrons, and develop a continuum kinetic code to solve these equations and study space-charge effects. While we will treat the general case in future work, we focus here on the particular regime in which the beam is almost laminar. We show that in this regime the averaging procedure can be used to obtain a reduced set of fluid equations describing the non-relativistic radial-longitudinal beam dynamics due to space charges. These fluid equations have the remarkable property to be isomorphic to the two-dimensional Euler equations for a fluid of uniform density. This analogy is very powerful to understand the stability of given beam density distributions, and explain beam spiraling [1, 4] and breakup phenomena [10] observed in isochronous cyclotrons.

REDUCED FLUID MODEL FOR THE BEAM

Starting Model

In this work, we make a number of simplifying assumptions that we will relax in future work. These assumptions allow us to make substantial analytic progress, and as we will show below, they lead to a model than contains all the key physics describing beam spiraling and beam breakup.

In order to compare our results with previous numerical results [1, 4], we focus on the case of a coasting beam. We restrict our study to the two-dimensional radial-longitudinal plane, and consider a non-relativistic beam. With these three restrictions in mind, we can consider the

* cerfon@cims.nyu.edu

TRANSVERSE-LONGITUDINAL COUPLING BY SPACE CHARGE IN CYCLOTRONS

C. Baumgarten, Paul Scherrer Institute, Villigen, Switzerland

Abstract

Based on a linear space charge model and on the results of PIC-simulations with OPAL , we analyze the conditions under which space charge forces support bunch compactness in high intensity cyclotrons and/or FFAGs. We compare the simulated emittance increase and halo formation for different matched and mismatched particle distributions injected into a separate sector cyclotron with different phase curves.

INTRODUCTION

Isochronous cyclotrons have no longitudinal focusing by their operation principle. Hence the phase width (bunch length) of the beam is constant for low intensity machines and tends to increase in the presence of space charge forces leading to a limitation of the maximal beam current. The usual strategy to overcome this limitation is to raise the phase acceptance and reduce the energy spread by the installation of one or more flat-top cavities. Flat-top operation raises the intensity limit, but at the cost of a reduction of the average energy gain and the installation of additional expensive hardware.

The PSI Injector II cyclotron is an example of an alternative mode of high intensity operation for cyclotrons. The installation of two bunchers in the injection line increases the longitudinal space charge force and allows for operation in the space charge dominated regime as predicted in Ref. [1, 2]. The former flat-top cavities are now operated as additional accelerating cavities. In this mode the bunch length remains strikingly short even at high beam currents (see for instance Ref. [3, 4, 5, 6, 7]).

Numerous papers have been published that (predicted or) described this effect [1, 2, 8, 9], but due to the complexity and non-linearity of the phenomenon the debate has not finished yet, i.e. the exact conditions to reach this regime are only approximately known and the properties of a beam (i.e. the optimal distribution in phase space at a given intensity) that matches the requirements of space charge dominated operation are not precisely understood.

In preceeding papers we described a method to compute the parameters of matched beams for the space charge dominated regime [10, 11, 12]. The method is based on a linear approximation, strictly valid only for particles close to the center of the bunch. Therefore the applicability of this approach and the underlying model is questionable.

Here we present simulation results obtained with the parallel space charge solver of OPAL -cycl that enables to study the behavior of high intensity beams with a state-of-the-art PIC code [13, 14]. The results show that the predictions of the linear (matching-) model are surprisingly powerful. In fact, the linear model does not only allow to compute the parameters of a matched beam with minimal halo production and minimal emittance increase, it also allows to understand the sensitivity of the bunches with respect to the phase slip. With some additional arguments the model also allows to derive a consistent picture of how the effects are related to the "negative mass instability".

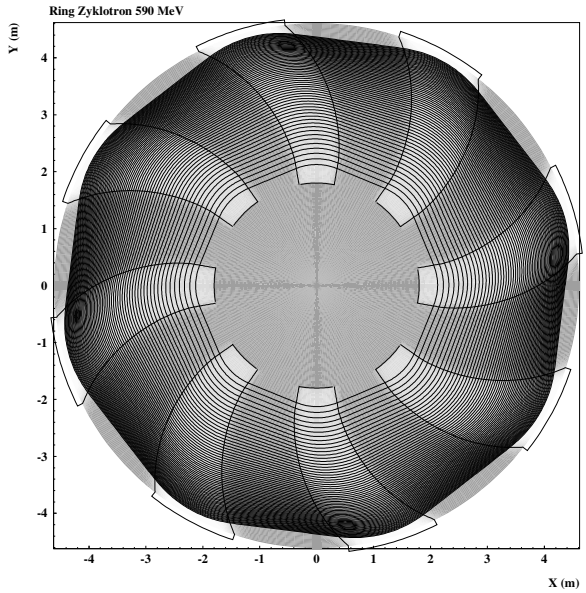

Figure 1: Top view of the idealized ring machine with some equilibrium orbits.

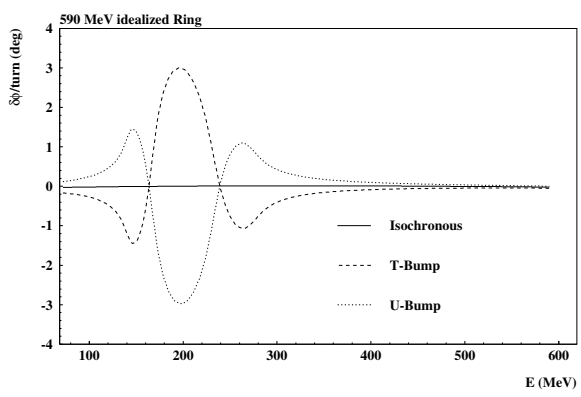

Figure 2: Phase shift per turn vs. radius of the idealized ring machine with bump "U" and bump "T".

ISBN 978-3-95450-128-1

OPTIMIZING THE OPERATIONAL PARAMETERS OF THE SFC BY USING PSO ALGORITHM

Shi Lei-Tai,* Jiang Pei-Yong, IMPCAS, Lanzhou 730000, China
Luo Hao, XiChang Satellite Launch Center of China, Xichang 615000, China

Abstract

HIRFL-SFC is a Sector-Focused Cyclotron which plays an important role in scientific experiments in IMP. The SFC was equipped with four groups of harmonic coils, for orbit correction and single turn extraction. There was not a code to calculate the currents of harmonic coils, thus the Orbit-PSO code was developed. Comparing the orbit of 7 MeV $^{12}C^{4+}$, the current of harmonic coils, injection energy and voltage of Dee were calculated by the Orbit-PSO code which contain of PSO(particle swarm optimization) method and the orbit calculation code.

INTRODUCTION

In HIRFL-CSR, various heavy-ions beam are utilized for research in mass measurement, biotechnology and materials science. HIRFL was equipped with a variable-energy Sector-Focused Cyclotron (K=69) [1] which provides various heavy ions. SFC is a three-spiral sector machine with one 180 degree Dee. The extraction radius is 0.75 m and harmonic number 1 and 3 are used. Dee voltage of up to almost 90 kV. The magnetic field can be adjusted by a group of main coils, 11 groups of trim coils and 4 groups of harmonic coils. The beam is extracted by means of three electrostatic channels. Three differential probes are used to measure the position of beam along radius.

SFC always extracts beam with hardness because the operational parameters of harmonic coils based on empirical observations, so it is of much importance to develop the Orbit-PSO code for calculating the currents of harmonic coils, injection energy and voltage of Dee.

THE PROGRAM (ORBIT-PSO) FOR OPTIMIZING THE PARAMETERS

The Orbit-PSO code mainly includes three parts: the PSO algorithm [2], the orbit calculation and post analysis. The orbit of 7 MeV $^{12}C^{4+}$ is considered as the referential orbit, because the carbon beam was utilized for cancer therapy frequently. Generally, $^{12}C^{4+}$ is extracted from ECR, accelerated to 7 MeV by SFC, stripped to be $^{12}C^{6+}$, injected into the CSRm and accelerated to different energy for cancer therapy. Thus we have experienced parameters of 7MeV $^{12}C^{4+}$ for SFC.

* shileitai@impcas.ac.cn

Particle Swarm Optimization (PSO)

Particle swarm optimization (PSO) is a computational method that optimizes a problem by iteratively trying to improve a candidate solution with regard to a given measure of quality. The system is initialized with a population of random solutions what dubbed particles. Each particle keeps track of its coordinates in the problem space which are associated with the best solution (fitness) it has achieved so far. And it is also guided toward the best known positions in the problem space, which are updated as better positions are found by other particles. this is expected to move the swarm toward the best solutions.

Magnetic Field

The isochronous magnetic field for different beam, which was calculated by the codes of EQUIL and OPTCC, was provided by a group of main coil, eleven groups of trim coils and four groups of harmonic coils. Figure 1 shows the magnetic field distribution along the radius of SFC. The maximum deviation between isochronous magnetic field and real magnetic field can reach 20 Gauss.

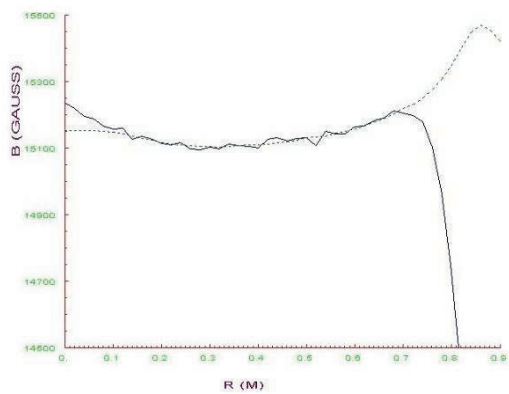

Figure 1: Magnetic field distribution along the radius.

Figure 2 shows the layout of the harmonic coils and Figure 3 shows the magnetic field produced by all coils for 7MeV $^{12}C^{4+}$. For each group of harmonic coils, the currents can be calculated by the equation of:

$$I_A = I * cos(\theta) \quad (1)$$
$$I_B = I * cos(\theta + 120) \quad (2)$$
$$I_C = I * cos(\theta + 240) \quad (3)$$

where I is the current and θ is the phase of each group of harmonic coils. The Eqs. (1-3) distribute the currents to the

BEAM OPTICAL SIMULATION IN A PROPOSED MAGNETIC EINZEL LENS

M. H. Rashid# and A. Chakrabarty, VECC, 1/AF- Bidhannagar (Salt Lake), Kolkata- 700064, India

Abstract

Magnetic scalar potential and field distributions along the central axis of a magnetic einzel lens consisting of a pair of axisymmetric iron yoked anti-solenoids have been evaluated using a simple closed form of analytical expressions. The magnetic field distribution is used to track single charged particles as well as ion beam through lens segmentation method. The method facilitates in evaluation of optical properties as well as aberration coefficients of the lens. Application of such doublet solenoid lens in transporting low energy ion beam introduces nominal rotation of the beam as well as least entangling between transverse phase spaces of the beam. So, instead of single solenoid, it is always beneficial to use a magnetic einzel lens in beam optical systems.

INTRODUCTION

The early application of the lens is traced back with the advent of electron microscope, which need very powerful, flexible lens with least aberrations. The lenses are used widely in beam handling devices like ion-implanters, spectrometers, charge and mass analyzers and beam transport lines associated with particle accelerators.

An einzel lens, at the first instance, indicates an electrostatic rotationally symmetric uni-potential lens consisting of three coaxial electrodes. The electric field has exact mirror symmetry about the centre and charged particles passing through the lens are unaffected energy-wise and focused down-stream in transverse direction.

A magnetic einzel lens (MEL) [1, 2] is envisaged in the similar way using two equally and oppositely charged solenoids such that the magnetic field has exact mirror symmetry about the centre in between the solenoids and charged particles with some rigidity passing through the lens are theoretically unaffected rotation-wise. The total magnetic scalar potential on the axis is just superposition of the potentials at the circular openings of the solenoids and given by a closed form of analytical expressions. The magnetic field and its derivative are obtained as analytical expressions. The field configuration depends on the solenoid geometrical parameters and its excitation. The advantage of a MEL over electrostatic one should be mentioned that no electric insulation is needed and voltage breakdown does not happen. But it consumes and dissipates electric power and there is an essential need for cooling. Operation and removal of astigmatism is straight forward as the beam emerges finally without beam rotation in such lens. Magnetic materials with high magnetic permeability are used in such lens to reduce magneto-motive force (electric power) and shield the stray magnetic field.

#E-mail: haroon@vecc.gov.in

Details of aberration coefficients have been discussed in [2, 3, 4]. The aberrations rotate and blur the image shape with increased size. Lens berrations can be reduced by decreasing the convergence angle of the system, so that charged particles are confined close to the axis of the lens. The ratio of the solenoid length and diameter affects both aberration and magnification, so the geometrical dimension should be optimized while designing a MEL.

MAGNETIC EINZEL LENS

For a pair of coaxial wire loops with the origin of the z-axis at the centre of the gap between the loops, the potential and field respectively are given by Eqs. 1 and 2. They are obtained by superposition of potentials created by the two loops passing some electric current, 'NI'. The potential and field along the axis depends on the geometrical parameters (pole gap '2s' and diameter '2R') of the lens by the current loops (solenoid).

$$\phi_1(z) = \frac{(NI)R}{\pi s}\left(z_+ \tan^{-1} z_+ - z_- \tan^{-1} z_-\right) \quad (1)$$

$$B_1(z) = \frac{-\mu_0 NI}{2\pi s}\left(\frac{z_+}{1+z_+^{\,2}} + \tan^{-1} z_+ - \frac{z_-}{1+z_-^{\,2}} - \tan^{-1} z_-\right) \quad (2)$$

Where $z_\pm = (z \pm s)/R$.

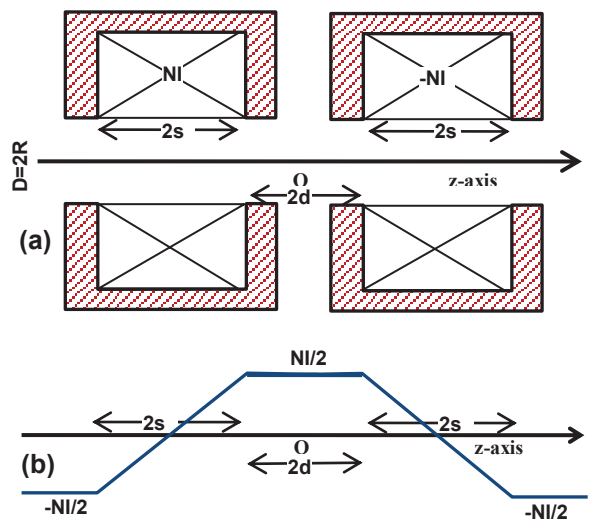

Figure 1: (a) Sketch of the MEL consisting of two solenoids, (b) Plot of scalar potential on the axis due to magneto-motive force NI.

Magnetic Potential and Field

We extend the single solenoid lens to two coaxial similar solenoids to form a MEL of diameter '2R' as shown in Fig. 1. The spacing between the two solenoids is 2d and the centres of the individual solenoids are situated

ISBN 978-3-95450-128-1

FEASIBILITY STUDY OF INTENSE BEAM MATCHING AT THE SPIRAL INFLECTOR USING ELLIPTICAL SOLENOID

A. Goswami*, P. Sing Babu and V. S. Pandit
Variable Energy Cyclotron Centre, 1/ AF, Bidhannagar, Kolkata-700 064, India

Abstract

A solenoid magnet with elliptical pole face aperture creates unequal focusing forces in the two transverse planes and thus can be utilized for beam matching with unequal sizes as required by spiral inflector for efficient transmission. In this work the beam optical properties of an elliptical solenoid have been studied, including the effect of space charge. An envelope model has been developed and utilized to study the feasibility of using an elliptical solenoid for transverse matching of an intense beam to the acceptance of a spiral inflector.

INTRODUCTION

The injection system of 10 MeV-5 mA proton cyclotron [1] being developed at VECC consists of a 2.45 GHz (80 keV) microwave ion source and two solenoids to transport and match the beam at the spiral inflector [2]. An elliptical solenoid [3] will be placed just before the inflector for transverse matching of the beam. In an elliptical solenoid the elliptic apertures at both ends generate transverse field components which result in unequal focusing forces in two transverse planes. This asymmetric focusing characteristic can be utilized for matching of an intense axisymmetric beam to the spiral inflector, requiring unequal phase ellipses in both planes [2]. In this paper, we have derived the equations of motion in canonical form in the combined linear self-field and applied magnetic field of the elliptical solenoid and obtained a set of envelope equations for uniform density beam. We have modelled a small magnet and computed the magnetic field using a 3D code which is then used in the envelope equations to study the beam optical properties of the magnet. We have also performed detailed study for transverse matching of an axisymmetric intense beam to the input of the spiral inflector.

THEORY

Let an intense continuous beam of particles of charge q and mass m propagating through an elliptical solenoid with an axial momentum $P = m\gamma\beta c$, where β and γ are the relativistic parameters and c is the speed of light. In the laboratory frame, we use a Cartesian coordinate system x, y and z. Here $s = z$ is the distance along the axial direction and x, y are the transverse coordinates from the beam axis. Under paraxial approximation, the components of the magnetic field can be expressed as [3]

$$B_x(x, y, s) = -\left(B_s'(s) - D(s)\right)x/2 \tag{1a}$$

$$B_y(x, y, s) = -\left(B_s'(s) + D(s)\right)y/2 \tag{1b}$$

$$B_s(x, y, s) = B_s(s) \tag{1c}$$

where $B_s(s)$ and $B'_s(s)$ are the field and its derivative on the axis of the solenoid. Here $D(s)$ is related to the field gradient along x and y directions and depends on the elliptic cross-section of the solenoid.

The dimensionless Hamiltonian H for transverse motion of particles in the applied field of the elliptical solenoid and self-field of the beam is given by

$$H = -\frac{qA_s}{P} + \frac{1}{2}\left[\left(p_x - \frac{qA_x}{P}\right)^2 + \left(p_y - \frac{qA_y}{P}\right)^2\right] + \phi^S \tag{2}$$

where p_x and p_y are transverse canonical momentum and H is normalized to $\gamma m\beta^2 c^2$. Here $\phi^S = q\phi/(m\gamma^3\beta^2 c^2)$ is the normalized space charge potential. The components of the vector potential $\mathbf{A}$ can be obtained by using the gauge $xA_x + yA_y = 0$, which yield $A_x(s) = -B_s(s)y/2$, $A_y(s) = B_s(s)x/2$ and $A_s(s) = D(s)xy/2$. Using the components of the vector potential, the Hamiltonian in Eq. (2) can be expressed as

$$H = -Jxy + \frac{1}{2}\left[(p_x + Ky)^2 + (p_y - Kx)^2\right] + \phi^S \tag{3}$$

where $K = qB_s/(2m\gamma\beta c)$, $J = qD/(2m\gamma\beta c)$ are functions of s. The equations of motion of a particle can be easily derived from the Hamiltonian (3) as

$$x' = p_x + Ky \quad , \quad p_x' = Jy - K^2 x + Kp_y - \frac{\partial\phi^S}{\partial x}$$

$$y' = p_y - Kx \quad , \quad p_y' = Jx - K^2 y - Kp_x - \frac{\partial\phi^S}{\partial y} \tag{4}$$

where all the variables are function of s. We assume a uniform density beam (KV distribution) with elliptical symmetry. The space charge potential ϕ^S will depend on the spatial elements of the beam matrix $\boldsymbol{\sigma}$ viz σ_{11}, σ_{33} and σ_{13} that is, on the size and orientation of the beam ellipse where for a continuous beam, the $\boldsymbol{\sigma}$ matrix defines the shape of a 4D hyper-ellipsoid $\hat{\mathbf{x}}^T\boldsymbol{\sigma}^{-1}\hat{\mathbf{x}} = 1$. Here $\hat{\mathbf{x}} = (x, p_x, y, p_y)^T$ represents the canonical variables and the "T" denotes the transpose of matrix. The potential ϕ^S in the coordinate system (x, y, s) can be written as [4]

*animesh@veccal.ernet.in

EMITTANCE MEASUREMENTS AT THE STRASBOURG TR24 CYCLOTRON FOR THE ADDITION OF A 65 MeV LINAC BOOSTER

A. Degiovanni#, TERA, Novara, Italy and EPFL, Lausanne, Switzerland
U. Amaldi, S. Benedetti, D. Bergesio, A. Garonna, G. Molinari, TERA, Novara, Italy
E. van Lier, R.L. Watt, ACSI, Richmond, B.C., Canada
D. Brasse, M. Pellicioli, M. Rousseau, J. Schuler, IPHC, Strasbourg, France
S. Braccini, E.V. Kirillova, LHEP-AEC, University of Bern, Bern, Switzerland

Abstract

The long term plans of IPHC foresee the installation of a linac that will boost the energy of the protons of the Strasbourg TR24 cyclotron from 24 MeV to 65 MeV. A Cell Coupled Linac, designed by the TERA Foundation, could be used for this purpose. To compute the transverse acceptances of the linac, the horizontal and vertical emittances of the extracted proton beam need to be measured. The secondary emission detector BISE (Beam Imaging with Secondary Electrons) built by TERA and under development at the Bern 18 MeV IBA cyclotron will be used in Strasbourg for the final measurements. The results of the preliminary measurements of the transverse beam profiles are reported together with the development of BISE, the description of the linac structure and the calculation of the expected output current based on the dynamics of the accelerated proton beam.

INTRODUCTION

The Cyrcé cyclotron (CYclotron pour la ReCherche et l'Enseignement) has recently been installed at IPHC (Institut Pluridisciplinaire Hubert Curien) for the development of new radiolabelled molecules based on the research and production of radio-isotopes for diagnostics and medical treatments. The TR24 cyclotron produced and commercialized by ACSI (Canada) delivers a 16-25 MeV proton beam on two extraction ports with intensity from few nA up to 500 μA. The facility will start soon to produce ^{18}F (half-life period 110 min) and ^{64}Cu (half-life period 12,7h). Using standard targets, 15 possible isotopes can be produced with this accelerator.

The long term plans of IPHC foresee the installation of a linac for boosting the energy of the protons from 24 MeV to 65 MeV. The TERA Foundation has developed in the last decades high RF frequency Cell Coupled Linacs (CCL) designed to be coupled with cyclotrons to boost their energy for applications in proton therapy [1]. A 3 GHz CCL, designed by the TERA Foundation, could be used for this purpose.

To compute the transverse acceptances of the linac, the horizontal and vertical emittances of the extracted proton beam need to be measured. Preliminary measurements were conducted at IPHC, in collaboration with ACSI. Further measurements are planned with the secondary emission detector BISE (Beam Imaging with Secondary Electrons) built by TERA and under development at the Bern 18 MeV IBA cyclotron [2].

#alberto.degiovanni@cern.ch

CYCLOTRON BEAM MEASUREMENTS

The TR24 installed at IPHC in Strasbourg is shown in Fig. 1. The cyclotron has two exit ports. One is equipped with targets for cell irradiation, while the second one is not used at the moment. The second extraction beam port has been commissioned for performing the beam measurements and is shown in Fig. 1.

Figure 1: Picture of the TR24 cyclotron installed at IPHC in Strasbourg. The water cooled beam dump provided by ACSI is visible at the end of the beam pipe.

Preliminary beam profile measurements have been performed at the beginning of July 2013 using Gafchromic™ EBT3 films and adding two pieces of beam pipe in order to obtain profiles at different distances from the extraction point. Meanwhile, the BISE detector is under development and test at the Bern cyclotron.

Preliminary Measurements at IPHC

The absence of a dedicated extraction beam line limited the first measurements to an analysis of beam profiles at different positions from the extraction port (0 m, 0.4 m and 0.7 m), obtained by connecting two pieces of beam pipe (100 mm diameter) to the exit port 2 of the cyclotron. The alignment of the beam pipe was based on results of simulations of beam trajectories in the cyclotron. The pieces of beam pipes were electrically isolated by placing polymeric gaskets, so that it was possible to monitor the beam current on the wall of the beam pipe and on the beam dump, during the irradiation.

ISBN 978-3-95450-128-1

DESIGN OF ACHROMATIC BENDS FOR THE HIGH ENERGY BEAM TRANSPORT SYSTEM OF HCI AT IUAC DELHI

Abanimohan Mandal, Dinakar Kanjilal, Gerald Oscar Rodrigues, Sarvesh Kumar
Inter-University Accelerator Centre, New Delhi, India

Abstract

The high energy beam transport system of the High Current Injector (HCI) being currently developed at IUAC will transport heavy ion beam of maximum energy ~1.8 MeV/u with mass to charge ratio (A/q) of 6 from drift tube linac (DTL) to the superconducting linear accelerator (LINAC) in the zero degree beam line of the existing 15UD Pelletron. The whole transport path (~50 m) consists of four 90 degree bends. Since the beams coming from DTL are expected to have an energy spread of 0.5%, the magnetic bends have to be achromatic. The transport system is designed considering the restrictions imposed by the existing beam hall and the other space constraints. The first three 90 degree achromats have the configuration of Q1Q2Q3MQ4MQ3Q2Q1 and the fourth one has configuration of Q1Q2MQ3Q4Q4Q3MQ2Q1 where Q stands for magnetic quadrupole and M stands for 45 degree bending magnet. Each achromat has been designed so that its total length is restricted to 7 m to fit into the available space. The maximum dispersion occurs at the middle of Q4. Beam dynamics codes like GICOSY and TRACE3D have been used to design the achromats and the detail of optics is presented.

INTRODUCTION

The HCI currently being developed at Inter University Accelerator centre (IUAC) is an alternate injector system based on electron cyclotron resonance (ECR) ion source. The 18 GHz high temperature superconducting based ECR called PKDELIS [1] was designed in collaboration with PANTECHNIK, France. The ions of A/q equal to 6 will be analysed by a large acceptance combined function 90 deg. analyzing magnet [2] placed on a 200 kV high voltage platform. The extracted ions are pre-accelerated to 8 keV/u and bunched using a multi-harmonic buncher to match with the input longitudinal emittance requirement of radio frequency quadrupole (RFQ). The ions of energy 180 keV/u coming out of RFQ will be transported to a room temperature DTL for further acceleration. Several quadrupole magnets and a 48.5 Mhz RF buncher will be used for transverse and longitudinal emittance matching to DTL input. The DTL enhances the energy of the ions to 1.8 MeV/u. This whole injector system will be housed in a beam hall called BH-III. The ions from DTL will be transported to an existing super conducting LINAC approximately 50 m away in a separate beam hall called BH-I. The whole beam transport system of HCI is divided into three sections as follows:

- Low energy beam transport section (LEBT) from ECR to RFQ
- Medium energy beam transport section (MEBT) from RFQ to DTL
- High energy beam transport section (HEBT) from DTL to superconducting LINAC

The HEBT has four 90 deg. bends. Since the ions coming out of DTL are expected to have energy spread ~0.5%, all these bends have been designed to be achromatic using two 45 deg. dipole magnets along with several quadrupole magnets. The present paper describes the design aspects of these achromatic bends.

LAYOUT OF BEAM HALLS

The layout of different beam halls in the accelerator building complex at IUAC is shown in Fig. 1. BH-1 consists of seven beamlines for the existing pelletron. The zero deg. line from the first switching magnet in vault area is used for augmenting energy of the beam coming from 15UD pelletron [3]. The bunched beam having FWHM ~1-2 ns from pelletron is further bunched by a superconducting niobium quarter wave resonator to ~150 ps and then injected into three LINAC cryostats [4] in BH-II. Each cryostat houses eight super conducting quarter wave resonators. The beam from LINAC is switched to four beamlines in BH-II. BH-III is situated on the eastern side of BH-I which is 33 m x 10 m in size housing the HCI. The schematic layout of HCI is shown in Fig. 1.

DESIGN OF ACHROMATIC BENDS

The HEBT has four 90 deg. bends, the first one being in BH-III and the other three are in BH-I. While designing each achromat, besides the input beam characteristics, the stress has been given on the geometrical constraints in the building layout. In BH-III, the major constraints are two pillars near first 90 deg. bend which restrict the overall length of the achromat, as it is necessary to have image point of the achromat before the first pillar to make space for the RF buncher and diagnostic equipment. The overall length available is ~ 7 m. To avoid multiple designs and to reduce cost all the dipoles magnets have been designed to have same specifications. Similarly care has been given on the type of quadrupole magnets used. The first three achromats have been designed identical, called type-I, whereas the last one has different configuration called type-II to accommodate the existing beam lines in BH-I.

Design of Type-I Achromat

This achromat has been designed with the input beam characteristics given in Table 1.

ISBN 978-3-95450-128-1

GETTING UNIFORM ION DENSITY ON TARGET IN HIGH-ENERGY BEAM LINE OF CYCLOTRON U-400M WITH TWO

I. Ivanenko#, I. Kalagin, V. Kazacha, N. Kazarinov, JINR, Dubna, Moscow Region, 141980, Russia

Abstract

Formation of a uniform ion distribution in the existing beam line of U400M cyclotron with the help of octupole magnets has been studied. The simulation was performed for $^{40}Ar^{17+}$ ions with energy of 41.3 MeV/amu. The required level of beam non-uniformity on the target with diameter of 60 mm is ±7.5%. Two octupoles with static magnetic fields have been used to achieve the desired uniformity of the beam density in both coordinates simultaneously. The results of calculations are presented. This method of improving the uniformity of the beam will be implemented soon at Flerov laboratory of JINR.

INTRODUCTION

The high energy beam line of the U-400M cyclotron is intended for the irradiation of the microchips by the flow of accelerated heavy ions for determination of the possible damages by radiation. This requires the non-uniformity of density of irradiation on target is not worse than 7.5%. Various methods are used to obtain a high uniformity of the ion density distribution on the target. A simple method is to send the beam from an accelerator through a thin scattering metal foil [1]. The multiple beam scattering results in approximately Gaussian angular distribution of the particles. The target is irradiated by the particles being on flat top of a Gaussian distribution.

The possibility of obtaining a uniform distribution of particles on a target by means of two magnetic scanners (horizontal and vertical ones) and the experimental implementation of this method were described in [2,3].

Sometimes a combination of electrostatic and magnetic scanners is utilized for these purposes [4].

An electrostatic lens is used also for getting the uniform particle distribution on the target in [5].

Utilization of the non-linear magnetic elements gives the possibility to refuse rather complex systems of scanning of the beam.

The scheme for obtaining a uniform distribution of the particle density on the target using the doublet of quadrupoles and one octupole was given in [6].

A method to achieve the same goal by using a pair of magnetostatic octupole lens was proposed in [7,8].

The possibility of obtaining a uniform distribution of the ions on the target in the high-energy channel of the U-400M cyclotron with the help of two magnetostatic octupoles was examined in this work.

SCHEME OF THE ION BEAM LINE

The layout of the ion beam line is represented in Fig. 1. All distances between the optical elements of the beam line, parameters of all quadrupoles and bending magnets are presented in [9].

SIMULATION RESULTS

The $^{40}Ar^{17+}$ ions with kinetic energy W of 41 Mev/amu were chosen for calculations. Table 1 shows the values of the initial Twiss's parameters $\alpha_{x,y}$, $\beta_{x,y}$ [cm], rms emittances $\varepsilon_{x,y}$ [π mm×mrad], the horizontal dispersion function η_x [cm] and its derivative η'_x calculated at the point of the beam extraction from the cyclotron [10].

Table 1: Initial Beam Parameters

α_x	β_x	α_y	β_y	ε_x	ε_y	η_x	η'_x
-17	1927	-0.3	54.3		1.5	118	1.0

It was assumed in the calculations that the relative mean-square spread of the ion longitudinal momentum was equal to 2 10^{-3}. The values of the vertical dispersion function η_y and its derivative η'_y were equal to zero.

The calculations were carried out with the following requirements:

- The quadrupole gradients were chosen so that the sizes of the beam inside the quadrupoles would not exceed 80% of their aperture.
- The values of the found gradients should not exceed the maximum values of gradients of the existing quads.
- The irradiated target is a circle with a diameter of 60 mm. The uniformity of the distribution of the ion density on the target should not exceed the value of ± 7.5%.

Figure 1: Layout of the high-energy beam line for ion transportation from the U-400M cyclotron. Here Q1 –Q15 are the quadrupoles, BM1 – BM2 are the bending magnets, and T is the target.

#ivan@nrmail.jinr.ru

ISBN 978-3-95450-128-1

CORRECTION OF VERTICAL SHIFTING OF EXTRACTED BEAM AT THE TEST OPERATION OF DC-110 CYCLOTRON

I.A. Ivanenko, B.N. Gikal, N.Yu. Kazarinov, I.V. Kalagin, V.I. Mironov, E.V. Samsonov,
FLNR, JINR, 141980 Dubna, Russia

Abstract

The specialized heavy ion cyclotron DC-110 has been designed and created by the Flerov Laboratory of Nuclear Reactions of Joint Institute for Nuclear Research for scientifically industrial complex "BETA" placed in Dubna (Russia) [1]. DC-110 cyclotron is intended for accelerating the intense Ar, Kr, Xe ion beams with fixed energy of 2.5 MeV/nucleon. The commissioning of DC-110 cyclotron has been carried out at the end of 2012. The project parameters of the ion beams have been achieved.

During commissioning of cyclotron, the vertical displacement of the beam at the last orbits and at the extraction channel was revealed. The calculations and experiments have shown that the reason of this displacement is the radial component of magnetic field at the median plane of the cyclotron, which appears because of asymmetry of the magnet yoke. Correction of the vertical displacement of the beam has been achieved by creating an asymmetry of current distribution in the main coil of the cyclotron electromagnet.

EXPERIMENTAL TESTING OF THE EXTRACTED BEAM POSITION AND DIMENSION

Commissioning of the DC-110 cyclotron has been done at the end of 2012. During the experimental testing of the cyclotron, the extracted beam position and dimension was analyzed. The beam tracks on the constructed elements of extraction system has shown that the beam at the last orbits and during the extraction has a vertical displacement. The extraction system consist of electrostatic deflector and passive magnetic channel. At the Fig. 1 the beam track at the deflector entrance, R=894 mm, has 3 mm of vertical displacement above median plane.

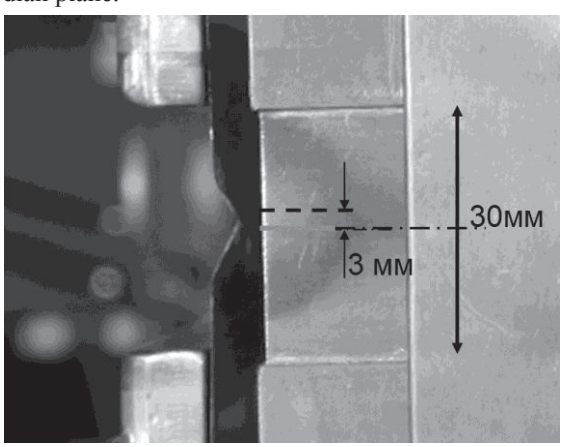

Figure 1: The beam track at the deflector entrance.

At the magnetic channel exit the beam track already has shown 5 mm of vertical displacement. At the distance of 1.1 meter after magnetic channel, in the extracted beam transport line, the luminophore probe is placed. The beam track at the probe has shown 16 mm of vertical displacement and aperture losses, Fig. 2.

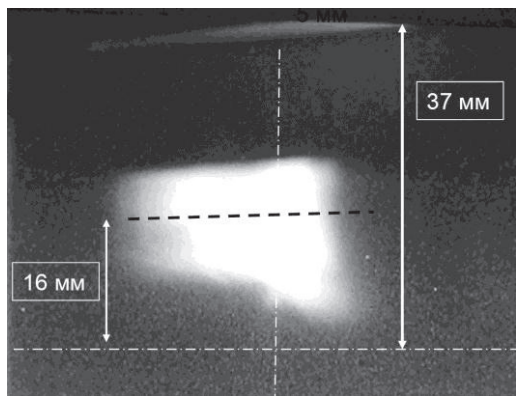

Figure 2: The beam track at the luminophore probe.

ESTIMATION OF MAGNET AXIAL ASYMMETRY INFLUENCE ON BEAM DYNAMIC AT EXTRACTION AREA

The main reason of the vertical displacement of the beam at the last orbits and at the extraction channel is the radial component of magnetic field, Br, on the median plane of the cyclotron. Br component appears because of vertical asymmetry of the magnet yoke.

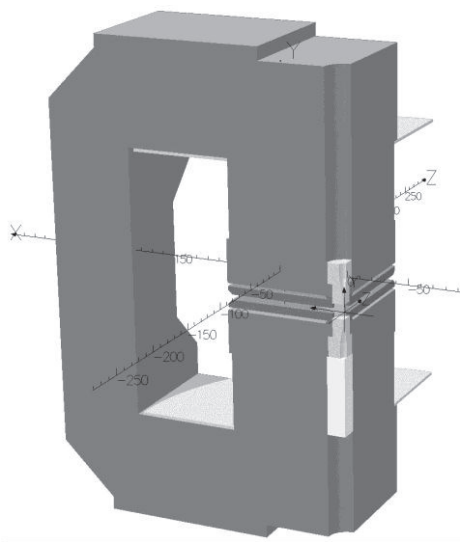

Figure 3: The model of asymmetric yoke of DC-110 cyclotron magnet.

ISBN 978-3-95450-128-1

TRANSVERSE PHASE-SPACE DISTRIBUTIONS OF LOW ENERGY ION BEAMS EXTRACTED FROM AN ECR ION SOURCE*

S. Saminathan†, J.P.M. Beijers, S. Brandenburg, H.R. Kremers, V. Mironov
Kernfysisch Versneller Instituut, University of Groningen, Zernikelaan 25,
9747 AA Groningen, The Netherlands

Abstract

Transverse phase-space distributions of low-energy ion beams extracted from ECR ion sources often show higher-order effects caused by ion-optical aberrations. Understanding these effects is mandatory to keep emittance growth and the resulting beam losses in low-energy beam transport lines under control. We present results of an experimental and theoretical study of beam extraction and transport in the AGOR injection line at KVI. Particle tracking simulations have been performed of a multi-component neon ion beam extracted from an ECR ion source to calculate 4D phase-space distributions at various positions along the beam line. The simulations compare well with beam profile and emittance measurements.

INTRODUCTION

Ion beams extracted from Electron Cyclotron Resonance (ECR) ion sources have relatively large and correlated transverse emittances compared to other types of ion sources. This, together with the high currents (up to tens of mA's) and low energies (up to tens of keV/amu) of the extracted multiply-charged ion beams often leads to significant losses during the subsequent beam transport. This is even a greater problem in the new generation of fully superconducting ECR ion sources because of their larger magnetic fields and extracted ion currents. Much work is being done by various groups to better understand and minimize these beam losses using beam diagnostic and/or simulation tools. However, there are often significant discrepancies between quantitative simulations and measurements, see e.g. [1]. Reasons for these disagreements could be a poor knowledge of the initial phase-space distributions of the extracted ion beams and/or poor handling of higher-order beam effects.

At the AGOR cyclotron facility of the Kernfysisch Versneller Instituut (KVI), University of Groningen, we have performed a study of the formation and extraction of helium and neon ion beams from the KVI ECR ion source and the subsequent transport through the low-energy beam line [2]. The study consists of detailed simulations of beam transport and measurements of beam profiles and transverse emittance distributions at various locations along the beam line. To check the validity of this approach we have first applied it to an essentially mono-component He^+ beam [3]. The simulation results compare very well, both qualitatively and quantitatively, with measurements. Here we present the results of simulations and beam profile measurements of a multi-component neon beam. First we briefly describe the experimental setup and simulation tools, then the results are presented and discussed and we finish with conclusions and outlook. In both simulations and measurements described below the parameters have been chosen such as to optimize the production and transport of a Ne^{6+} ion beam with a kinetic energy of 144 keV.

EXPERIMENTAL SETUP AND SIMULATION TOOLS

The KVI-AECR (Advanced Electron Cyclotron Resonance) ion source and first section of the low-energy beam transport line including the 110° analyzing and 90° bending magnets, a magnetic quadrupole triplet and electrostatic quadrupole singlet and three BaF_2 viewing targets VT1-3 are schematically shown in Fig. 1. The ion source is a 14 GHz AECR ion source with an electrostatic accel-decel extraction system and is described in detail in Ref. [4]. The analyzing magnet is a double-focusing one with a geometrical acceptance of 120 mm in the horizon-

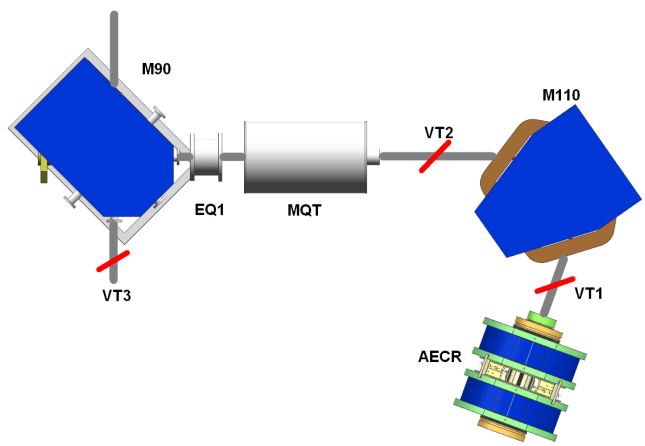

Figure 1: AECR ion source and first section of the low energy beam transport line. The locations of the three viewing screens are indicated as VT1, VT2 and VT3.

* This work is part of the research program of the "Stichting voor Fundamenteel Onderzoek der Materie" (FOM) with financial support from the "Nederlandse organisatie voor Wetenschappelijk Onderzoek" (NWO). It is also supported by the University of Groningen and by the "Gesellschaft für Schwerionenforschung GmbH" (GSI), Darmstadt, Germany.

† Present address: TRIUMF, 4004 Wesbrook Mall, Vancouver, BC V6T 2A3, Canada

ISBN 978-3-95450-128-1

MEASUREMENT OF RADIAL OSCILLATION AND PHASE OF ACCELERATING BEAM IN KOLKATA SUPERCONDUCTING CYCLOTRON

Jedidiah Pradhan†, Malay Kanti Dey, Jayanta Debnath, Atanu Dutta, Uttam Bhunia, Santanu Paul, Md. Zamal Abdul Naser, Vinay Singh, Ankur Agrawal, Alok Chakrabarti, VECC, Kolkata, India

Abstract

This paper describes various measurements performed on the beam behaviour with the help of the main probes and the differential probe to have a clear insight of the accelerating beam and the difficulties of beam -extraction process in the K500 superconducting cyclotron at Kolkata. Beam shadow measurements with three probes at three sectors were done to get the information of beam-centering and radial oscillations. The radial oscillation amplitude is estimated from the measurements. A differential probe was used to measure the turn separation and its modulation due to radial oscillation. With the help of magnetic field detuning method, the beam phase history was also measured.

INTRODUCTION

The beam behaviour studies were carried out to have a clear insight of the accelerating beam and the difficulties of beam -extraction process in the superconducting cyclotron (SCC) at Kolkata. We have accelerated the beam of Ne^{4+} and N^{2+} under 2nd-harmonic operation and carried out different probe measurements. The probe is made of insulated copper electrode which collects beam current and conducted through a cable to be measured by electrometer. There are such three probes separated at nearly 120 degree apart were used to measures the current versus radius. One of the probe which we called main probe(Mp) moves on spiral path along the centre of hill whereas the other two probes (Bore probe, BP & Deflector probe, DP) moves straight radially. The convenience of three probes is that current can be collected on one probe and cut off from this probe by moving another probe in, to determine orbit centre. The main probe (mp) is attached with differential probe to measure turn separation. To obtain information on the coherent and incoherent radial oscillations we have used both differential probe and shadow measurement cast by one probe on another at different locations of the probes. Beam shadow measurements are well known technique and are performed at many radial position of cyclotron. The radial position of reference particle of the beam is assumed to be the location where the beam current drops to 50% during shadow measurement. The orbit-centre was obtained from such measurements by finding its deviation from equilibrium orbit which is calculated for three sector cyclotron using measured field data. It was found that a large off centering in the extraction region where ν_r =1 could not survive the beam upto extraction energy. Later it was clear from magnetic field measurement that significant first harmonic imperfections in the extraction region which accounts for the unexpected off centering. The radial motion of orbit centre under measured field imperfection was simulated and compared with observed data. An empirical relation was deduced to be used with beam shadowing measurement to obtain radial coherent oscillation in three sector cyclotrons. The present analysis being general unlike others [1] where we have included scalloped orbit with three dee system and decreasing radial gain per turn due to acceleration in order to apply in our system. The turn separation was measured by differential probe and its modulation due to radial oscillation was studied to estimate dee voltage. The shadow width which is the radial extent where the beam current is taken over by other probe is used to estimate the largest incoherent betatron amplitudes present in the beam. The paper also describes the measurement of particle phase history which also accounts for the loss of beam in the cyclotron.

METHOD OF MEASUREMENT AND ANALYSIS

Orbit Centre

A beam is centered when the geometrical centre of the cyclotron coincides with the orbit centre. A number of shadow measurements were performed for different radial positions of the probes. The first probe is fixed at some radius and the second probe is moved to obtain equal beam current density on both probes. The third probe is placed well outside during measurement. Similarly the third probe was moved and repeats the measurement while second probe was kept outside. The measurement sequence of the probes follows the direction of acceleration viz DP-BP-MP. The measured data are plotted as a function of the position of fixed probe (Fig. 1). The equilibrium orbit is computed in a perfect magnetic field where only 3N harmonic are present and shifted from geometric centre so that positions of three probes matches the measured values so obtain. The radial motion of orbit centre is calculated and compared with observed values.

Radial Coherent Oscillation

Particles displaced from the equilibrium orbit oscillate harmonically about it both vertically and radially. The radius of such particle performing coherent radial oscillation at the nth turn is given by:

†jpradhan@vecc.gov.in

ISBN 978-3-95450-128-1

BEAM DYNAMICS IN PRESENCE OF IMPERFECTION FIELDS NEAR THE EXTRACTION ZONE OF KOLKATA SUPERCONDUCTING CYCLOTRON

J. Debnath#, M.K. Dey, J. Pradhan, S. Paul, A. Dutta, U. Bhunia, Md. Z.A. Naser, V. Singh, A. Chakrabarti, Variable Energy Cyclotron Centre, 1/AF, Bidhan Nagar, Kolkata -700064, India

Abstract

The superconducting cyclotron at Kolkata has accelerated the ion beams up to the extraction radius producing neutrons via nuclear reactions. After that the beam extraction process has been tried exhaustively. But rigorous beam extraction trials indicate towards some kind of error field, which was not possible to balance with the trim coil operated in harmonic-coil mode. It is found that the beam is being off-centred by a large amount after crossing the resonance zone and it is not reaching the extraction radius in proper path. This paper will be emphasizing the effect of various kind of error field on the beam. However, the magnetic field is being measured again to know the exact distribution of the field.

INTRODUCTION

The superconducting cyclotron [1] at VECC is a multi-particle, variable energy machine, having bending limit of K_b=500 corresponding to maximum magnetic field of 50 kG and the focusing limit of K_f=160 which is a design feature of the magnet determined by the hill-valley flutter field and the spiraling of the sectors. So the maximum kinetic energy (in MeV/u) is limited either by $(E/A) = K_b(Q/A)^2$ or by $(E/A)=K_f(Q/A)$. The optimum isochronous field is produced by a pair of superconducting coils (main coils), the iron core and 14 trim coils. The superconducting cyclotron has mainly two beam probes.

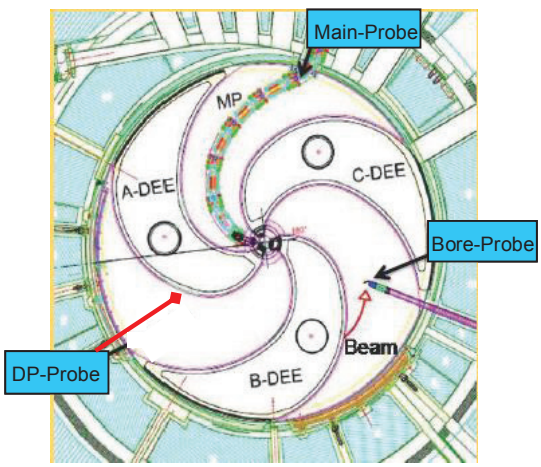

Figure 1: Schematic of the three probe locations.

One 'main-probe' (MP) running along the spiral central line of a hill. Another 'bore scope probe', running straight across another hill, is sometimes used as a second beam current measuring probe. One of the extraction element ports was used temporarily for installing the third beam current measuring device, which we call the 'deflector probe' (DP). With these three probes and the beam shadowing technique, beam off-centring were quantified at different radii.

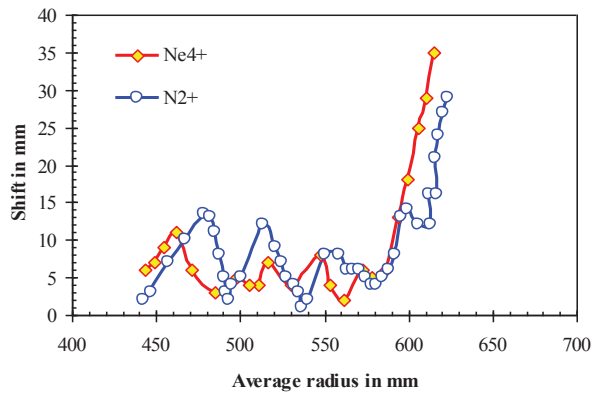

Figure 2: Beam off-centering as a function of R_{av}.

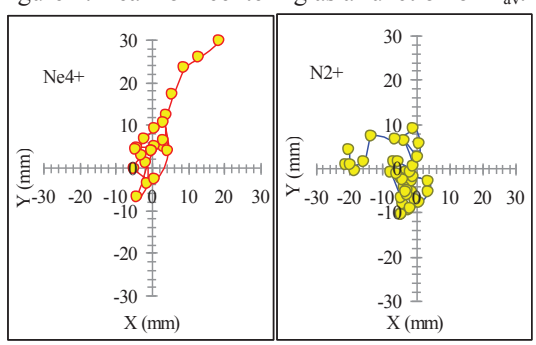

Figure 3: Locus of the Beam-centre for Ne^{4+}, h=2, ν_{RF}=19MHz and N^{2+}, h=2, ν_{RF}=14MHz beam.

Ne^{4+} beam in 2nd harmonic RF mode (ν_{RF}=19MHz) has been accelerated up to the maximum radius but we could not extract it. We have tried to measure the beam off-centering and beam phase to understand the problem. It was observed that the coherent oscillation amplitude of the beam is ~5 mm up to radius ~580 mm. Beyond that radius, the beam continuously shifts in one direction as shown in Fig. 2 and as a result of large off-centering it is lost before reaching the deflector entry. Figure3 shows the locus of the beam centre as a function of radius obtained by beam shadowing experiment. From the beam shadowing measurements one can calculate the average

#jdebnath@vecc.gov.in

ISBN 978-3-95450-128-1

ANALYSIS OF PHASE BUNCHING IN THE CENTRAL REGION OF THE JAEA AVF CYCLOTRON

N. Miyawaki#, H. Kashiwagi, S. Kurashima, S. Okumura, TARRI, JAEA, Gunma, Japan
M. Fukuda, RCNP, Osaka University, Osaka, Japan

Abstract

Phase bunching generated in the central region of an AVF cyclotron was analysed by a simplified geometric trajectory model for particles travelling from the first to the second acceleration gap. The phase difference between particles and a reference particle at the second acceleration gap depends on combination of four parameters: the acceleration harmonic number (h), a span angle of the dee electrode, a span angle from the first to the second acceleration gap, a ratio between a peak dee-voltage and an extraction voltage of an ion source. In the JAEA AVF cyclotron, phase bunching was realized for h = 2 and 3. The geometric conditions of phase bunching for h = 1 were unrealistic for the case of the JAEA AVF cyclotron with an 86 degree dee electrode. The phase difference at the second acceleration gap for an initial particle phase width of 40 RF degrees, estimated by the geometric trajectory analysis, was reduced to 8.9 RF degrees for h = 2 and to 27.7 RF degrees for h = 3, but was expanded to 43.7 RF degrees for h = 1. The reduction of the phase width was consistent with the results obtained by orbit simulations. The practical phase bunching was demonstrated by the phase width measurement for an internal beam of the JAEA AVF cyclotron.

INTRODUCTION

The central region of the JAEA AVF cyclotron [1] had been remodelled [2] to improve the beam phase width reduction for production of a high-quality beam with an energy spread of the order of 10^{-4} which is required to reduce a chromatic aberration effect caused in the focusing lenses for microbeam formation [3]. In general, reduction of a phase width is controlled by a phase slit installed in the central region. An external buncher in an injection beam line is indispensable for improvement of beam intensity and quality under the condition of the phase defining. Further phase bunching effect is obtainable by optimizing configuration of the central region geometry. Feasibility of phase bunching generated in the central region with an internal ion source was explored by Reiser et al. [4] in the 1960's. In a design of the central region for external injection, the generation of phase bunching was reported by Aldea [5]. However, there was little discussion for phase bunching in recent years because phase bunching achieved by an external buncher was sufficient for usual operation. In a design process for remodelling the central region of the JAEA AVF cyclotron, we analysed the mechanism of phase bunching by a simplified geometric trajectory model [6] and realized the phase bunching effect in the central region [2].

In this paper, we described the mechanism of the phase bunching generation and its application to the central region of the JAEA AVF cyclotron.

#E-mail: miyawaki.nobumasa@jaea.go.jp

MECHANISM OF PHASE BUNCHING

Phase bunching generated in the central region originates in energy gain modulation produced in the rising slope region of an acceleration voltage waveform at the first acceleration gap, and reduces phase difference between particles and a reference particle at the second acceleration gap. In general, a span angle θ_P from the first to the second acceleration gap is not always equal to a span angle θ_{Dee} of the dee electrode because the initial beam phase for acceleration to obtain maximum energy gain at the second acceleration gap depends on the position of a dee or a puller electrode. Consequently, the beam phase at the second acceleration gap can be changed by the electrode position and shape at the first acceleration gap. Moreover, the phase difference at the second acceleration gap is proportional to a bending angle from the first to the second acceleration gap. The bending angle is related to the energy gain at the first acceleration gap. The most effective phase bunching can be achievable at the first and second acceleration gaps, because the ratio of the energy gain to the total kinetic energy is largest.

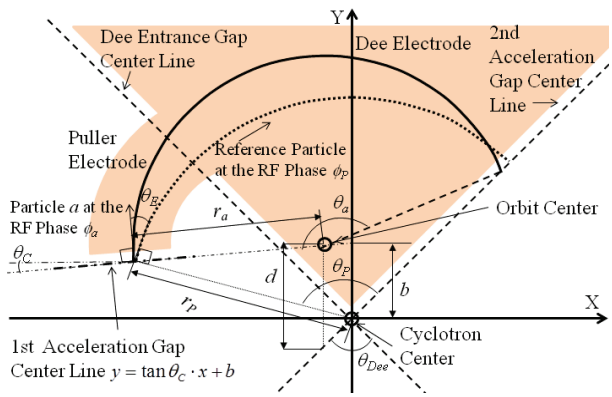

Figure 1: Layout of geometric analysis model.

The mechanism of phase bunching was investigated by the simplified geometric trajectory analysis model for particles travelling from the first to the second acceleration gap in homogeneous magnetic field. The layout of the geometric analysis model is shown in Fig. 1. In this model, the Y axis corresponds to the axis of the dee electrode. The center line of the first acceleration gap

ISBN 978-3-95450-128-1

STUDY OF BEAM CAPTURE IN COMPACT SYNCHROCYCLOTRON

S. Kostromin, G. Karamysheva, N. Morozov, E.Samsonov, JINR, Dubna, Russia

Abstract

Capture efficiency and main aspects of the beam dynamics during first turns and in a period of one synchrotron oscillation were studied in synchrocyclotron with driving magnetic field of ~5 Tesla. Corresponding simulations of the beam motion were done by means of numerical integration of the full equations of motion in the electro-magnetic field of accelerator. Main physical parameters for input data were taken similar to them for IBA S2C2.

TOOLS AND INITIAL DATA

To study the mentioned above processes so called 3-D (transverse and longitudinal) tracking code was used. Code is basing on numerical integration of full equations of motion in cylindrical coordinate system using t (time) as independent variable. This is the main difference from the tools used in [1].

Input parameters for these calculations are approximately reconstructs electromagnetic field of IBA S2C2 and were synthesized from data [1]-[3].

The dependence of RF-frequency on time which is needed for the particles tracking was calculated by means additionally developed procedure. Constructed curve ensures stable RF-phase of the synchronous particle. Driving magnetic field and corresponding $f_{RF}(t)$-curve for constant φ_s=60°RF inside the acceleration cycle where synchronous particle exists are presented in Fig. 1. RF-field was calculated by means of approximation [4] assuming two accelerating gaps (180°-dee) and constant with radius voltage U=10kV.

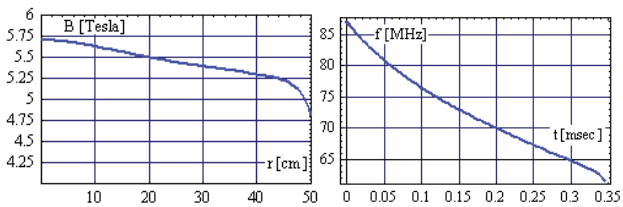

Figure 1: Driving magnetic field (left) and $f_{RF}(t)$ inside the acceleration cycle.

Kinetic energy of accelerating particle in our approximation is given by:

$$\mathrm{W} = 2qU\cos\varphi_s \cdot N$$

where q is particle charge, N - number of passed turns (two accelerating gaps per turn are assumed here). So, the time needed to get total energy $\mathrm{E} = \sqrt{(qB(r)\cdot r\cdot c)^2 + E_0^2}$ and take radius r in the driving magnetic field (see Fig. 1) defined by the equation

$$\mathrm{t} = \int_0^{t_0} \frac{1}{f} dt = \int_1^N \frac{E_0 + 2qU\cos\varphi_s \cdot N}{qB(r)\cdot c^2} dN$$

where E_0 is the rest energy of the particle. This equation defines a connection between points in curves in Fig. 1.

For simulation of the beam acceleration from ion source output slit a bunch of 10000 particles was generated. Distribution of particles on transverse phase planes (r, P_r) and (z, P_z) is of Gaussian shape (see. Fig. 2) and matched with the parameters of the synchrotron central region optics which is taken similar to IBA S2C2 (see Fig. 3) [3]. Starting beam emittances are $\varepsilon_r \approx 50\pi\cdot$mm·mrad and $\varepsilon_z \approx 200\pi\cdot$mm·mrad.

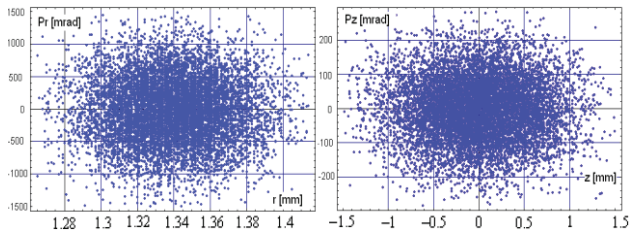

Figure 2: Distributions of particles on phase planes (r, P_r) and (z, P_z).

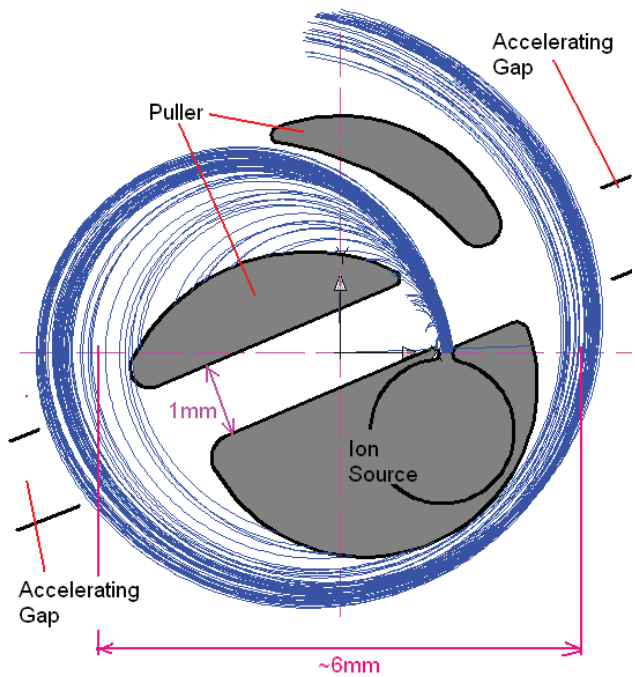

Figure 3: Central region elements and particles trajectories on the 1st turn.

ISBN 978-3-95450-128-1

BEAM TRACKING SIMULATION FOR A 9 MeV CYCLOTRON

S.Y. Jung, H.W. Kim, S.H. Kim, Y.H. Yeon, H.S. Song, Y.S. Lee, J.S. Chai,#
Sungkyunkwan University, Suwon 440-746, Korea

Abstract

Recently, the development of a 9 MeV cyclotron for production of radioisotope has been carried out. It has four sector magnet and RF cavity which resonance frequency is 83.209 MHz. The internal ion source was adopted and the central region was designed to accommodate the starting beam. In this paper, the design of the central region to optimize the initial circumstances for H^- beam and the study of extraction were described. The electric and magnetic field distribution were designed by electrostatic and magnetic solver in OPERA-3D TOSCA. A numerical code was developed to simulate the particle tracking and used to evaluate the performance during the acceleration in the designed EM field. The beam characteristics including the beam orbit, motion of the center of orbit, energy gain was investigated for central region and the entire acceleration characteristic until extraction was discussed.

INTRODUCTION

A 9 MeV cyclotron for the production of short-lived radioisotope has been developed. The cyclotron has four sector magnet having deep-valley structure for higher vertical focusing effect and RF cavity of which resonant frequency is 83.209 MHz. It adopted internal Penning Ion Gauge (PIG) ion source to produce H^- beam [1,2]. According to the use of internal ion source, the central region has been designed by iterative process considering the initial condition of the beam [3,4]. The optimal condition of the starting particle was determined to accommodate the beam at the first acceleration gap. The beam characteristic during the acceleration process was investigated to estimate the efficiency loss and minimize the beam loss caused by inappropriate central region design. It can decrease the beam current at the aimed energy level or damage the component inside the cyclotron. The thin carbon foil was used for extraction due to its high efficiency of stripping and the lower cost [5]. In this paper, the performance of the single particle beam starting from the central region of the cyclotron until it is extracted by carbon foil was described.

CENTRAL REGION

The electric and magnetic field distribution was designed by OPERA-3D TOSCA. The geometry of the electrode to accelerate the early beam was configured and initial parameters of the particle were investigated by including the ion source in the geometry. Then the beam properties in central region were evaluated with particle tracking calculation.

#jschai@skku.edu

Electric Field Distribution

The three dimensional modelling was carried before the electrostatic field was analysed in OPERA-3D TOSCA. In order to correlate the acceleration gap angle in cavity, the overall shape of the centre dee was determined based on the four gaps placed on the lines of ±15° from the x axis of cyclotron. The electric field generated by the model was evaluated with the single particle tracking simulation. Then, the position of the gap was gradually corrected based on the information of the particle passing through it and improved after few steps of iteration.

Figure 1 shows the optimized electric potential distribution. The electrode tip was included right after the chimney of ion source to effectively pull the particles by higher electric field. For more realistic analyse, the horizontally inserted PIG ion source was included in the simulation as shown in Fig. 2.

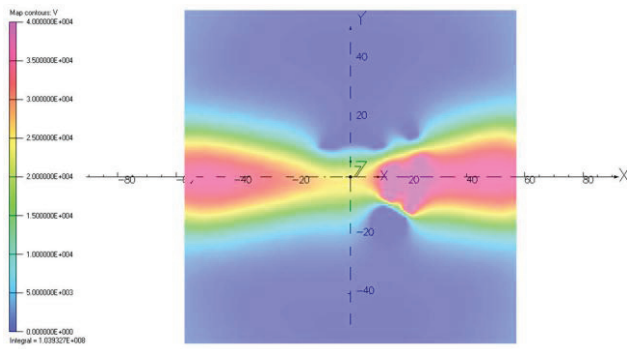

Figure 1: Electric potential distribution in central region.

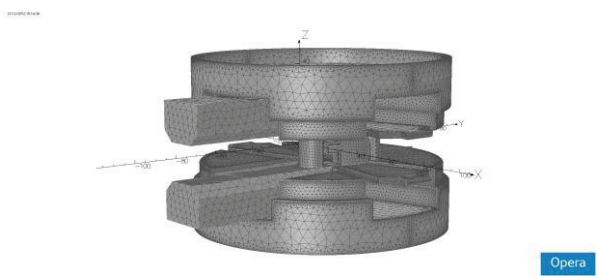

Figure 2: Electric field analysis in TOSCA.

Magnetic Field Distribution

The magnetic flux in central region was generated by a pair of centre pole which radius is 57mm and controlled by changing the current density of the electromagnetic coil.

For the control of vertical focusing, the bump of magnetic flux in central region was intentionally created. In order to minimize the beam loss which occurred when the particle hits the upper and lower center dee, the

ISBN 978-3-95450-128-1

BEHAVIOR OF SPACE CHARGE DOMINATED BEAM ENVELOPE IN CENTRAL REGION OF HIGH CURRENT CYCLOTRON

R. Azizi, H. Afarideh#, V. Afzalan, Department of Energy Engineering & Physics, Amirkabir University of Technology, Tehran, 15875-4413, Iran
M. Ghergherhchi, J.S. Chai, WCU Department of Energy Science/School of Information & Communication Engineering, Sungkyunkwan University, Suwon 440-746, Korea

Abstract

In this paper the space charge effect in the two first turn after injection has been investigated. In order to determine beam envelopes, two corresponding equations were chosen. In addition, all steps of calculation were done by MATLAB program. It should be mentioned limiting current and also magnetic, electrical field and edge effect has been considered. As far as, the high current cyclotron with 0.8π mm mrad emittance has been studied and current alters till 10 mA.

INTRODUCTION

In this paper, the space charge and beam envelope in the two first turn was investigated. And also specification of an IBA cyclotron -CYCLONE30 HC- which has four sectors, two delta type resonators and mulicaspe ion source was considered. At hill center the maximum and average magnetic field are 1.7 T and 1.03 T, respectively. The ion source produces proton beam with 30keV energy and 15mA current, and in next a sinuousal buncher bunches this beam. Finally, the beam is injected axially into the inflector.

More serious effect of space charge is defocusing along with injection. Moreover, weak vertical focusing causes an increase beam envelope. In order to compute the space charge is dominated by beam envelope, the K-V (Kapchisky - Vladimirsky) equation was used. Beam envelope oscillation has been investigated by the variation of beam current and Dee voltage.

DISCUSSION

Beam envelopes are represented by couple Eqs. 1,2 where X(s) and Y(s) are the beam envelopes in x-z plane and y-z plane respectively, and s is the distance along the equilibrium orbit [1]:

$$X'' + k_x - \frac{2K}{X+Y} - \frac{\varepsilon_x^2}{X^3} = 0 \quad (1)$$

$$Y'' + k_y - \frac{2K}{X+Y} - \frac{\varepsilon_y^2}{Y^3} = 0 \quad (2)$$

k_x, k_y are the periodic focusing strength of magnet with the period N. These quantities are equal to $\frac{v_r}{\rho}$ and $\frac{v_z}{\rho}$, respectively where ρ is the radius curvature of particle and K is the generalized perveance which is obtained from Eq. 3.

$$I = \frac{I_0}{2}\beta^3\gamma^3 K \quad (3)$$

where I_0 is the characteristic current which is defined as $I_0 = 4\pi\varepsilon_0 mc^3/q$. β and γ are usual relativistic terms.

The important values which have been used in simulation are shown in Table 1.

Table 1: Main Parameters used in Simulation

Injection energy	30 keV
Dee voltage	50 kV
Hill angle in central region	54 °
Valley angle in central region	36 °
Emittance	0.8 πmm mrad

In order to study the behavior of a beam passing through each bending magnet (dipole), we assumed the magnets as thin lens so the focal length of the thin lens could be obtained by the following formula (Eq. 4):

$$f = -\frac{\tan\alpha}{\rho} \quad (4)$$

where α_1 is the entrance angle to hill and α_2 is the exit angle from hill.

The exit angle from hill is equal to the entrance angle to valley and entrance angle to hill is equal to exit angle from valley, but these angles vary before and after the boundary field. The flaring and edge effects are noted when the beam passes from the boundary of bending magnet, and in this article these effects have been applied by using thin lenses. Since the thin lens does not change the beam radius, so the beam motions can be predicated according to the transfer matrices [2]. A linear decreasing field is considered in order to simulate fringe field in simulation. The fringe field changes the optics of the dipole and causes oscillation in the beam trajectory around the mean orbit.

$$\begin{pmatrix} x_2 \\ x'_2 \\ y_2 \\ y'_2 \end{pmatrix} = M \begin{pmatrix} x_1 \\ x'_1 \\ y_1 \\ y'_1 \end{pmatrix} \quad (5)$$

where

#hafarideh@aut.ac.ir

ISBN 978-3-95450-128-1

INVESTIGATION ON THE TRANSVERSE EMITTANCE GROWTH OF INTENSE BEAM DURING BUNCHING

P. Sing Babu*, A. Goswami† and V. S. Pandit#
Variable Energy Cyclotron Centre, 1- AF, Bidhannagar, Kolkata-700 064, India

Abstract

A 2D particle in cell (PIC) code is developed to study the transverse dynamics of space charge dominated beam during bunching. The linear increase in the current within the specified bunch width due to density modulation during the transport is included in the method. Simulation shows emittance growth during bunching induced by the space charge effect for nonuniform distribution.

INTRODUCTION

In high current accelerators for example cyclotron, only a fraction of the injected dc beam from an external ion source is accepted for further acceleration. The typical value of phase acceptance of cyclotron is ~ 10 % of an rf cycle. Beam current in this phase acceptance can be improved by using a suitable buncher in the injection line [1-3]. To compress the dc beam longitudinally one needs to impose a velocity modulation at the buncher gap. In the case of high intensity beams, increase of current in the specified bunch affects the transverse dynamics. In general, the collective process in intense beams is provided by the Vlasov-Maxwell equations [4]. The average behaviour of transverse beam dynamics during beam bunching is studied using envelope equations [5-8]. The transverse component of space-charge force increases after the buncher because of the compression of the beam as the beam advances in the transport line. Generally a PIC simulation is used for self-consistent study of space charge dominated beam dynamics [9-12]. However, in the case of bunching where longitudinal compression takes place and optimization of transport parameters are also involved, such calculations become cumbersome and take long time. In the present paper we have studied the transverse beam dynamics in the presence of beam bunching using a linear increase of beam current in the specified bunch width from the buncher position to the time focus. The evolution of beam envelope and emittance growth have been estimated for various initial particle distributions.

PIC SIMULATION METHOD

In the PIC method, the beam is represented by a large number of macroparticles. Each macroparticle usually represents many individual ions maintaining the charge to mass ratio of a single ion [9]. Equations of motion of macroparticles are solved in the laboratory frame. After passing through the buncher gap the current in the bunch increases which also increases the line charge density. We have used a linear increase of beam current in the specified bunch width from the buncher position to the time focus. If the current in the bunch at location s is $I(s)$ then the space-charge density of each macroparticle becomes

$$Q_{xy}(s) = Q_{xy}(0) I(0) \left(1 + \frac{(\eta - 1)s}{L}\right). \quad (1)$$

Where $Q_{xy}(0)$ is the density of each macroparticle at s =0, η is the bunching factor, L is the drift distance of time focus from buncher.

The equations of motion of macroparticles in the laboratory coordinate system are given by,

$$\frac{d\mathbf{r}_\perp}{ds} = \frac{\mathbf{v}_\perp}{\beta c} \quad (2a)$$

$$m(s)\frac{d\mathbf{v}_\perp}{ds} = \frac{q(s)}{\gamma^2 \beta c}\mathbf{E}^{sc} + q(s)\mathbf{v}\times\mathbf{B}^{ext} \quad (2b)$$

where $\mathbf{v} = (\mathbf{v}_\perp, \mathbf{v}_\parallel)$ is the component of the velocity in transverse and longitudinal direction, $\mathbf{r}_\perp = (x, y)$, $\mathbf{v}_\perp = (v_x, v_y)$ are the component of the position and velocity in transverse direction respectively. $q(s) = q.I(s)/I(0)$ and $m(s) = m.I(s)/I(0)$ are the charge and mass of each macroparticle at location s. The terms $\mathbf{E}^{sc}$ and $\mathbf{B}^{ext}$ are the self-electric field and external magnetic field respectively. In the analysis, we have included the effect of self-magnetic field by multiplying a factor of $1/\gamma^2$ in the electrostatic space-charge force terms.

RESULTS

The injection system consists of a 2.45 GHz microwave ion source and a solenoid based transport system to focus and match the beam at the entrance of spiral inflector [13, 14]. The schematic diagram of the transport system is shown in Fig. 1.

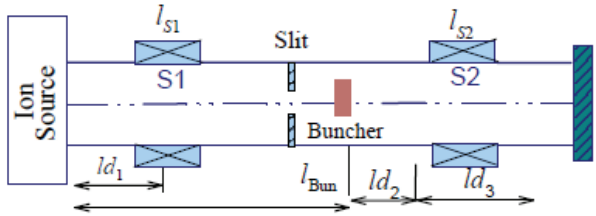

Figure 1: Schematic diagram of the beam bunching system.

*psb@vecc.gov.in, †animesh@vecc.gov.in, #pandit@vecc.gov.in

ISBN 978-3-95450-128-1

COLUMBUS - A SIMPLE ION SOURCE

M. Frank, Ch. Wolf, E. Held, Gymnasium Ernestinum, Coburg, Germany

Abstract

A simple ion source had to be designed for a cyclotron for school- and teaching purposes. It is adjustable to find the ideal position of the ion source.

The hydrogen gas is stored in a hydro-stick and controlled by a mass-flow-controller.

INTRODUCTION

The protons for our cyclotron are produced in the ion source which was built after the pattern of Tim Koeth [1], which he used first in his cyclotron.

This paper is about the conception of a simple ion source, COLUMBUS, for a school project [2].

A specific design of the ion source was required due to the cyclotron's small size and the low number of revolutions, cf. Figure 1. It was designed for adjusting the position of the ion source itself and the proton's angel of emission.

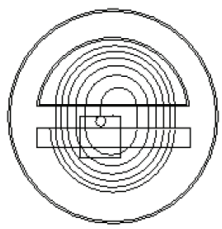

Figure 1: Revolutions of the protons.

FUNCTION & DESIGN

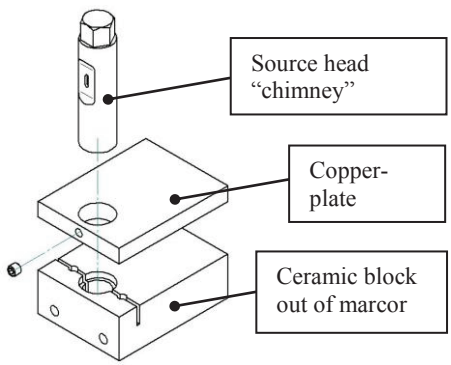

Figure 2: The basic setup of our ion source.

An ion source supplies the cyclotron with charged particles – in our case with protons accelerated by an electric field.

The protons are produced by collision ionization. Electrons emitted from a glowing tungsten filament showered by hydrogen gas are accelerated by a DC voltage of 100...200V. They are forced on a helical orbit by the uniform magnetic field. On their path they ionize the hydrogen gas.

The housing block of the ion source consists of a ceramic block out of macor and contains a filament of tungsten in an ionization-room. The macor block is covered by a copper plate, which holds the source-head – the so-called "chimney" – and is used as an acceleration-electrode for the electrons emitted from the glowing filament, cf. Figure 2.

Gas Feed

The ionized hydrogen-atoms, i.e. the protons rise into the chimney and exit through a tiny slit into the gap between the dee and the dummy-dee.

The hydrogen gas is stored in a hydro-stick, a small tank containing 10 litre of hydrogen gas at a pressure of 10 bar. After reducing the pressure to 0.3 bar the hydrogen gas is introduced into the housing-block by a mass-flow-controller (MFC) which allows a precise dosage of the hydrogen gas. The MFC will control the total pressure to approximately 10^{-4} mbar.

Positioning

For the setup of the ion source, it is considered that the ion source remains adjustable in direction of the gap, so that the ideal position can be found by experiments.

Normally the ion source is centred in the cyclotron. However, in our case – with our small cyclotron and such a small amount of revolutions ($\leq$ 10) - it is better to optimize the starting position of the first path. Due to this fact the ion source will not be fixed mounted but it will be stuck under the dummy-dee instead, cf. Figure 3.

Because of the low energy of the protons emitted from the ion source the angle of emission shall be adjustable for a better acceleration and to prevent that the protons remain in the gap between the dees.

This possibility is given by a rotatable source-head. The ideal angle of emission will be found by experiments.

ISBN 978-3-95450-128-1

RUTGERS 12-INCH CYCLOTRON: DEDICATED TO TRAINING THROUGH RESEARCH AND DEVELOPMENT*

Timothy W. Koeth#, IREAP, University of Maryland, College Park, MD, 20742, U.S.A.
Aaron J. Rosenberg, James E. Krutzler, Timothy S. Ponter, William S. Schneider,
Department of Physics and Astronomy, Rutgers University, Piscataway, NJ, 08854, U.S.A.
Daniel E. Hoffman, Gas Dynamics Laboratory, Princeton University, Princeton, NJ, 08554, U.S.A.

Abstract

The Rutgers 12-Inch Cyclotron is a 1.2 MeV proton accelerator dedicated to beam physics instruction.[1] The 12-inch cyclotron project began as a personal pursuit for two Rutgers undergraduate students in 1995 and was incorporated into the Modern Physics Teaching Lab in 2001.[2] Since then, student projects have been contributing to the cyclotron's evolution through development of accelerator components. Most of the Rutgers 12-Inch Cyclotron components have been designed and built in house, thus giving its students a research and development introduction to the field of accelerator physics and associated hardware.

INTRODUCTION

With the exception of a few institutions, accelerator science and engineering is relegated to the national labs and is not commonly found at the universities. The development of a small educational cyclotron is well within the capabilities of a standard Modern (Senior) Physics Lab course and in doing so brings accelerator science to the pool of young students at that critical time when they are deciding their scientific paths.

To fulfil academic requirements, Rutgers undergraduate physics students take two semesters of a Modern Physics Lab course where they typically perform twelve standard lab experiments. Since 2001, one or two exceptional students are chosen from the fall semester's lab participants for an independent cyclotron project the follwing spring. The "cyclotron students" are assigned a single, semester-long project which provides them a real life experimental research experience in a modern physics context and introduces them to the field of accelerator physics. At the end of the semester, the cyclotron students compose one joint report and collaboratively present their work to their classmates and instructors during an oral session. The Rutgers 12-Inch Cyclotron has had, to date, eighteen students; six of them have redirected their career goals to pursue accelerator physics in both academia and industry.

The student projects continually contribute to the cyclotron's evolution and improved operation. For example, the first pair of students designed pole tips that would improve beam focusing.[3] They were followed by two students that had the pole tips machined, which they installed and characterized with a home-built magnetic field mapping system.[4] The resulting magnetic field provided the necessary focusing enabling an exceptional beam physics experience for subsequent students.[5] To further illustrate the impact of our educational program, this paper discusses two student-designed and -built components which have performed well and have general application to other accelerator facilities.

Due to the small size of the 12-inch cyclotron, standard components need to be miniaturized. We will describe our internal cold cathode Penning Ion Gauge (PIG) type ion source as well as the electrostatic deflector that measures the ion beam final energy.

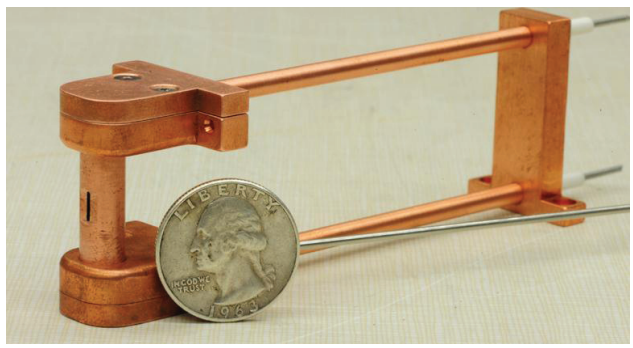

Figure 1: Miniature PIG ion source assembly with 0.7 x 4 mm slitted aperture.

ION SOURCE

The ion source has been our cyclotron's most challenging component to conquer. Early filament based designs generated mere nanoamps of protons and would only operate a few hours. With the promise of many hours of service, we set out to build a cold cathode Penning Ion Gauge (PIG) source, the results is shown in Fig. 1. Our Mark-III PIG has yielded a robust source of simple construction, outlined in Fig. 2. It uses two tantalum cathodes pinned to stainless steel leads that are seated in boron-nitride cups which are housed in copper bases. The chimney, chimney bases, and HV lead shields are also all copper. Cooling is through conduction to the upper and lower chamber lids.

*This work privately supported by the Rutgers Cyclotroneers and a Rutgers Physics Department donor-funded Instructional Equipment Fund.
#:koeth@physics.rutgers.edu -

BEAM PHYSICS DEMONSTRATIONS WITH THE RUTGERS 12-INCH CYCLOTRON*

Timothy W. Koeth#, IREAP, University of Maryland, College Park, MD, 20742, U.S.A.

Abstract

The Rutgers 12-Inch Cyclotron is a research grade accelerator dedicated to undergraduate education.[1] From its inception, it has been intended for instruction and has been designed to demonstrate classic beam physics phenomena. The machine is easily reconfigured, allowing experiments to be designed and performed within one academic semester. Our cyclotron gives students a hands-on opportunity to operate an accelerator and directly observe many fundamental beam physics concepts, including axial and radial betatron motion, destructive resonances, weak and azimuthally varying field (AVF) focusing schemes, DEE voltage effects, and more.

INTRODUCTION

With the expanse of Proton Beam Radio Therapy, medical isotope and industrial facilities as well as numerous research labs, the demand for personnel trained in accelerator science and engineering is at an all time high. However, even upon graduation most undergraduate physics and engineering students are unaware of the option to pursue accelerator physics as a career. The Rutgers 12-Inch Cyclotron, Fig. 1, was built to introduce students to accelerator physics, let them explore many parameters of acceleration and focusing, and gain experience with standard accelerator hardware. Relative to other accelerator facilities, it is safe and accessible; reaching a maximum energy of 1.2 MeV protons, the Rutgers Cyclotron is not a radiological hazard and is easily approachable while operating.

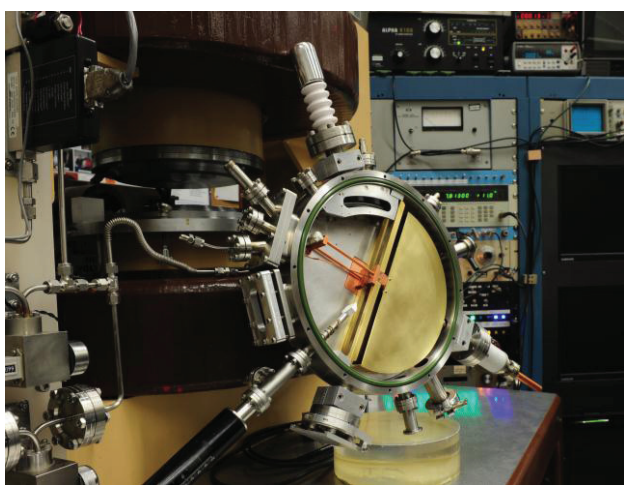

Figure 1: The Rutgers 12-Inch Cyclotron.

*This work privately supported by the Rutgers Cyclotroneers and a Rutgers Physics Department donor-funded Instructional Equipment Fund.

#:koeth@physics.rutgers.edu

Figure 2: Poletips for use on the Rutgers Cyclotron.

The H-frame cyclotron magnet has 12 inch diameter poles and approximately a 2-inch gap; the pole tips can be up to 1-inch thick and are easily removable – to date, we have four sets of pole tips and one of each set is shown in Fig. 2. They consist of two weak focusing (one "good" and one intentionally "bad" for educational purposes), a radial sector AVF and a spiral sector AVF, all with a maximum central axial field, $B_z(r=0)$, of 1.2 Tesla.[2,3] The magnet's upper and lower coils are independently energized for intentional field imbalance so as to shift the median plane. The cyclotron has a single 5-inch radius DEE with a 0.9 inch vertical aperture and a matching dummy DEE. The Radio Frequency (RF) supply is tuneable from 2 to 30 MHz with power adjustable up to 1.5 kW; it can be operated in continuous or pulsed mode and is capable of achieving a peak DEE voltage of 10 kV.[4] The ion source is an internal cold cathode PIG source that operates in excess of 40 hours before requiring service.[5] Beam diagnostics include a radial probe carrying an electrically isolated phosphor plate, which provides transverse beam images as well as beam current measurements at all radii. A removable electrostatic deflection channel intercepts the ion beam at the 4-inch radius and is used as a velocity filter to measure ion energy.[6] The operating pressure of 1E-5 Torr is provided by a standard 4-inch diffusion pump stack. The cyclotron chamber's position can be moved horizontally with respect to the magnet's center. A full 3D SIMION model has been developed and extensively verified with every configuration of our cyclotron.[7]

ORBIT STABILITY DEMONSTRATIONS

Weak focusing (WF), empirically discovered in the first cyclotrons, and subsequently studied by R.R. Wilson, is an ideal introduction into orbit stability.[8,9] WF fields are, at some level, still present in all cyclotrons -

ISBN 978-3-95450-128-1

CYCLOTRON INJECTION TESTS OF HIGH-INTENSITY H2+ BEAM

F. Labrecque, B.F. Milton, BCSI,Vancouver, BC V6P 6T3, Canada
L. Calabretta, L. Celona, INFN-LNS, Catania, Italy
J. R. Alonso, D. Campo, J. M. Conrad, D. Winklehner, M. H. Toups,
MIT, Cambridge, MA 02139, USA
R. Gutierrez-Martinez, L. Winslow, UCLA, Los Angeles, CA 90095, USA

Abstract

A test stand designed for high-intensity q/a = 0.5 beams has been assembled at the development labs of Best Cyclotron Systems, Inc. (BSCI) in Vancouver, Canada. The Versatile Ion Source (VIS) ECR source from LNS-INFN Catania delivers high-current, high-quality beams of H_2^+ ions to a small 1 MeV cyclotron under development at BCSI. A primary goal is to design systems capable to deliver 10 mA of protons (5 mA H_2^+) on neutrino-producing targets for the DAEδALUS and IsoDAR experiments. Progress and status of the R&D program are presented.

INTRODUCTION

Members of the neutrino community have proposed the IsoDAR and DAEdALUS experiments to, respectively, search for sterile neutrinos and CP violation in the neutrino sectors [1,2,3]. Both experiments require accelerators able to supply 10 mA proton beams. In particular, DAEdALUS needs 800 MeV protons, while IsoDAR will use a beam of 60 MeV protons. To achieve this high current, molecular H_2^+ ions will be injected and accelerated in the cyclotrons, easing space-charge effects at injection and allowing stripping extraction at the top 800 MeV/amu energy.

Capture efficiency in the central region of a compact cyclotron is typically 10%; if the beam can be effectively pre-bunched at the cyclotron RF frequency, a factor of two improvement could be obtained. Hence currents from the (CW) ion source must be around 25 to 50 mA. Space charge is important at these current levels and can prevent reaching this goal.

A first-phase R&D program to test injection of high-intensity H_2^+ beams is underway at BCSI. This project, a collaborative effort between MIT, LNS-INFN (Catania), and BCSI, utilizes the VIS source shipped from Catania and mounted on a test stand assembled at the Vancouver development labs of BCSI. The source delivers beam to an axially injected 1 MeV cyclotron that is being built by BCSI. Characterization of the source for H_2^+ beam production has taken place this summer. Inflection and acceleration tests will be completed in early 2014.

THE TEST STAND

Figure 1 shows the layout of the test stand. The VIS source, has produced 40 mA of proton current [4]. In a test stand at LNS-INFN (Catania), 15 mA of H_2^+ was observed, by adjusting only the inlet gas pressure and microwave power but no other changes.

A solenoid with a 44 cm effective length, and10 cm bore is located 50 cm from the extraction point of the source. It provides primary focusing, and also the means of separating protons from H_2^+ ions. The test stand was, originally configured for H^- and did not allow for a bend to analyze the beam. We decided to test solenoid focusing to separate the beams instead of developing a Wien filter. Indeed, a Wien filter has a significant disadvantage in that the electrical field destroys space-charge compensation, with a resulting deleterious effect on the beam emittance.

An emittance meter can be installed in a 6-way iso-160 vacuum T located about 1.5 m after the solenoid.

The drift tube buncher will be placed at about 1.7 m after the solenoid. Molybdenum grids 0.1 mm thick, are mounted on the accelerating gaps between the electrode and ground. The grids have a square mesh size of 5 mm.

A Bergoz 100 mm bore DCCT is a primary current monitor. After this device another 6-way iso-160 vacuum T houses a collimator and movable beam stop.

Finally come two magnetic quadrupoles, which can be rotated around the beam axis, and the last solenoid magnet. These allow flexible adjustment of beam focus and shape at the entrance of the spiral inflector inside the cyclotron magnet.

CENTRAL REGION

The 1 MeV cyclotron central region is critical to establish the injection feasibility of H_2^+ molecules at the levels required by the DAEδALUS and IsoDAR experiments. The final injection system consists of a Spiral Inflector (SI) to bend the beam onto the median plane and a set of electrodes connected to the two RF cavities that drive the beam along the first acceleration turns. The design of this system is a compromise between the characteristics of the DEAδALUS/IsoDAR cyclotrons and the properties of the small cyclotron developed by BCSI. These elements were designed by iterating between the 3D particle paths in the median plane and different models of SI in order to determine the optimal beam-matching conditions. The 3D electrostatic structures of the SI and the central region were studied by means of dedicated MATLAB codes and OPERA Vector Field, applying the back/forward particle integration technique. The SI was designed to transport the 60 keV beam of

ISBN 978-3-95450-128-1

DESIGN OF THE INJECTION INTO THE 800 MeV/amu HIGH POWER CYCLOTRON*

M. Haj Tahar, F. Méot, N. Tsoupas , BNL, Upton, Long Island, New York, USA
L. Calabretta†, INFN/LNS, Catania, Italy; A. Calanna, CSFNSM, Catania, Italy

Abstract

We present the design of the injection into a separated sector cyclotron (SSC) aimed at the production of a high power beam of 800MeV/amu molecular H_2^+ for ADS-Reactor applications. To work out the beam line parameters and beam dynamics simulations, including the first accelerated turns, we used the ray-tracing code Zgoubi and the OPERA magnetic field map of the cyclotron sector. We simulated the injection path of the H_2^+ and evaluated radial injection scheme in order to evaluate the parameters so derived. The paper details and discusses various aspects of that design study and its outcomes.

INTRODUCTION

The present paper addresses an attempt to find an appropriate injection design for our SSC: the cyclotron complex consists of an injector cyclotron accelerating H_2^+ molecules from 50 KeV/amu up to 60 MeV/amu. The beam is then injected to our 6-sector cyclotron by means of electrostatic and magnetic elements, and accelerated up to 800 MeV/amu. In order to do so, 6 RF cavities, 4 single-gap and 2 double-gap are used, which are PSI-like. A plot of the OPERA magnetic field map in the median plane, for one sector is shown in Fig. 1. There are many considerations that explain the magnetic field shape [1]:

- The azimuthal variations show that the field is decreasing in the central region which ensures more focusing of the beam.
- The superconducting coils of each sector, which are simply wound around the hills, are tilted by $\pm 3°$ in order to reduce the field at inner radii and increase it at outer radii: the magnetic field has to follow the γ(r) law in order to keep the isochronicity, where γ stands for the Lorentz factor.
- The isofield lines show that one edge of the sector has spiral shape while the other is quite straight: even though it is better to have spiral edges to increase the vertical focusing, the design of the magnet becomes problematic when it comes to using superconducting coils, because of the expansion radial force exerted from the inner region of the coil towards the outer radii. A superconducting magnet with a convex shape of the coil would be very difficult to build.

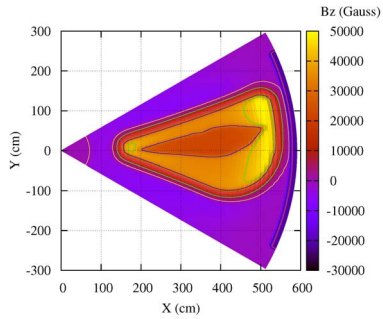

Figure 1: Plot of the z-component of the magnetic field in the median plane for one sector, with the isofield lines.

BEAM DYNAMICS AT INJECTION

Orbits at various energies from injection to nearby extraction are shown in Fig. 2. It can be easily seen that the distance between consecutive turns (that have the same step size in energy) decreases quickly. In fact, the transverse separation of the turns is very important to consider in our design because it has to be maximized in order to allow clean injection. The step width per turn can be described by the formula [2]:

$$\frac{dR}{dn_t} = \frac{U_t}{m_0 c^2} \frac{R}{(\gamma^2 - 1)\gamma} \tag{1}$$

where U_t denotes the energy gain per turn. However, this assumes that the condition of isochronicity is perfectly satisified. It can be deduced from Eq. 1 that both the energy gain per turn and the injection radius should be made as big as possible in order to increase the step width per turn at injection as well. The transverse separation of the turns as a function of the kinetic energy is shown in Fig. 3.

The first orbit suitable for acceleration is the first closed orbit shown in Fig. 2 This orbit is very important to study in order to match the injected beam properly. Paraxial rays were generated around this orbit in order to compute the transfer matrix of the sector. From that, the betatron functions of the sector ensuring the 6-fold symmetry were computed. The beam envelope of the entire cyclotron was then obtained by multi-turn tracking of a set of particles generated around the eigen ellipse. Both axial and radial beam envelopes are shown in Fig. 4 and 5 respectively. All the results obtained here assume a H_2^+ beam energy of 60 MeV/amu and a normalized emittance of 13.5 π mm.mrad.

INJECTION LINE

The injection system needs to transport the beam from a point outside the cyclotron ring to the first orbit suitable for acceleration. The main constraints of the design are:

* Work supported by Brookhaven Science Associates, LLC under Contract No. DE-AC02-98CH10886 with the U.S. Department of Energy.
† calabretta@lns.infn.it

PROPOSAL FOR HIGH POWER CYCLOTRONS TEST SITE IN CATANIA

L. Calabretta, L. Celona, L. Cosentino, G. Gallo, D. Rifuggiato, Cui Tao, INFN-LNS, Catania, Italy
J.R. Alonso, W. Barletta, A. Calanna, D. Campo, J.M. Conrad, MIT, Cambridge, MA 02139, USA
R. Johnson, L.A.C. Piazza, BCSI, Vancouver, BC, Canada

Abstract

The IsoDAR and DAEδALUS experiments will use cyclotrons to deliver high-intensity (10 mA peak current) proton beams to neutrino-producing targets. Cyclotrons with similar high current but with lower energies are also useful to produce medical radioisotope. To investigate the feasibility of these very high beam current we proposed the construction of a dual cyclotron able to accelerate ions with q/A=0.5, in particular He^{++}, up to 7 MeV/A and protons up to 28MeV.

The application of this machine, the main characteristics and the planned activity of the project are presented.

INTRODUCTION

A small cyclotron with 700 mm extraction radius, able to accelerate ions with q/A=0.5 (H_2^+ ionized hydrogen molecule and He^{++}) up to the maximum energy of 7 MeV/A, is presented here. This cyclotron is based on the design of central part of a bigger cyclotron already studied in the context of the experiments DAEδALUS (investigation of CP-violation) and IsoDAR (to search for sterile neutrinos) [1, 2, 3].

One of the goals of the project is to check experimentally the acceleration of H_2^+ beams with current up to 5 mA. To achieve this goal, we need also a very powerful ion source able to supply H_2^+ current in the range 25-50 mA. Up to now our present ion source VIS [4] has been able to supply about 10 mA of H_2^+. We planned to upgrade this source or to use other sources developed in other laboratories to supply the request current. Moreover, using this cyclotron it will also be possible to accelerate He^{++} beams up to a maximum energy of 28 MeV and or a deuteron beam up to 14 MeV. This cyclotron will be able to produce a helium beam current in excess of 0.5 mA when equipped with the AISHA ion source, under construction at INFN-LNS in Catania [4]. With this high-current He beam, through the reaction $^{96}Zr(\alpha, n)^{99}Mo$, we could produce enough ^{99}Mo to satisfy about 50% of the Italian needs. ^{99}Mo is the parent generator of ^{99}Tc, the most used radioisotope in the medical field. The production of ^{99}Mo inside a target of ^{96}Zr should simplify the purification of ^{99}Mo. The production of the ^{99}Mo radioisotope via accelerators is extremely interesting, building up an alternative way to the production by nuclear reactors that are at the end of their life. Using the helium beam we could also produce the ^{211}At radioisotope through the reaction of $^{209}Bi(\alpha, 2n)^{211}At$. Targets and procedures to prepare and separate these radioisotopes will be the charge of a private company that has already expressed interest in it.

Table 1: Cyclotron Parameters

R axial hole	29 mm	R pole	800 mm
N. Sectors	4	Hill width	30° ÷ 36°
Valley gap	1400 [mm]	Pole gap	60 [mm]
Diameter	2800 [mm]	Full height	1800 [mm]
Total weight	52 [tons]	Vacuum	10^{-5} Pa
Cavities λ/2	Double gap	Acc. Voltage	70 [kV]
Main Coil size	200x240 [mm^2]	2nd Coil size	30x240 [mm^2]
Parameters for ions with q/A=0.5, H_2^+, He^{++}			
E_{inj}	70 [keV]	E_{max}	7 [MeV/amu]
B_0	1.08 [T]	Bmax	1.90 [T]
RF Harmonic	4th	Freq.	32.5 [MHz]
Main coil curr. density	2.8 [A/mm^2]	2nd coil curr. density	-1.1 [A/mm^2]
Parameters for proton beam			
E_{inj}	70 [keV]	E_{max}	28 [MeV]
B_0	1.12 [T]	Bmax	2.0 [T]
RF Harmonic	2nd	Freq.	34.3 [MHz]
Cur. density Main coil	2.3 [A/mm^2]	Cur. density 2nd coil	4 [A/mm^2]

A serious effort is dedicated to finding a design of the iron and of the coils of the cyclotron that allow the use of this cyclotron also to accelerate protons up to 28 MeV.

LAYOUT OF THE CYCLOTRON

The test site cyclotron consists of a four sectors cyclotron, mounted with median plane in the vertical direction, Fig.1. The iron return yoke has a large empty area at the position corresponding to the cyclotron's valley to allow easy access at the median plane. In Fig. 1 the main sizes of the cyclotron iron are shown. The cyclotron main features are presented in Table 1, in particular the different settings for acceleration of ions with q/A=0.5 and protons are also presented. To achieve the isochronous magnetic field, we use a double pair of coils mounted one on the other. The coil shown in Fig. 1 consists of a main coil and a second small coil that are fed independently. The two coils can be fed with current flowing in the same direction or opposite direction just to fit the isochronous magnetic

ISBN 978-3-95450-128-1

THE CYCLOTRON COMPLEX FOR THE DAEDALUS EXPERIMENT

A. Calanna[1], D. Campo[1] ,J. M. Conrad, MIT, Boston, USA
L. Calabretta, INFN-LNS, Catania, Italy, F. Meot, M. Tahar Haj, BNL, Upton, USA

Abstract

The cyclotron complex for the DAEδALUS CP-violation neutrino experiment consists of a compact cyclotron able to accelerate high-current (5 electrical milliamps) H_2^+ beams up to an energy of 60 MeV/amu, cleanly extract this beam with two electrostatic deflectors, and transport it to a superconducting ring cyclotron (D-SRC) able to accelerate the beam up to 800 MeV/amu. H_2^+ is dissociated with thin stripping foils for efficient extraction as protons then the beam impinges on a megawatt-class target for neutrino production. The D-SRC is similar in size and engineering concept to the SRC at RIKEN. Space-charge dominated beam dynamics simulations using OPAL have been performed for an eight-sector geometry, and indicate acceptable transmission and low beam losses. Subsequent engineering magnet-design studies [1] pointed to a six-sector configuration as more practical. Results of the studies conducted to date are presented.

INTRODUCTION

The goal of DAEδALUS is the search for a nonzero CP-violation parameter δ [2,3]. This experiment needs three neutrino sources produced by a proton beam with energy of about 800 MeV/amu. In this paper we discuss one of the DAEδALUS Superconducting Ring Cyclotrons, D-SRC, which has to be driven with a proton beam power of 1.6 MW. Further information on the scheme to produce decay-at-rest sources driven by such cyclotrons can be found in [2,3], as well as all constraints discussion, the R&D successes, including construction of a beam-line test-stand [4], and future plans.

Significant changes have been made to the previous eight-sector-design of the D-SRC [5], which did not allow four PSI-like RF cavities to be hosted. The new six-sector-design solves this problem. The new magnetic sector is described in this report, as well as evaluating the other solution, and the reasons that drove the DAEδALUS collaboration together with the Technology and Engineering Division (T&ED) of the MIT Plasma Science and Fusion group to the final choice. T&ED developed the magnet conceptual design to provide very preliminary cost estimates to fabricate a single magnet sector [1]. The conceptual design includes solid modelling and analyses for the conductor and winding pack design, high temperature superconductor and copper current leads for the magnet, structural design of the magnet cold mass, cryostat and warm-to-cold supports, cryogenic design of the magnet cooling system, and magnet power supply sizing. Injection system preliminary study is reported in [6].

[1] Present address: LNS-INFN, Catania, Italy

Here we present the features of the new design and the results of beam dynamics simulation achieved without space-charge effects.

THE SECTOR MAGNET EVOLUTION

In the design presented in [5] there were three major blocking points:

- the variable coil cross section, which could cause complications to the cooling system and the natural flow of the LHe. Moreover, arrangements with tilted coils are acceptable but add complexity to the wounding process;
- there wasn't enough room to host PSI-like RF cavities;
- the residual radial force was too high.

We studied two very different options. The first solution, option A, is an eight-sector machine, Fig. 1. The difference with [5] is based on the consideration that even if we have an eight-sector machine we don't need symmetry eight at energies below 400 MeV/amu. First, we shaped the iron to free the space up to radii smaller than 400 cm, and then we designed a new coil that has symmetry four at the lower radii and symmetry eight at the outer radii. The optimization process led us to reach almost the same precision in the field isochronism and for the vertical focusing (maybe a little bit better) than in the previous design.

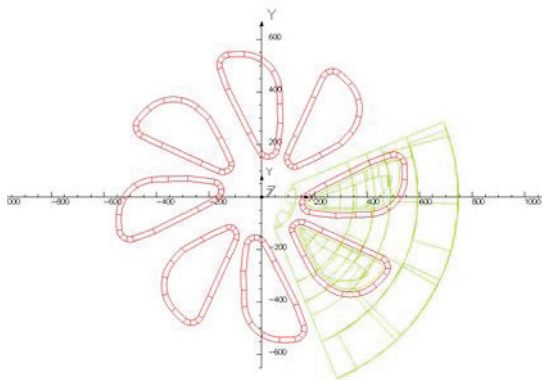

Figure 1: Option A layout.

Improvements are:

- we have four valleys in which the space between coils is 95 cm, large enough to install RF cavities;
- the current density has been decreased from 34A/mm^2 to 28.33 A/mm^2. We could stress again the current density parameter up to 34 A/mm^2 and adapt the coil. In this way we could gain more space for the cavities or the injection tools;
- cross-section is constant and it is 20x30 cm^2, without any negative curvature.

ISBN 978-3-95450-128-1

HIGH INTENSITY COMPACT CYCLOTRON FOR ISODAR EXPERIMENT

D. Campo, J. Alonso, W. Barletta, L. Bartoszek, A. Calanna, J. M. Conrad, M. Toups,
MIT, Cambridge, USA
L. Calabretta, G. Gallo, C. Tao, INFN-LNS, Catania, Italy
M. Shaevitz, Columbia University, New York, USA
A. Adelmann, PSI, Villigen, Switzerland
J. Yang, CIAE, Beijing, China
R. Gutierrez Martinez, L. Winslow, UCLA, Los Angeles, USA

Abstract

The scientific international community in recent years has focused an increasing interest on the neutrino properties. The aim of the IsoDAR (Isotope Decay At Rest) experiment is to look for the existence of sterile neutrinos. To perform this experiment, a cyclotron able to deliver proton beam current up to 10 mA is proposed. This cyclotron is very similar to the DAEδALUS injector cyclotron (DIC), but, due to the required higher average beam current and the experimental underground site, it poses a new ambitious goal in terms of technical solutions.

INTRODUCTION

The existence of the neutrino states beyond the "standard" 3ν paradigm was predicted to explain some anomalies that were experimentally observed. The IsoDAR experiment's aim is the observation of the "so-called" sterile neutrinos by studying the oscillation of electron antineutrinos [1, 2, 3].

In the IsoDAR experiment, the electron antineutrinos are produced by ^{8}Li decay. A high-current proton beam strikes a beryllium target in order to produce a high flux of neutrons. Moreover, the interaction between the neutrons and the ultra-pure ^{7}Li sleeve surrounding the target produce a lot of ^{8}Li. The target is ~15 meters from a kiloton-scale detector and the produced antineutrinos would oscillate into and out of the sterile state within the volume of the detector. It will be possible to observe this sinusoidal event rate, which is a function of the distance from the target.

The whole experimental setup has to be installed underground, inside KamLAND, so a compact cyclotron able to accelerate a 5 mA beam of H_2^+ molecules up to the final energy of 60 MeV/amu is an optimal solution.

The design of this accelerator arises from the DAEδALUS injector cyclotron [4], but it takes into account solutions for transport and assembly of the machine through the constricted access apertures of the Kamioka mine. Moreover, the required beam intensity is about six times higher than the maximum intensity delivered by the 30 MeV compact cyclotrons used in the medical isotope production centers. In particular, during the beam injection, the space-charge effects are a crucial issue. To mitigate this effect, we propose to inject an H_2^+ beam at an energy of 70 keV, which has a generalized perveance value comparable to the value of existing high-intensity proton commercial cyclotron. The test stand, installed by a collaboration between MIT, INFN-LNS, and Best Cyclotron Systems Inc. (BCSI) [5] at the BCSI laboratory in Vancouver, will produce useful information in order to verify the feasibility of the beam injection and to check the critical issue.

THE ISODAR CYCLOTRON

The IsoDAR cyclotron has the same magnetic circuit as the DIC, while the acceleration system and the central region are different in order to improve the high-intensity beam production. It is a four-sector machine, with a pole radius of 220 cm and a large vertical gap of 10 cm; the hill angular width is 25.5° in the central region and increases up to 36.5° in the extraction region. A couple of coils at room temperature complete the system. Each coil has an inner radius of 223 cm and a size of 200 x 250 mm^2; the current density is 3.167 A/mm^2. The average magnetic field varies between 1.05 ÷ 1.2 Tesla, while the minimum and maximum values are 0.28 Tesla in the valley and 2.11 Tesla in the hill. The outer part of the pole has a special design to allow the ν_r=1 resonance crossing at the end of the acceleration. Introducing a small off-center in the beam orbit, the first harmonic precession produces a growing of the inter-turns orbit separation at the extraction region. A large inter-turn separation is mandatory to achieve an extraction efficiency of 100% using electrostatic deflectors.

Four RF double-gap cavities are placed in the four magnet valleys. The design of the λ/2 cavities allows production of an accelerating voltage that rises from 70 kV at the inner radii to 250 kV at the outer radius. A main difference of the IsoDAR cyclotron with respect to the DIC is the harmonic operation mode, harmonic 4th and 6th, respectively. Using a lower harmonic mode will allow improvements to the beam capture in the injection region and achievement of the required high-intensity transmission. Moreover, the thermal power losses of the cavities will be a little lower. Another huge difference vs. the DIC is the duty cycle: the IsoDAR cyclotron will work in continuous-wave mode, while the duty cycle of the DIC is only 20%. The higher beam power poses a serious constraint on the amount of the beam losses.

ISBN 978-3-95450-128-1

HIGH INTENSITY BEAM STUDIES USING THE KURRI FFAGS

C.T. Rogers, S.L. Sheehy, C. Gabor, D.J. Kelliher, S. Machida*, C.R. Prior
STFC/RAL/ASTeC, Harwell Oxford, United Kingdom
Y. Ishi, J-B. Lagrange, Y. Mori, T. Uesugi
KURRI, Kyoto, Japan

Abstract

Increasing the repetition rate of FFAG accelerators is one way of obtaining high average beam current. However, in order to achieve beam powers of up to 10 MW for applications like ADSR, the number of particles per bunch in an FFAG has to be approximately the same as in a high power synchrotron. Collective effects such as space charge then become crucial issues. To understand high current beam behaviour in FFAGs, an international collaboration has been established to carry out an experimental programme using the FFAGs at Kyoto University's Research Reactor Institute, KURRI. The goal is to demonstrate acceleration of high bunch charge and identify the fundamental limitations. In this paper, we will show simulation results toward the first beam experiment which is planned towards the end of 2013.

KURRI FFAGS

Kyoto University Research Reactor Institute currently has two scaling FFAGs of interest, which we refer to as the ADSR-FFAG and ERIT-FFAG. The former is a 150 MeV proton driver for a test reactor where basic ADSR concepts can be examined. The latter is a 11 MeV demonstrator of neutron production using an internal target which is also used for ionisation cooling. Both FFAGs have been successfully commissioned and have achieved their initial goals. The experiments discussed may be performed on either machine depending on their availability.

For illustration, this paper will mostly discuss ERIT-FFAG. This machine can be injected with up to 6×10^{11} particles per pulse, equivalent to a Laslett tune shift for a uniform beam of -0.25 assuming a bunching factor of 0.25 and 100% unnormalised emittance of 100π mm mrad. The accelerator parameters for ERIT-FFAG are listed in Table 1.

Table 1: General Parameters of the ERIT-FFAG

Parameter	Value
Mean radius	2.35 [m]
Sectors	8
Max. B field	0.9 [T]
Field index, k	1.92
FD radio	3
Horiz. tune, Vert. tune	1.74, 2.22
Horiz./Vert. acceptance	7000/2000 [π.mm.mrad]
Rev. frequency	3.01 [MHz]
RF voltage	200 [kV]
Harmonic number	6

PROPOSED EXPERIMENT

The purpose of the proposed experiment is to verify three specific aspects of high intensity beam behaviour in FFAG accelerators. Firstly, whether FFAGs face the same challenges in terms of space charge tune shift as synchrotrons. Secondly, whether we can keep a large ratio of beam size to aperture to accommodate more particles. Thirdly, whether beam intensity may affect ionisation cooling.

In scaling FFAGs, magnet nonlinearities are not perturbations but essential ingredients in helping to maintain zero chromaticity and a scaling orbit. Compared to synchrotron nonlinearities, those in scaling FFAGs are relatively strong. In addition, magnet misalignments excite harmonic components beyond the ideal lattice periodicity, and therefore lead to non-systematic resonances. Denser resonance lines in tune space may limit the maximum tune shift/spread more strongly than in a synchrotron.

In an FFAG the orbit moves radially outward throughout acceleration like in a cyclotron. The horizontal acceptance is much larger than the vertical. Enlarging the beam emittance in the horizontal plane at injection is one way to suppress space charge tune shift/spread. However, this is only possible if there is no coupling between the horizontal and vertical planes so that the vertical beam size does not get larger.

Finally, experiments on ERIT-FFAG have demonstrated the use of ionisation energy loss to suppress emittance growth from an internal Beryllium foil. The presence of collective effects in passage of charged particles through material, which may be an issue for ionisation cooling systems, could also be addressed experimentally at KURRI.

Diagnostics

Relevant experimental measurements will rely on two kinds of diagnostics available in the KURRI FFAGs: beam position monitors using probes or electro-static plates; and beam size measuring devices using collimators combined with beam current monitors.

The beam position at all locations in the FFAG can be obtained by installing available beam position monitors sequentially, assuming the orbit is not affected by the probes. This method would allow for comprehensive position mon-

* shinji.machida@stfc.ac.uk

ISBN 978-3-95450-128-1

DEVELOPMENT OF NEW COMBINED SYSTEM FOR PRODUCTION OF FDG AND NaF RADIOPHARMACEUTICALS

F. Dehghan, S. Jaloo, H. Afarideh*, Department of Energy Engineering and Physics,
Amirkabir University of Technology, Tehran, 15875-4413, Iran
M. Ghergherehchi, J. S. Chai, WCU Department of Energy Science/School of Information & Communication Engineering, Sungkyunkwan University, Suwon 440-746, Korea
M. Akhlaghi, Research center for Nuclear Medicine,
Tehran University of Medical Sciences, Tehran, 14117-13137, Iran

Abstract

In this work, we present a new combined system which produces FDG and NaF in separate runs. The needed ^{18}F for synthesis these radiopharmaceuticals are obtained by bombardment of highly enriched water (H_2O_{18}) with proton. The aim is development of routine systems to use with baby cyclotrons. In this study, the various chemical steps and required reagents as well as different reagent delivery methods has been investigated. This evaluation has been done with purpose of optimizing the performance of a conceptually simple device integrated into a fully automated synthesis procedure for radiosynthesis of FDG and NaF. In this system, we have used AVR microcontroller to control the process and LabVIEW software for monitoring the operation of system. Furthermore, Geiger Muller counters have been used to determine the activity to insure the accuracy of the systems operation.

Keywords: FDG and NaF radiopharmaceutical, AVR microcontroller, LabVIEW, Geiger Muller counter, highly enriched water.

INTRODUCTION

^{18}F-FDG is the most important radiopharmaceutical used in oncology for early diagnosis of cancers and for assessing response to therapy. But ^{18}F-FDG has known limitations in detecting blastic malignant skeletal lesions. The initial staging of patients diagnosed with certain cancers includes imaging with ^{18}F-FDG PET and ^{99m}Tc-methylenediphosphonate (^{99m}Tc-MDP) bone scintigraphy as separate studies. ^{99m}Tc-MDP bone scintigraphy is the method of choice for evaluation of osseous metastases, since it allows a whole-body survey at a relatively low cost.

^{99m}Tc-MDP conventional planar image have limitations related to spatial resolution and lack of specificity. However, recently the combined technology like PET-CT is used to better localizing the diagnosed cancer. Since all nuclear medicine centers are not equipped with PET-CT and/or they intend evaluate the possible bone metastasis while assessing response to therapy, the use of ^{18}F-NaF PET is considered as a suitable radiopharmaceutical for PET bone scans which has been approved by the Federal Drug Administration in February 2011. In several studies the role and efficiency of the combined ^{18}F-FDG/^{18}F-NaF PET/CT for detection of malignancy was compared to ^{18}F-FDG PET/CT and showed that the sensitivity for detection of osseous lesions or skeletal disease was increased compared to the separate ^{18}F-FDG PET/CT scans. So the simultaneous availability of ^{18}F-FDG and ^{18}F-NaF are important for PET centers. The commercially available synthesis modules like Simians EXPLORA FDG[4], GE-FDG-MX, GE-FDG-FX or GE-FDG FastLab have limitation to produce ^{18}F-NaF. So this radiopharmaceutical should be produced manually or by using a separate available kit-based module or a homemade one [1-3].

In this project we decide to design a synthesis module with capability of producing of both ^{18}F-FDG and ^{18}F-NaF by one time load to produce them in the same day.

MATERIALS AND METHODS

In order to designing and construction of an automated synthesis module, considering of following points are necessary.

Hardware

The set up of the apparatus is shown schematically in Fig. 1. Part (a) and part (b) are relevant to producing ^{18}F-NaF and ^{18}F-FDG respectively. Manipulation of all reagent solutions and solvents is performed by a vacuum and pressure of auxiliary gas (helium).

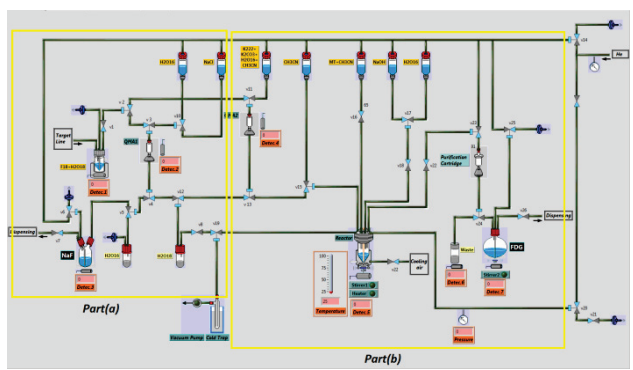

Figure 1: Schematic of the automated system for synthesis of ^{18}F-NaF (Part (a)) and ^{18}F-FDG (Part (b)).

Since the labeling of [^{18}F] fluoride onto Mannose Triflate (fluorination) is occurred at the reaction vessel, so this vessel is an important portion in a module. Therefor designed reactor must be covering several properties like

*corresponding author: hafarideh@aut.ac.ir

^{62}ZN RADIOISOTOPE PRODUCTION BY CYCLOTRON

M. Ghergherehchi, J. S Chai*, SungKyunkwan University, Suwon, 440-746, South Korea
H. Afarideh, Amirkabir University of Technology, Tehran, 15875-4413, Iran

Abstract

Natural Cu target was irradiated with proton beam in the energy range of 15 to 30 MeV at a beam current of 100 μA for 15 min. In this irradiation radioisotope of 62Zn was produced as a generator and then decayed to ^{62}Cu radioisotope. The ^{62}Cu is emitting β+ and known as PET radioisotope. Excitation function of ^{62}Cu via ^{nat}Cu (p, 2n) ^{62}Zn, ^{62}Cu and ^{63}Cu (d, 3n) ^{62}Zn reactions were calculated using Alice and Talys codes and then were compared with the reported measurement by experimental data and ENDF-2013 data. Production yield versus target thickness were evaluated with attention to reaction cross section data obtained from Alice and Talys codes, and stopping power and range of protons in target materials using SRIM code. The production yield also examined experimentally and found that the optimum irradiation yield achieved to be 5.9 mci/μAh at protons of 100 μA current and 30MeV energy. A radiolabeling process also was performed using $^{62}Zncl_2$ and antitumor compound, Bleomycin (BLM) as a possible tumour imaging particle tracking.

INTRODUCTION

The short- lived generator produced β+ emitter ^{62}Cu (T= 9.7 min), has found application in blood flow studies in heart and brain using positron emission tomography (PET). This is of special interest for clinics having PET but no cyclotron. This radio isotope is obtained via the ^{62}Zn/^{62}Cu generator system, the parent ^{62}Zn (T=9.3h) being produced via the ^{63}Cu (p, 2n) process at medium-sized cyclotron [1]. Considering that cyclotron available for routine radioisotope productions accelerate particles of proton and very seldom deuteron that the maximum of proton's energy is 30 MeV and that of deuteron is 15 MeV and only the reaction resulting from proton and deuteron are accomplishable for generating zinc-62. Our irradiated target was natural copper and contains both ^{65}Cu and ^{63}Cu therefore, we'll analyse the reaction creating from ^{65}Cu and ^{63}Cu in this study. The aim of this work was the investigation of excitation function of ^{nat}Cu (p, 2n) ^{62}Zn→ ^{62}Cu and ^{63}Cu (d, 3n) ^{62}Zn reactions and their comparison with ENDF-2013 database.

The Alice/ Talys Code

The ALICE/ASH code is a modified and advanced version of the ALICE/91 code. This code has been written to study the interaction of intermediate energy nucleons and nuclei with target nuclei. The code calculates energy and angular distributions of particles emitted in nuclear reactions, residual nuclear yields, and total nonelastic cross-sections for nuclear reactions induced by particles and nuclei with energies up to 300 MeV. The parameters used in the ALICE/ASH code are as follow: (i) the Weisskopf–Ewing model for equilibrium calculations (ii) The hybrid model and geometry dependent hybrid model (GDH) for pre-equilibrium emissions [2]. TALYS aims to comprise important aspects such as physical quality, flexibility, robustness, completeness and efficiency into one software package [3].

Calculation of the Physical Yield and the Target Thickness

Theoretical physical yield can be calculated by the following equation:

$$Y = \frac{N_L \cdot H}{M} I(1-e^{-\lambda t}) \int_{E_1}^{E_2} \left(\frac{dE}{d(\rho x)}\right)^{-1} \sigma(E) dE \quad (1)$$

where Y is the product activity (in Bq) of the product, N_L is the Avogadro number, H is the isotope abundance of the target nuclide, M is the mass number of the target element, r (E) is the cross-section at energy E, I is the projectile current, dE/d (ρx) is the stopping power, λ is the decay constant of the product and t is the time of irradiation.

To achieve the optimum physical dimensions of the target such as the thickness, the SRIM codes [4] (the stopping and range of ions in matter); were accomplished. SRIM is a group of programs which calculate the stopping and range of ions (up to 2 GeV/amu) into matter using a quantum mechanical treatment of ion-atom collisions. This calculation is produced very efficient by the use of statistical algorithms which allow the ion to make jumps between calculated collisions and then averaging the collision results over the interfering gap.

The physical thickness of the target layer is chosen in such a way for a 90° geometry beam/target to ensure that the incident beam exits the target layer with a predicted energy; so the required thickness of the layer will be smaller with a coefficient 0.1.

ENDF-2013

The ENDF Evaluated Nuclear Data Formats are used all over the world to encode nuclear data evaluations for use in research and nuclear technology.

RESULT AND DISCUSSION

^{63}Cu (p,xn)^{63,62}Zn

Figure 1 show the excitation function obtained from the reaction of ^{63}Cu(p,xn)^{63,62}Zn .Considering this figure we'll find out that the cross section of ^{62}Zn generation, that is our desirable reaction is the best in the energy limit of 14 MeV to 30 MeV .This radioisotope isn't generated in the energy below than 14MeV and ^{63}Zn is one of our

ISBN 978-3-95450-128-1

RADIOCHROMIC FILM AS A DOSIMETRIC TOOL FOR LOW ENERGY PROTON BEAMS

S. Devic, Medical Physics Unit, McGill University, Montréal, Québec, Canada
S. Aldelaijan, Saudi Food and Drug Authority, Riyadh, Saudi Arabia
F. Alrumayan, M. Shehadeh, F. Alzorkani, and B. Moftah,
King Faisal Specialist Hospital and Research Centre, Riyadh, Kingdom of Saudi Arabia

Abstract

We tested EBT3 and HDV2 models of GAFCHROMIC™ films for dose measurements at low energy proton beam quality. Proton beam (CS30 Cyclotron at KFSHRC) has energy of 26.5 MeV and Bragg peak position at 6 mm depth. Beam output was calibrated using TRS-398 reference dosimetry protocol with calibrated ion-chamber in water and the film was calibrated in terms of dose to water by exposing calibration film pieces within a solid water phantom at depth of 3 mm. Pieces of EBT3 films were irradiated to doses of up to 10 Gy with both 4 MV photon and 26.5 MeV proton beams, while pieces of the HDV2 radiochromic films were irradiated to doses of up to 128 Gy in proton beam. Irradiated pieces of the EBT3 films were tested for activation using Germanium detector and by measuring and subsequently decomposing decay curve over a period of 40 minutes after irradiation.

EBT3 film model response was 3 times higher for 26.5 MeV proton than 4 MV photon beam quality, and when irradiated in proton beam the EBT3 film model was 24 times more sensitive than HDV2 film model. For the EBT3 film model we identified three proton-activation processes resulting in short-lived ^{15}O, ^{13}N, and ^{11}C radioisotopes. The EBT3 film model can be used for measurements for doses of up to 10 Gy using a green colour channel of the scanned images, while the red colour channel of the HDV2 scanned film images can be used for measurements of much higher doses.

INTRODUCTION

External radiotherapy proton beams commonly range in energies between 70 to 250 MeV and are produced using dedicated synchrotrons. Our institution, KFSH&RC, is in a possession of a CS-30 cyclotron which is a positive ion machine capable of accelerating four different particles: protons at 26 MeV, deuterons at 15 MeV, Helium-3 at 38 MeV and Helium-4 at 30 MeV. Accurate dosimetric characterization of a radiation field is crucial for its subsequent use in both research and clinical applications. As a part of our research project in adapting the CS-30 cyclotron for research irradiations (of cells and small animals) as well as intraoperative radiotherapy with protons (pIORT), we developed a radiochromic film based reference dosimetry system for 26 MeV proton beam.

Because of their ability to minimize beam perturbation effects caused by the presence of dosimeter body (i.e. such in ionization chambers), and because of their structure that match biological tissue in energy absorption and transfer properties, the use of tissue equivalent and energy independent radiochromic films became an interesting investigational path in proton beam dosimetry. Radiochromic film (RCF) [1,2] is a 2D high resolution dosimeter that is convenient for in vivo and in vitro dose measurements [3,4]. It has all advantages of conventional radiographic film systems without the need for wet processors, making this film type an important dosimetric tool. They can be cut in any arbitrary shape or size and can be handled in ambient light with much less detriment compared to radiographic film. In addition, they have properties equivalent to those of water and have been shown to have a response independent of beam quality in a relatively broad energy range including proton beams [5].

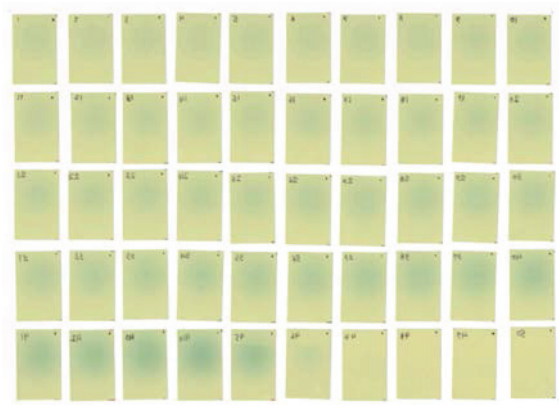

Figure 1: Pieces of HDV2 GAFCHROMIC™ film model stacked together within a plastic phantom in order to measure the per cent depth dose of the proton beam.

Relatively high dose rate of the CS-30 proton beam, which is characteristic of cyclotrons used for radiopharmaceutical production, requires use of a less sensitive radiochromic film model. The HD-V2 model GAFCROMIC™ film was introduced recently as a replacement of the previous HD-810 film model. It has a dynamic range between 10 – 1000 Gy and it was introduced for Gamma Knife and Stereotactic Radio Surgery (SRS) quality assurance and commissioning processes in addition to other industrial applications. It has a nominal thickness of 105 microns consisting of an 8 microns active layer and a 97 microns polyester substrate. The advancement over the HD-810 model is attributed to the addition of a yellow dye marker which is anticipated to correct for inhomogeneities arising from variation in the

ISBN 978-3-95450-128-1

CHARACTERIZATION OF THE CS30 CYCLOTRON AT KFSH&RC FOR RADIOTHERAPY APPLICATIONS

Belal Moftah, Faisal Alrumayan, Faisal Alzorkani, and Mamoun Shehadeh,
King Faisal Specialist Hospital and Research Centre, Riyadh, Kingdom of Saudi Arabia
Saad Aldelaijan, Saudi Food and Drug Authority, Riyadh, Saudi Arabia,
Slobodan Devic, Medical Physics Unit, McGill University, Montréal, Québec, Canada

Abstract

The 26.5 MeV beam of the CS30 Cyclotron at King Faisal Specialist Hospital and Research Centre (KFSH&RC) was characterized dosimetrically for the use in radiobiological experiments for pre-clinical and radiotherapy studies. Position of the beam's Bragg peak was measured with a stack of 100 pieces of HD-V2 model GAFCHROMIC®films (105 microns thick each). This film type was specifically designed for measurement of very high doses, ranging up to 1,000 Gy. The response of the film was calibrated in terms of dose to water by exposing calibration film pieces within a solid water phantom. Percentage depth dose (PDD) of the proton beam was measured using a calibrated parallel-plate chamber in water. The position of the Bragg peak was found to be at around 6 mm when 10 to 20 nA proton beam current was used. For beam profile measurements, pieces of GAFCHROMIC® EBT3 film were irradiated at 40, 70 and 100 cm from the primary collimator, where the Gaussian shaped beam profiles had values of 12, 26, 45 mm at FWHM, respectively. Proton beam characteristics in terms of the output and beam size appear to be acceptable for pre-clinical studies and radiotherapy applications.

INTRODUCTION

The use of protons in the field of radiation therapy has been growing in recent years due to the ability to localize their dose deposition with relatively low entrance and exit doses[1][2]. High cost of proton radiotherapy facilities is the limiting factor of spreading this modality. For radiopharmaceutical cyclotrons, another limitation is their low energy protons, which prevent them from treating deeply seated tumors. However, low energy radiopharmaceutical cyclotrons can still be utilized to treat superficial tumors as well as surgical beds [2].

The CS30 Cyclotron at KFSH&RC was built to produce positron emitters such as F-18 for positron emission tomography (PET) imaging. It is capable to accelerate four different particles at different energy levels. This facility has proton and neutron beam lines connected to experimental vaults and a gantry-based neutron treatment room. For this project, the cyclotron is used to accelerate proton beam up to 26.5 MeV for beam characterization and dose measurements on beamline 2. One unique goal of the current work is to adapt the CS30 cyclotron for intra-operative proton radiation therapy (IOpRT) technique.

MATERIALS AND METHODS

The CS30 Cyclotron at KFSHRC is a positive ion machine [3]. For beam characterization measurement, proton ions beam was used. Target stations are available on seven beamlines as well as on an internal target. For beam characterization measurements, beamline 2 was chosen due to its location in separate vault as shown in Fig. 1. This gives the flexibility to work on the beamline without interrupting the production of radiopharmaceuticals. Before beam current was sent externally to the target, the beamline was pumped down to 10^{-4} mbar using two means for vacuum pumps: the roughing pump and diffusion pump. The temperature of the water cooling system was ±10 °C.

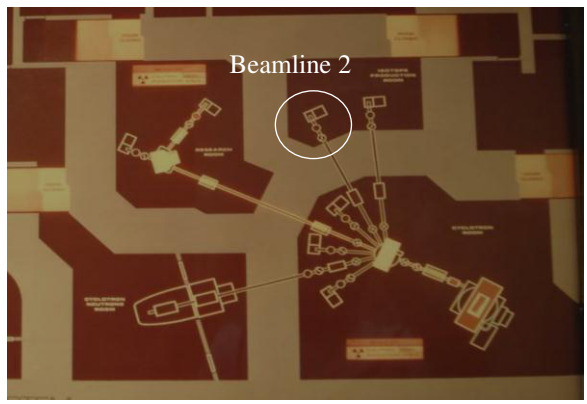

Figure 1: A general layout of the CS30 beamlines.

The CS30 cyclotron was used to deliver a beam current of 100 nA at 26.5 MeV for our measurements. Although the cold cathode internal ion source of the CS30 cyclotron, is quite reliable to deliver 100 µA internally and 20 µA externally, for these particular measurement, beam current needed is only 100 nA. Therefore, in order to have better control on the beam intensity and reach high stability level at such low current, few parameters were taken into consideration during the measurements.

ISBN 978-3-95450-128-1

PROTON THERAPY AT THE INSTITUT CURIE – CPO: OPERATION OF AN IBA C235 CYCLOTRON LOOKING FORWARD SCANNING TECHNIQUES

A. Patriarca, S. Meyroneinc, Institut Curie – CPO, Orsay, France

Abstract

Since 1991, more than 6100 patients (mainly eye and head&neck tumours) were treated at the Institut Curie – Centre de Protonthèrapie d'Orsay (IC – CPO) using Single Scattering and Double Scattering (DS) proton beam delivery technique. After 19 years of activity, a 200 MeV synchrocyclotron has been shut down and replaced by a 230 MeV C235 IBA proton cyclotron. This delivers beam to two passive fixed treatment rooms and to one universal nozzle equipped gantry (DS, Uniform Scanning – US, Pencil Beam Scanning – PBS). In the past two years of operation more than 95.5% of the scheduled patients (near 500/year) were treated without being postponed. According to IBA recommendations, we have realized preventive maintenance and we have improved some diagnostic tools allowing us to reduce the number of downtime events from 499 in 2011 to 351 in 2012 [1]. In order to enhance cancer treatment capabilities we are now involved in the transition towards scanning particle therapy, requiring even more accurate quality assurance protocols. We describe here the main cyclotron issues looking forward the scanning technique, the main goal being the progress of our reliability performances.

ACCELERATOR OPERATION

More than 900 patients have been treated with the IBA C235 cyclotron from its commissioning in July 2010 until now (see Fig. 1). During the 51 weeks per year scheduled for the therapy, the day average activity is near 12 hours, so that the accelerator operation is in an almost two-shift mode. During the week night the machine is idle and over the week-end all is shut down. An on call system is activated every time the clinical activity ends.

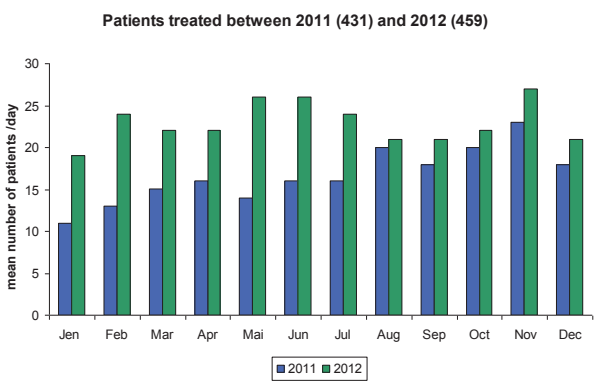

Figure 1: Patients treated (average per day) with the C235.

The beam delivery technique used to distribute the dose over the tumour volume is the passive spreading. This choice was motivated by the previous treatment experience of the centre coupled to the need to ensure a clinical break as short as possible between the shutdown of the existing synchrocyclotron and the start up of the new cyclotron. Actually we were able to start again the treatments a month after the shutdown.

Thanks to the change in the machine we have increase our uptime from 92% in 2009 to 95.9% in 2012. This is still improving as we are probably in the "early life failures period" of the equipment according to the Weibull model [2]. In order to reduce the number of possible issues, we perform regular maintenance interventions together with the local IBA team (3 engineers). The main guidelines in the servicing of the accelerators and ancillaries are discussed in the paper.

MAINTENANCE

We have from two to four hours per week for regular servicing as changing the ion source, servicing some power supplies units or fixing some beam line or treatment room issues. If this is not possible during this scheduled week time, we have also dedicated Saturdays or 1.5 days each 3 months. But the main maintenance is once a year when we open the cyclotron and the activity is off during one week.

In order to define priorities in the maintenance planning, IBA has a list of 256 procedures where the periodicity is well defined. Additional checks on the cyclotron operation are monthly performed by the IC – CPO team. Here we find some examples:

- Cyclotron efficiency (around 45%) via radial track (see Fig.2)
- Main Coil pancakes resistance
- Cooling (Main Coil and general)
- Water resistivity
- Vacuum
- Extraction system (deflector leakage current)
- Radio Frequency system (amplifiers efficiency and lifetime)

Nevertheless, even if we try to anticipate, we have experienced some critical failures affecting the clinical activity. We describe now a few preventive and curative interventions that we have made.

ISBN 978-3-95450-128-1

PERFORMANCE OF IBA NEW CONICAL SHAPED NIOBIUM [^{18}O] WATER TARGETS

F. Devillet*, J.-M. Geets, M. Ghyoot, E. Kral, O. Michaux, B. Nactergal, V. Nuttens,
IBA RadioPharma Solutions, Louvain-la-Neuve, Belgium
J. Courtyn, IBA Molecular Europe, Paris, France
R. Mooij, L. Perk, BV Cyclotron VU, Vrije Universiteit, Amsterdam, The Netherlands

Abstract

Background: Because of an ever increasing demand for Fluoride-18 ($^{18}F^-$), efforts are made to increase the performance of the ^{18}F-target systems. Moreover, given the particularly high cost of ^{18}O enriched water, only a small volume of this target material, at the very most a few milliliters, is desired.

Procedure: Four conical shaped targets with different target chamber sizes (Conical 6 – 2.4 ml; Conical 8 – 3.4 ml; Conical 12 – 5 ml; Conical 16 – 7 ml) were tested using IBA Cyclone® 18 MeV cyclotrons. The insert volumes of the new Conical targets are identical to the cylindrical insert volumes: LV – Conical 6; XL – Conical 8; 2XL – Conical 12; 3XL – Conical 16. Fluoride-18 saturation activity yields and pressure curves were completed. Radionuclidic impurities were measured, even if the new target is using the same principle of Niobium body [1] with Havar® window.

NEW TARGET DESIGN

When designing this new conical shaped Niobium insert (Figure 1), the objectives were multiple:

- reduce the enriched water volume;
- improve the cooling of this insert;
- increase the produced activity;
- reduce and improve auxiliary parts.

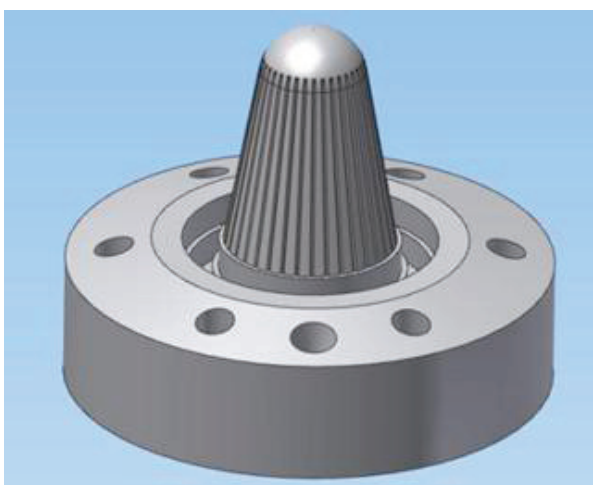

Figure 1: New conical shaped Niobium insert [2].

The cooling has been improved thanks to the drilled channels on the outside of the insert chamber. Another deep channel has been foreseen to be able to cool the beam strike area next to the target window (Figure 2, green circle).

Maintenance has been simplified by using less pieces and o-rings. The insertion of the flow lines is now done directly inside the Niobium (Figure 2, blue circle). This solution improves the purity of the ^{18}F-Fluoride, because there is no contact between the product and small o-rings as it was the case with the old cylindrical design (Figure 3, red circle). The maintenance interval is expected to be longer.

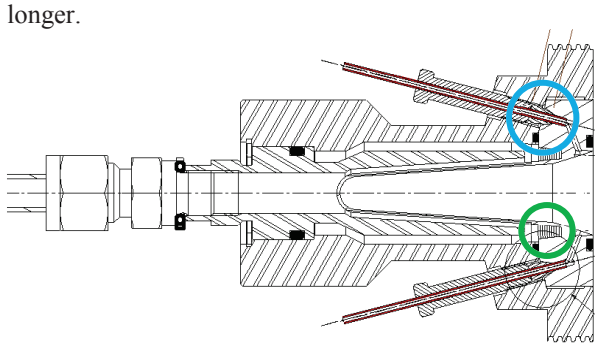

Figure 2: New conical design.

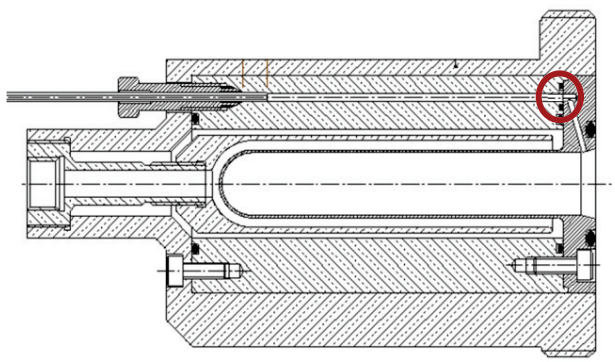

Figure 3: Old cylindrical design.

Another benefit of this new design is the target weight. It is now much lighter and avoids the target misalignment with the beam that was at the origin of many target and synthesis yield problems. A handle has been added to make the target manipulation easier (Figure 4).

Compared to the cylindrical design, this conical shape allows sending the [^{18}O]-water back to the beam strike area, and when emptying the target at the end of the shot, the water flows naturally to the transfer line making the remaining activity inside the target as low as possible.

* Fabienne.devillet@iba-group.com

ISBN 978-3-95450-128-1

EXPERIMENTAL STUDY OF RESONANCE CROSSING WITH A PAUL TRAP

H. Sugimoto, KEK, Ibaraki, Japan

Abstract

The resonant instability of charged particle beams during betatron resonance crossing is systematically investigated by both an experimental and a numerical approach. The present experiment is based on the fact that charged particle beams observed from its rest frame are almost equivalent to single-species plasmas confined in a plasma trap system. Tune excursion in a Non-Scaling Fixed-Field Alternating Gradient (NS-FFAG) accelerator with many identical FODO cells is emulated by ramping the plasma confinement force. It is experimentally and numerically confirmed that the resonance crossing is not harmful as long as the crossing speed is sufficiently high. We also address that a linear coherent stop band around quarter-half integers severely limits the machine performance at high-density beams. This band exists even without machine imperfection, thus the performance of NS-FFAGs is restricted as in high-power synchrotron accelerators.

INTRODUCTION

NS-FFAG [1] accelerators are expected to be a candidate for use in muon acceleration, as well as for medical purposes based on carbon and proton hadron therapy owing to their possibility of high repetition rate. One of the fundamental subjects in NS-FFAG is resonance crossing. The beam orbit and optics in NS-FFAG is widely varied during acceleration because guiding and focusing forces felt by the beam depend on the beam energy. Consequently, the beam transverses a few or more resonances before extraction and the resonance crossing may lead to serious beam losses or degradation of beam quality. Past theoretical and numerical studies suggest that emittance growth is negligible or tolerable when the crossing speed is sufficiently high [2].

In this study, we carry out systematic experiments on betatron resonance crossing without using any accelerators, but using a novel experimental tool named "S-POD (Simulator for Particle Orbit Dynamics)" developed at the Beam Physics Laboratory at Hiroshima University. S-POD is based on the physical equivalence between non-neutral plasmas in a plasma trap and charged particle beams propagating a linear focusing channel [3]. Particle-in-Cell (PIC) simulation corresponding to this experiment is also conducted. Based on a large number of experimental and numerical observations, we discuss the fundamental feature of resonance crossing including space-charge-driven resonances.

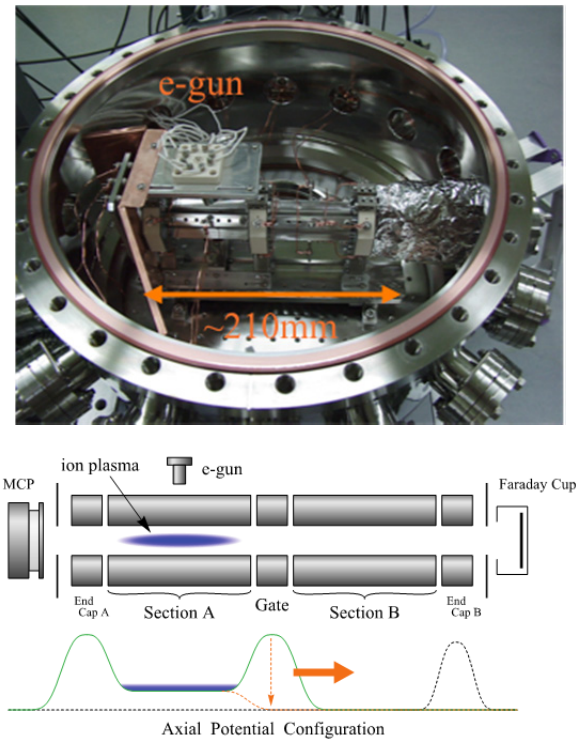

Figure 1: The linear Paul trap developed at the Hiroshima University and its schematic.

S-POD

Principle

Figure 1 shows the S-POD apparatus employed for the present experiment. S-POD is basically a linear Paul trap (LPT) system, and composed of five quadrupole-electrode sections. For the present experiment, ions are confined within the Section A as indicated in the lower panel of Fig.1. Similar to conventional LPTs, the plasma confinement in transverse (x- and y-) direction is achieved by an applied radio-frequency (rf) electric field with quadrupole symmetry. Static voltages are also applied to these electrodes to form a potential barrier for the longitudinal plasma confinement. Since the aperture size (5mm in radius) is much shorter than the longitudinal dimension of the confinement region (75mm), the potential barrier is square-well-like rather than harmonic. It is thus reasonably expected that the plasma is an infinitely long charge column along the longitudinal direction. This fact enables us to focus on betatron beam dynamics in the present study.

ISBN 978-3-95450-128-1

IMPROVEMENT OF THE CURRENT STABILITY FROM THE TRIUMF CYCLOTRON*

T. Planche, Y.-N. Rao, R. Baartman, TRIUMF, Vancouver, BC, Canada

Abstract

The $\nu_r = 3/2$ resonance, driven by the third harmonic of the magnetic gradient errors, causes modulation of the radial beam density in the TRIUMF cyclotron. Since extraction is by H^- stripping, this modulation induces unwanted fluctuations of the current split between the two high-energy beam lines. To compensate field imperfections, the cyclotron has sets of harmonic correction coils at different radii, each set constituted of 6 pairs of coils placed in a 6-fold symmetrical manner. The 6-fold symmetry of this layout cannot create a third harmonic of arbitrary phase, and so a single set of harmonic coils cannot provide a full correction of third harmonic errors driving the $\nu_r = 3/2$ resonance. However, the outermost two sets of harmonic correction coils are azimuthally displaced. We took advantage of this fact to achieve a full correction of the resonance. This greatly reduces rapid fluctuations of the beam current in the high-energy beam lines.

An active feedback system has also been implemented to compensate for the slow fluctuations ($\sim$ 1 minute range and above). This feedback acts on the amplitude of the first harmonic B_z correction produced by the outtermost set of harmonic coils. A proper choice of the phase of this first harmonic correction allows us to affect the split ratio, without changing the energy of the extracted beams.

INTRODUCTION

A large part of the results presented in this paper have already been reported in the proceedings of an earlier conference [1].

The TRIUMF cyclotron accelerates H^- ions, which enables the use of charge exchange extraction. To extract beam to several high-energy (480 MeV) beam lines simultaneously, stripping foils are inserted at azimuths differing by 60°, at almost the same radius. Each foil takes part of the beam, converting H^- ions into protons for extraction. The fraction of beam taken by each foil depends on the radial density of the beam. Any fluctuation of the radial beam density in the region of a foil will cause variations of the current extracted to each individual beam line.

Such fluctuations are observed in the TRIUMF cyclotron, where variations of radial beam density in the high-energy region lead to undesirable fluctuations of the beam current split between beam line 1A and 2A. The main source of these fluctuations is related to the crossing of the 3/2 half-integer resonance.

*TRIUMF receives federal funding via a contribution agreement through the National Research Council of Canada.

MECHANISM DRIVING CURRENT INSTABILITIES

The horizontal tune crosses the half-integer value 3/2 around 428 MeV, as shown on Fig. 1. For reference, the relation between energy and average beam radius is also given in this figure. As discussed in [2], since the 6-fold symmetry of the TRIUMF cyclotron is imperfect, there exists in that region enough third harmonic field error to drive this resonance. After crossing the resonance the ellipse occupied by the beam in the horizontal phase becomes mismatched, and begins to rotate at the frequency ($\nu_r - 3/2$) [3]. This precession of the horizontal phase space induces oscillations of the radial beam density, as shown in Fig. 2.

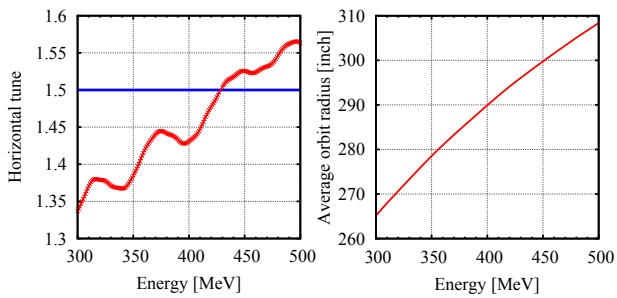

Figure 1: Left: horizontal tune variation with energy in the TRIUMF cyclotron. Right: average closed orbit position with energy. Results were obtained from simulation (using CYCLOPS [4]).

These oscillations could also be measured using one of the radially moving probes equipped with two diaphragms, shadowing each other, and displaced radially by 0.762 mm. Examples of measurement results are presented in Fig. 3. One can see on this figure a current density modulation starting around 428 MeV (~296 inch) and propagating all the way to 480 MeV (~305 inch).

If all cyclotron parameters are fixed, these radial oscillations are fixed in radius and so they cannot be the cause of the fluctuation with time of the split ratio between extraction lines 1A and 2A. But as is clear from Fig. 3, even a slight fluctuation in rf voltage can cause a large change in radial density at the location of the foil, making the split ratio between high-energy beam lines unnecessarily sensitive to the accelerating voltage. To stabilize the energy gain per turn to the required level ($\ll 0.1\%$) is very difficult since the TRIUMF resonator system is itself mechanically unstable, suffering 5 Hz oscillations driven by turbulence in the cooling water. Thus, to get rid of the fluctuations in extracted current, it is necessary to correct the field harmonics driving the 3/2 resonance.

ISBN 978-3-95450-128-1

SPACE CHARGE COMPENSATION MEASUREMENTS IN THE INJECTOR BEAM LINES OF THE NSCL COUPLED CYCLOTRON FACILITY*

Daniel Winklehner#, Daniela Leitner, Guillaume Machicoane, Dallas Cole, Larry Tobos,
NSCL, East Lansing, MI, 48824, USA

Abstract

In this contribution we report on measurements of space charge compensation (alternatively called "neutralization" here) in one of the injector beam lines of the Coupled Cyclotron Facility (CCF) at the National Superconducting Cyclotron Laboratory (NSCL) using a retarding field analyzer (RFA). The beams were produced by the superconducting electron cyclotron resonance ion source (ECRIS) SuSI. The measured neutralization values were between 0% and 60% and agreed reasonably well with a theoretical prediction using an adaptation of the formula presented by Gabovich et al. [1]. A dependence on beam intensity, radius and pressure could be observed.

INTRODUCTION

Space charge compensation is a well-known phenomenon for high current injector beam lines. For beam lines using mostly magnetic focusing elements and for pressures above 10^{-6} Torr, compensation up to 98% has been observed [2]. However, due to the low pressures required for the efficient transport of high charge state ions, ion beams in ECR injector lines are typically only partly neutralized and space charge effects are present. Current state-of-the-art Electron Cyclotron Resonance Ion Sources (ECRIS) are able to produce many emA of total extracted beam and several hundred eμA in a single species. Thus, realistic beam transport simulations, which are important to meet the acceptance criteria of subsequent accelerator systems, have to include non-linear effects from space charge, but also space charge compensation. In general, the self-electric field of the beam arising from the space charge of the collective of beam particles acts as a defocusing field on the beam.

Space Charge Compensation

Space charge compensation (for positively charged ions) takes place when slow electrons created by the interaction of the beam ions with the residual gas of the beam line accumulate inside the beam envelope (attracted by the positive space charge potential of the beam), thereby lowering the effective potential. The two main processes contributing to the creation of secondary ions and electrons are charge-exchange and ionization. To first order, electrons are created only through ionization. In both cases, slow secondary ions are created which are expelled by the beam potential. By measuring the energy distribution of these secondary ions, the beam potential can be found. By comparison the measured value with the calculated potential of an uncompensated beam, the neutralization factor f_e can be derived.

*Work supported by the National Science Foundation
#winklehner@nscl.msu.edu

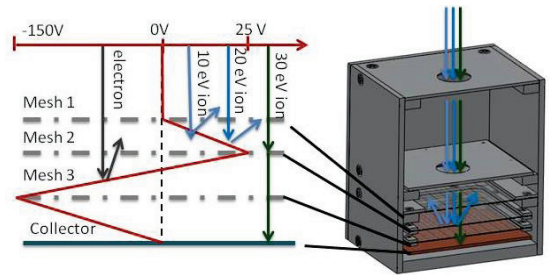

Figure 1: 3D CAD model of the RFA is shown on the right. The picture on the left depicts the working principle of the RFA. The retarding grid is biased at 25 V, the electron suppressor is biased at -150 V. Two 5 mm diameter apertures collimate the incoming secondary ions.

Theoretical Prediction

Following the derivation in [1], the potential difference between the beam center and beam edge ($\Delta\phi = \phi_{center} - \phi_{edge}$) for a compensated beam can be expressed in SI units as:

$$(\Delta\phi)^2 = 3\mathcal{L}\left(\frac{M}{m_e}\right)\left(\frac{\varphi_i}{V_0}\right)\frac{n_b q e^2}{(4\pi\varepsilon_0)^2}\left(\frac{q}{n_g\sigma_e}+\frac{v_b\sigma_i r_b}{2v_i\sigma_e}\right) \quad (1)$$

with $\mathcal{L}$ a Coulomb logarithm, M the beam ion mass, φ_i the gas ionization potential, V_0 the source voltage, v_i the plasma ion velocity, n_b the ion beam density, n_g the residual gas density, σ_i the total ion production cross-section, σ_e the electron production cross-section, and r_b the ion beam radius. From this, f_e can be calculated using:

$$f_e = 1 - \frac{\Delta\phi}{\Delta\phi_{full}} \quad (2) \quad \text{where:} \quad \Delta\phi_{full} = \frac{I}{4\pi\cdot\varepsilon_0\cdot\beta c} \quad (3)$$

with $\Delta\phi_{full}$ the full potential drop in an uncompensated beam, ε_0 the vacuum permittivity and βc the beam velocity. The theoretical predictions presented here are using an adaptation of this model for lower neutralization by replacing the quasi-neutrality of the beam plasma (beam ions + secondary ions = e^-) with a simple non-neutral condition for the electron density [3], changing Eq. 2:

$$f_e = 1 - \sqrt{f_e}\cdot\frac{\Delta\phi}{\Delta\phi_{full}} \quad (4)$$

MEASUREMENT SETUP

Retarding Field Analyzer (RFA)

The RFA used in this work is a three grid device with a two aperture collimation system at the entrance. Both apertures have a diameter of 10 mm. The three grids are highly transparent (90%) copper meshes (with a combined theoretical transparency of ~73%). A CAD model of the RFA is shown in Fig. 1, as well as a cartoon of the working principle. The three meshes are

ISBN 978-3-95450-128-1

TRANSMISSION OF HEAVY ION BEAMS IN THE AGOR CYCLOTRON*

A. Sen †, M.A. Hofstee, M.J. van Goethem, S. Brandenburg
Kernfysisch Versneller Instituut, Rijksuniverseteit Groningen
Zernikelaan 25, 9747 AA Groningen, The Netherlands

Abstract

During the acceleration of intense low energy heavy ion beams in the AGOR cyclotron feedback between beam intensity and pressure, driven by beam loss induced desorption, is observed. This feedback leads to an increase in the pressure in the cyclotron and limits the attainable beam intensity. Calculations and measurements of the pressure dependent transmission for different beams agree reasonably well. Calculation of the trajectories of ions after a charge change shows that the desorption is mainly due to ions with near extraction energies, hitting the outer wall at a shallow angle of incidence. For heavy ions like $^{206}Pb^{27+}$ several charge changes are needed before the orbit becomes unstable. Our calculations indicate that these ions make thousands of turns before finally hitting the wall. Ion induced desorption for relevant ions and materials has been measured; it explains the observations in the cyclotron semi-quantitatively.

INTRODUCTION

The experiments in the framework of the TRIμP program at the KVI required the AGOR cyclotron to produce a wide range of high intensity heavy ion beams, for example ^{206}Pb at 8 MeV/amu and ^{20}Ne at 23.3 MeV/amu. Since issues related with the acceleration of high intensity beams of in particular heavy ions at low energy (e.g. ^{208}Pb at 8 MeV/amu) have not been addressed in the design of AGOR, an upgrade program was initiated which included an investigation of beam transmission of heavy ions at low energies. Experiments showed that the transmission strongly depends on injected beam intensity, which was varied over a few orders of magnitude, with a substantial decrease in transmission at higher injected intensities,and an increase in pressure.

During acceleration beam particles collide with the rest gas atoms leading to beamloss. The observed pressure rise is caused by desorption due to the lost ions which deposit their energy on the walls of the cyclotron vacuum chamber and liberate materials. A positive feedback is created between the pressure rise and beamloss. In this paper we investigate the various components of the beam loss cycle individually, to determine their contribution to the reduced beam transmission.

* This work has been financially supported by the Foundation FOM, the Dutch funding agency NWO and the EU-FP7, Grant Agreement n 262010 - ENSAR.

† sen@triumf.ca

TRANSMISSION AT LOW INTENSITIES

At low intensities the majority of the vacuum induced beamlosses come from charge changing collisions with the restgas in the cyclotron. The number of beam particles lost depend on the cross-section of interaction, the pathlength of the beam particle and the local density of the rest gas.

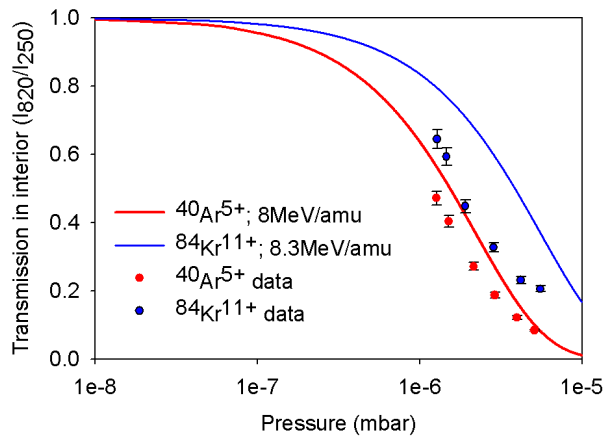

Figure 1: Transmission of $^{84}Kr^{11+}$ and $^{40}Ar^{5+}$ at 8 MeV/amu, comparison of simulations with experimental results.

There are several semi-empirical models which predict the cross sections of ion-atom collisions ([1] and [2]) as a function of the beam energy. Using these semi-empirical models for the cross section, the total transmission is estimated for beams accelerated in the AGOR cyclotron. We compare these calculations to transmission measurements as shown in Figure 1.

We define the transmission as the ratio of the beam current at a radius 820 mm,maximum radius where the read out is not affected by probe efficiency, to the beam current at radius 250 mm. Qualitatively both simulations and experiments show the same exponential dependence on the pressure inside the cyclotron. The overestimation we observe for the calculated values is due to systematic errors in both the pressure measurements and the calculated cross-sections [3].

ORBIT DYNAMICS

Charge changed particles are not accelerated anymore along with the rest of the beam particles due to a change in their charge over mass ratio. Under the influence of the magnetic field, these particles circulate in the cyclotron along a complex trajectory until they eventually, possibly

ISBN 978-3-95450-128-1

TRACKING IN A CYCLOTRON WITH GEANT4

F.W. Jones, T. Planche and Y.-N. Rao,
TRIUMF*, 4004 Wesbrook Mall, Vancouver V6T 2A3, Canada

Abstract

The tracking and simulation toolkit Geant4 [1] has been conceived and realised in a very general fashion, with careful attention given to the modeling of electric and magnetic fields and the accuracy of tracking charged particles through them. As evidenced by the G4Beamline application, Geant4 offers a unique simulation approach to beam lines and accelerators, in a 3D geometry and without some of the limitations posed by conventional optics and tracking codes. Its visualization tools allow detailed examination of trajectories as well as a particle's-eye view of the acceleration process. Here we apply G4Beamline to the TRIUMF cyclotron, describing the generation and input of the field data, accuracy of closed orbits and tunes, stability of multi-turn tracking, and tracking accelerated orbits.

INTRODUCTION

Originally conceived to meet the simulation needs of a new generation of high energy physics detectors at the LHC and elsewhere, the Geant4 software toolkit has become the mainstay simulation resource in a wide range of applications, from underground and underwater detectors to space experiments and medical physics. With its object-oriented architecture and C++ implementation, Geant4 has proved to be adaptible to many types of problems. One of the fundamentals is its precise tracking of charged particles in electric and magnetic fields, with user control of tracking error limits and a flexible interface for defining fields.

Geant4 can be useful in accelerator studies simply as a versatile and accurate ray-tracer with 3D geometry and fields, but it offers much more: the wide range of physics models can be used to simulate decays, foil scattering, production targets, collimators, ionization cooling, and so on. The tracking can include polarization, multiple particle species, and precise detection of particle losses.

A notable related development is the G4Beamline[2] application, which puts together the Geant4 components with a powerful scripting and analysis interface that is designed for the needs of accelerator physicists. It allows accelerators and beam lines to be defined, layed out, populated with beams, and instrumented with virtual detectors. Data output options in a variety of formats are provided.

In the course of using G4Beamline for TRIUMF applications, we found it to be easy to adapt an OPERA field map for a dipole magnet to G4Beamline and use it to do accurate ray-tracing for analysis of the aberrations. This raised the question: could G4Beamline handle a really large and complex field map, e.g. for the TRIUMF 500 MeV cyclotron? If so, could it track accurately enough to exhibit repeatable equilibrium orbits? If we added a time-dependent dee-gap field, could it accelerate to the maximum energy? This prompted the present study, where the cyclotron model is a good vehicle to test both the spatial accuracy of Geant4 tracking as well as the time-of-flight accuracy needed to produce isochronism and successful acceleration.

*TRIUMF receives federal funding via a contribution agreement through the National Research Council of Canada

FIELD MAP ADAPTATION

The reference field map of the TRIUMF cyclotron has been in use for over 30 years. It is expressed in Fourier harmonics as a function of radius, derived from the original survey data at 3-inch and 1-degree intervals, together with the trim coil contributions.

In addition to predefined beam line elements, G4Beamline offers several options for specifying electric and magnetic fields, which can be placed at arbitrary locations in the simulation "world". Overlapping and superimposed fields are automatically combined, to first order in the contributing fields. Here we have utilized the `fieldmap` element which reads in a self-describing ascii file containing the mesh information (2D cylindrical or 3D cartesian) and componentwise field data. For converting the TRIUMF data to this format we re-used some existing C++ code to process the Fourier data and evaluate the field components on a 3D cartesian grid of 0.5" spacing.

Geant4 by design handles arbitrary ions but due to limitations in the G4Beamline "external beam" input options, we have conducted all our tests using proton beams instead of H^-. To preserve isochronism it is sufficient to scale the magnetic field globally by the ratio of masses m_p/m_{H^-} as will be verified in the next section.

In this study we have used the default tracking settings provided by G4Beamline, including the most general and safe 4th-order Runge-Kutta integrator (one of several offered by Geant4) and relatively stringent error controls. G4Beamline currently implements only an 8-point linear interpolation method for field evaluation, and the limitations of this are discussed below.

EQUILIBRIUM ORBITS AND ISOCHRONISM

A first test of Geant4 tracking is to track known equilibrium orbits (EOs) and see if they close with sufficient accuracy, and to measure their time-of-flight to see if the particle velocity and path-length are also accurately accounted for.

We tracked 95 EOs from CYCLOPS[3] H^- orbit data based on the same field, from 0.1 to 520 MeV, using a small converter program to simply assign the same coordinates and energy to the protons and write out a "BLTrack-

ISBN 978-3-95450-128-1

AN ALL-PURPOSE ACCELERATOR CODE, ZGOUBI*

François Méot, BNL C-AD, Upton, Long Island, New York, USA

Abstract

A brief history of the ray-tracing code Zgoubi is given, illustrated with its numerous capabilities, up to the most recent 6-D tracking simulations in the largest accelerators.

INTRODUCTION

The ray-tracing code Zgoubi is being developed since the early 1970's for the design, development and operation of spectrometers, beam lines and circular accelerators. A Users' Guide is available [1] and provides extensive description of its methods and contents, whereas a voluminous documentation is available on web, *e.g.*, Ref. [2].

The code is a genuine compendium of numerical recipes allowing the simulation of most types and geometries of optical elements as encountered in accelerator assemblies. It provides built-in fitting procedures that make it a powerful design and optimization tool. It can account for synchrotron radiation, spin tracking, in-flight decay and other Monte Carlo based simulations. The high accuracy of the Zgoubi integrator allows efficient, long-term multi-turn tracking, in field maps and analytical models of fields. In particular, being based on stepwise integration Zgoubi allows taking full profit of modern high-accuracy magnet and RF system 4-D design codes (space + time), since it can directly use the field maps they produce.

A SHORT RETROSPECTIVE

1970s-1980s Period

Zgoubi and its integrator were first written for the design and development of the SPES-II spectrometer at the 3 GeV synchrotron SATURNE, Saclay [3]. The author inherited a copy of the code from Saby Valero at the "Theory Group" at SATURNE in 1985, for the purpose of a design collaboration with GSI regarding the KAOS spectrometer, still in operation nowadays [4]. This is also when the first version of the Users' Guide was written [5]. Zgoubi was at that time in use since a few years for the design of the high-resolution energy-loss spectrometer SPEG, still in operation at GANIL [6]. It was used as a beam line and spectrometer tool in a number of labs as CERN, JINR-Dubna, TRIUMF, etc.

SATURNE had then, second half of the 1980s, projects of a solenoidal partial snake (an idea that had emerged at the AGS, BNL) in complement with tune jump techniques then in use, to overcome depolarizing resonances [7]. The sophistication of the stepwise ray-tracing method was considered an appropriate candidate for an accurate evaluation of the technique, thus spin, together with periodic tracking, were installed in Zgoubi [8]. The code was later used in various spin studies in the following years, as the Neutrino Factory, super-B, ILC and, Section 4, RHIC.

1980s-early 2000s Period

Computer capabilities were in fast development, with prospects of CPU speed as well as memory capacities no longer being a concern in long-term, multi-particle beam and polarization transport simulations. Essentially, that period has seen the extensive development of Zgoubi for periodic machines, a daring and challenging technique in view of its excessive sophistication in regard to the paraxial machines that rings are, notwithstanding the culture of the guardian of truth "Hamiltonian integrators". The aim was to allow the use of the highest accuracy transport method: stepwise ray-tracing in realistic field models, This is addressed in the following two sections, more can be found in review and conference papers by the author, regarding, *e.g.*, LHC, Neutrino Factory muon rings, FFAGs, hadrontherapy and other electrostatic rings.

THE ZGOUBI METHOD

The Lorentz Equation

The *Lorentz* equation governs the motion of a particle of charge q, relativistic mass m and velocity $\vec{v}$ in electric and magnetic fields $\vec{e}$ and $\vec{b}$, and the *Thomas-BMT* equation which governs spin motion, write respectively (reference frame in Zgoubi defined in Fig. 1)

$$\frac{d(m\vec{v})}{dt} = q\,(\vec{e} + \vec{v} \times \vec{b})\,, \quad \frac{d\vec{S}}{dt} = \frac{q}{m}\,\vec{S} \times \vec{\omega}.$$

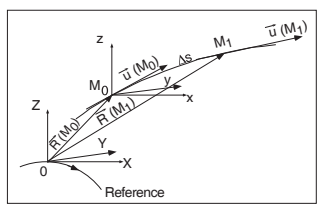

Figure 1: Position and velocity of a particle, pushed from location M_0 to location M_1 in Zgoubi frame.

Noting $()' = d()/ds$, $\vec{u} = \vec{v}/v$, $ds = v\,dt$, $\vec{u}' = d\vec{u}/ds$, $m\vec{v} = mv\vec{u} = q\,B\rho\,\vec{u}$, with $B\rho$ the rigidity of the particle, these equations can be rewritten in the reduced forms

$$(B\rho)'\,\vec{u} + B\rho\,\vec{u}' = \frac{\vec{e}}{v} + \vec{u} \times \vec{b}, \quad (B\rho)\,\vec{S}\,' = \vec{S} \times \vec{\omega} \quad (1)$$

with for the latter,

$$\vec{\omega} = (1+\gamma G)\vec{b} + G(1-\gamma)\vec{b}_{//} + \gamma(G + \tfrac{1}{1+\gamma})\tfrac{\vec{e}\times\vec{v}}{c^2},$$

G the gyromagnetic factor, γ the Lorentz relativistic factor. Both equations are solved using a truncated Taylor series

$$\vec{a}(M_1) \approx \vec{a}(M_0) + \vec{a}\,'(M_0)\,\Delta s + \ldots + \vec{a}^{(n)}(M_0)\,\frac{\Delta s^n}{n!} \quad (2)$$

where $\vec{a}$ stands for either the position $\vec{R}$ and velocity $\vec{u}$ which solves the motion, or for the spin $\vec{S}$. A scalar form of Eq. 2 is used to push the rigidity $B\rho(M)$ and time $T(M)$ in the presence of electric fields. The coefficients $a^{(n)} = d^n a/ds^n$ are obtained from the fields and their derivatives, provided using analytical models or field maps.

* Work supported by Brookhaven Science Associates, LLC under Contract No. DE-AC02-98CH10886 with the U.S. Department of Energy.

OPTIMIZING THE RADIOISOTOPE PRODUCTION WITH A WEAK FOCUSING COMPACT CYCLOTRON*

C. Oliver#, P. Abramian, B. Ahedo, P. Arce, J.M. Barcala, J. Calero, E. Calvo, L. García-Tabarés, D. Gavela, A. Guirao, J.L. Gutiérrez, J.I. Lagares, L.M. Martínez, T. Martínez, E. Molina, J. Munilla, D. Obradors, F. Olivert, J. M. Pérez, I. Podadera, E. Rodríguez, L. Sánchez, F. Sansaloni, F. Toral, C. Vázquez, CIEMAT, Madrid, Spain

Abstract

A classical weak focusing cyclotron can result in a simple and compact design for the radioisotope production for medical applications. Two main drawbacks arise from this type of machine. The energy limit imposed by the non RF-particle isochronism requires a careful design of the acceleration process, resulting in challenging requirements for the RF system. On the other hand, the weak focusing forces produced by the slightly decreasing magnetic field make essential to model the central region of the machine to improve the electric focalization with a reasonable phase acceptance. A complete analysis of the different beam losses, including vacuum stripping, has been performed. The main cyclotron parameters have been obtained by balancing the maximum energy we can obtain and the maximum beam transmission, resulting in an optimum radioisotope production.

INTRODUCTION

The growing demand of PET radioisotopes as diagnostic tools in hospitals makes interesting the design of compact cyclotrons. Superconducting magnets can be used to increase the magnetic field, minimizing the particle acceleration region and consequently reducing the overall cyclotron size. However, such strong magnetic fields, far beyond the iron saturation level, make difficult to obtain strong focusing forces by using azimuthally varying magnetic configuration, as it is typically used in synchronous cyclotron machines. To avoid moving to very expensive solutions with non-standard magnetic materials or auxiliary superconducting coils, classical cyclotrons, based on weak focusing forces, can result in an alternative for accelerating particles at relative low energies (<10 MeV) with a simple design.

AMIT CYCLOTRON

One of the main goals of the Spanish AMIT (Advanced Molecular Imaging Technologies) project is the development of a compact cyclotron of 8.5 MeV, 10μA proton beam for ^{11}C and ^{18}F single doses production for PET diagnostics. The superconducting AMIT cyclotron (Fig. 1) is a 180º Dee weak focusing machine, with a 60 kV accelerating peak voltage imposed by the non RF-particle isochronism and with stripping mechanism for beam extraction. A trade-off between machine size and cost results in a magnetic field of 4 T as an optimum value. In the same way an internal H^- ion source has been chosen to reduce the overall cyclotron footprint.

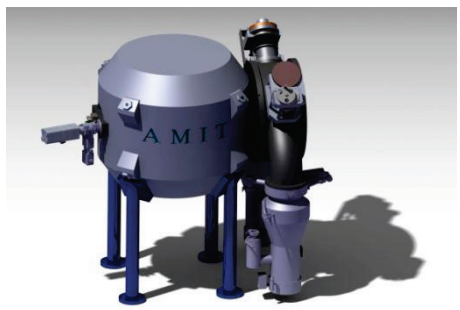

Figure 1: AMIT cyclotron overview.

The beam dynamics of the AMIT cyclotron is mainly determined by two features:

- **Weak focusing machine:** In this type of cyclotrons, beam focusing is obtained by using a slightly radial decreasing magnetic field. As a consequence, there is no synchronism between particles and the RF field, limiting the time that they can be properly accelerated and, consequently, the maximum beam energy we can achieve. In order to reach higher energies, high accelerating voltages are required.
- **Compact machine:** The compactness of the AMIT cyclotrons has resulted in the choice of a 4 T magnetic field and an internal ion source. On one hand, such a magnetic field results in very small orbits in the central region which, in combination with the high voltage, leads to a non-trivial design of the ion source and puller. On the other hand, the gas throughput needed for the internal ion source causes a low vacuum level in the cyclotron (~10^{-4}-10^{-5} mbar), resulting in a poor beam transmission through the cyclotron, stressed if the number of turns is not kept low.

This paper summarizes the most important beam dynamics features of the AMIT cyclotron. CYCLONE code [1] has been used for orbit simulations.

OPTIMIZATION OF RADIOISOTOPE PRODUCTION

The radioisotope production is determined by the properties of the beam hitting the target, namely, the beam energy and current. Although the dependence with the

*Work supported by the AMIT project, a CDTI funded project (CENIT CIN/1559/2009)
#concepcion.oliver@ciemat.es

ISBN 978-3-95450-128-1

OPERATIONAL EXPERIENCE AT THE INTENSITY LIMIT IN COMPACT CYCLOTRONS

G. Cojocaru and J. Lofvendahl, TRIUMF, 4004 Wesbrook Mall, Vancouver, BC, V6T 2A3, Canada

Abstract

Compact cyclotrons are a cost-efficient choice for medical radioisotope production since negative hydrogen ions can be used at energies well below 100 MeV. The stripping extraction technique allows quite large circulating currents without the need for separated turns. Space charge limits are in the range of 1 to 2 mA, but operating for long periods at these levels is a challenge for many reasons, among them being the sputtering of metal surfaces where unaccepted beam is deposited. These limits and others observed during our 22 years of 24 hours/365 days of quasi continuous operation of TR30 cyclotrons will be explored.

INTRODUCTION

TR30s are compact, low energy, high current H- cyclotrons originally designed and developed by TRIUMF and Advanced Cyclotron Systems Inc. (ACSI) [1]. They are four sector machines with two 45^0 Dees in opposite valleys. Due to their external ion source, and thus low tank pressure, the beam gas stripping is minimal. This combined with negligible electromagnetic stripping results in no beam losses between 1 MeV and the maximum energy. Extraction is done above 15 MeV by passing and stripping H- beam through graphite foils located at the desired energy, making this process very simple and efficient. Dual extraction with two carousels is performed on regular basis. The first TR30 (TR30-1) was commissioned in 1990 [2] and was initially producing 500μA extracted proton beams at energies up to 30 MeV. In 1995, after an upgrade program [3, 4], this cyclotron's capabilities were increased to 1 mA at 30 MeV. In 2002 another TR30 (TR30-2) was build and installed by ACSI at TRIUMF site. Both these machines are used by TRIUMF and NORDION for medical radioisotope production. Several other TR30s were built and installed by ACSI at different locations and are intensively used for same applications [5].

Our more than 22 years operational and maintenance experience with TR30-1 and 10 years with TR30-2, along with the nature of our production schedule (24 hours/365 days), have helped us to evaluate the long term performance stability of these cyclotrons. Both beam intensity and uptime are critical parameters in estimating the limits of our machines and we are evaluating the cyclotron output and performance in terms of charge delivered (mAh). Both factors have to be considered concurrently in order to assess the long term performances of our cyclotrons. Operating these machines for long periods at mA level is a challenge. Fundamental intensity limits were considered by R. Baartman in [6] and will be also presented in another paper in these Proceedings.

CYCLOTRONS SUBSYSTEMS

We are detailing here the failures and lifetimes of several components and how these are affecting our cyclotrons performances based on accumulated statistical data.

Ion Source and Injection Line

The beam levels extracted out of our ion sources are dependent on our production demands. We are running between 2 mA and 10 mA, with an estimated average of 6mA extracted H- beams. At this level the filament lifetime is about 35 days. A filament change takes about 5 hours (cool-down, filament replacement, pumping down and filament conditioning) and is the type of maintenance that is scheduled without affecting production. A new filament is not altering the cyclotron output, other than the downtime.

The components in the Injection Line that have a relatively high rate of failure are the inflector and the buncher. We have experienced about 10 TR30-1 inflector failures in the past 10 years and a similar rate in TR30-2. They usually fail before affecting the injected beam intensity, and maintenance and recovery takes about 4 days (cool-down, replacement, vacuum recovery, inflectors conditioning and tuning and tank RF conditioning). Figure 1 shows a TR30-2 deteriorated inflector, as opposed to a new inflector in Fig. 2. TR30-2 buncher is failing at a rate of about once every 3 years and is preceded by beam amplitude deterioration. TR30-1 buncher has a more robust design and a low rate of failure. Beam amplitude is recovered in about 2 days after a buncher repair. Gradual physical deterioration of ion source components and especially the extraction optics combined with limited accessibility due to the nature of our application affects the overall beam transmission.

Extraction Foils

There is typical beam deterioration during the lifetime of an individual foil, due to its physical depreciation. As a result, the beam size is growing along the beam lines, and eventually, cannot be compensated with beam lines and injection line optics tunes. A foil change will be necessary. Figure 3 shows a 5 foils carousel ready to be installed, while Fig. 4 shows a used set of foils. Every new foil needs additional beam tuning. To estimate the foils lifetime we considered our statistics on 2325 foils

ISBN 978-3-95450-128-1

TUNING OF THE PSI 590 MeV RING CYCLOTRON FOR ACCEPTING AND ACCELERATING A REBUNCHED 72 MeV PROTON BEAM

M. Humbel, Ch. Baumgarten, J. Grillenberger, W. Joho, H. Müller, H. Zhang,
Paul Scherrer Institut, CH-5232 Villigen PSI, Switzerland

Abstract

In the past year the production of a 1.42 MW proton beam at a relative loss level of 10^{-4} at PSI's high power proton facility became routine operation. In addition, the inaugurated buncher based beam injection into the 590 MeV Ring cyclotron made a remarkable step forward. In particular, an almost dispersion free setting of the beamline region around the 500 MHz rebuncher in the 72 MeV transfer line has been established and a perfect matching of the dispersion into the Ring cyclotron has been achieved. This buncher-operation optimized facility setting could be advanced up to the ordinary stable standard 2.2 mA production proton beam. With the buncher voltage turned on, at the moment the beam, extracted from the Ring cyclotron is limited to below 1 mA due to raising losses, mainly generated by space charge induced distortions of the beam bunches. For a better understanding of these effects a substantial effort in modelling of the accelerated beam is under way. In particular, the influence of the trim coil fields is partly implemented into the OPAL simulation code and the insertion of an additional bunch shape monitor in the Ring cyclotron is proposed.

INTRODUCTION

PSI's three stage accelerator facility is on the way to reach proton beam currents beyond 3 mA [1]. To achieve higher intensities longitudinal and transversal effects have to be considered. In transversal direction the gap between the last two turns can be broadened by raising the voltage of the RF amplitude yielding a reduction of the number of turns. Along propagation direction in contrast the bunch length will reach the boundaries of the phase acceptance of the Ring cyclotron at about 2.7 mA despite the installed flattop system. In order to longitudinally shrink the bunches a rebuncher [2] has been inserted in the middle of the transfer line between Injector 2 and the Ring cyclotron. The diagnostic elements involved in the tuning of the Ring cyclotron for the acceleration of the bunched beam are shown in Fig. 1.

DEMANDING MATCHING CONDITIONS

The beam bunches leave the Injector 2 at a phase width of 1.5 RF-degrees. While travelling across the 56 m long 72 MeV transfer line to the Ring cyclotron the bunches elongate to a 4σ phase width of 40 RF-degrees. Due to the high charge density the acceleration of the rebunched beam imposes stringent boundary conditions on the beam properties in the buncher region and for the matching of the beam at the injection into the Ring cyclotron.

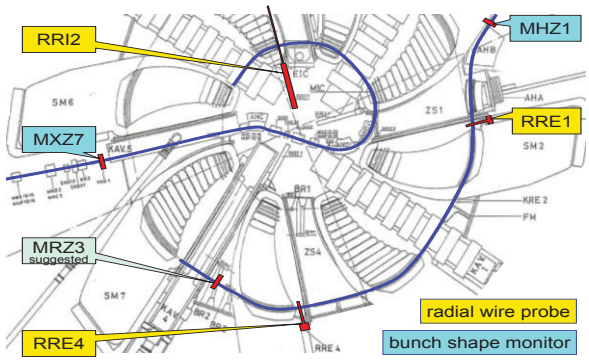

Figure 1: Bunch shape monitors and radial wire probes involved in the tuning of the PSI Ring cyclotron for the acceleration of a bunched beam. The proposed new time structure probe MRZ3 is labelled in mint.

Dispersion Free Section at the Buncher Position

In a matched beam, each particle moves along the equilibrium trace corresponding to its velocity. While crossing the buncher the slow particles are converted into fast ones and vice versa, but leave there position unchanged, yielding the fact, that the particles start to oscillate around the equilibrium trace according to their obtained velocity. To avoid this effect the dispersion D and the dispersion gradient D' have to remain zero in the buncher surroundings. This condition has been achieved in the 72 MeV Beam line by optimising the R-matrix elements r16 and r26 of the initial beam conditions and by adjusting the first quadrupole triplet QXA1/2/3 at the beginning of the beamline (Fig. 2).

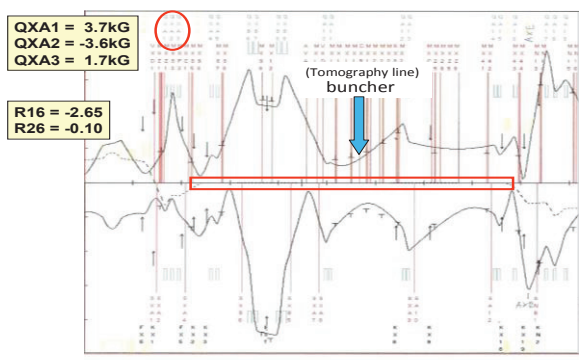

Figure 2: TRANSPORT-fit of the 72 MeV-transfer line with dispersion free buncher region.

ISBN 978-3-95450-128-1

ACTIVATION ANALYSIS WITH CHARGED PARTICLES: THEORY, PRACTICE AND POTENTIAL

M. Anwar Chaudhri
The Institute of Biomaterials, F.A. University of Erlangen-Nuernberg, 91058 Erlangen, Germany

Abstract

Activation analysis using charged particles (CPA) from cyclotrons and other similar accelerators is presented. Its advantages over neutron activation analysis using thermal neutron (NAA) is presented. Also some of the difficulties involved with the CPA are also highlighted along with the practical solutions to overcome these difficulties. Our "special theory" [1] is presented that makes the CPA as simple as the NAA. A practical example is given where the Effect of French Atomic Tests of the 197's in the Pacific on the Australian East Coast was studied with CPA. By making use of empirically constructed excitation functions of Lange and Muenzel [2] we have estimated the detection sensitivities of all the elements and isotopes with Z from 20 to over 90, through 1, 2 &3 particles-emission under irradiation with protons, deuterons and alpha particles of up to 36 MeV and have presented these in graphical form [3].

INTRODUCTION

Activation analysis with slow neutrons from a reactor is the most commonly used radio-analytical method. However, certain elements such as Al, Si, Ti, Cd, Tl, Pb, Bi, etc. can not be conveniently or at all activated with slow neutrons. Furthermore, for biomedical samples, due to the presence of large quantities of Na, radiochemical separation is required before NAA can be carried out. Particle induced X-ray emission Analysis (PIXE) is another accelerator based technique which is simple and has multi-elemental measurement capabilities. But PIXE is not so convenient for measurement for elememts lighter than F. Furthermore, its detection sensitivity is limited to around ppm (or µg/g) range.

Charged particle activation analysis tends to overcome many of these short comings. It can be non-destructive and elements lighter than F can be conveniently and accurately determined and sensitivities of as low as ppb (µg/kg) range can be achieved in favourable circumstances. Furthermore, this technique has multi-elemental detection capability.

METHOD

Mostly energetic protons energy, ca. 8-10 MeV have been used for CPA, although other charged particles, such as deuterons, He-3 and He-4 also offer a great deal of potential in this field.

However, unlike the NAA there are a number of practical difficulties in CPA which have to be overcome. These are:

1. Energy loss and heat generation in the sample under irradiation with charged particles. This can be minimised by cooling the sample holder with water, air or even liquid Nitrogen. In the case of powdered samples the heat generation problem can also be overcome by mixing the sample with analytical grade Graphite and thus making it conductive.
2. Simultaneous and controlled "identical" irradiation .of the sample and the standard is absolutely essential in CPA. It can generally be achieved by keeping the irradiation conditions energy, beam-intensity, etc., stable and monitoring the beam carefully. Alternatively, one can also mount the sample and the standard on a special target holder and rotating it at a constant speed during irradiation. This assures that the sample and the standard have been irradiated under identical conditions.

The trace element to be determined has to be uniformly distributed in the matrix. This condition is generally met in many types of samples, especially in biological fluids and organs, which are freeze-dried and /or ashed and then homogenized.

Chaudhri et al. [1], have presented a simplified theory of CPA which reduces it to the simplicity of NAA. According to this theory the induced activity in an unknown sample A is related to the induced activity in the standard (with known concentration of the element being determined) A_s with the following equation:

$$A_s / A = Cs\ Qs / C\ Q\ \mathbf{X}\ (dE/dx) / (dE/dx)s. \qquad [1]$$

Where C is the concentration, in appropriate units in the sample, Q is the charge collected to induce activity A and dE/dx is the stopping power of the incoming beam in the sample-matrix at the "mean-energy" of the incident particles. This "mean-energy" is given by $[E_i + E_0] / 2$ where Ei and E_0 are respectively the incident energy and the lowest energy for which an appreciable amount of induced activity would be produced. Various terms with the subscript "s" refer to the standard. In Eq. (1) all quantities are measured or can be taken from the published tables with the exception of C, which can then be calculated.

Chaudhri et al. [4] have recently shown, through extensive calculations, that this theory produces the best results as compared to any other approximation for CPA and it's a lot simpler.

ISBN 978-3-95450-128-1

FABRICATION OF HYDROPHOBIC SURFACES FROM HYDROPHILIC BeO BY ALPHA-IRRADIATION-INDUCED NUCLEAR TRANSMUTATION

E. J. Lee, M. G. Hur*, Y. B. Kong, Y. D. Park, J. H. Park, S. D. Yang, Advanced Radiation Technology Institute, Korea Atomic Energy Research Institute, Jeongeup, Republic of Korea
J. M. Son, National Cancer Center, Goyang, Republic of Korea

Abstract

Hydrophobic surfaces were simply fabricated by irradiating hydrophilic BeO surfaces with an alpha particle beam from a cyclotron. In this research, BeO disks were irradiated under conditions of ~25 MeV in alpha particle energy and ~315 nA/cm^2 in beam current density with different fluences.

After the alpha irradiation, the wetting property of alpha-irradiated BeO surfaces was analyzed by measuring water contact angles (CAs). The changes in the morphology and chemical composition of BeO surfaces were analyzed using a 3D optical surface profiler and X-ray photoelectron spectroscopy.

C and F atoms were created, and consequently, hydrophobic CF_2 functional groups were formed by the alpha irradiation of hydrophilic BeO. The amount of CF_2 functional groups on the surface increased as the fluence increased. Accordingly, the CA of alpha-irradiated BeO surfaces gradually increased as the fluence increased. In conclusion, hydrophilic BeO surfaces could be easily converted to hydrophobic surfaces by the alpha irradiation.

INTRODUCTION

Wettability is one of the most important properties related to various phenomena such as adhesion, printing, cleaning, painting, lubrication, and so on [1].

It has been revealed that the wettability is controlled by two factors, the surface roughness related to the morphology and the surface energy concerned with the chemical composition [2]. Among various methods to control the wettability, irradiation technique is known to be a simple process that can modify both the surface roughness and the surface energy simultaneously [3,4]. Although many irradiation methods using ion implantation, plasma treatment, and synchrotron radiation have been developed [5-7], the method utilizing irradiation-induced nuclear transmutations has not been reported as far as we know.

Here, we present a simple route to change hydrophilic BeO into a hydrophobic surface via alpha-irradiation-induced nuclear transmutation. The alpha-irradiated BeO disks were characterized using a 3D optical surface profiler, an X-ray photoelectron spectroscopy, and contact angle measurement. The wettability of BeO was controlled from hydrophilicity to hydrophobicity by simply increasing the fluence.

*hur09@kaeri.re.kr

EXPERIMENTAL

BeO disks with a diameter of 35 mm and a thickness of 2 mm (BeO >99.5%, Thermalox995^{TM}, Materion, USA) were used as irradiation targets. BeO disks were irradiated with an alpha particle beam generated from a cyclotron (MC-50, Scanditronix, Sweden) at Korea Institute of Radiological and Medical Sciences (KIRAMS). The irradiation process was carried out at room temperature in a vacuum chamber. The energy of the alpha particle beam was ~25 MeV, and the current density of the beam was ~315 nA/cm^2. Fluences of the alpha particle beam irradiating the samples were 5.97 x 10^{14} and 4.53 x 10^{15} cm^{-2}.

The wettability was analyzed by a water contact angle (CA) measured with a CA measurement system (SEO Co., Ltd., Phoenix 300 Plus). The volume of a water drop used for the CA measurement was 4 μL.

The morphologies of pristine and alpha-irradiated BeO disks were characterized with a 3D optical surface profiler (Nano System Co. Ltd., NV-2000). The chemical compositions of pristine and alpha-irradiated BeO disks were investigated with X-ray photoelectron spectroscopy (XPS) using a Mg and Al Kα X-ray source in a SIGMA PROBE (Thermo VG) spectrometer. All the XPS spectra were charge-compensated to C 1s at 285.0 eV [8,9].

RESULTS AND DISCUSSION

Main nuclear transmutations which can be induced by the alpha irradiation of BeO are ^{16}O(α, n)^{19}Ne and ^{9}Be(α, n)^{12}C. Fluorine atoms are created by the formal reaction and following β^+ decay with a half-life of 17.22 s. On the other hand, Carbon atoms are directly produced by the latter reaction.

To evaluate the effect of the alpha irradiation to the wettability of BeO, water contact angles (CAs) of pristine and alpha-irradiated BeO disks were measured (Fig. 1). The pristine BeO disk showed a CA of 42.1±1.2° indicating that the surface was originally hydrophilic. When the fluence was 5.97 x 10^{14} cm^{-2}, the CA slightly increased to 50.3±2.5°, but the surface of the alpha-irradiated BeO disk was still hydrophilic. The CA further increased, and finally a hydrophilic surface transformed to a hydrophobic surface with a CA of 90.8±1.7° when the fluence was further increased to 4.53 x 10^{15} cm^{-2}.

In order to explain the behavior of CA change, changes in the morphology and the chemical composition were investigated as follows because the wettability is determined by the surface chemistry as well as by the

ISBN 978-3-95450-128-1

DESIGN OF ULTRA-LIGHT SUPERCONDUCTING PROTON CYCLOTRON FOR PRODUCTION OF ISOTOPES FOR MEDICAL APPLICATIONS

M. K. Dey#, A. Dutta Gupta, A. Chakrabarti, VECC, Kolkata, India

Abstract

A new design has been explored for a superconducting-coil-based compact cyclotron, which has many practical benefits over conventional superconducting cyclotrons. The iron yoke and poles in conventional superconducting cyclotrons have been avoided in this design. The azimuthally varying field is generated by superconducting sector-coils. The superconducting sector-coils and the circular main-coils have been housed in a single cryostat. It has resulted in an ultra-light 25 MeV proton cyclotron weighing about 2000 kg. Further, the sector coils and the main coils are fed by independent power supplies, which allow flexibility of operation through on-line magnetic field trimming. Here, we present design calculations and the engineering considerations, focused on making the cyclotron ideally suited for the production of radioisotopes for medical applications.

INTRODUCTION

Historically, various designs of cyclotron have evolved to adapt them to various applications, especially in medical applications, apart from its use as a research tool in atomic, nuclear and solid-state physics experiments [1]. Due to its compactness and the cost factor, the cyclotrons have become the ideal choice for the production of short-lived proton-rich radio-isotopes used in biomedical applications [2, 3, 4, 5]. More than 350 cyclotron installations worldwide are engaged in the production of radio-nuclides, mostly the PET and SPECT isotopes (^{11}C, ^{13}N, ^{15}O, ^{18}F, ^{123}I, ^{203}Tl, ^{67}Ga) used in medical diagnostics, as well as the isotopes for therapeutic applications, e.g., ^{64}Cu, ^{103}Pd, ^{186}Re etc. The production of ^{99m}Tc in a proton cyclotron is also a matter of great contemporary interest [6].

These installations generally use low energy cyclotrons (9 MeV to 30 MeV) with several hundred micro-ampere beam currents to satisfy user demand for these radioisotopes [7, 8, 9]. There has been ongoing effort since nineteen eighties towards developing new designs of such cyclotrons using superconducting magnets to lower the weight, power consumption and radiation background. The recent trend is to develop extremely compact superconducting cyclotron, optimized to produce unit does on demand [10].

One remarkable step towards an ultra-light cyclotron was the design proposed by Finlan, Kruip and Wilson using a superconducting magnet with iron sectors contained within the room temperature bore of the magnet was [11]. The major reduction of weight was obtained by getting rid of iron yoke enclosing the superconducting magnet. This was unique feature of this design over all other conventional superconducting cyclotrons [12, 13, 14, 15]. Oxford Instruments built 12 MeV H^- cyclotron based on this design weighing only 3.5 tons [16]. The isochronous field and adequate flutter was achieved three iron sectors placed in the warm bore of the superconducting main coils. Isochronous fields for protons or H^- ions up to 60 MeV can be produced in such an arrangement.

Moving ahead in the same direction, present authors proposed a design in which the iron sectors have been replaced by superconducting sector coils [17]. The isochronous field along with sufficient flutter is obtained by optimizing the sector coils and the superconducting circular coils. A magnetic field bump at the centre of the machine generated by a small superconducting circular coil provides the necessary magnetic focusing in this low flutter zone. Inside the main sector coils, sector shaped trim coils have been used for further fine tuning of the average field. Independent excitations of the main coils and trim coils allow the flexibility of operation through online magnetic field tuning. Thin iron shims have been used on the face of sector coils for finer shaping of the magnetic field. Magnetic shielding is done using separate a-few-mm thick iron cylinders outside the superconducting magnet. The weight of a 25 MeV H^- cyclotron based on this design is estimated to be about 2 tons. In this paper we present the design calculations for this cyclotron and the engineering aspects.

DESIGN FEATURES AND SPECIFICATION

The proposed design is for a fixed field, fixed frequency, compact superconducting cyclotron, accelerating negative hydrogen ions and extracting proton beams using stripper mechanism. The present design is for a maximum energy of 25MeV proton (H^-) beam, which is good enough for ^{99m}Tc production [6]. However, the concept can be applied for designing cyclotrons of other energies as well, from 12MeV to 30MeV or a little higher energy also.

The cyclotron magnet consists of two sets of circular main coils at the outer radius (MC1, MC2), four 45° sector coils, two trim coils inside each sector and two small circular coils at the centre (CC1, CC2). Figure 1 shows the geometry of sector and circular coils. All the coils are superconducting and they are contained in a single cryostat. In this design calculations we have considered NbTi superconducting wire (1.1×1.7 mm^2) from Bruker Advanced Supercon (4.2 K, 4 T, J~3000 A/mm^2, Cu:NbTi ratio from 10 to 20). The number of

#malay@vecc.gov.in

PARASITIC ISOTOPE PRODUCTION WITH CYCLOTRON BEAM GENERATED NEUTRONS*

J.W. Engle+, E.R. Birnbaum, M.E. Fassbender, K.D. John and F.M. Nortier#
LANL, Los Alamos, NM 87544, USA

Abstract

Several LINAC and cyclotron facilities worldwide generate high intensity beams with primary beam energies in the range 66 MeV to 200 MeV for isotope production purposes. Many of these beams are almost fully subscribed due to the high demand for isotopes produced via proton induced reactions, leaving little beam time available for production of smaller quantities of research isotopes. Modelling and preliminary experimental measurement of the high power proton beam interaction with targets at the Isotope Production Facility (IPF) at Los Alamos show a high potential for parasitic small scale production of isotopes utilizing the secondary neutron flux generated around the target. Such secondary neutron flux can also be exploited by cyclotron facilities, especially emerging modern commercial 70 MeV machines with total beam currents approaching 1 mA and more.

INTRODUCTION

Popular radioisotopes whose production requires a proton beam with primary energy of 30 MeV or higher include ^{124}I, ^{123}I, ^{67}Ga, ^{111}In, ^{11}C, ^{18}F, ^{13}N, ^{13}O, ^{82}Sr, ^{68}Ge, ^{22}Na and ^{48}V [1]. Some of these isotopes are exclusively made in large quantities at facilities with energy capability beyond 60 MeV. Limited beam time for small-scale production of other research isotopes is therefore a known problem at most operating intermediate energy isotope production facilities such as those listed in Table 1. Usually the production of one or two commercial isotopes dominates operations, consuming most of the beam time.

Table 1: Operating Intermediate Energy Isotope Production Facilities

Facility	Country	Beam Energy and Current	Type
IPF, LANL	USA	100 MeV, 250 µA	LINAC
BLIP, BNL	USA	200 MeV, 100 µA	LINAC
INR	Russia	160 MeV, 120 µA	LINAC
iThemba	South Africa	66 MeV, 250 µA	Cyclotron
PSI	Switzerland	72 MeV, 100 µA	Cyclotron
TRIUMF	Canada	500, 70 MeV, 100 µA	Cyclotron
ARRONAX	France	70 MeV, 2x375 µA	Cyclotron

* Work supported by Los Alamos National Laboratory and U.S. Department of Energy
+ jwengle@lanl.gov, # meiring@lanl.gov

THE LANL EXPERIENCE

Production operations also dominate irradiations at the 100 MeV Isotope Production Facility of the Los Alamos National Laboratory (LANL), which is based on a linear accelerator. Presently, the production of the commercial isotopes ^{82}Sr and ^{68}Ge represents more than 95% of the production volume. Tightly scheduled routine production runs proceed at a beam current of 230 µA, employing a standardized production target stack consisting of two RbCl targets and one gallium target [2]. Recent decline in beam availability resulted in the concurrent decline of small-scale production of research isotopes to almost non-existent levels. This prompted the consideration of alternative parasitic production approaches.

Secondary Neutrons at IPF

The IPF's high proton beam current produces a secondary neutron flux with a scale that is typically beyond the reach of low energy cyclotrons (<30 MeV) and energetically distinct from reactor neutron fluxes. This potential for research in novel methods of isotope production and materials science is as yet unexploited. Current irradiations utilizing a standard production target stack result in a secondary neutron flux of ~10^{12} n s^{-1} cm^{-2}, approaching the scale of medium flux research reactors at the location directly behind the target stack (see Fig. 1).

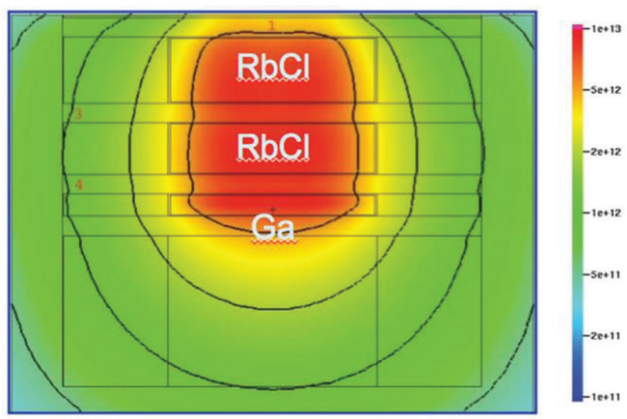

Figure 1: Neutron flux distribution (n s^{-1} cm^{-2}) around the IPF target stack as predicted by MCNPX [3]. The proton beam direction is downward.

Parasitic Production Potential at LANL

Parasitic production target material inserted at the rear of the target stack may advantageously utilize this neutron flux. As the energetics of the IPF neutron field are also predicted to differ significantly from typical reactor

ISBN 978-3-95450-128-1

THE UNIVERSITY OF WASHINGTON CLINICAL CYCLOTRON A SUMMARY OF CURRENT PARTICLES AND ENERGIES USED IN THERAPY, ISOTOPE PRODUCTION, AND CLINICAL RESEARCH

Eric Dorman and Rob Emery
University of Washington Medical Center, Seattle, WA 98195, USA

Abstract

The University of Washington Clinical Cyclotron (UWCC) is a Scanditronix MC50 compact cyclotron installed in 1983. The cyclotron has now been in operation for 30 years and has been used to treat approximately 3000 patients. Its primary purpose is the production of 50.5 MeV protons used to bombard a beryllium target to produce neutrons for fast neutron therapy. The unique nature of the cyclotron is its variable frequency Rf system, and dual ion source chimneys; it is also capable of producing other particles and energies.

Our facility is now sharing beam time among multiple users:

- Fast neutron radiotherapy.
- Development of a Precision Proton Radiotherapy Platform.
- In vivo verification of precision proton radiotherapy with positron emission tomography.
- Routine production of 211-At.
- Routine production of 117m-Sn.
- Cyclotron based 99m-Tc production.
- Cyclotron based 186-Re production.
- Proton beam extracted into air, demonstrating a visual Bragg peak.
- Neutron hardness testing for electronic subsystems.

These multiple projects show the uniqueness of our hospital based facility and our commitment to therapy, radioisotope research and production, and clinical investigations.

HISTORY

In January 1979, the National Cancer Institute (NCI) published a Request For Proposal (RFP) for a "Clinical Neutron Therapy Program". The RFP requested medical centers, which met minimum qualifications outlined in the RFP, to respond with proposals to establish Clinical Neutron Therapy Programs utilizing dedicated neutron generators. The RFP outlined three major phases for the project: Acquire a high LET neutron generator to be dedicated to the project, acquire the necessary facilities to house the generator and treatment rooms, and undertake six years of clinical trials according to established protocols.

In April 1979, the University of Washington (UW) submitted a formal proposal to the NCI. In all, eleven medical centers responded to the NCI with proposals.

In September 1979, a contract between the NCI and the UW was awarded to build a Clinical Neutron Therapy Program. The NCI also awarded contracts to three other medical centers: MD Anderson Cancer Center, University of California at Los Angeles, and The Fox Chase Medical Center.

A RFP for the clinical neutron therapy equipment was issued by the UW in November 1979. Bids were submitted by The Cyclotron Corporation (TCC), Nucletronix/Scanditronix (SCX), and CGR-Medical. All manufacturers proposed a fixed-energy isochronous AVF cyclotron as the core of their neutron therapy system. Proton beam energies ranged from 42–60 MeV depending on manufacturer and machine specifications.

A variable energy option was added so that different dose distributions and comparative neutron beam studies could be performed over a range of energies at one facility. The variable energy option was also seen as giving the cyclotron more flexibility for research purposes. Although not intended for radioisotope production under the NCI contract, the use of the cyclotron for this purpose was envisioned in a separate grant proposal for the production of short-lived and positron-emitting isotopes.

In February 1980, SCX was selected as the vendor. The SCX system was judged to have a number of advantages in magnetic field, Rf, vacuum, extraction, ion source, and beam transport systems. In addition to the technical advantages, the SCX system offered the low bid among the three vendors for the "complete" system.

February 14, 1980, purchase order T-485501 was issued by the UW to SCX for the clinical neutron therapy equipment at a cost of $4,700,000. The core of the system is a MC50 cyclotron.

Subsequent to execution of the initial fabrication contract, permission was sought and granted by NCI to modify the design of the cyclotron to provide for the addition of deuteron acceleration capability. SCX gave assurance that this modification would not detract from the neutron production capability nor affect its reliability. This late change was very important to the flexibility of the cyclotron and the role it currently plays in research at the UW.

March 1980 – September 1982, Cyclotron and related equipment was fabricated at the SCX facility.

November 1982, Treatment units and beam line components delivered to UW.

April 1983, Cyclotron delivered to the UW.

June 1983, First beam on the therapy target.

October 19, 1984, First patient treated!

ISBN 978-3-95450-128-1

A MULTI-LEAF FARADAY CUP ESPECIALLY FOR PROTON THERAPY OF OCULAR TUMORS

C. Kunert#, J. Bundesmann, T. Damerow, A. Denker, Helmholtz-Zentrum Berlin, Germany
A. Weber, Charité Universitätsmedizin Berlin, Germany

Abstract

For tumor therapy with protons it is crucial to know the beam range with a high accuracy. The Multi-leaf Faraday Cup (MLFC) offers a quick and precise range or energy measurement. To adapt the principle of a MLFC to the eye tumor therapy requirements is a challenging task, due to the necessary accuracy in the sub mm regime. The first prototype has 42 channels; each consists of a 10 µm copper foil, connected to an ammeter, next to a 25 µm Kapton foil. An incoming proton beam creates a current of some pA in a certain channel with respect to its energy.

MOTIVATION

The eye tumor therapy benefits from the radiation therapy with protons in a lot of cases. Since 1998 the University Hospital Charité Berlin provides together with the Helmholtz-Zentrum Berlin (HZB) a treatment facility using the HZB isochronous cyclotron [1]. The main benefit of proton beams in tumor therapy is the determined range in tissue in contrast to the commonly used photon radiation. Additionally the protons create the highest dose just before stopping. This depth dose curve is called Bragg peak and an example is shown in Fig. 1.

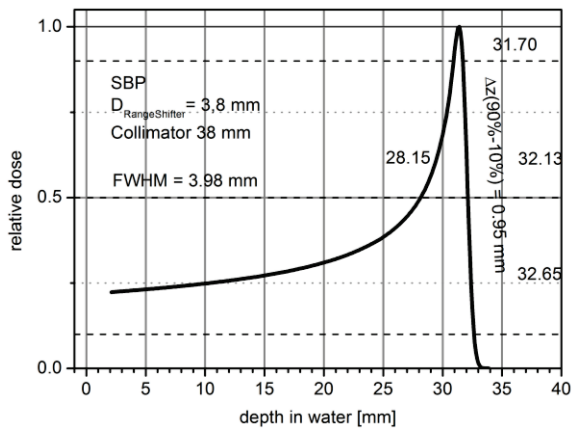

Figure 1: Typical Single Bragg Peak (SBP) of the HZB cyclotron.

With such proton beams are very well determined radiation fields achievable, the dose can be delivered mainly to the tumor tissue, and critical tissues, which are highly sensitive to radiation, can be spared. In our case this leads to a tumor control of 96% after 5 years and in most cases the eyesight can be conserved.

The eye contains several critical structures in its small volume of 6-7 cm³, e.g. the optical nerve or the macula. Figure 2 shows a typical planned dose distribution for a melanoma located near the optical nerve. The positioning of the radiation field is crucial for the successful therapy with low side effects. Due to the small structures in the eye compared to other organs the necessary precision is in the sub mm regime. Therefore the positioning of the patients has to be done very precisely and the range of the proton beam has to be known with a resolution of 0.1 mm or better.

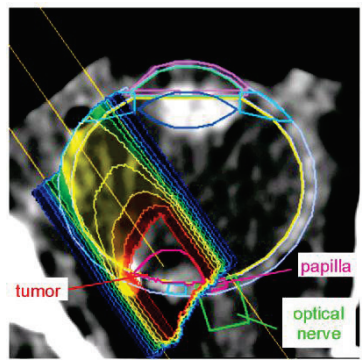

Figure 2: Planned radiation field with marked critical structures and the tumor.

Due to necessary quality checks, a range measurement has to be done in every therapy and after unexpected shut downs, e.g. an accidental shut-down due to instabilities in the power supply network. Thus, it would be a great advance to perform the necessary quality check in a short time to keep the therapy interruption as short as possible.

THE MLFC

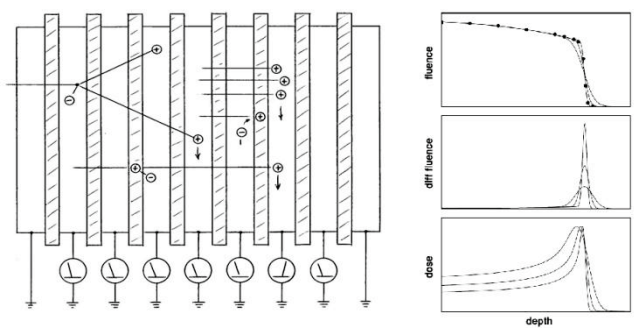

Figure 3: Principle of a MLFC and the comparison (top to bottom) of the fluence, differential fluence (range) and the Bragg peak as a function of depth [2, 3].

One idea for a quick and precise range measurement is a Multi-Leaf Faraday Cup. This is a stack of alternating conductor and insulator plates (Fig. 3). Each conductor is connected to the ground potential via an ammeter. Incoming protons stop in a certain plate and this additional positive charge creates a current by pulling

#christoph.kunert@helmholtz-berlin.de

OPERATION MODE OF AIC-144 MULTIPURPOSE ISOCHRONOUS CYCLOTRON FOR EYE MELANOMA TREATMENT *

K. Daniel, K. Gugula, J. Sulikowski, IFJ-PAN, Krakow, Poland
I. Amirkhanov, G. Karamysheva, I.Kiyan, N. Morozov, E. Samsonov, JINR, Dubna, Russia

Abstract

Computational and experimental results concerning acceleration and extraction of the 60 MeV proton beam at AIC-144 cyclotron of the Institute of Nuclear Physics (Krakow, Poland) are considered. A proton beam of the AIC-144 cyclotron is accelerated without large losses in the radial region of 12-62 cm and is extracted from the cyclotron with a pretty good overall efficiency of ~35%. The beam was used for successful treatment of 15 patients in 2011-2012.

INTRODUCTION

The AIC-144 cyclotron is used at the Institute of Nuclear Physics, Polish Academy of Sciences, mainly as a source of deuteron and proton beams for isotope production on the internal target. In the past years several systems of the cyclotron have been modified in order to provide parameters of the external proton beam with an energy of 60 MeV necessary for eye melanoma radiotherapy which has been conducted at the INP since 2011 [1].

Important efforts have been made to increase reliability of the RF system operation at a frequency of 26.26 MHz and dee voltage of 60 kV. Stable operation of the RF system in this regime essentially increased the extraction efficiency of 60-MeV protons [2].

Magnetic field measurements were fulfilled in order to shape the specified level of the isochronous field with a required accuracy and to limit the 1st harmonic of the field imperfections to ~ 5 Gs [3].

Particle dynamics computations show that the beam is accelerated up to extraction system with tolerable phase drift and amplitudes of transverse oscillations. Main losses of the protons (~40%) occur at the radius ~62 cm (energy ~59.5 MeV) due to the action of the coupling resonance Q_r-$2Q_z = 0$ and the parametric one $2Q_z = 1$.

Experimental study of the beam acceleration and extraction confirms the main results of the computations. The RF phase of the beam just before the extraction is close to 10°RF, as measured using the Smith and Garren method [4].

The experimental extraction efficiency is ~50% after two electrostatic deflectors in comparison with the internal circulating beam intensity and approaches ~35% at a point out of the cyclotron.

IMPROVEMENT OF RF SYSTEM OPERATION

Between 2005 and 2007 the high-frequency system was revamped. The modernization included reduction of the contact resistance at the power stage of the generator, the acceleration chamber, the resonator, and the chamber connecting the resonator with the acceleration chamber.

After ten year of operation some high-frequency elements became stale. These elements, in the form of sheets, were connected by bolts, and the contact impedance between them was not sufficiently low. It resulted in unstable power output and accelerating voltage in the cyclotron.

In order to improve the connectivity and prevent future degradation, copper elements were covered with copper sheets. Welded joints were used in place of the screwed ones. The contact force was increased and the contacts in the areas where welding was not possible were cleaned.

Reduction of the contact resistance for high-frequency current resulted in a 50% decrease in power loss and an increase in the amplitude of the high-frequency voltage at the accelerating electrode from ~50 kV to 65 kV.

LATEST SHAPING OF MAGNETIC FIELD

The latest AIC-144 magnetic field mapping and shaping campaign was conducted in 2011-2012 [3]. The main goals of that campaign were the following:

- verification of the cyclotron magnetic field in comparison with the 2006 mapping;
- shaping of the new magnetic field regime in view of the new requirements to the central magnetic field bump and an increase in the final energy of the accelerated proton beam;
- correction of the 1st harmonic of the magnetic field in the extraction region of the cyclotron.

Verification of the Magnetic Field

A small (~5 Gs) change was observed in the average magnetic field against the previous (2006) one at the same conditions of the magnet. This difference was corrected by a small change, ~(5-10) A, in the excitation current in the cyclotron trim coils. Fig. 1 shows the initial deviation of the average magnetic field from the required one and the deviation after the correction of the trim coil current.

*Work suported by RFFR, the grant No13-01-00595a….

ISBN 978-3-95450-128-1

SECONDARY PARTICLE DOSE AND RBE MEASUREMENTS USING HIGH-ENERGY PROTON BEAMS

M. Ghergherehchi, J. S Chai, SKKU, Suwon, South Korea
D. H. Shin, NCC, Goyang, South Korea

Abstract

High- and intermediate-energy protons are not able to directly form a track in a CR-39 etch detector (TED). Such detectors, however, can be used for the detection and dosimetry of the beams of these particles through the registration of secondary charged particles with sufficiently high values of linear energy transfer (LET). The studied were realized in a clinical proton beam of the NCC Korea, with primary energy of 72 to 220 MeV (1.1 to 0.4 KeV/ μm). The contribution of the secondary particle dose and the value of RBE both increase with decreasing proton energy. A strong agreement between experimentally obtained results and the predicted total cross sections was verified by the Alice code. Stimulation of the secondary particle dose by the Geant4 code also predicted results in agreement by experimental results. It is clear that higher cross sectional values lead to an increased production of secondary particles. This secondary particle dose is highly important for applications such as radiotherapy, radiobiology, and radiation protection.

INTRODUCTION

The concept of radiation protection is based on a connection between the radiation quality and quantity, often referred to as linear energy transfer (LET). There are several techniques used for LET spectra measurements. In order to create particle tracks, a solid-state nuclear track detector (SSNTD) was exposed to nuclear radiation (neutrons or charged particles), etched, and examined microscopically [1]. Heavier, high-energy, charged particles, particularly protons are now being used in radiotherapy. When energy levels are sufficiently high, secondary particles with high LET are produced through nuclear interactions, which may change therapeutic beam characteristics [2]. Dosimetry measurements are understood and transformed into biological efficiency by means of a biological weighting function. The goal of the current experiments was to study qualitative and quantitative changes in the secondary particle microdosimetry with the aforementioned proton energy.

EXPERIMENTAL PROCEDURES

Material and Methods

Irradiation was performed at the National Cancer Center (NCC) in Korea. CR-39 plates of 20 × 20 × 0.75 mm were used throughout this study. The samples were irradiated by various proton energies using a Cyclotron with a beam current of 5nA over time periods ranging between 1–3 min. CR-39 track detectors (available from Intercast Europe SpA via Natta 10/a 43100, Parma, Italy) were used. Two corners of each detector were irradiated. One corner was irradiated with ^{252}Cf fission fragments and the other corner was irradiated with ^{241}Am alpha particles at the Sungkyunkwan University. The task was completed to check the exact etching conditions and to determine the bulk etching rate [3].

LET Spectrometer Base on Chemically Etched CR-39 TED

After irradiation, each piece of the CR-39 detector was etched in a 70°C 6N NaOH solution, as this is the most popular and commonly recommended etchant [4]. The etching time was 15 h, which corresponded to the removal of an approximately 20-μm-thick layer on each side of the detector. After etching, the CR-39 samples were cleaned in running water for 30 min and dried. The value of V was calculated by combining at least 2 of the previously mentioned track parameters. Final optimization was presented through comparison of the removed layer recalculated from V-values and directly measured through fission fragment track diameters. The resulting V-spectra were corrected for by using the critical detection angle. Anisotropy can be obtained easily by the Alice code [5]. By taking into account the anisotropy the critical and solid angles are easily corrected to determine the V-spectra. V-distributions were then transformed into LET spectra using calibration curves [6] with the heavy charged particles. This calibration curve, based on irradiation with 12C to 56Fe ions and LET in water ranging from 7.9–200 keV/μm, was based on extrapolated data extended to the much higher values of LET. The etched tracks were observed using an optical microscope. The microscope image was viewed with a high-quality camera connected to a PC-based image analyzer. With a magnification of 1000 pixels, the single field-of-view area considered was approximately 4.71×10^{-4} cm^2. The image analyzer displays images on a monitor and tracks appear as dark spots on a clear white background.

Integral Dosimetry and Microdosimetry Characteristics and RBE Calculated from LET Spectra

Dose characteristics and clinical radiobiological effectiveness for the particles having LET values higher than 10 keV/μm can be obtained from the LET spectra by the following:

*Jschai@skku.edu

ISBN 978-3-95450-128-1

THE RADIO FREQUENCY FRAGMENT SEPARATOR: A TIME-OF-FLIGHT FILTER FOR FAST FRAGMENTATION BEAMS*

T. Baumann, D. Bazin, T. N. Ginter, E. Kwan, J. Pereira, C. S. Sumithrarachchi
NSCL, Michigan State University, East Lansing, MI 48824, USA

Abstract

Rare isotope beams produced by fragmentation of fast heavy-ion beams are commonly separated using a combination of magnetic rigidity selection (mass-to-charge ratio) and energy-loss selection (largely dependent on proton number) using magnetic fragment separators. This method offers isotopic selection of the fragment of interest, however, the purity that can be achieved is often not sufficient for neutron-deficient isotopes (towards the proton drip line) where much more abundant isotopes closer to stability can not be separated out. A separation by time-of-flight can clean things up. The Radio Frequency Fragment Separator deflects isotopes based on their phase relative to the cyclotron RF using a transverse RF field, effectively separating by time-of-flight. This method is in use for the production of neutron deficient rare isotope beams at NSCL.

INTRODUCTION

Rare isotope beams that are produced in fast fragmentation reactions give access to a large range of radioactive isotopes for in-beam nuclear physics experiments, from the most neutron-rich isotopes that have ever been observed up to the proton drip line for many elements. Many experiments require beams of high purity, and for neutron deficient rare isotopes in particular this is often difficult to achieve using magnetic fragment separators. The problem originates from a low momentum tail produced in the fragmentation process, which occurs for projectile energies between 50 MeV/u and 200 MeV/u. This causes much more abundant fragments that are closer to stability to spill into the acceptance window of the desired isotope.

The Radio Frequency Fragment Separator (RFFS) [1] at the National Superconducting Cyclotron Laboratory (NSCL) was built to address this problem. It uses the time structure of the particle beams that are accelerated by the coupled cyclotrons to deflect unwanted fragments based on the difference in velocity. In this paper we will give a brief summary of how the RFFS functions and focus on two recent experiments that give a real world view of its performance.

Function of the RF Fragment Separator

The RFFS is basically the combination of an RF driven electric deflector that diverts the particle beam vertically at a specified phase of the cyclotron RF, and a set of slits that blocks unwanted particles. The detailed parameters of the RFFS are given in Ref. [1]. Figure 1 shows a side view of the RF cavity.

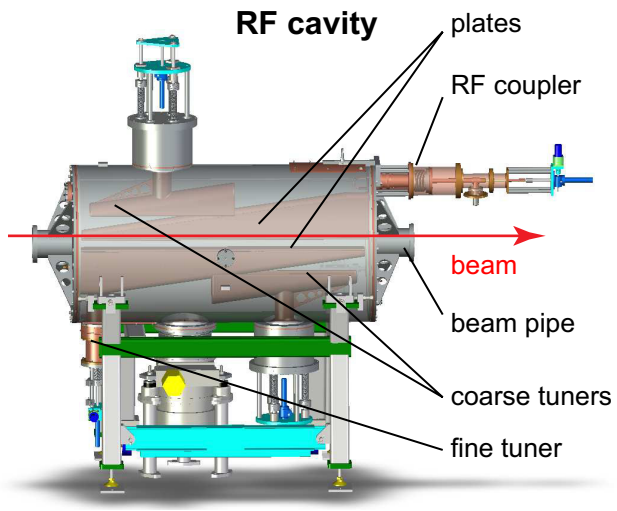

Figure 1: Side view of the RFFS cavity.

The length of the electrodes is 1.5 m which covers approximately 140° of the phase with typical beam velocities of around $0.4c$ and the given cyclotron frequency of about 25 MHz. The vertical gap between the electrodes is 5 cm, and the nominal operating peak voltage is 100 kV.

Following the RF deflector, the particle beam is focused on a pair of vertical slits in the RFFS focal plane box. These slits are adjustable in order to block the unwanted parts of the beam depending on their vertical position. The RFFS focal plane box also contains detectors to perform the particle identification. A pair of parallel plate avalanche counters (PPACs) gives position and angle information, a 250 μm plastic scintillator timing, and a stack of Si PIN detectors energy-loss information.

Under normal operating conditions, the phase of the RFFS is set such that the fragment of interest receives the maximum deflection, and unwanted fragments that are less deflected are blocked by the slits. The deflected beam position is then corrected by a pair of steering magnets before reaching the experimental setup. This method has the advantage that in case of a failure of the RF deflector, the possibly highly intense unwanted beam will still be blocked by the slits, minimizing the risk of damaging rate sensitive detectors.

EXPERIMENTAL EXAMPLES

The RFFS is one of the tools that are available at NSCL to provide rare isotope beams to facility users. Two recent experiments will serve as examples of neutron deficient rare isotope beams that benefited from the use of the RFFS.

* Work supported by NSF grants

ISBN 978-3-95450-128-1

GANIL OPERATION STATUS AND UPGRADE OF SPIRAL1

O. Kamalou, O. Bajeat, F. Chautard, P. Delahaye, M. Dubois, P. Jardin, L.Maunoury,
GANIL, Grand Accélérateur National d'Ions Lourds, CEA-DSM/CNRS-IN2P3,
Bvd H. Becquerel, BP 55027 14076 Caen Cedex 5, France

Abstract

The GANIL facility (Grand Accélérateur National d'Ions Lourds) at Caen produces and accelerates stable ion beams since 1982 for nuclear physics, atomic physics, radiobiology and material irradiation. Nowadays, an intense exotic beam is produced by the Isotope Separation On-Line method at the SPIRAL1 facility. It is running since 2001, producing and post-accelerating radioactive ion beams of noble gas type mainly. The review of the operation from 2001 to 2013 is presented. Due to a large request of physicists, the facility will be enhanced within the frame of the project Upgrade SPIRAL1. The goal of the project is to broaden the range of post-accelerated exotic beams available especially to all the condensable light elements as P, Mg, Al, Cl, etc. The upgrade of SPIRAL1 is in progress and the new beams would be delivered for operation by the end of 2015.

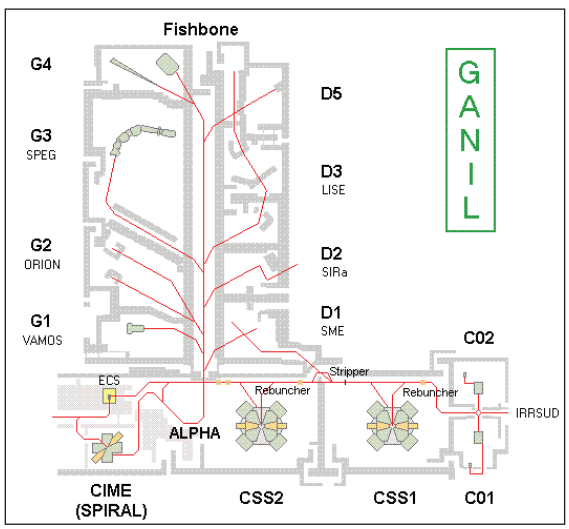

Figure 1: GANIL layout.

OPERATION REVIEW

Multi-beam delivery is routinely done at GANIL using its 5 existing cyclotrons. Up to five experiments can be run simultaneously in different rooms with stable beams (Fig. 1):

1. Beams from C01 or C02 are sent to an irradiation beam line IRRSUD (<1MeV/u).
2. A charge state of the ion distribution after the ion stripping downstream CSS1 is sent to atomic physics, biology and solid states physics line D1 (4-13MeV/u).
3. A high-energy beam out of CSS2 is transported to experimental areas (<95MeV/u).
4. An auxiliary experiments shares the previous CSS2 beam (10% of the pilot experiment time)
5. Finally, stable beams from SPIRAL1 source can be sent to LIRAT (<10 keV/q) or post-accelerated by CIME and used for testing detector for example.

During radioactive beam production with SPIRAL1, the combinations are reduced to the four first (cases 1, 2, 3, 4) and radioactive beam is sent to the experimental areas.

2001-2012 GANIL OPERATION STATUS

Since 2001 (Fig. 2), more than 40000 hours of beam time has been delivered by GANIL to physics, which correspond to 92 % of scheduled experiments.

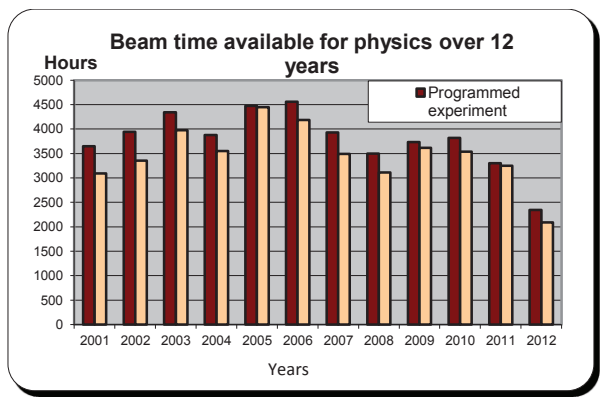

Figure 2: Beam time available for physics over 12 years.

The number of beam delivered per year (Fig. 3) has increased until 2010. Owing to the construction and assembly of the new SPIRAL2 accelerator, the running time has been shrinked to devote more human ressources to the project, in particulier in 2012 with only 2000 hours of running time (instead of 3500 hours per years).

ISBN 978-3-95450-128-1

IN MEMORIAM: HENRY G. BLOSSER

S.M. Austin, F. Marti, NSCL, MSU, East Lansing, MI 48824, USA
M.K. Craddock, University of British Columbia & TRIUMF, Vancouver, BC, Canada

Abstract

Henry G. Blosser, physicist and cyclotron designer, died on March 20, 2013 after an extended illness. Henry was a world-renowned accelerator physicist who founded the Cyclotron Laboratory at Michigan State University. Henry's influence extended to many cyclotron construction projects during his 60 years of active participation in the field.

INTRODUCTION

Henry (also known as Hank to his early collaborators) was a passionate accelerator physicist who devoted most of his professional life to the design and construction of cyclotrons. He always pushed the envelope to obtain more precise beams, higher energy and lower cost. From 1958 when he joined Michigan State University until 1993 he was the laboratory accelerator group leader and developer of new machines for nuclear science. After 1993 his efforts concentrated on the medical applications of cyclotrons.

Henry was a very active participant in the Cyclotron Conferences and we will miss his insightful comments.

Figure 1: Henry Blosser, sailor.

EARLY YEARS

Henry was born on March 16, 1928 and grew up in Harrisonburg, Virginia, USA. Influenced by a High School buddy, he joined the Navy after studying business for a year at the University of Virginia (UVA). His Navy experience could be detected in his PA announcements which often started with "Now hear this…" He returned to UVA, where he received his B.Sc. in math in 1951 and his M.Sc. in 1952 and Ph.D. in 1954, both in physics. His Ph.D. thesis adviser was Frank Hereford. Henry joined Oak Ridge National Laboratory and soon became group leader of the cyclotron project. This group pioneered the use of digital computers to design a new generation of sector focused cyclotrons that overcame the limitations in energy of classical cyclotrons (T. Welton and M.M. Gordon). The development of the Thomas-type electron cyclotrons at the University of California [1] gave new impulse to implementing Thomas' proposal of sector focused cyclotrons [2] for nuclear physics. Another electron model was built at ORNL [3] to study the effect of imperfection resonances on orbit stability, and successfully demonstrated that they would not prevent acceleration up to $\beta = 0.69$.

THE K50 YEARS

The completion of the electron analogue at ORNL coincided with an interest at Michigan State University (MSU) in strengthening the Physics Department Nuclear Physics group. The construction of a cyclotron as part of an effort to attract promising faculty was supported by MSU President Hannah. Henry was approached to lead the effort. At age 30 he moved to MSU in 1958 as an Associate Professor and Director of the future Cyclotron Laboratory. He hired Morton M. Gordon from the University of Florida to help with the theoretical work, and Thelma Arnette to do computer programming. By 1961 they had completed a design and received funding from the National Science Foundation to build the K50, a precision cyclotron. The cyclotron began operation three and a half years later. Its precise proton beams set a new standard for cyclotrons and made possible experiments with resolutions comparable to Van de Graaff accelerators. Its high-resolution capability was used by Henry and his collaborators, in his only purely nuclear physics experiment, to delineate in unique detail the nature of bismuth-208 excitations. That established the feasibility of the many experiments that followed and established the unique strength of the Cyclotron Laboratory. Over the next 14 years, the K50 supported a research program that put MSU nuclear physics on the map. The successful cyclotron was copied (with some modifications) at Princeton [5].

ISBN 978-3-95450-128-1

CONSTRUCTION OF THE RARE RI RING AT THE RIKEN RI BEAM FACTORY

M. Wakasugi and Rare-RI Ring Collaborators, RIKEN, Japan

Abstract

The Rare RI Ring (R3) heavy-ion storage ring is now under construction at the RIKEN RI Beam Factory. The aim of this ring is high-precision mass measurement of extremely short-lived and rarely produced unstable nuclei (rare RIs). Our target performance for mass determination is accuracy on the order of 10^{-6} ($\sim$ 100 keV), even for a single event. We use isochronous mass spectrometry to reduce measurement times to less than 1 ms. The R3 structure is based on cyclotron motion to achieve the target accuracy. Since an isochronism in R3 is established over a wide momentum range, rare RIs with a large momentum spread, $\Delta p/p = \pm 0.5\%$, are acceptable. Another significant feature of the R3 system is an individual injection scheme in which a produced rare RI itself triggers the injection kicker. This allows efficient use of unpredictably produced rare RIs. Ultra-fast response is required of the kicker system to establish the individual injection scheme. Technical challenges are forming a precision isochronous magnetic field and development of a fast response kicker system. This paper describes the R3 and its construction status.

INTRODUCTION

Mass measurement is one of the most important contributions to research on nuclear properties, especially for short-lived unstable nuclei far from the β-stability line. In particular, high-precision mass measurements of nuclei located around the r-process pass (rare RI) are required for nucleosynthesis. The r-process is a promising candidate for solving the mystery of nucleosynthesis for elements heavier than iron. Supernovae and neutron star collisions are proposed as sites of r-process nucleosynthesis. A precision in mass determination on the order of 10^{-6} ($\Delta m/m$) is required to constrain environmental conditions such as temperature and neutron flux in these sites. The RIKEN RI Beam Factory is the world's most powerful RI production facility, and has allowed access to rare RIs [1, 2, 3]. Nuclei around the r-process pass have extremely short lifetimes (on the order of ms) and rare production rates, making precise mass measurement difficult. Our motivation in constructing the R3 is to establish a method that allows determination of nuclear masses with precision on the order of 10^{-6} and measurement times of less than 1 ms.

Some experimental methods for precise mass measurement have been established. An ion-trapping-based method using a slow RI beam [4] achieves excellent mass resolutions of better than 10^{-7}. Schottky mass spectrometry conducted in a storage ring is also an elegant method that can achieve mass resolutions of 10^{-6}, as demonstrated at ESR/GSI [5]. But measurement times in these methods exceed 1 s, making them unsuited to rare RIs. Another candidate for fast mass measurement is isochronous mass spectrometry (IMS) conducted in a storage ring; measurements for nuclei with lifetimes of 50 ms were demonstrated at ESR/GSI using this method [6]. However, the mass resolution achieved in IMS has so far been on the order of 10^{-5}, which is insufficient for our purposes. The reason for this is that the isochronous mode of ESR provides relatively small acceptance, in momentum space in particular, because the lattice was originally designed as a strong focusing storage ring. Since the lattice design of R3 is based on cyclotron motion, it can provide isochronism in a wide range of momentum. Acceptances in momentum and m/q value were designed to be much larger than that of the isochronous mode of ESR. We expect significant improvement in IMS mass resolution as long as the isochronous field is precisely formed in R3. Therefore, IMS using R3 will be capable of both high precision and fast measurement.

Another desired feature for R3 is to efficiently take advantage of opportunities for measurement of unpredictably produced rare RIs. We adopted an individual injection scheme in which the produced rare RI itself triggers the injection kicker magnets. To achieve this, full activation of the kicker magnetic field must be completed within the flight time of the rare RI from the originating point of the trigger signal to the kicker position. Development of an ultra-fast response kicker system is therefore a key issue for establishing the individual injection scheme.

The R3 design study has continued for over a decade, and construction began in 2012. Construction of the infrastructure and fabrication of major R3 hardware have been generally completed. We are now setting up and testing all equipment, including power supplies, the control system, and the vacuum system. Commissioning is planned for 2014.

R3 IMS PRINCIPLES

Since design of the R3 beam orbit is based on cyclotron motion, its circulation frequency is described by the cyclotron frequency f_c,

$$f_c = \frac{1}{2\pi}\frac{q}{m}B, \quad (1)$$

where q/m is the charge-to-mass ratio and B is the magnetic field. The frequency is independent of beam momentum so long as the R3 isochronism is secure. Since the mass and magnetic field are relativistically given by $m = m_0\gamma$

ISBN 978-3-95450-128-1

CYCLOTRON PRODUCTION OF Tc-99m

Ken Buckley, TRIUMF, Vancouver, Canada

Abstract

Concern over past and impending shortages has led to renewed interest in the cyclotron production of Technetium-99m (Tc-99m) - the most used radionuclide in Nuclear Medicine. TRIUMF has led a collaboration to implement the irradiation of Molybdenum-100 (Mo-100) solid targets on cyclotrons previously used only for the production of PET radionuclides. Solid targetry and target transfer systems have been implemented on the GE Medical Systems PETtrace at two centres and the ACSI TRPET at one centre. Irradiations have occurred at 100 μA on the PETtrace and 230 μA on the TRPET. Progress continues towards the design goals of 130 μA and 300 μA respectively. Due to the presence of other molybdenum isotopes in the enriched Mo-100 target material the purity of the resulting technetium is affected by beam energy and irradiation time.

INTRODUCTION

The radioisotope Tc-99m is used in approximately 80% of nuclear medicine imaging procedures at a volume equivalent to approximately one scan per second worldwide [1]. Tc-99m with a half-life of 6 hours is also the decay product of molybdenum-99 which has a half-life of 66 hours. The Mo-99/Tc-99m generator was developed at Brookhaven National Laboratory in 1958 [2]. The generator consists of an alumina column loaded with molybdenum-99. As the Mo-99 decays the Tc-99m builds up on the column and can be eluted by simply rinsing the column with saline yielding Tc-99m in the form of pertechnetate. The development of the generator allowed the simple distribution of Tc-99m to a large geographic area. This easy availability, combined with the desirable decay characteristics of a 140 keV gamma ray and 6 hour half-life have led to the popularity of Tc-99m in clinical nuclear medicine.

Starting in 2009 the National Research Universal (NRU) reactor at Chalk River Laboratories in Ontario Canada was off line for 15 months. This reactor previously supplied 30 % of the world's supply of Mo-99 and is one of 5 that at the time supplied the world's demand for Mo-99. The coincident shutdown of the Petten reactor in the Netherlands resulted in a shortage of Tc-99m in nuclear medicine clinics around the world and raised concerns over the potential fragility of the supply. This concern, coupled to the use of weapons grade highly enriched uranium as the target material for the reactor production of Mo-99, resulted in an effort to develop alternative sources of Tc-99m. The Canadian government funded two consecutive programs through the federal agency Natural Resources Canada. TRIUMF has led a collaboration of four institutions through the Non-reactor Isotope Supply Program and the Isotope Technology Acceleration Program. The collaborators are the British Columbia Cancer (BCCA) Agency in Vancouver British Columbia, the Center for Probe Development and Commercialization (CPDC) in Hamilton Ontario, and the Lawson Health Research Institute (LHRI) in London Ontario. These facilities produce only PET isotopes which, almost exclusively, are produced by irradiating liquids and gases which are easily transported through sealed small diameter (eg. ≤ 3mm) piping. The target material, and produced radioisotopes, are always fully contained while in the cyclotron facility and thus do not typically pose a radioactive contamination hazard. As such the required radiation protection practices are significantly less onerous than those of a commercial production facility irradiating and transporting solid targets.

The feasibility of direct production of Tc-99m was first reported by Beaver & Hupf in 1971 employing the Mo-100(p,2n)Tc-99m reaction [3]. Low current irradiations with molybdenum of both natural isotopic abundance and enriched in mass 100 indicated sufficient production rates that compact commercial medical cyclotrons could supply a metropolitan area. Presumably due to the availability and low cost of Mo-99/Tc-99m generators there was little effort to develop molybdenum targets with high current capabilities, until Targholizadeh reported a thick molybdenum target produced by electrospray [4].

CYCLOTRON FACILITIES

The CPDC & LHRI have GE Medical Systems PETtrace 880 cyclotrons capable of delivering 130 μA of 16.5 MeV protons. The BCCA has an ACSI TRPET cyclotron capable of delivering 300 μA of 19 MeV protons. The intention of this project is to fully utilize the beam power of the cyclotrons.

PETtrace Cyclotron Description

The PETtrace 880 cyclotron is an H- machine with an internal PIG source and dual beam extraction probes allowing simultaneous irradiation of two targets. Targets are arranged on the periphery of the vacuum tank on individual beam ports. There are six ports identified as 1 through 6. One extraction probe serves target ports 1-3 while the other extraction probe serves ports 4-6. Each port has a set of beam collimators followed by a vacuum isolation valve and each port is electrically isolated allowing measurement of the beam current striking the target. The beam port diameter is 15 mm. Radiographs of irradiated target plates were performed according to the method of Avila-Rodriguez [5] to confirm the beam distribution.

The cyclotron vacuum is achieved by a single oil diffusion pump that affords a typical beam-on operating pressure of 1E-5 mbar.

ISBN 978-3-95450-128-1